DOT/FAA/TC-19/12

Federal Aviation Administration
William J. Hughes Technical Center
Aviation Research Division
Atlantic City International Airport
New Jersey 08405

Study of Mishap Kinematics, Damage, and Injury Interactions for Wide-Body and Narrow-Body Transport Aircraft

August 2019

Final Report

This document is available to the U.S. public through the National Technical Information Services (NTIS), Springfield, Virginia 22161.

This document is also available from the Federal Aviation Administration William J. Hughes Technical Center at actlibrary.tc.faa.gov.

U.S. Department of Transportation
Federal Aviation Administration

NOTICE

This document is disseminated under the sponsorship of the U.S. Department of Transportation in the interest of information exchange. The U.S. Government assumes no liability for the contents or use thereof. The U.S. Government does not endorse products or manufacturers. Trade or manufacturers' names appear herein solely because they are considered essential to the objective of this report. The findings and conclusions in this report are those of the author(s) and do not necessarily represent the views of the funding agency. This document does not constitute FAA policy. Consult the FAA sponsoring organization listed on the Technical Documentation page as to its use.

This report is available at the Federal Aviation Administration William J. Hughes Technical Center's Full-Text Technical Reports page: actlibrary.tc.faa.gov in Adobe Acrobat portable document format (PDF).

Technical Report Documentation Page

1. Report No.	2. Government Accession No.	3. Recipient's Catalog No.
DOT/FAA/TC-19/12		

4. Title and Subtitle	5. Report Date
STUDY OF MISHAP KINEMATICS, DAMAGE, AND INJURY INTERACTIONS FOR WIDE-BODY AND NARROW–BODY TRANSPORT AIRCRAFT	August 2019
	6. Performing Organization Code

7. Author(s)	8. Performing Organization Report No.
Lance C. Labun John (Jack) P. Cress Dale Kennedy	

9. Performing Organization Name and Address	10. Work Unit No. (TRAIS)
Labun LLC 1342 E. Louis Way, Tempe, AZ 85284 Vortechs Helicopter Analytics, 19275 Reavis Way Prunedale, CA 93907 Dale Kennedy 565 E Sunburst Lane, Tempe, AZ 85284	11. Contract or Grant No. NIAR 065591

12. Sponsoring Agency Name and Address	13. Type of Report and Period Covered
U.S. Department of Transportation Federal Aviation Administration Orlando CMO-29 5950 Hazeltine National Drive Citadel International Bldg Orlando, FL 32822	Final Report
	14. Sponsoring Agency Code AIR-600

15. Supplementary Notes

The FAA William J. Hughes Technical Center Aviation Research Division COR was Allan Abramowitz.

16. Abstract

This study investigated the mishap outcomes for two classes of transport aircraft: narrow-body, single-aisle aircraft; and wide-body, two-aisle aircraft. The mishaps included survivable and nearly survivable mishaps of passenger-carrying, western–built aircraft. Only mishaps with detailed mishap investigations available in the public record are included. The analysis of each class of aircraft characterizes the kinematics of the mishaps, the damage outcomes, and the injury outcomes. Ultimately, this study, together with a prior study of regional jets, is part of a larger effort by the FAA and other agencies to make air travel safer by understanding how occupants are injured in mishaps and by attempting to provide guidance to build aircraft that offer occupants an improved chance of survival.

17. Key Words	18. Distribution Statement
Aircraft crashes, Aircraft kinematics, Aircraft damage, Aircraft crash injuries, Transport aircraft crashworthiness, Narrow-body, Wide-body	This document is available to the U.S. public through the National Technical Information Service (NTIS), Springfield, Virginia 22161. This document is also available from the Federal Aviation Administration William J. Hughes Technical Center at actlibrary.tc.faa.gov.

19. Security Classif. (of this report)	20. Security Classif. (of this page)	21. No. of Pages	22. Price
Unclassified	Unclassified	203	

TABLE OF CONTENTS

LIST OF FIGURES

LIST OF TABLES

LIST OF ACRONYMS

AGL	Above ground level
ANOVA	Analysis of variance
BLM	Binary logistic model
CI	Confidence interval
CSTRG	Cabin Safety Technical Research Group
Fin	Vertical stabilizer
L	Localized
LCL	Lower confidence limit
N	None
N–B	Narrow-body
NS	Non-survivable
PS	Partially survivable
RJ	Regional jet
S	Survivable
SFO	San Francisco International Airport
UCL	Upper Confidence Limit
W	Widespread
W–B	Wide-body

EXECUTIVE SUMMARY

The purpose of this study was to quantify the outcome of fixed-wing transport aircraft in two classes: wide-body (W–B) and narrow-body (N–B). The information will be used to establish crashworthiness guidelines for composite fuselage commercial aircraft. The results of this study are meant to compliment the results of a prior study on regional jet (RJ) aircraft. The aircraft in this study are mostly metal airframes. To set standards for crashworthiness in composite airframes, the response of metal airframes was studied. For the purposes of this study, W–B aircraft are western–built aircraft with two internal aisles, and N–B aircraft are western–built aircraft with a single aisle. The mishaps of interest are those that are potentially survivable. The mishap outcomes of interest are the damage to the aircraft and the injuries to the occupants. The analyses were conducted independently on the N–B and W–B mishaps.

Each mishap has been identified with a particular mishap scenario. An analysis of the kinematics, the damage, and the injuries has been conducted for each scenario and for a larger dataset in which all of the impacts were from the air. The kinematics of the crashes have been quantified and the distributions for the key impact parameters have been determined and are presented. For two critical velocities—the vertical velocity and airspeed—the 90^{th}-percentile values have been determined. The damage and injury outcomes are presented in a two-velocity plot using the 90^{th}-percentile values as a reference. The method developed in the RJ study for quantifying damage to the aircraft has been applied in these two analyses. The damage quantification was focused on the fuselage where the occupants are located and on the types of damage leading to injury. Results show that the damage metric correlates well with the injuries experienced in the mishaps.

The two aircraft classes had similar injury fractions at approximately 17 percent fatalities, 8 percent serious injuries (generally, an injury requiring hospitalization as used by the NTSB), and 75 percent minor or no injuries. Although the details in the cause-of-death information varied from investigation to investigation, reported thermal fatalities accounted for 5 percent of all occupants in both classes of aircraft and for approximately 30 percent of all fatalities.

Binary logistic models were constructed using the kinematic data. The models attempt to predict the probability of injury or, equivalently, the fraction of fatal and serious injuries in each mishap based on the kinematic parameters. In both classes of aircraft, the best models were those that combined several kinematic parameters to estimate the injury probability.

The fact that the injury probability correlated well with the damage metric serves to validate the objective of crashworthiness design criteria. That objective is to minimize the number of serious injuries in a potentially survivable mishap by design of the aircraft, seats, and restraints. Minimizing these injuries not only directly reduces fatalities and serious injuries, but also improves the chances of escape should there be a post-crash fire.

1. INTRODUCTION

The objective of the two studies reported here was to investigate the damage and injury characteristics of two classes of transport aircraft: narrow-body (N–B) and wide-body (W–B). In previous efforts [1], one study investigated a mishap type—ditching—and another study investigated an aircraft class—regional jets (RJs). In these studies, the damage and injury characteristics for mishaps involving N–B aircraft (single-aisle) and W–B aircraft (two-aisle) were investigated. The objective was to better understand and quantify the occupant survivability for these two classes of aircraft in much the same way as the RJ study. These two studies contribute to a larger objective of defining the crashworthiness of transport aircraft with metal fuselage structures on at least a semi-quantitative basis. The ability to describe the crashworthiness of these metal aircraft will set expectations for the crashworthiness of polymer-composite and other nontraditional fuselage structures in current and future transport aircraft.

As the two studies evolved, it became apparent that the two study classes have minimal overlap in characteristics. The 86 N–B, single-aisle aircraft had a maximum of six seats across, and most were in the 100,000–250,000 lb weight class with just nine in the 250,000–400,000 lb weight class. In contrast, the 29 W–B two-aisle aircraft ranged from seven to ten seats across, and all except two weighed more than 400,000 lb. Although these two classes of aircraft are not formally defined for industry or regulatory purposes, they represent two distinct populations of aircraft.

Each class of aircraft was treated as a separate study in this report. The same basis was used for selecting mishaps for inclusion in each study. The objective of the studies required detailed information about each mishap. Consequently, to be included, a mishap must have had a thorough investigation conducted and documented in a report that is accessible and, preferably, written in English. The mishaps for each study were selected from those mishaps included in the Cabin Safety Technical Research Group (CSTRG) database. The mishaps were selected for each study by first creating a list of aircraft models with which to query the database. Based on experience with the RJ study, the two lists included only western manufactured aircraft, because the probability of finding thoroughly conducted investigations in English for aircraft manufactured elsewhere was quite small.

Each mishap was assigned to a scenario based on characteristics of the mishap. As described in the “Mishap Scenario” sections, the same list of scenarios was used to categorize the mishaps: runway overruns, compromised landings, landing short, post-landing loss of control, and loss of control during takeoff. The list of scenarios was based on the scenarios used in the RJ study but with two added scenarios related to the local wind environment. The W–B study included 29 mishaps. When these are broken down into scenarios, the sample size for each scenario is generally small, which is not desirable for establishing the statistical significance of the quantitative findings. The situation is better in the N–B study, in which 86 mishaps are usable in the dataset. Even when categorized into the scenarios, the sample sizes are reasonable.

The analyses of the two datasets were conducted separately. Therefore, all the information and discussion for each class of aircraft is grouped together. This presentation provides information on each class of aircraft and enables the findings to supplement each other and the findings from the RJ study. Some readers may be interested in only one class of aircraft; consequently, the report is

written with some redundancy of explanation considering that some readers may not be reading the entire report and may not have read the RJ report.

2. METHODS

This report describes the analysis of mishap data from two types of transport aircraft: N–B and W–B. The study is intended to supplement the work done on RJ aircraft mishaps in a prior report [1]. The methods used in this study are based on those used in the RJ study to assure that the results can be compared. Methods that are unique to one study or the other will be described in the appropriate section of the study.

2.1 SELECTING THE MISHAPS FOR STUDY

The mishap search was conducted by specifying a particular aircraft type in passenger operation. Only impact-related mishaps were sought, and mishaps with and without official reports were reviewed for inclusion. Consequently, a typical query would look like:

AIRCRAFT TYPE = (e.g. A320, B747 etc.)

OPERATION = PASSENGER

IMPACT RELATED = Yes

CONTAINS OFFICIAL ACCIDENT REPORTS = not ticked or ticked (two queries)

Access to a formal report was important to accomplish the objective of this study. Data on the aircraft, the kinematics of the impact, the aircraft damage resulting from the impact, and the injuries resulting from the impact are all needed to accomplish the objectives of the study. Ticking the box for “Official Reports” returned only those mishaps for which the database had the report field filled with a report identifier or for which the database contained a copy of the report. For many mishaps that were returned when the query was run without requiring a report, either a report could be located or sufficient information could be found so that the mishap could be included in the study.

The output from these queries for the W–B aircraft delivered 273 candidate mishaps and the output from the N–B queries delivered 719 candidate mishaps. Quite a few of the mishaps were events such as ground collisions with vehicles or other aircraft. These were eliminated from consideration, as were turbulence mishaps resulting only in passenger or crew injury. The lists of mishaps were reviewed by reading the summary description in the database and verifying that the nature of the mishap was suitable for inclusion in the study. For the list of suitable mishaps, the reports and other information were sought, mostly through Internet access. Where available, reports were downloaded from the Internet and the link stored in a cell of the Microsoft® Excel® workbook. One limitation placed on the nature of the mishap was that the mishap be survivable (S), partially survivable (PS), or at least close to survivable. Mishaps involving disintegration of the aircraft with deceleration forces beyond human survivability and without survivable volume were not included. In as much as knowledge of the damage to the aircraft and its influence on the number of severe and fatal injuries is an objective of the study, mishaps in which the impact-generated damage could not be determined were also eliminated. This criterion eliminated a few mishaps with severe post-crash fires because knowledge of the impact-induced damage was lost in the fire.

Several mishaps identified by the query for this study were used in the water-mishap study; these water-related mishaps were included in this study if the primary impact was on terrain.

2.2 ORGANIZING THE DATA

After selecting the final list of mishaps for each aircraft type, the detailed data for these mishaps were extracted from the CSTRG database. The data for each study were stored in an Excel workbook for that study consisting of four tabs: Mishap Data, Kinematics, Damage Data, and Injury Data. The list of mishap IDs was saved as a text list and imported to the CSTRG database as a custom list. The custom list and the Export Wizard were used to export the data for each worksheet. The fields for each data query are provided in appendix A. For consistency and efficiency, the data queries for the two studies were kept as similar as practical. Each data field became a column and each mishap became a row.

After importing the data from the CSTRG, fields were added to the worksheets for additional data and in anticipation of the analysis. Each worksheet was manipulated for analysis in two forms: in one form, the mishaps appeared in reverse chronological order (newest at the top), and in the other form, the mishaps were sorted by scenario. The worksheet sorted by scenario was used when the data were analyzed to compare or organize the results between different mishap scenarios.

The data for each mishap were reviewed for completeness and were supplemented with any additional information available from the investigation report. The report file was opened and read, and the missing data, where available, were extracted and inserted into the database. The kinematics data, where available, were extracted from the report. The mishaps with incomplete kinematics data were identified as candidates for accident reconstruction. The reconstructions were done by Mr. Jack Cress[1]; all reconstructions were jointly reviewed and agreed on between the authors—Mr. Cress and Dr. Lance Labun.

Information on the damage to the aircraft floor, seats and restraints, and interior appointments was often minimally described in the reports. Consequently, it was necessary to infer the interior damage from the descriptions of the evacuation and from photos of the exterior damage. Similarly, information on the functionality and use of doors and exits was often found under different topics throughout the report, including the sections on survivability, evacuation, damage, and injury. Information from these different sections of the report was integrated and recorded in the worksheet. Columns were set up to perform various mathematical and logical operations on the data and to save the results. The results from these manipulations and calculations are presented as tables and plots in this report where appropriate.

2.3 KINEMATIC PARAMETERS

The kinematic parameters describe the dynamics and attitude of the aircraft as the impact occurs. The airspeed was used as the longitudinal velocity because it is the most commonly reported and readily available value. The vertical velocity is the velocity of the aircraft perpendicular to the horizon and is positive downward. Lateral velocity was determined in the reconstructions, but the lateral velocity was not one of the kinematic parameters studied in detail. The three aircraft attitude angles were pitch (positive nose upward), yaw (positive nose to the right of direction of travel), and roll (positive right wing downward). There were three axes of deceleration recorded and

[1]Cress, Jack, Vortechs Helicopter Analytics, Prunedale, CA. vortechsanalytics@att.net, (831) 229-6773.

analyzed: longitudinal deceleration (negative for loss of airspeed), vertical deceleration (positive for loss of downward vertical velocity), and lateral acceleration (absolute value). The lateral acceleration was analyzed as an absolute value because it has two directions—left and right. Intuitively, the aircraft damage and occupant injuries incurred increase as the peak lateral deceleration increases in either direction. However, the analysis will not detect this increase if the positive (right) and negative (left) signs on the deceleration are retained. By taking the absolute value, the increasing trend was retained without having to treat the positive values as a separate parameter from the negative values.

Roll and yaw were combined into a single parameter named the "off-nominal angle". This value was obtained by adding the absolute value of roll angle to the absolute value of yaw angle. The absolute value is justified on the basis that the aircraft is symmetric about its axes in both yaw and roll; therefore, in terms of damage and injuries, the outcome is the same regardless of whether the direction is right or left. Intuitively, the aircraft damage and injuries incurred increase as either the roll angle or the yaw angle become larger (further from zero), regardless of the direction (left or right). However, if the positive and negative signs are retained in the analysis, the mishaps with negative angle values tend to cancel out the mishaps with negative angle values, and the result appears to be that the damage and the injuries do not depend on these angles. The two angles were summed together to create a single parameter because there are very few mishaps with non-zero roll and yaw angles. Summing the angles reduced the number of parameters to be analyzed with only a small loss of detail, considering that there were so few non-zero values in the dataset.

The pitch angle represents a special case of the bi-direction problem described above for the roll and yaw angles. Pitch response is not obviously symmetric about zero. If the pitch angle exceeds a critical angle, the tail will make ground contact first. This tail strike causes the nose of the aircraft to rotate sharply downward, causing potentially high vertical accelerations at the forward end of the fuselage. For a nose low impact, the nose gear contacts first (if extended) and typically fails, leading to the second contact being the nose of the aircraft. These are two very different situations and the resulting damage and injury patterns are expected to be very different. In the W–B dataset, there are three nose-down (-) mishaps, 11 nose-level mishaps (zero), and 15 nose-up (+) mishaps. Because of the small number of negative mishaps in the W–B dataset, the author chose to treat the pitch parameter as a single algebraic (+/-) parameter. With only three values in two different scenarios, treating positive and negative pitch as two separate variables would not be productive. The effect of treating it as a single, algebraic parameter is to slightly reduce the modeled slope for dependence of damage and injury fraction on the pitch angle.

2.4 KINEMATICS RECONSTRUCTION TECHNIQUES

Each reconstruction was initiated by thoroughly reading the published accident investigation report and searching for other data sources, including contemporaneous news reports and photographs, and professional journals and websites for supplemental information. Information sought to support the reconstruction included:

a. Aircraft gross weight
b. Atmospheric characteristics
c. Wind conditions
d. True airspeed
e. Ground speed (calculated)

f. Velocity reference (V_{ref})
g. Control positions (primarily flaps)
h. Landing-gear position
i. Aircraft damage (location, deformation)
j. Design guidance and regulatory requirements for structure
k. Ground topography and obstacle interaction (if pertinent)
l. Sequence of impacts (in which multiple impacts of significant magnitude occurred)
m. Ultimate aircraft configuration and wreckage distribution (accounting for sequence and loss of major components)

The acquired information was analyzed to estimate (if unreported) and resolve the primary impact parameters, velocity, and attitude into the aircraft's reference frame. This reference frame was adapted from the "Aircraft Crash Survival Design Guide" [2]. The reference is a right-hand coordinate system with the *X* axis as the longitudinal axis (about which the aircraft rolls); the forward direction is positive (see figure 1). The *Y* axis is the lateral axis about which the aircraft pitches; positive along this axis is to the right. The *Z* axis passes vertically through the aircraft and is the axis that the aircraft yaws about; downward along this axis is positive. In the final presentation, *Z* was reported as positive downward. The conversions from earth reference frame to aircraft reference frame used the guidance from "Dynamics of Flight" [3] by Bernard Etkin.

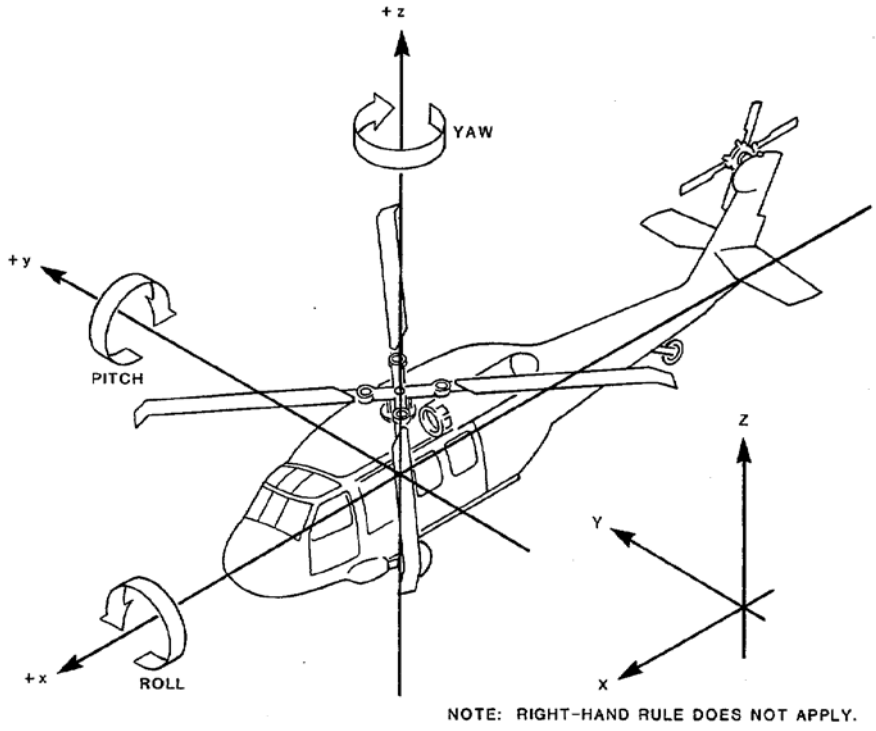

Figure 1. Axes and attitude angles in aircraft coordinate system

After establishing the component velocities and attitude angles in the aircraft reference frame, the peak deceleration forces (G-loads) were determined for each axis. The methods used were those described in "Summary of Equations of Motion for Several Pulse Shapes" [4] by Turnbow. For

terrain impacts, the reconstructions used engineering judgment for the pulse shape and the applicable Turnbow equations to convert the velocity change into a peak deceleration.

2.5 SCENARIOS

The mishaps in both of these studies cover a diverse range of circumstances. Consequently, grouping the mishaps into scenarios for analysis proved to be useful. These scenarios are consistent with those used in the RJ study. Scenario F, the most common scenario in both datasets, covers runway overruns following landing or following an aborted (while still on the ground) takeoff. These mishaps are characterized by relatively low velocities and low, idle-level, or reverse thrust from the engines. Scenario F includes both aborted takeoffs and poor, yet controlled, landings in which the aircraft remained on the runway until it exceeded the length boundary of the runway. Scenario G is characterized as "compromised landing with mild impact" and includes landings where a failure of some type occurred that damaged the aircraft, but the aircraft generally remained under control and on or near the runway. These mishaps include gear-up landings, landing-gear collapses, tail strikes, and landings hard enough to cause limited structural damage. These mishaps generally end with the aircraft on the runway. Tail strikes during takeoff are included in scenario G as the best fit in terms of outcome and kinematics. Scenario G was the second most common in the W–B dataset. Scenario H consists of impacting terrain short of the runway during an attempted approach or landing; these impacts are characterized by relatively low descent rates and moderate airspeeds. Scenario H mishaps may occur well away from the prepared area of the airport and, consequently, some impacts are into rough terrain. Scenario J covers hard landings that result in loss of control of the aircraft sufficient to cause excursion from the runway and severe damage to the aircraft. Scenario J was the second most common scenario in the N–B dataset. Scenario K is loss of control on takeoff due to contaminated wings, mismanaged engine failure, or a misconfigured aircraft. Scenario K includes misjudged and mishandled go-around attempts; the common characteristics in this scenario are the engines at high thrust and the intent to fly rather than to land. A decision to put the aircraft back on the ground beyond the bounds of the airport was considered a scenario K mishap.

Two new scenarios were created compared to those developed in the RJ study. These two new scenarios are variations on two already defined scenarios. In reading the older N–B and W–B mishaps, several investigations described wind shear or otherwise severe yet localized winds contributing to a poor landing or loss of control on takeoff. Scenario M is similar to scenario H with the addition of wind as a contributing influence. For many of the analyses in this report, scenarios H and M mishaps are combined into a single scenario because the outcome is essentially the same. The reason to identify the M events separately was a desire to reveal any trend related to wind-shear events. As with scenario K, in the N–B mishaps, several mishaps were influenced if not actually caused by wind shear. Consequently, scenario L was created to identify loss of control on takeoff with a strong effect of wind shear. As it happens, no usable scenario L events were found among the W–B mishaps.

2.6 POTENTIALLY SURVIVABLE CRASHES

The concept of a potentially survivable crash has evolved in the field of crashworthiness. A survivable crash (S) is defined to be a crash in which: 1) the occupied volumes of the aircraft are maintained (i.e., not crushed or even briefly compromised); and 2) the decelerations along all three

primary axes of a restrained occupant remain below the human tolerance for fatality. Crashes in which part of the occupied volume is compromised, and the part remains preserved, or in which a part of the aircraft experiences decelerations beyond human tolerance, are considered to be PS. A non-survivable (NS) mishap is one in which either no occupant volume remained anywhere in the aircraft or acceleration loads exceeded human tolerance throughout the aircraft. Note that this definition for survivability does not consider the actual injuries experienced in the crash. The usefulness of this concept lies in determining design requirements for occupant protection based on structural and kinematic parameters.

A survivability rating was assigned to each mishap. The damage data, primarily the loss of occupant volume, were reviewed, and each crash was assigned a rating of S, PS (some occupied volume was lost), or NS (all occupied volume was lost). If a particular area of a transport aircraft is crushed, then that volume can readily be considered as not livable space. One difficulty with assigning survivability to fixed-wing transport aircraft is the volume near fuselage breaks. If this localized volume were always considered to be NS, then in the W–B data, 15 crashes would be PS because 15 of the 29 mishaps have at least one fuselage break. Looking back to the W–B data, seven mishaps with one or more breaks were rated S rather than PS. A couple of these "breaks" were not complete open breaks, so that volume could have been survivable. This example is indicative of the judgment involved in rating the survivability of a given mishap. Although all of the mishaps were assigned a survivability rating, the analysis was conducted only on the scenario G–M mishaps.

2.7 DAMAGE METRIC

The general damage to the mishap aircraft is reported in each investigation report. Unfortunately, less information is generally provided at the level of detail needed for survivability considerations than would be desired. Two important considerations for survivability are the integrity of the occupant restraint load path (belt/seat/floor/structure) and the sustainment of a survivable volume for each occupant. Many reports, particularly more recent ones, made specific reference to the disruption of the floor and the integrity of the seats as observed after the crash. Both of these observations are critical to knowing the integrity of the restraint load path. For the occupant to be restrained through the duration of the crash, the seat must remain attached to the floor, and the floor must remain structurally sound. Severe disruption of the floor also interferes with evacuation.

In reviewing the report for each mishap, several descriptors for damage were recorded on the data worksheet. Damage information was recorded by segment of the fuselage. The five segments used were: the cockpit, the forward cabin, the overwing cabin, the aft cabin, and the tail. These segments were selected based on the observation that when aircraft break up, they often break at manufacturing joints or at "structural discontinuities." The segment labeled "cockpit" breaks away from the forward end of the uniform cross section, which is labeled "forward cabin." The flight attendant seat is usually, but not always, in the cockpit segment with the galley. The forward cabin often breaks away from the segment labeled "overwing cabin." The extent of the overwing section is taken to be the length of fuselage between the wing fairings. Structurally, this segment is defined by the wing box. The "rear cabin" is defined as the uniform cross-section segment from the end of the wing fairings back to the "tail," in which the tail is taken to begin at the point where the underbelly begins to slope upward rather than remain level. Each of the four joints had a cell in the datasheet and a Y (for yes) was recorded for each joint where a break was reported or could be

inferred to have occurred. Where a break did not occur, an N (for no) was recorded. The seat rows were assigned to each section on the basis of seat maps. If available, the seat map in the report was used; in the absence of a map in the report, the most relevant seat map that could be located on the Internet was used to assign seat rows to each segment. Very few aircraft had passenger seating in the tail, but some had flight attendant seating there. Consequently, a few injuries were recorded in the tail segment.

In addition to the fuselage breaks, the other damage descriptors were: underside skin and structural damage, floor disruption, seat failure, and loss of occupant volume. Considered the least direct threat to the occupants, damage to the underside skin of the aircraft was determined from photographs and descriptions in the investigation reports. The information in the investigation reports was supplemented by performing Internet searches for images of the wreckage. The damage severity for each aircraft segment was recorded as Widespread (W), Localized (L), or None (N). In a similar fashion, the floor disruption was recorded as W, L, or N based on photographs and descriptions in the reports. However, it should be noted that very few of the reports or Internet sources contained photographs of the aircraft interiors after the crash; therefore, most of the information on interior conditions came from the report's text. In addition to the investigation report section on damage, the condition of the interior was often referred to in the survivability or in the evacuation section. Similarly, for seat failures, the reports commented when there were seat failures and, in some cases, actually stated that seat failures had not occurred. In certain mishaps, the integrity of the seats could be inferred from the descriptions of the evacuation. Last, the loss of occupied volume was recorded as W, L, or N, based on external photos and information in the text of the reports.

To be able to describe or quantify the damage in each mishap in a single figure, the individual damage descriptors were combined into a more encompassing damage indicator, referred to as the damage metric. For this approach to the analysis, the different damage severities and types were weighted based on the influence of that damage for increasing the number of injuries. Therefore, the severity of the damage was given a weighting by assigning a multiplier of 2 for each segment containing that type of damage rated W, a multiplier of 1 for each segment rated L, and 0 for each segment rated N. The underside skin-damage values were weighted by a factor of 1; the floor disruption values were multiplied by 2; and the seat failure was multiplied by a factor of 3. The score for each segment in which loss of occupied volume occurred was multiplied by 4. Each fuselage segment that had a break at its forward end had 3 added to the segment score. The five terms were added up for each fuselage segment to create a damage metric value for the segment. Therefore, the damage to each segment of an aircraft was identified with a single value; by adding the values for each segment together, a single value for the aircraft could be obtained.

In some cases, a few cells were missing information, as indicated by NI (no information), which is counted as zero in the damage factor. By counting up the number of NI cells in each mishap, those mishaps whose damage metrics may be significantly affected by the absence of information could be identified. The effect of the missing cell was to reduce the value of the damage metric because NI was assigned a zero value. Several means for working around this missing data were considered, but none were deemed satisfactory. The number of cells containing no information is given in the two tables reporting the damage metric values. The total damage metric for these mishaps was lower than would have been recorded had all of the information been available.

2.8 BINARY LOGISTIC REGRESSION ANALYSIS

The binary logistic approach interprets injury data as having just one of two outcomes for each occupant: severe injury (fatal or serious—also referred to in this report as Fat+Ser) or minor/no injury. In this view, the expectation is that for each model parameter (i.e., regressor variable), the fraction of severe injuries will be low (near zero) for low values of the parameter, and the severe-injury fraction will increase to the limit value of one as the value of the parameter increases. For example, it is expected that the fraction of severe injuries will increase as the impact velocity increases. When the fitted model does not meet this expectation, it is likely because unaccounted for (i.e., not modeled) parameters/mishap conditions are affecting the severe-injury count. For example, one or more high-impact velocity mishaps in a scenario class may have very low severe injuries associated with them and if some mishap observations in the same scenario class have high severe-injury counts with lower impact velocities, it is likely the resultant model will not meet the aforementioned expectation. The equation that the regression fits assumes that the dependence on the parameter is a linear function. Therefore, the logistic equation being fitted is an exponential with a linear form to the exponent (referred to as the linear predictor). The output variable $\hat{p}$ is the estimated probability that an occupant is severely injured. The number of occupants on a similar mishap aircraft meeting the model parameters can be multiplied by the estimated probability of an occupant being severely injured to provide an estimated number of fatally and seriously injured occupants. For an *n* parameter (i.e., *n* regressor) model, the equation contains one constant and *n* coefficients.

The form of the equation eq. (1) is:

$$\hat{p} = \frac{1}{1+e^{-(\beta x)}} \tag{1}$$

Therefore, the linear form for a single parameter (i.e., with single regressor) of eq. (1) is:

$$\hat{p} = \frac{1}{1+e^{-(\beta_0+\beta_1 x_1)}} \tag{2}$$

The response variable for all modeling was the binary injury level of the occupants (Fat+Ser and minor/no injury). The event of interest for all modeling is the Fat+Ser injury events. Several kinematic variables were evaluated as candidate regressor variables. These include Airspeed (ft/sec), Vertical Velocity (ft/sec), Flight Path Angle (degrees), Pitch Angle (degrees), Peak Vertical Deceleration (Gz), and Peak Longitudinal Deceleration (Gx). The Peak Lateral Deceleration (Gy) was treated as the absolute value. The absolute values of the yaw and roll angles were taken and summed to create a parameter named Off-Nominal Angle. Each of these kinematic variables was modeled individually in an attempt to create usable single-regressor variable models. The same parameters were also combined as multiple-regressor variables to develop multi-parameter binary logistic regression models in an attempt to identify usable models for predicting injury fraction.

The software used to accomplish these binary logistic regression analyses was Minitab® Version 16. All statistical analysis and modeling was performed using a level of significance (α) of 0.10. Therefore, the confidence intervals (CIs) presented in the analysis are all 90 percent. The

interpretation of these 90 percent CIs is that in repeated aircraft crash instances that meet the general parameters and conditions for the cases analyzed (e.g., fixed-wing aircraft type, water impacts), 90 percent will result in an estimated probability of Fat+Ser injuries to occupants that falls within the indicated CI. The regression analysis includes hypotheses tests to determine if the constant and the regressor coefficient(s) have non-zero values. The software calculates a *p*-value, and if this *p*-value is <0.100, then the constant or the coefficient is likely non-zero. The software then calculates three goodness-of-fit statistics: Pearson, Deviance, and Hosmer-Lemeshow. These test statistics have resultant *p*-values, and *p*-values <0.100 indicate the resultant model is a poor fit. The Summary Measures of Association consist of three metrics that indicate the strength of the model's ability to accurately predict the Fat+Ser injury probability for new crash events that can be categorized in the same manner as those used to develop the model. The three metrics are the Somers' D, the Goodman-Kruskal Gamma, and Kendall's Tau-a. These three metrics vary in value typically from 0 to 1.0, with the larger values indicating stronger model predictive ability. Occasionally, one or more metrics may be negative. This happens when the number of concordant pairs is less than the number of discordant pairs. In this instance, the measures are indicating weak-model predictive ability. Metric values near zero indicate weak-model predictive ability. In this study, the summary measures of association have been converted to strength of model predictive capability based on the following ranges: 0–0.29 (including negative values) = Low; 0.30–0.75 = Medium; and 0.76–1.00 = High.

One additional evaluation of the binary logistic model (BLM) is made with regard to its prediction. This subjective evaluation by the author is whether the model predicts a slope (sign + or – of β_n), which is consistent with the author's intuitive expectation. Therefore, if a model predicts decreasing probabilities of severe injury with increasing impact velocities, that model would be labeled "counterintuitive."

3. W–B IMPACT STUDY

3.1 SELECTING MISHAPS FOR THE STUDY—W–B

The overall mishap-selection process and data-extraction process were described previously in section 2 of this report. The intent in this study is to analyze the mishaps of a particular class of aircraft rather than a particular type of mishap (such as ditching). The term W–B has no formal definition in the regulatory environment, but the term generally refers to aircraft with two lengthwise aisles rather than one. Aircraft with one aisle are also being studied and are referred to in this work as N–B aircraft. Rather than try to query the database by weight class or other database fields, a list of W–B aircraft was assembled (see table 1), and the CSTRG database was queried for each type on the list. Only western-built W–B aircraft were included because experience with the RJ study revealed that very few mishaps involving non-Western-built aircraft had thorough enough reports available to provide the information needed for this study. The series of W–B queries retrieved 273 candidate mishaps. Reviewing the summaries in the CSTRG reduced the list to 55 that appeared to be suitable to the study. Reading the reports and information on these 55 resulted in 29 mishaps being included in the study. The list of mishaps used in the W–B study is provided in appendix B.

Table 1. W–B aircraft types sought in the CSTRG database

A300	A380	DC10
A310	B747	L1011
A330	B767	MD11
A340	B777	
A350	B787	

One mishap, 19710730A, appears twice in the dataset, and the identifier is notated as –T and –L for takeoff and landing. In this mishap, a 747-100 took off from San Francisco International Airport (SFO) and struck its tail on the landing light array hard enough to cause aircraft damage and injuries to passengers. That portion of the mishap is designated 19710730A-T. After assessing damage and injuries, and dumping fuel, the aircraft crew returned to SFO rather than continue the trans-Pacific flight. On landing, the aircraft veered off the runway. Once the aircraft came to a halt, an emergency evacuation was conducted. This latter mishap is designated 19710730A-L.

3.2 ANALYSIS

This section describes the analysis of the data gathered regarding W–B mishaps and describes in detail the methods, results, and conclusions for the analysis.

3.2.1 Aircraft Population—W–B

Although a diverse population of aircraft was sought, ultimately the population studied consisted of those airplanes that have experienced mishaps of the type of interest and sufficiently well documented to provide the required information. The aircraft in the dataset are characterized by such design features as number of engines, location of engines, wing position, weight class, and seats per row. Tables 2–9 provide data characterizing the mishaps and the aircraft involved. Table 2 lists the specific aircraft types and the number involved in the study.

Tables 3–5 characterize the aircraft in the dataset in terms of aircraft design. All aircraft in this study were powered by non-propeller turbine engines. The database differentiates between turboprop and turbojet but does not differentiate high-bypass and low–bypass turbojet engines. The majority of aircraft in this study were in weight class E, greater than 400,000 lb (see table 3). Only two aircraft weighed less than 400,000 lb. The W–B aircraft had one of two engine configurations (see table 4)—either engines on wings or engines on wing plus one engine under the vertical stabilizer (referred to as “fin” for brevity). The 13 aircraft with the wing and fin configuration had three engines (see table 5); eight aircraft in the study had two engines, and eight aircraft had four engines. All of the aircraft in the W–B study were of the low-wing configuration.

Table 2. Aircraft type and quantity in W–B study

A330-200 (2)	B747-400 (2)	DC10-30 (3)
A340-300 (1)	B767 (1)	DC10-30CF (2)
B747-100 (2)	B767-300 (2)	L1011 (2)
B747-200 (2)	B777-200 (3)	L1011-385 (2)
B747-300 (1)	DC10-10 (3)	MD-11 (1)

Table 3. Weight category populations—W–B

Weight Category	Number of Aircraft in the Dataset
C (100,000–250,000 lb)	0
D (250,000–400,000 lb)	2
E (> 400,000 lb)	27

Table 4. Aircraft engine configuration—W–B

Engine Configuration	Number of Aircraft With Configuration
Engines on Wing	16
Engines on Wing & Fin	13

Table 5. Number of engines on aircraft—W–B

Number of Engines	Number of Aircraft in the Dataset
2	8
3	13
4	8

Being two-aisle aircraft, the W–B aircraft have more than six seats across. None of the aircraft in the W–B study overlapped with those in the N–B study that had a maximum of six seats across. All aircraft had a maximum number of seats across equal to at least seven, with nine seats across being the most common configuration (see table 6). The number of passenger seats is shown in table 7 with the number of people aboard. The “total people aboard” is from the database and includes crew members and infants. In the analysis, crew members were tracked separately from passengers in the dataset, and infants were not counted. The total of all occupants in the W–B study was 6902.

Table 6. Maximum seats per row—W–B

Total Seats per Row (Maximum)	Number of Aircraft
7	3
8	3
9	13
10	10

Table 7. Number of passenger seats—W–B

	Total Passenger Seats	Total People Aboard[†]
Average Number	310	238
Median Number	295	218
Greatest Number	428	410
Least Number	214	81

[†] Total people aboard includes passengers and crew.

The mishaps included in the study cover a range of scenarios and severity. These mishaps cover most phases of flight, although approach and landing predominate (see table 8). The study mishaps were all from the low-altitude phases of flight. Ten of the mishaps resulted in "substantial" damage, whereas 19 mishaps led to aircraft described as "destroyed." Fatalities occurred in 14 of the 29 mishaps, and serious injuries occurred in 23 of the 29 mishaps.

Table 8. Phase of flight—W–B

Phase of Flight	Number of Mishaps (No.)	Fraction of Mishaps (Percent)
Aborted Takeoff	2	7
Takeoff	4	14
Climb	0	0
Flight	1	3
Approach	5	17
Go-around	3	10
Landing	14	48
Total	29	100
Characterized as 'Overrun,' including both takeoff and landing. (counted above)	8	28

Injuries caused by the impact are the primary interest (see table 9). In many investigation reports, minor injury counts are combined with no-injury counts; consequently, these two counts are combined throughout the analysis for consistency. The distribution of injuries within the aircraft will be discussed later in the report. The injury numbers in this table are from the CSTRG database and count all aboard the aircraft, including children without seats.

Table 9. Overview severity of injuries—W–B

	Total Occupants/ Mishap	Total Fatalities/ Mishap	Total Severe Injuries/ Mishap	Total Minor-No Injury/ Mishap
Median	218	0	10	200
Average	238	41	20	177
Maximum	410	228	106	410
Minimum	81	0	0	0

An emergency evacuation was conducted in 19 of the 29 mishaps. If an evacuation did not occur, either there was no perceived danger of fire or the mishap was so catastrophic that the escape of the few survivors could not be characterized as an evacuation.

3.3 MISHAP SCENARIOS—W–B

The W–B mishaps cover a diverse range of circumstances. For this study, grouping the mishaps into scenarios for analysis proved to be useful. The 29 mishaps were classified into seven scenarios (see table 10). Detailed descriptions of each scenario are provided in section 2 of this report. Scenario F consists of runway overruns either following landing or following an aborted takeoff. Scenario F is one of the two more common scenarios within the W–B dataset (seven mishaps). The seven scenario G mishaps are characterized as "compromised landing with mild impact," and this scenario includes landings in which a failure of some type occurred that damaged the aircraft. The six scenario H mishaps include impacting terrain short of the runway during an attempted approach or landing; these impacts are characterized by relatively low descent rates and moderate airspeeds. The five scenario J mishaps were hard landings that resulted in loss of control of the aircraft sufficient to cause excursion from the runway and severe damage to the aircraft. Scenario K constitutes two loss-of-control-on-takeoff mishaps; these mishaps were due to such issues as a mismanaged engine failure or a misconfigured aircraft. Scenario K includes misjudged and mishandled go-around attempts, the common characteristic being the engines at high thrust and the intent to fly rather than to land. A decision to put the aircraft back on the ground beyond the bounds of the airport was considered a scenario K mishap rather than an overrun.

Table 10. Number of mishaps by scenario—W–B

Scenario	Number of W–B Mishaps (no.)	Fraction of W–B Mishaps (percent)
Scenario F—Runway overrun (landing or takeoff)	7	24
Scenario G—Compromised landing (mild, but damaging impact)	7	24
Scenario H—Impacted terrain short of runway (reduced speed and thrust during approach)	6	21
Scenario J—Hard landing with loss of control post-impact	5	17
Scenario K—Loss of control during or following takeoff or go-around attempt (includes wing contamination)	2	7
Scenario L—Loss of control on takeoff or go-around attempt worsened by wind influence	0	0
Scenario M—Impacted terrain short of runway due to wind influence	2	7
Total	29	100
Scenarios H+M	8	28
Scenarios K+L	2	7

Two new scenarios were created compared to those developed in the RJ study. These two new scenarios are variations on previously defined scenarios. Scenario M is similar to scenario H, landing short, with the addition of local wind influence as described in the investigation report. For many of the analyses in this report, the scenario H and M mishaps are combined into a single scenario H+M because the outcome is essentially the same. The W–B dataset contained no mishaps identified as belonging in scenario L.

To determine the extent to which the study sample of the W–B mishaps represented the frequency of each scenario in the population of all W–B mishaps, the larger sample of mishaps returned by the original query (273) was reviewed. The summary descriptions were read, and those mishaps with sufficient information were assigned to one of the scenarios. There were 47 mishaps that were of a suitable type for inclusion and could be assigned to a scenario. The remaining mishaps either had insufficient information or were not applicable to this study. The study sample tracked the larger sample (see table 11) well; this correlation indicated that the sample of mishaps analyzed was representative of the larger population of mishaps and, therefore, of the entire population of W–B mishaps.

Table 11. Number of mishaps by percent in each scenario—W–B

	29 Mishaps Studied in Detail (percent)	47 Mishaps From Query With Assignable Scenario (percent)
Scenario F—Runway overrun (landing or takeoff)	24	31
Scenario G—Compromised landing (mild impact)	24	29
Scenario H—Impacted terrain short of runway (during on approach)	21	18
Scenario J—Hard landing with loss of control post-impact	17	12
Scenario K—Loss of control during or following takeoff (includes wing contamination)	7	6
Scenario L—Loss of control on takeoff or go-around due to wind influence	0	0
Scenario M—Impacted terrain short of runway due to wind influence	7	4
	100	100
Scenario H+M	28	23
Scenario K+L	7	6

3.3.1 Mishap Kinematics Scenario G–M—W–B

The larger dataset of all mishaps excluding the overruns (22 mishaps identified as scenarios G–M) will be reviewed first, and then the individual scenarios will be analyzed. For the purpose of setting design guidelines and test conditions, knowledge of the larger set of data may be more beneficial. In this analysis, the data for scenarios G–M are grouped together. These scenarios have the common attribute that the impact occurred in the air or in the attempt to become airborne. Being airborne caused at least two factors to be different compared to the overrun scenario (F): 1) the velocity was generally higher, and 2) the attitude and velocity had an additional degree of freedom. The overrun scenario is analyzed in a later discussion, in which each scenario is reviewed separately.

The data are presented in several graphical ways to facilitate the reader's interpretation of where critical transitions may be occurring. In the following section, the kinematic data are presented as combined histogram frequency charts and as cumulative percentile charts. The histograms are created to show the number of mishaps that occurred within ranges or "bins" for each parameter. In the percentile distribution curves, the value for each mishap is ranked in ascending order and then assigned a percentile value based on the number of events. The percentile value for a particular mishap means that X percent of the events occurred at a lower value of the parameter than the value for a particular mishap. Therefore, the plot can be used to determine either where a mishap falls in the hierarchy of mishaps or, for a particular percentile, the corresponding parameter

value. In the Microsoft® Excel® version of the histogram plot, the bin is labeled with the highest value in the range of that bin. Therefore, the range for a given bin is from the label on the bin adjacent on the left side of the given bin to the label on the bin itself. In figure 2, the lowest bin contains all events with vertical velocity less than -40, and the second bin contains the mishaps with vertical velocity greater than -40 and less than or equal to -20.

The first kinematic parameter analysis is for the vertical velocity (see figure 2). Vertical velocity is normally positive for the downward direction, but one aircraft in the W–B study crashed inverted, and another impact occurred during takeoff and, therefore, had a negative vertical velocity. The red curve presents the cumulative percentile of crashes; 50 percent (11 mishaps from 10th percentile to 60th percentile) of these 22 mishaps have vertical velocities from 0 to 20 ft/s inclusive. All four of the mishaps in the bin labeled "0" in figure 2 are exactly zero.

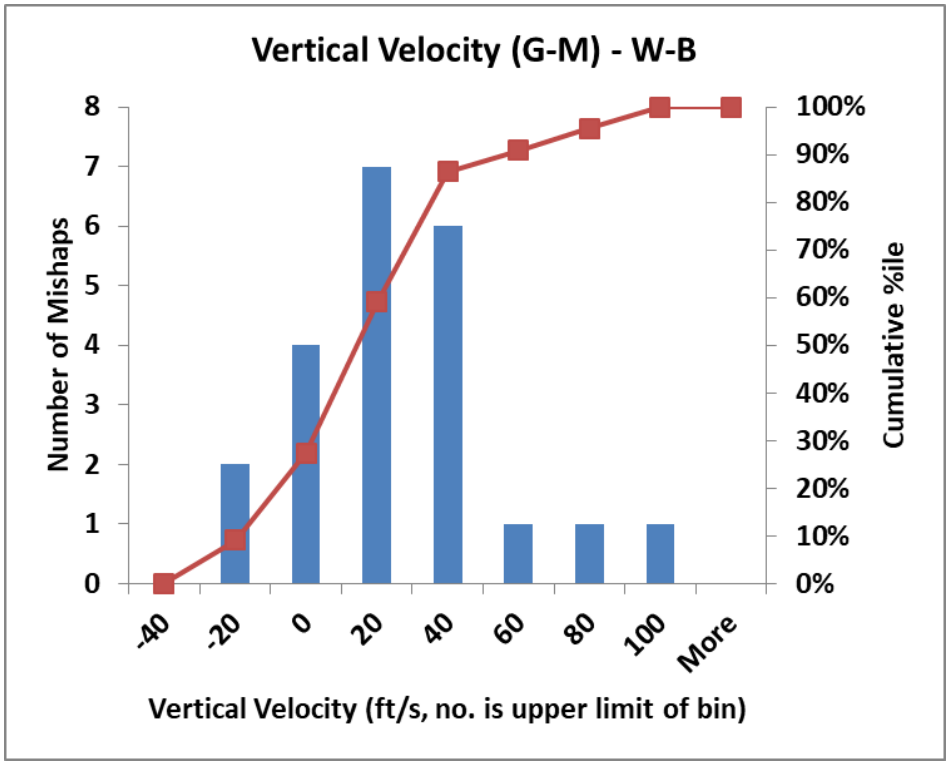

Figure 2. Vertical velocity distribution scenarios (G–M)—W–B

The airspeed is the velocity along the flight path; the data for scenarios G–M cover a wide range (see figure 3). The median and average values for airspeed both fall between 200 and 250 ft/s. The fact that these metrics are approximately equal is a confirmation that they represent the central tendency of the sample set. The one very low-velocity event occurred when an aircraft went off the runway late in the rollout and dropped into a water catchment area (therefore, not called an overrun but a loss of control after landing). The cumulative percentile curve, as does the median value, indicates that approximately 60 percent of the mishaps in the dataset had airspeeds of 250 ft/s or less.

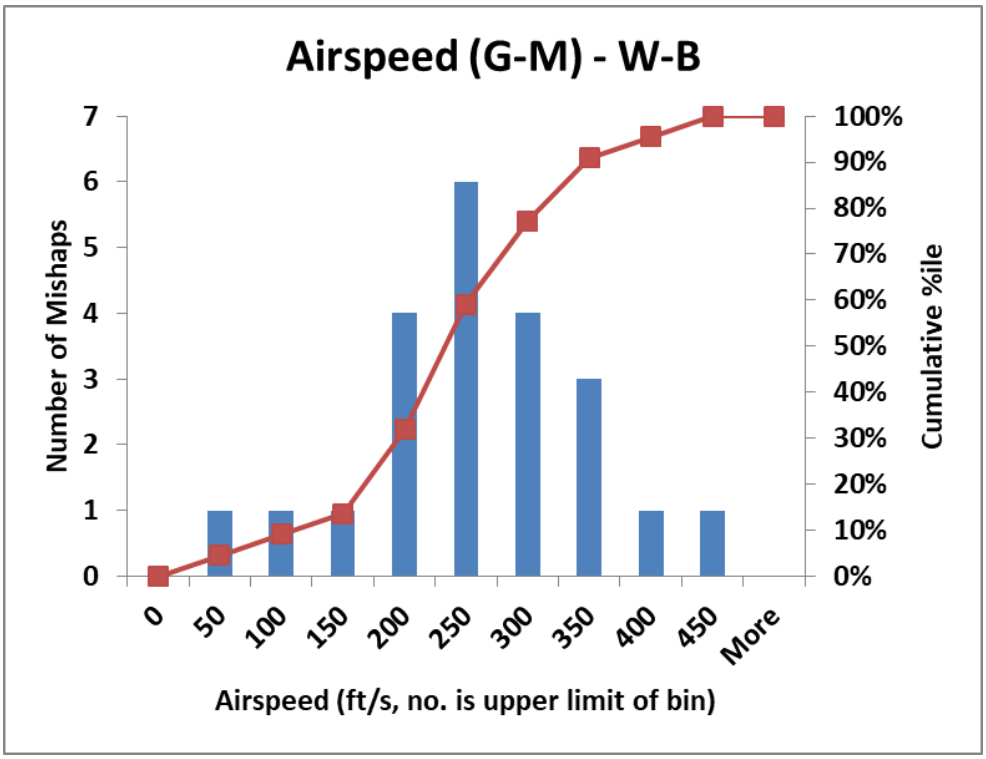

Figure 3. Airspeed distribution scenarios (G–M)—W–B

The flight-path angle is the angle between the path of the aircraft center of gravity and the horizon (see figure 4); descent is a negative angle. The flight-path angle can be estimated as the ratio between the airspeed and the vertical velocity (arcsine). The W–B dataset for scenarios G–M (see figure 5) contain just one positive value. The positive-value flight-path angle occurred as the result of a tail strike during takeoff. This mishap appears in the dataset twice (both as scenario G) because there was also a hard landing with damage on return to the airport.

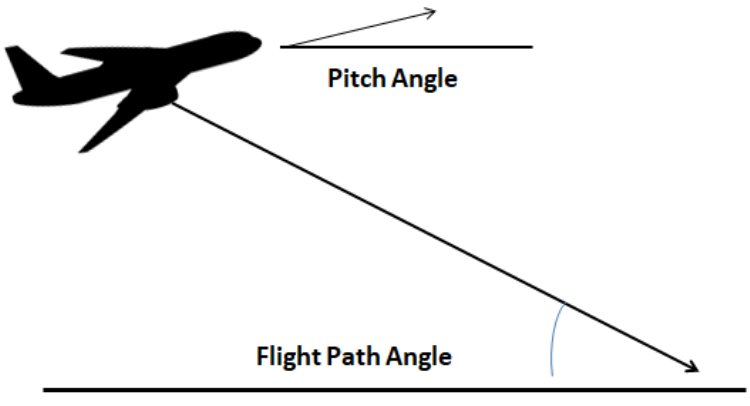

Figure 4. Flight-path and pitch-angle relationship

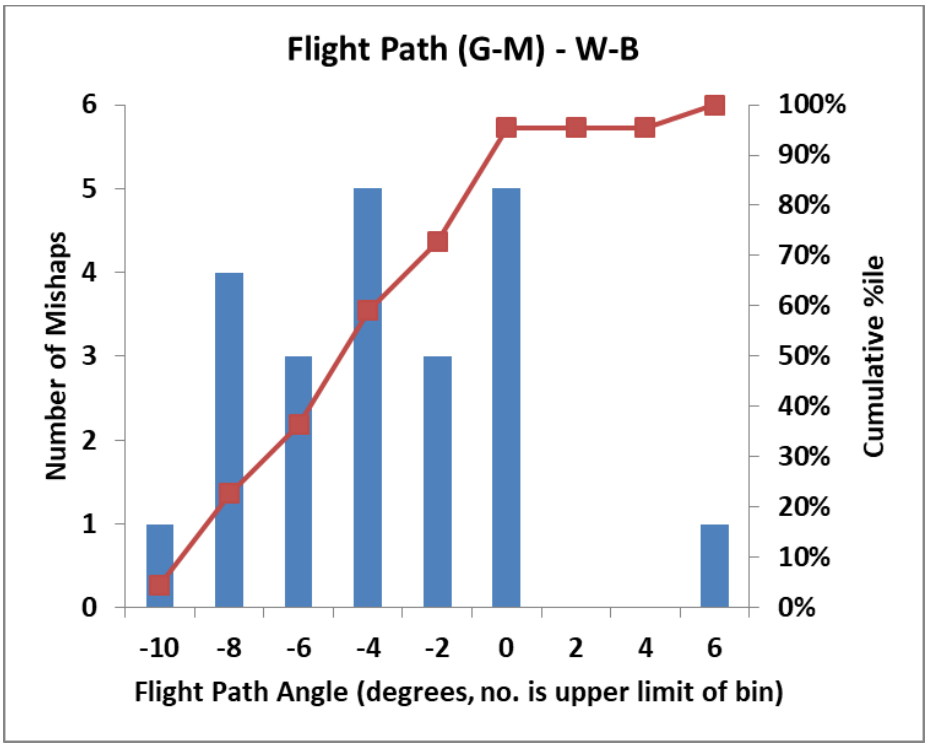

Figure 5. Flight-path angle distribution scenarios (G–M)—W–B

The pitch angle is the angle between the longitudinal axis of the aircraft and the horizon; nose-up is positive pitch angle. The pitch-angle chart (see figure 6) shows that, of the 22 mishaps, 1 impacted with the nose down (negative pitch) more than 8 degrees. The seven mishaps between -4 and 0 degrees consisted of one mishap with a pitch of -3 degrees and the other six mishaps with pitch angles of 0 degrees. Therefore, the most common pitch attitude was in the range -4 through 0 degrees with seven mishaps.

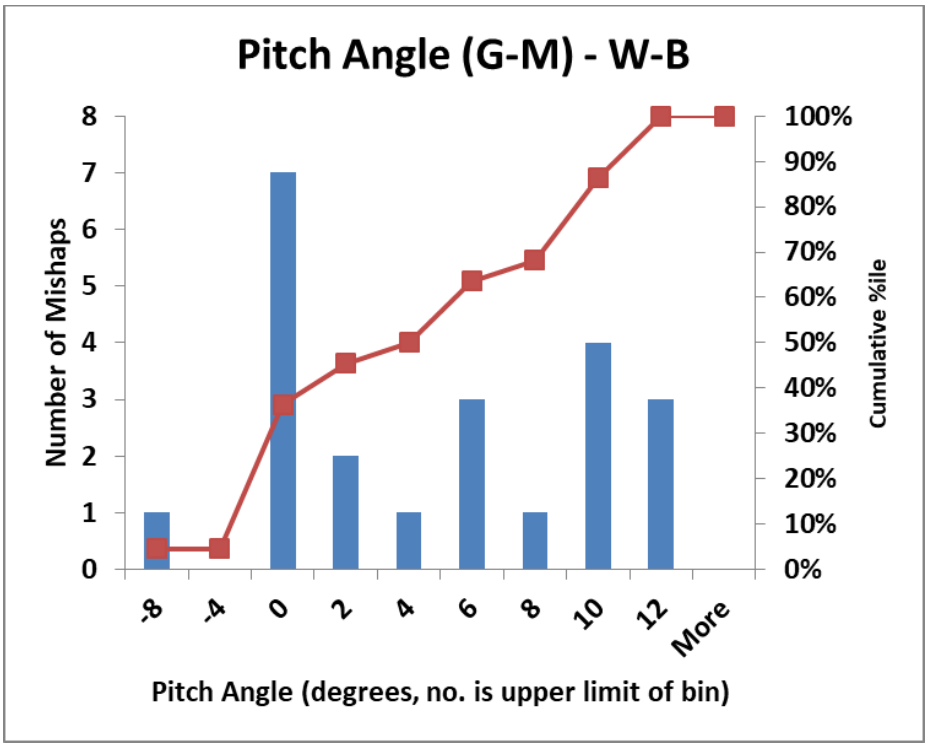

Figure 6. Pitch-angle distribution scenarios (G–M)—W–B

The roll angle (see figure 7) and yaw angle (see figure 8) at impact in many of these mishaps are very near neutral values because the aircraft impacts from controlled flight. However, in scenario K, in which control of the aircraft is sometimes lost, more extreme values of these two angles were recorded. It is readily apparent that approximately half of the G–M events occurred with the roll and yaw angles at the normal near-zero value. The absolute values are plotted considering the symmetry of the airplane. The important quantity is the magnitude of deviation from nominal attitude; the effect on the airframe presumably will be equal, regardless of which side is affected. The extreme values generally indicate a scenario K event.

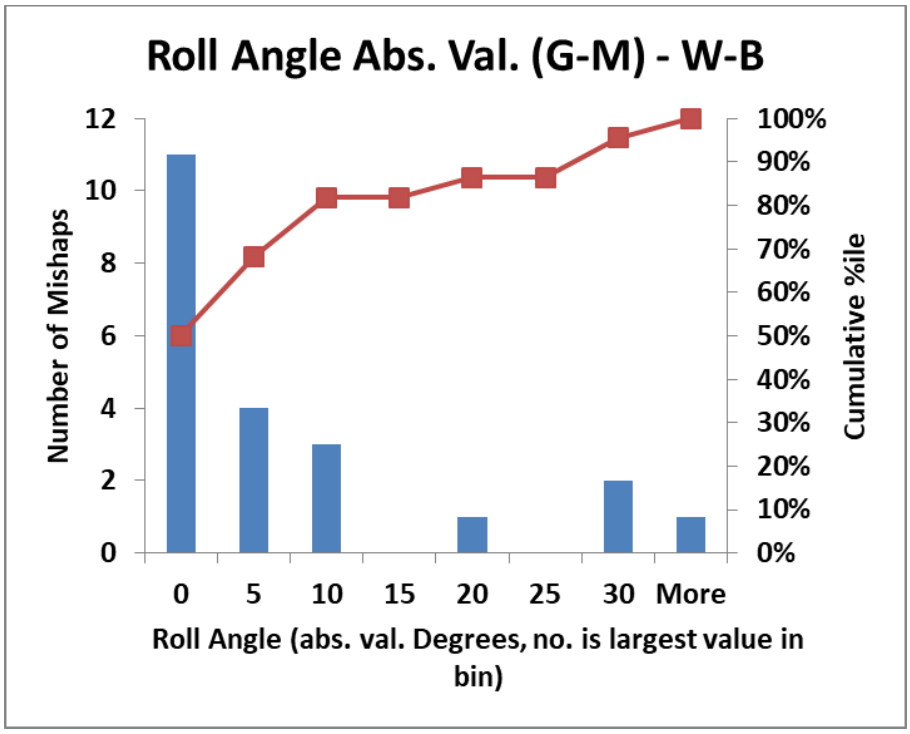

Figure 7. Roll-angle absolute-value distribution scenarios (G–M)—W–B

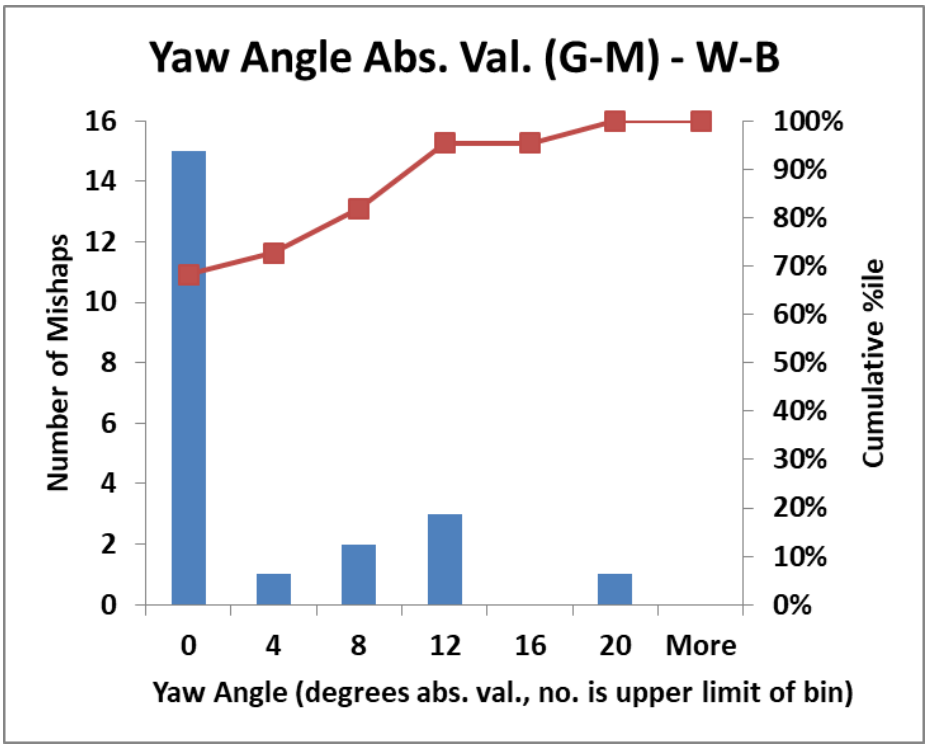

Figure 8. Yaw-angle absolute-value distribution scenarios (G–M)—W–B

Because there were few values different from zero for both roll and yaw, and considering that both of these angles are symmetric left and right, it was decided to combine them into a single parameter identified as the "off-nominal angle." This combined angle reduces the number of parameters for which to create single-parameter models. This value is calculated by adding the absolute value of roll angle and the yaw angle. The distribution of occurrences for this new parameter is shown in figure 9. The dominate value remains 0 with 9 of 22 mishaps having 0 off-nominal angles. Nearly 80 percent of the mishaps had a value less than 10 degrees.

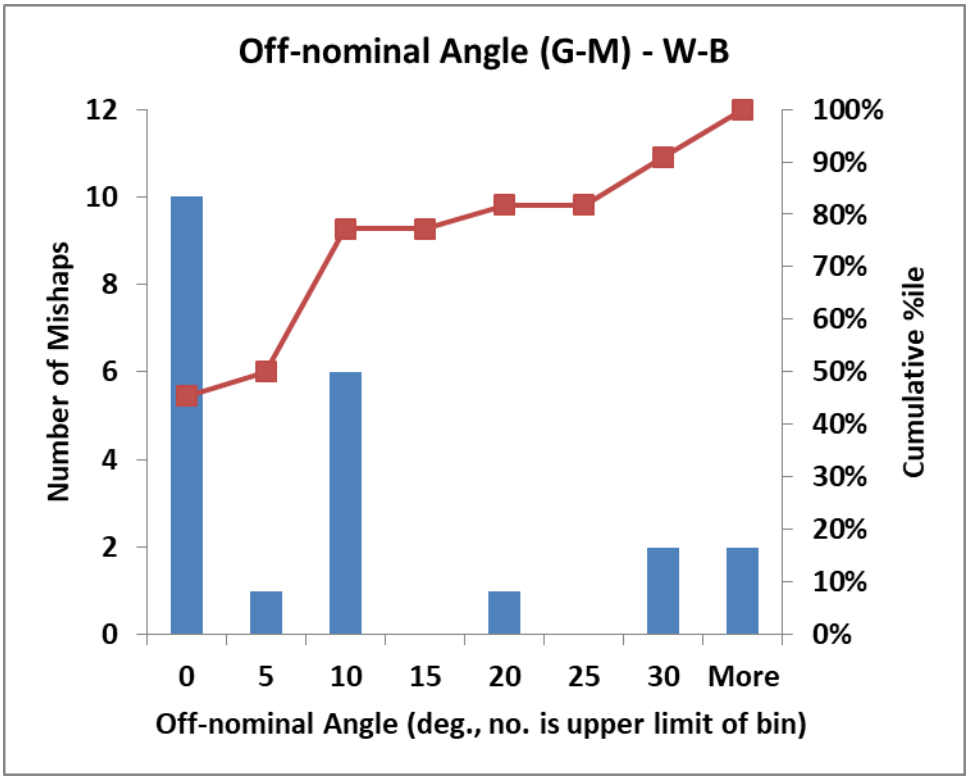

Figure 9. Off-nominal angle-distribution scenarios (G–M)—W–B

Most of the acceleration force values used in this study were estimated by aircraft impact reconstructions. The vertical acceleration (also referred to as "normal acceleration" in several reports) was recorded in a few aircraft. However, in those cases in which the acceleration was recorded, the recording frequency normally used for flight data was too low to capture the acceleration details in a crash event. As can be seen in the peak vertical deceleration histogram (see figure 10), the peak vertical deceleration was between 0 and 10 G in 16 of the 22 mishaps (three mishaps recorded zero vertical deceleration; eight recorded between 0 and 5 G vertical deceleration; and five recorded between 5 and 10 G vertical deceleration). Four mishaps exceeded 10 G vertical deceleration, and two events recorded negative decelerations because of inverted attitude. Two mishaps resulted in inverted impact (negative values) for the survivable segments of the aircraft.

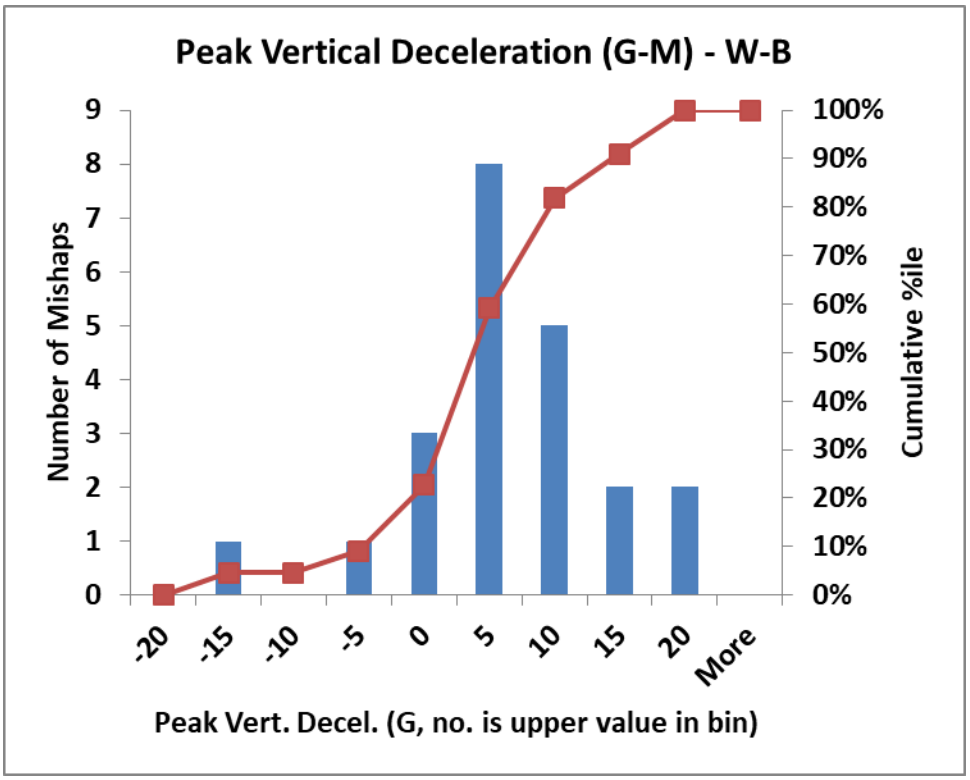

Figure 10. Peak vertical deceleration distribution scenarios (G–M)—W–B

For peak deceleration, greater negative values represent more severe crashes; therefore, the cumulative percentile chart has negative values increasing to the right. Rather than present a full histogram chart for the peak longitudinal deceleration histogram, a simple cumulative percentile chart is provided (see figure 11). The data indicate that most (approximately 68 percent) of the mishaps experienced deceleration forces under 5 G, and two mishaps recorded zero deceleration. The low deceleration levels reflect the long distances over which these large aircraft are generally brought to rest. The few mishaps, in which the longitudinal deceleration is high (large negative values), represent events for which the aircraft strongly interacted with the terrain or an obstacle such as a building. In events in which only the landing gear interacted, such as striking shallow ditches or less substantial vertical obstacles, the resulting deceleration on the aircraft was relatively modest. In this study and the N–B study, a new field was added to the damage worksheet to track how many of the mishaps involved the aircraft striking a vertical obstacle. Any obstacle with a vertical dimension equal or greater than the radius of the nose wheel was considered an obstacle regardless of its mass relative to the aircraft. Therefore, low-mass structures, such as light arrays, antennas, and fences, were included with sharp terrain discontinuities, trees, and buildings. Of the 22 scenario (G–M)—W–B mishaps, 8 involved interaction with a vertical obstacle. For the scenario (G–M) mishaps, the presence of a vertical impediment raised the magnitude of the average peak longitudinal deceleration from -4.2 to -9.5 G. The corresponding difference in average peak longitudinal deceleration for the runway overruns (scenario F) is -8.3 G for an impact involving an obstacle (four mishaps) compared to -0.8 G for the mishaps without an obstacle (three mishaps).

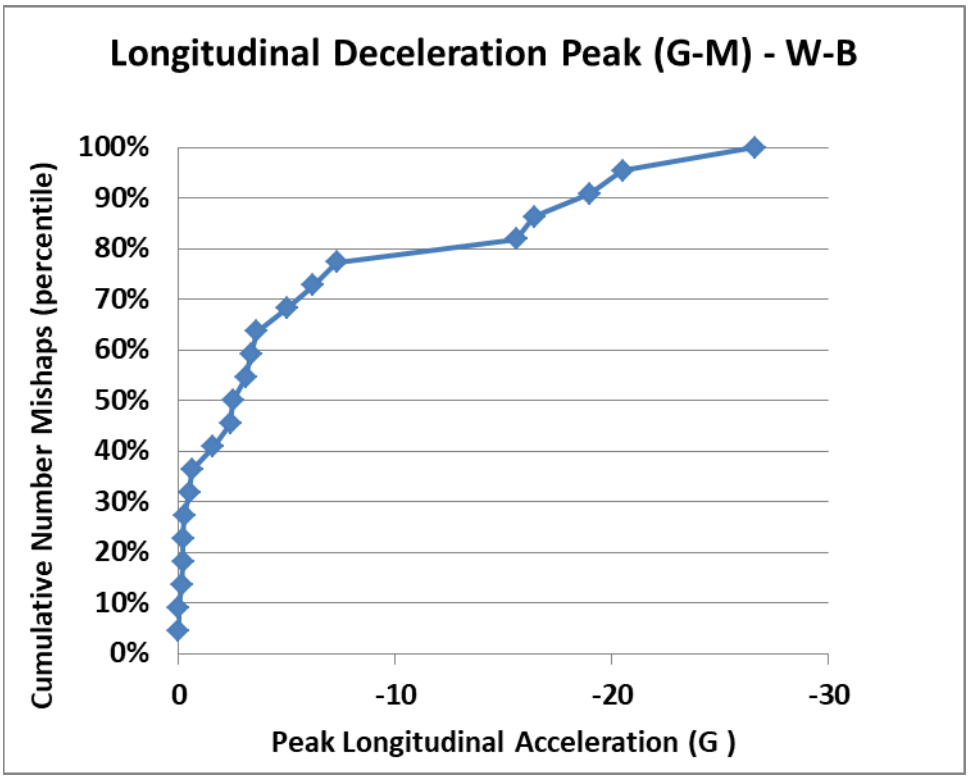

Figure 11. Peak longitudinal deceleration distribution scenarios (G–M)—W–B

The absolute value of the peak lateral deceleration is generally non-zero only when the roll or yaw angles have deviated from 0 degrees. As was seen previously in the angle charts, relatively few of the mishaps occur at extreme angles, and that fact is reflected in lateral deceleration values (see figure 12). Only 3 of the 21 mishaps experienced lateral deceleration greater than 5 G.

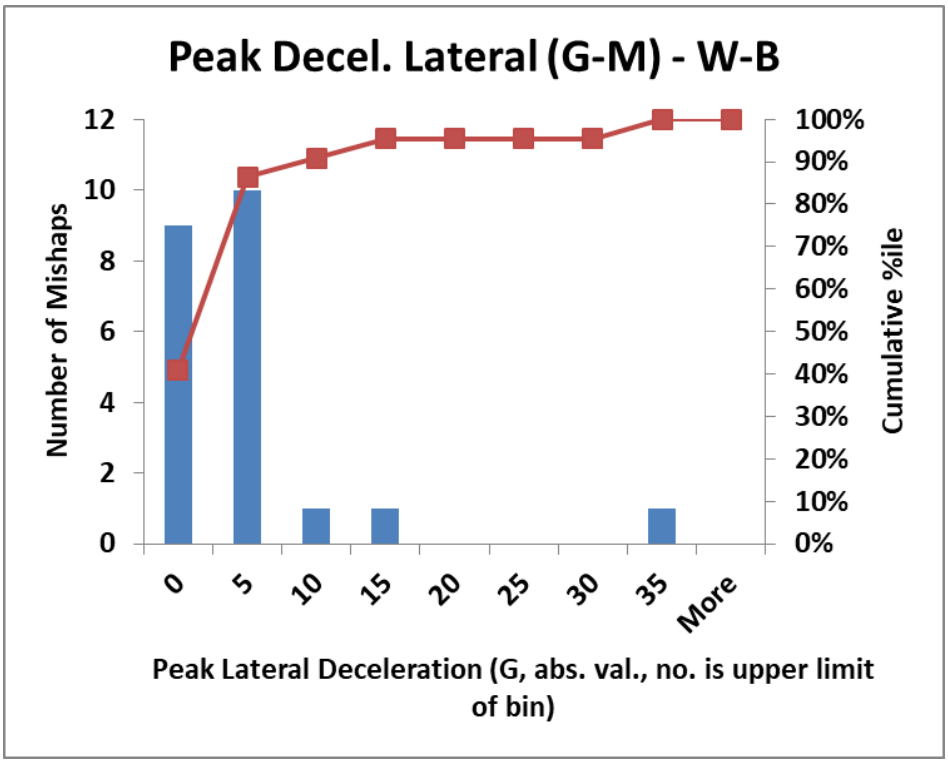

Figure 12. Peak lateral deceleration absolute-value distribution scenarios (G–M)—W–B

3.3.1.1 Velocities for Survivable Crashes—W–B

The basis for identifying the crashes as S, PS, and NS is discussed in section 2.6 of this report. The runway overrun mishaps (scenario F) are excluded from this analysis because there is generally just the longitudinal velocity, and the nature of the impacts are different from the impacts in which the aircraft was airborne.

The scenarios (G–M)—W–B dataset includes 22 mishaps: 4 mishaps were NS, four mishaps were PS, and the remaining 14 mishaps were S. Three of six mishaps within scenario H were identified as NS and one of two within scenario K was identified as NS. Three of the four PS mishaps were in scenario J, whereas the fourth was in scenario H+M. Looking only at the vertical velocity (see figure 13), two of the mishaps had inverted impacts (i.e., the vertical velocity was negative); both of these mishaps were in the S category. The 90th percentile[†] is marked with a reference line. The corresponding plot for airspeed is shown in figure 14.

[†] The 90th percentile is selected only as a convenient reference point; there is no technical nor regulatory reason for its selection.

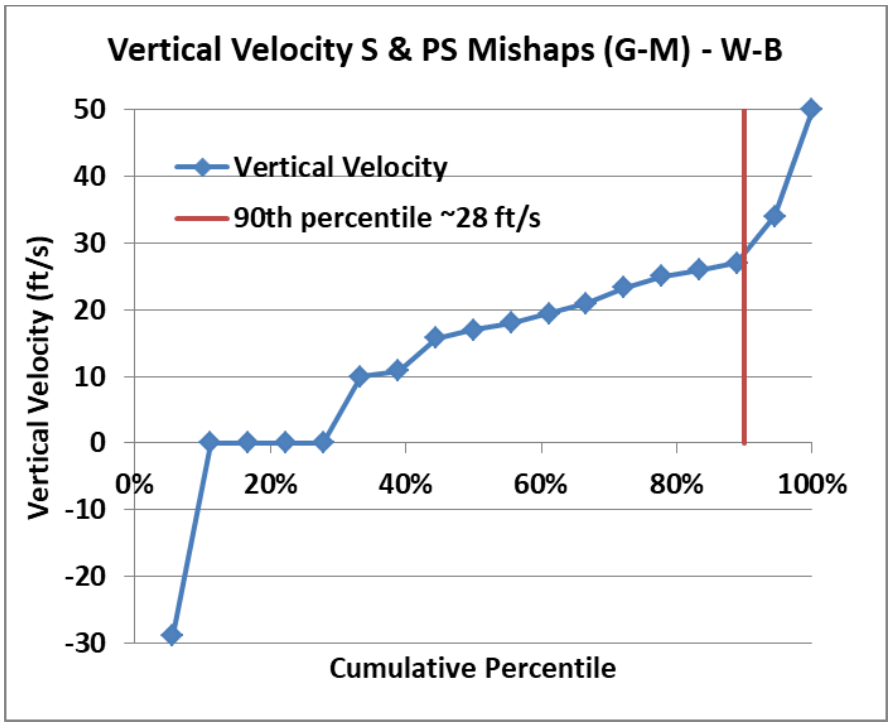

Figure 13. Vertical velocity for S and PS mishaps scenarios (G–M)—W–B

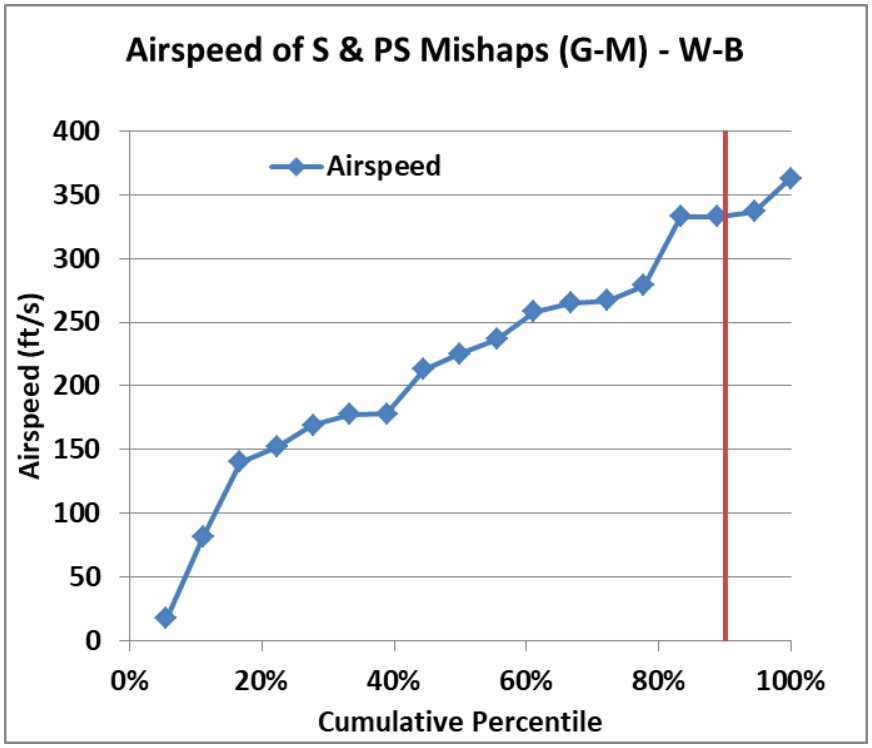

Figure 14. Airspeed for S and PS mishaps scenarios (G–M)—W–B

The 90th-percentile velocity was chosen as a reference velocity for creating a two-velocity plot (see figure 15) to show how the two primary velocities interact in mishap outcome. For each mishap, the airspeed is plotted as the *X* value, and the negative of the vertical velocity is plotted as the *Y* value. The sign of the vertical velocity is reversed because the resulting plot is more intuitive. The 90th-percentile curve is created just as the vector magnitude would be created, the square root of the "airspeed squared plus the vertical velocity squared." The result is the equation of an ellipse in which the *X* intercept is the 90th-percentile airspeed, and the *Y* intercept is the 90th-percentile vertical velocity. Three of the four NS crashes fall outside the 90th-percentile curve, as do four of the six PS mishaps. A first impression is that too many mishaps fall outside the 90th-percentile ellipse. However, looking back to the determination of the two 90th-percentile values (see figures 13–14), there are two mishaps on each curve greater than the 90th percentile and one mishap nearly on the 90th-percentile value. For the airspeed, there are actually three mishaps with nearly the same value as the 90th percentile. In both figures 13 and 14, the NS crashes are excluded in determining the 90th percentile; it is not surprising that the NS mishaps would be beyond the ellipse shown in figure 15. Looking only at airspeed, three values are approximately equal to the 90th percentile and one is beyond, as shown in figure 15. For the vertical velocity, one mishap is approximately equal to the 90th-percentile vertical velocity, and two are clearly beyond it.

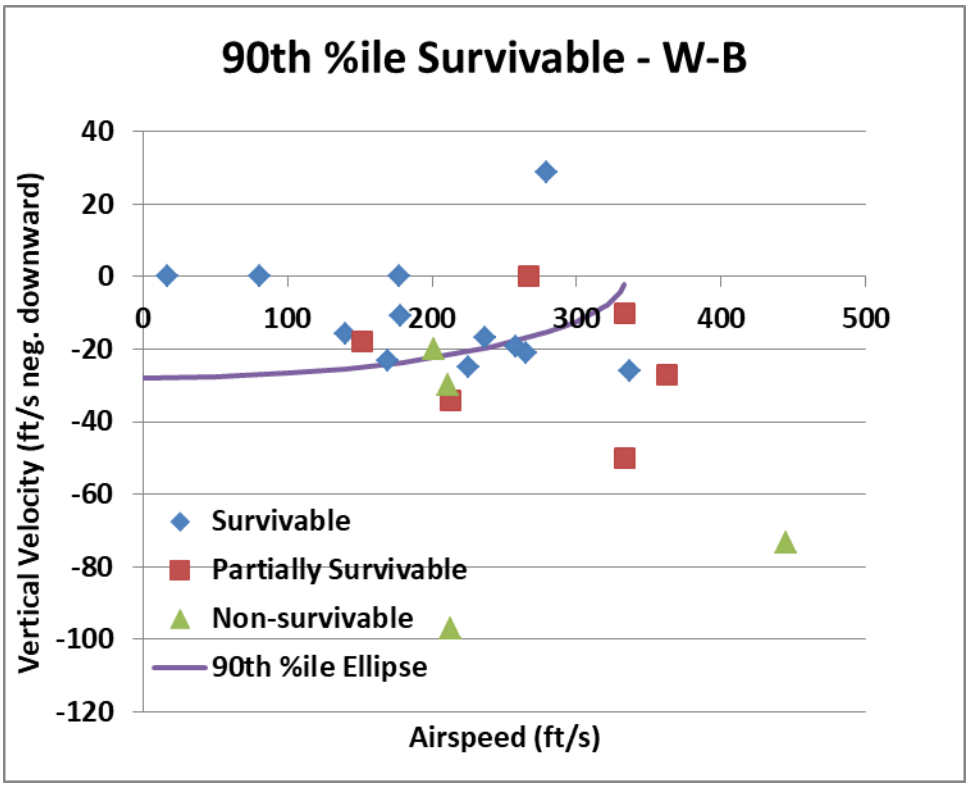

Figure 15. 90th-percentile survivable velocities for scenarios (G–M)—W–B

3.3.2 Kinematics of Each Mishap Scenario—W–B

The kinematic characteristics of the different scenarios are generally consistent with the nature of the scenario. The runway overruns (F) have a lower airspeed (longitudinal velocity) than the other scenarios (see table 12). A few of these events had a vertical velocity component in the impact due

to the terrain dropping off, ditches, or ravines. Both the median airspeed and the median longitudinal deceleration for scenario F have generally lower values than the other scenarios. The lower median longitudinal deceleration is likely a direct consequence of the lower airspeed and, therefore, the lower kinetic energy to be dissipated.

Table 12. Kinematics by scenario—W–B

Scenario {# of events in scenario}	Vertical Velocity Med./Avg. (ft/s)	Airspeed Med./Avg. (ft/s)	Flight Path Angle Med./Avg. (deg.)	Pitch Angle Med./ Avg. (deg.)	Vert. Accel. Med./ Avg. (G)	Long. Accel. Med./ Avg. (G)
F Runway overrun {7}	0.0/-2.2	118/156	0.0/0.4	0.0/0.0	1.0/2.9	-1.5/-5.1
G Compromised landing, no impact {7}	15.8/7.1	225/201	0.0/-1.6	5.4/5.4	2.0/2.3	-0.2/-0.2
H Impact terrain, short{6}	26.7/38.5	206/218	-8.0/-10.2	8.5/6.7	8.4/5.2	-16.0/ -12.6
J Hard landing, lose control {5}	26.0/21.0	213/216	-4.4/-4.4	2.0/1.2	2.0/0.9	-3.1/-3.1
K Loss of control takeoff {2}	36.7/36.7	356/356	-4.8/-4.8	0/0	10.0/ 10.0	-6.2/-6.2
L Loss of control takeoff due to weather influence (K influenced by weather) {0}	–	–	–	–	–	–
M Loss of control landing due to weather influence. (H influenced by weather) {2}	14.8†/14.8	296/296	-3.3/-3.3	4.3/4.3	8.3/8.3	-15.1/ -15.1
H + M Similar mishaps regardless of influence {8}	21.7/32.6	212/237	-6.8/-8.5	6.7/6.1	8.4/6.0	-16.0/ -13.2
G–M inclusive {22}	19.8/22.2	219/232	-4.5/-5.0	4.3/4.2	3.3/4.0	-2.8/-6.1

† Excel calculates the average value for the median of two values.

Scenario G, the compromised landing scenario, is characterized by some deficiency in the landing preparation or the aircraft, which leads to a poor landing outcome. Consequently, the kinematics (see table 12) approximate the kinematics of a near-normal landing. This scenario includes a tail strike that occurs during a go-around, a tail strike during landing, a brief runway excursion during roll-out following a crosswind landing, and a runway excursion and hard landings on the runway that result in structural damage.

The impacted terrain short scenario (H) involves the aircraft impacting the terrain short of the runway. Although airspeeds (see table 12) in this scenario are similar to those for scenario G, the vertical velocity at impact is generally higher. Because the terrain is not a runway, the outcomes are far less favorable in terms of damage and injury as will be discussed later.

The hard landings, loss-of-control scenario (J) exhibits airspeeds comparable to those of scenario H, reflecting the fact that the aircraft is likely not in a stabilized approach or some difficulty has arisen; the difference being that the aircraft remained airborne beyond the runway threshold. The average vertical velocities (see table 12) associated with scenario J are lower than those for scenario H. The average peak vertical deceleration for scenario J is also lower than for scenario H. In many scenario J mishaps, the vertical velocity was beyond the capability of the landing gear.

The W–B dataset incorporated only two scenario K mishaps—1) a failed go-around, and 2) an obstructed runway. In the RJ study [1], this scenario involved mishaps caused by wing contamination, but none of the W–B mishap investigations cited wing contamination. An aspect consistent with the RJ study is that the two impacts were catastrophic. The first was caused by a severe impact attitude resulting from a failed go-around, and the second was a collision with concrete barriers and heavy construction equipment on an obstructed (closed) runway.

The W–B dataset contained no scenario L mishaps in which loss of control on takeoff was associated with wind shear.

Two mishaps within the W–B dataset were assigned to scenario M. In these two mishaps, the aircraft was "knocked down" by wind shear short of the runway on what was otherwise a stabilized approach. The vertical velocity in one case was very high (19.5 ft/s) with a moderately high airspeed (258 ft/s); this impact occurred just short of the threshold, resulting in the aircraft colliding with the landing light structure. In the other mishap, the aircraft was still more than 1 mile from the threshold and in severe weather. The vertical velocity at impact was estimated to be 10 ft/s, but combined with a high airspeed of 333 ft/s.

3.3.3 Quantifying Damage—W–B

The definition and construction of the damage metric is presented section 2 of this report. This metric is the same definition used for the RJ study and is the same used for the N–B study later in this report. The five fuselage segments are:

- Cockpit
- Forward cabin
- Overwing cabin
- Aft cabin
- Tail

For the purposes of this study, the tail is defined to begin at the station where the uniform cross section of the fuselage ends and the lower surface of the fuselage slopes upward. The damage modes recorded in the analysis workbook are: underside fuselage damage, floor disruption, seat failure, fuselage breaks, and loss of occupied volume. The information in the database was supplemented by text from the investigation report and by photographs both in the report and found on the Internet. To record the severity of occurrence for each mode of damage in each segment of the aircraft, a cell for each segment and each damage mode was populated with: "none," "local," or "widespread." These values were weighted and accumulated to form the damage metric for each segment (see table 13). The damage for the W–B mishaps was thoroughly reported; only two

mishaps had any missing information. The worst of these was missing eight of 24 cells. The effect of any missing cell is to reduce the value of the damage metric because no information (NI) is assigned a zero value. Several methods for working around these missing data were considered, but none were deemed satisfactory. For the benefit of the reader, the column on the right (see table 13) lists the number of cells containing no information; the total damage metric for these mishaps will be lower than would have been recorded had all of the information been available.

Table 13. Damage metric for each mishap by segment—W–B

Reference # ID	Scenario (F–M)	Cockpit Damage Metric	Fwd Cabin Damage Metric	OW Cabin Damage Metric	Rr Cabin Damage Metric	Tail Damage Metric	Total Damage Metric	# of NI
20050802A	F	12	2	5	7	10	36	0
20001224A	F	0	0	0	0	0	0	0
19990923A	F	1	1	0	0	0	2	0
19960613A	F	10	7	7	10	5	39	0
19920730A	F	12	5	0	0	0	17	0
19820913A	F	1	0	1	1	0	3	0
19780301A	F	0	0	0	0	0	0	0
19710730A-T	G	0	0	1	6	1	8	0
20140620A	G	0	0	0	0	2	2	0
20120331A	G	0	0	0	0	1	1	0
20090420B	G	0	0	0	0	0	0	0
19930414A	G	2	4	1	3	0	10	0
19900324A	G	0	0	0	0	0	0	0
19710730A-L	G	0	0	1	6	0	7	0
20130706A	H	2	2	7	12	15	38	0
20080117A	H	1	2	2	4	1	10	0
20020415A	H	20	23	23	23	23	112	0
19970806A	H	20	19	19	23	23	104	0
19831127A	H	20	23	23	23	23	112	0
19721229A	H	10	13	16	16	16	71	0
19850802A	M	20	26	23	14	14	97	0
19731217A	M	0	0	2	14	10	26	0
20010824C	J	0	0	0	0	0	0	0
20001105A	J	2	2	1	0	0	5	0
19990822A	J	11	14	10	9	6	50	0
19921221A	J	6	11	13	2	2	34	8
19890719A	J	8	19	20	26	20	93	0
20100512A	K	20	23	23	23	23	112	0
20001031B	K	8	8	8	11	4	39	3

Each fuselage break (see table 14) that occurred was entered as damage to the segment on the aft side of the break. This choice was based on the observation that injuries related to a break tend to occur in the seats behind the break rather than ahead of the break. This insight is based on generalizing from those investigation reports in which detailed injury maps were provided. Unlike the RJ and N–B mishaps, several breaks in the W–B mishaps occurred away from the structural interfaces or assembly joints of the aircraft. Mid-segment breaks in the forward and aft cabins were recorded in separate fields for W–B mishaps. The formula for calculating the damage metric was

modified to count these mid-segment breaks. However, a limit of four breaks was placed on each aircraft; therefore, even in the event an aircraft was completely destroyed, only four fuselage breaks are counted. Therefore, the maximum damage metric remains 112.

Table 14. Number of fuselage breaks by scenario

	Number of Fuselage Breaks in Scenario	Fuselage Breaks/Mishap
Scenario F, Overruns (7 events)	4	0.57
Scenario G, Compromised Landing (7 events)	2	0.29
Scenario H+M, Short of Runway (8 events)	21	2.6
Scenario J, Hard Landing, Lost Control (5 events)	6	1.2
Scenario K, Lost Control during T-O (2 events)	6	3.0
Scenarios G–M (22 events)	35	1.6

The frequency of breaks (expressed as number of breaks per mishap) for each scenario is consistent with the nature of the scenario. The least-severe scenario (G) in which the aircraft remains on the prepared area of the airport has the lowest number of breaks per mishap. For scenario F, in which the aircraft travels beyond the prepared area of the airport and is more likely to strike an obstacle or change elevation, the number of breaks per mishap nearly doubles. For the two most severe scenarios (landing short of the runway and loss of control on takeoff or climb out), the number of breaks per mishap averages greater than one.

It may also be useful to identify in which segments the various forms of damage occur (see table 15). Damage to the underside skin depends on the angle of impact and the integrity of the landing gear after the impact, but in table 15, the underside damage is seen to be evenly distributed along the fuselage. Of 29 mishaps, 22 experienced at least one landing-gear failure. Floor disruption occurs most frequently in the rear cabin. Considering the front of the aircraft frequently encounters a vertical obstacle in the more violent scenarios, one might expect floor disruption to be more frequent in the cockpit and the forward cabin. In as much as the overwing segment is structurally the most robust, less frequent floor disruption might also be expected in this segment. The seat failures generally reflect the floor disruptions, although the cockpit has a markedly lower frequency of seat failures despite more frequent floor disruption. Cockpit seats are built robustly to allow for adjustment, and they are anchored individually to the floor. The loss of occupant volume shows a slow but steady decrease from the front to the rear. If anything, one might have expected this decrease to be more pronounced than it is. It might also be expected that more breaks would occur between the forward fuselage and the overwing segment rather than between the rear fuselage and the overwing segment.

Table 15. Number and type of damage occurrence for each segment—W–B

All Mishaps (29)	Cockpit (# of Mishaps)	Forward Cabin (# of Mishaps)	Overwing Cabin (# of Mishaps)	Rear Cabin (# of Mishaps)	Tail (# of Mishaps)
Underside Skin Damage	19	18	19	17	18
Floor Disruption	12	11	12	16	12
Seat Failure	7	10	10	14	10
Loss of Occupant Volume	11	11	10	9	8
Breaks	NA	9	8	12	8

Three mishaps were characterized by the maximum damage metric of 112. In the B747 crash short (scenario H) at Madrid, the fuselage was torn apart with very little, if any, survivable volume. The largest single piece of debris was around the wing box and landing gear structure, but the fuselage above the floor was mostly torn away. Similarly, the B767 that struck a hill short of Pusan was a scenario H. The only recognizable portions of the debris were the empennage, the wings, and one small portion of the rear cabin. The A330 that crashed during an attempted go-around (scenario K) in Tripoli tore itself apart sliding along the ground beyond the initial impact. The fatalities reported were due to trauma, and there was only one survivor. The B747 that impacted short against Nimitz Hill on Guam was torn apart with only a fraction of cabin volume remaining intact. This scenario H mishap's damage metric was 104 because of the preservation of some cabin volume in the forward and overwing segments.

Subdividing the damage metric data into segments and scenarios (see table 16), scenario H+M and scenario K are seen to result in far more damage than the two low-damage scenarios, with scenario J falling in between. To understand why three scenarios have much higher damage metrics than the other two, the kinematics of the scenarios should be considered. The damage metric tends to be higher when velocities and peak decelerations are also high (see table 17). The scenarios are ordered from highest damage metric to lowest. A second consideration comes into play, as evidenced by the very low average damage metric for scenario G despite relatively high velocities. In scenario G, the deceleration values are low, and these low values may be because most scenario G mishaps are stable approaches and end with the aircraft remaining on the airfield. Consequently, the aircraft does not encounter obstacles during its deceleration. Comparing the damage metric for scenario H+M to that for scenario J, the difference is substantial, although the vertical and longitudinal velocity changes are not as dramatically different. The vertical and longitudinal deceleration values are quite different and, again, this may be due to more of the scenario H+M mishaps occurring away from the prepared surface of the airfield, whereas most of the scenario J mishaps end on the airfield. This argument is supported by looking at the fraction of mishaps in each scenario in which the aircraft encountered a vertical impediment or discontinuity (right column of table 17). The two scenarios with the highest average damage metric also have high fractions of mishaps involving impediments. The exception is scenario F, in which the damage metric is low, but the fraction of impediments struck is high. This exception is

reasonable in that the impediments struck are often fences and lighting structures, and these impacts occur at low longitudinal velocity and essentially zero vertical velocity.

Table 16. Average damage metric of each segment by scenario—W–B

Scenario	Cockpit Average Damage Metric	Fwd. Cabin Average Damage Metric	OW. Cabin Average Damage Metric	Aft Cabin Average Damage Metric	Tail Average Damage Metric	Whole Aircraft Average Damage Metric
Scenario F	5.1	2.1	1.9	2.6	2.1	13.9
Scenario G	0.3	0.6	0.4	2.1	0.6	4.0
Scenario H+M	11.6	13.5	14.4	16.1	15.6	71.3
Scenario J	5.4	9.2	8.8	7.4	5.6	36.4
Scenario K	14.0	15.5	15.5	17.0	13.5	75.5

Table 17. Damage metric and kinematics by scenario—W–B

Scenario {# of events in scenario}	Aircraft Damage Metric (Avg. for Scenario)	Vertical Velocity Med./Avg. (ft/s)	Airspeed Med./Avg. (ft/s)	Vert. Accel. Med./Avg. (G)	Long. Accel. Med./ Avg. (G)	Vertical Obstacles Impacted (% of mishaps)
K Loss of control takeoff {2}	75.5	36.7†††/36.7	356/356	10.0/10.0	-6.2/6.2	50
H + M Similar mishaps regardless of influence {8}	71.3	21.7/32.6	212/237	8.4/6.0	-16.0/-13.2	63
J Hard landing, loss of control {5}	36.4	26.0/21.0	213/216	2.0/0.9††	-3.1/3.1	20
F Runway overrun {7}	13.1	0.0/-2.2†	118 /156	1.0/2.9	-1.5/5.1	57
G Compromised landing, no impact {7}	3.3	15.8/7.1	225/201	2.0/2.3	-0.2/0.2	14

† Negative average caused by one very large negative value.

†† Average is reduced by one large negative value (inverted impact); eliminating that mishap changes average for four mishaps to +3.3 G.

††† Excel calculates the average value for the median of two values.

The other kinematic parameters are the flight path angle and the attitude angles. In the following analysis (see table 18), the off-nominal angle is considered rather than the roll and yaw angles individually. The three scenarios with the highest damage metric values also have high median and average flight-path angles. The two scenarios with low damage metric values also have low flight path angles. The higher damage metric for scenario F is possibly due to the much higher percentage of vertical obstacles. For the off-nominal angle, scenario K does not follow the expected pattern—the average damage metric for the two scenarios is high, yet the median and

average for the angles are zero. There are only two of these mishaps compared to eight for the sum of the H and M scenarios. As might be expected, the H+M scenarios and the J scenarios have greater off-nominal angles associated with greater damage metric values. Similarly, the two scenarios with low values of damage metric have low off-nominal angles. The pitch angle treated as a monotonic variable (see table 18) exhibits no apparent pattern with the damage metric.

Table 18. Damage metric and kinematic angles by scenario—W–B

Scenario {# of events in scenario}	Aircraft Damage Metric (Avg. for Scenario)	Flight-Path Angle Med./Avg. (degr.)	Pitch Angle Med./Avg. (degr.)	Off-nominal Angle Med./Avg. (degr.)	Vertical Impediments Impacted (%)
K+L Loss of control takeoff {2}	75.5	-4.8†/-4.8	0†/0	0†/0	50
H + M Similar mishaps regardless of influence {8}	71.3	-6.8/-8.5	6.7/6.1	10.0/30.3	63
J Hard landing, lose control {5}	36.4	-4.4/-4.4	2.0/1.2	6.7/11.1	20
F Runway overrun {7}	13.1	0/-0.4	0.0/0.0	0/3.1	57
G Compromised landing, no impact {7}	3.3	-1.6	5.4	2.1	14

† Excel calculates the average value for the median of two values.

However, the pitch angle increases in magnitude away from zero in either direction, and the consequence of the increasing magnitude of the angle for the impact is different depending on the sign of the angle. For impacts with positive pitch angles, the aircraft rotates downward after contact of the main landing gear with the ground. For impacts at extreme positive pitch angles the aircraft rotates downward with a more severe vertical impact in the forward portions of the aircraft after contact of the tail with the ground. This type of impact will lead to nose landing gear collapse, crushing of the underside skin, fuselage breaks forward, and potentially to the disruption of the floor, and in the most severe cases to the loss of occupied volume forward in the aircraft. For the negative pitch angle impacts, the nose gear will impact first and usually collapse, followed by the nose and forward fuselage impacting the ground. These impacts have a greater likelihood of floor disruption and seat failure occurring and a greater likelihood of loss of occupied volume in the forward areas of the aircraft. For either the nose-up case or the nose-down case, the severity of damage and injury would be expected to increase with increasing angle. Pitch equal to zero or near zero represents a special case, and uniform damage and injury likelihood could be expected along the length of the fuselage. In the W–B dataset (see table 19), only scenarios J and F have both positive and negative pitch-angle mishaps. There are four scenarios with nose-up data; consequently, one may look for a trend there. The average damage metric value for nose-up mishaps varies over a wide range from 3.6 to 64.5, yet the average pitch angles for nose-up mishaps vary over a narrow range from 5.0 to 8.2 degrees with no strong pattern in the relationship with damage metric. It is interesting to note in scenario J that the average positive pitch angle is approximately equal to the average negative pitch angle, yet the damage metric for the negative pitch angle is higher than for the positive angle.

Table 19. Pitch angles resolved into positive and negative—W–B

Scenario {# of events in scenario}	Aircraft Damage Metric Nose up (Avg. for Scenario)	Nose-up Pitch Angle Avg. (degr.)	Aircraft Damage Metric Nose Down (Avg. for Scenario)	Nose-Down Pitch Angle Avg. (degr.)	Vertical Impediments Impacted (% Mishaps)
K+L Loss of control takeoff {2, 0+, & 0-}†	-	-	-	-	50
H + M Similar mishaps regardless of influence {8, 6+, & 0-}	64.5	8.2	-	-	63
J Hard landing, lose control {5, 3+, & 2-}	28	5.6	49	-5.5	20
F Runway overrun {7, 1+, & 1-}	17	5.0	0	-5.0	57
G Compromised landing, no impact {7, 5+, & 0-}	3.6	7.6	-	-	14

† The first value in the parenthesis is the number of mishaps; the second value is the number of mishaps with positive pitch angles; and the third value is the number of mishaps with negative pitch angles. The remainder of mishaps had zero pitch angle.

The damage metric plotted against the various kinematic parameters reveals fewer general trends than might be expected. In the case of airspeed (see figure 16), an upward trend in damage with increasing airspeed would be expected. However, no such clear trend is evident in either scenario F or in scenario G. This lack of trend for the airspeed may be due to the low average peak longitudinal decelerations (see table 17) in these two scenarios, which are characterized by long deceleration distances. Furthermore, scenario G in particular has a low fraction of mishaps encountering vertical impediments. In scenario F, although a greater fraction of vertical obstacles are met, the airspeeds have already decreased substantially (see table 17). The data for scenario H+M generally has the expected trend, but the scatter is quite wide. The scenario J data follow the expected trend, except for one outlier. Scenario K+L does exhibit the expected trend, but consists of only two mishaps.

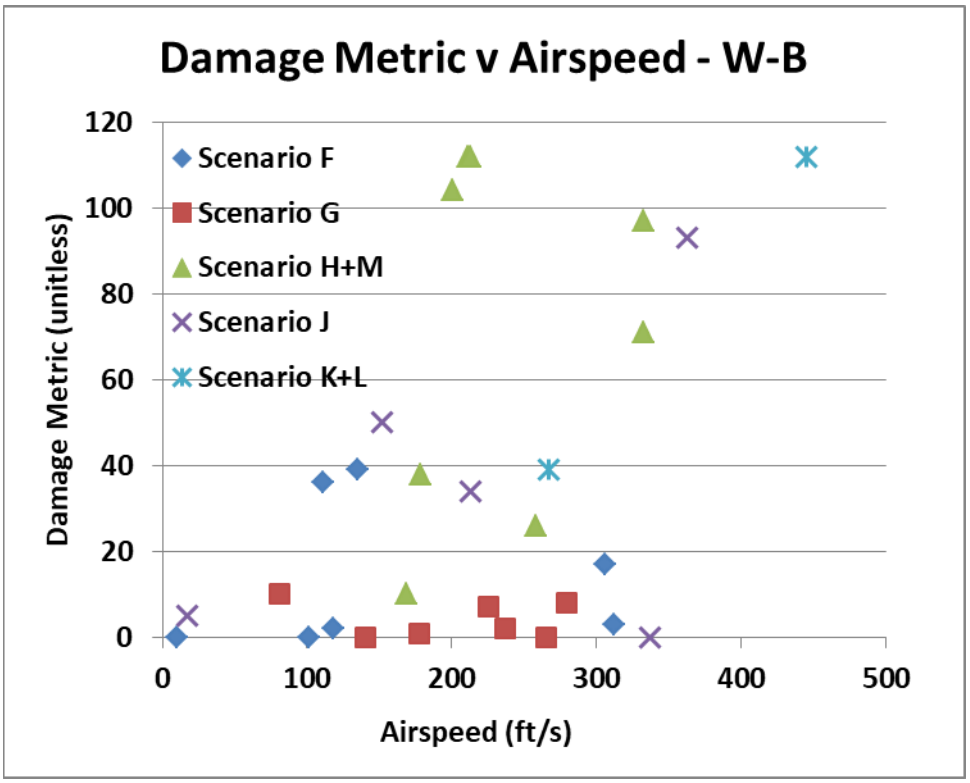

Figure 16. Damage metric vs. airspeed—W–B

In the vertical velocity plot (see figure 17), neither scenario F nor scenario G exhibit a trend. Scenario H+M and scenario J both exhibit very steep trends of increased damage with increased velocity, although scenario J data contain one apparent outlier. The two mishaps for scenario K have the expected relationship with the higher vertical velocity point also having the greater damage metric.

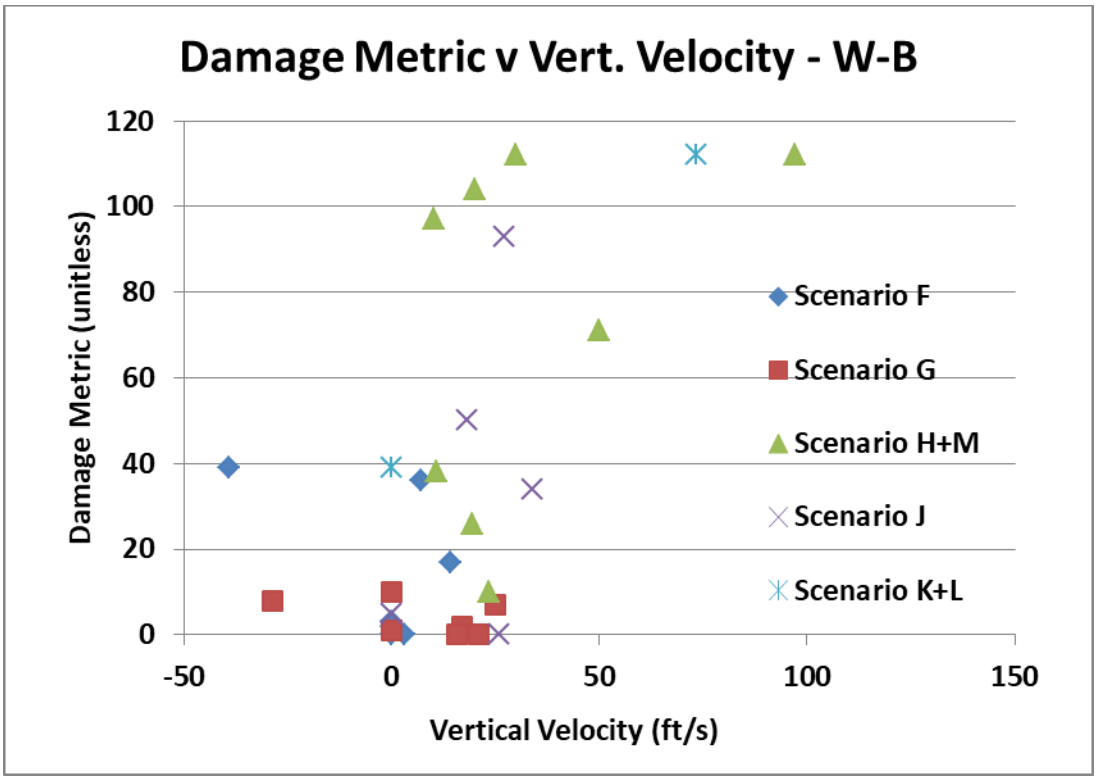

Figure 17. Damage metric vs. vertical velocity—W–B

The flight-path angle is not relevant for scenario F because it is near zero for all cases. Scenarios G, H+M, and J exhibit a strong upward trend of damage metric dependence (see figure 18), although there is quite a bit of scatter. The two scenario K mishaps do exhibit the expected relationship with the greater flight-path angle having the greater damage metric.

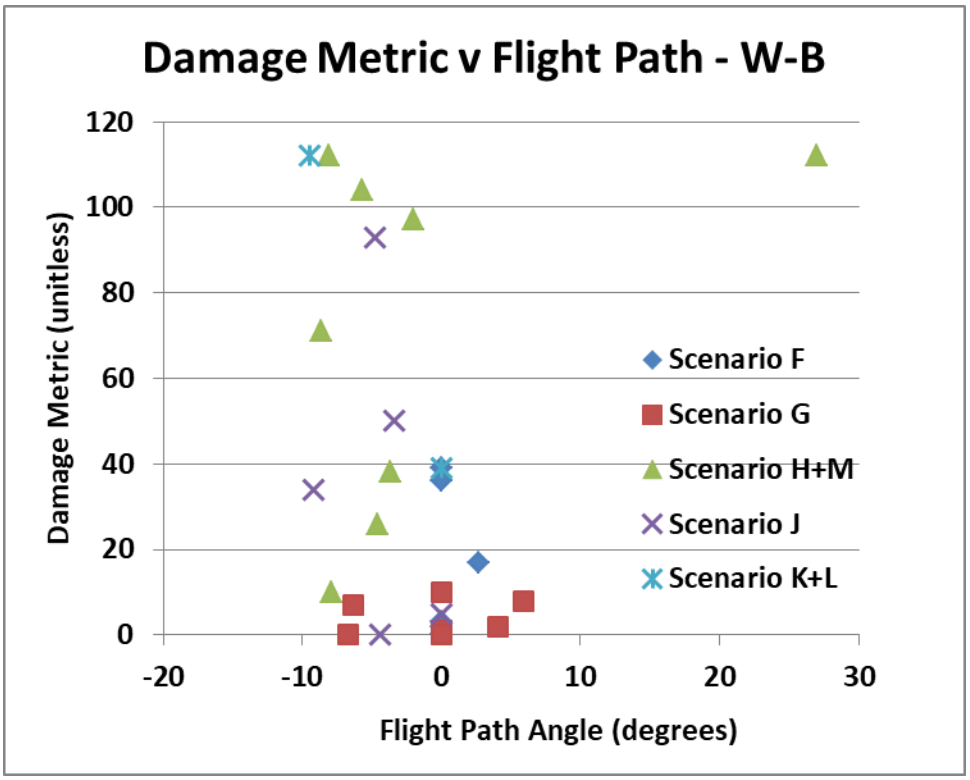

Figure 18. Damage metric vs. flight-path angle—W–B

The damage metric data for the pitch angle (see figure 19) does not show a trend for any of the scenarios. To try to improve the correlation, the few mishaps with negative pitch angles and those with zero pitch angle (12 of 29) were eliminated. In scenario F, only one mishap has a positive pitch angle so there can be no correlation or slope. Scenario G has just four mishaps with positive pitch and these four have a correlation coefficient of 0.18 together with a positive trendline slope. Scenario H+M has six mishaps with nose-up orientation. The correlation factor is low—0.03—because the points are widely separated in damage metric values, but the slope is positive as expected. Scenario J has the highest correlation coefficient at 0.55 based on four mishaps and the slope has the anticipated positive sense. There are no mishaps in scenario K+L with a positive pitch angle.

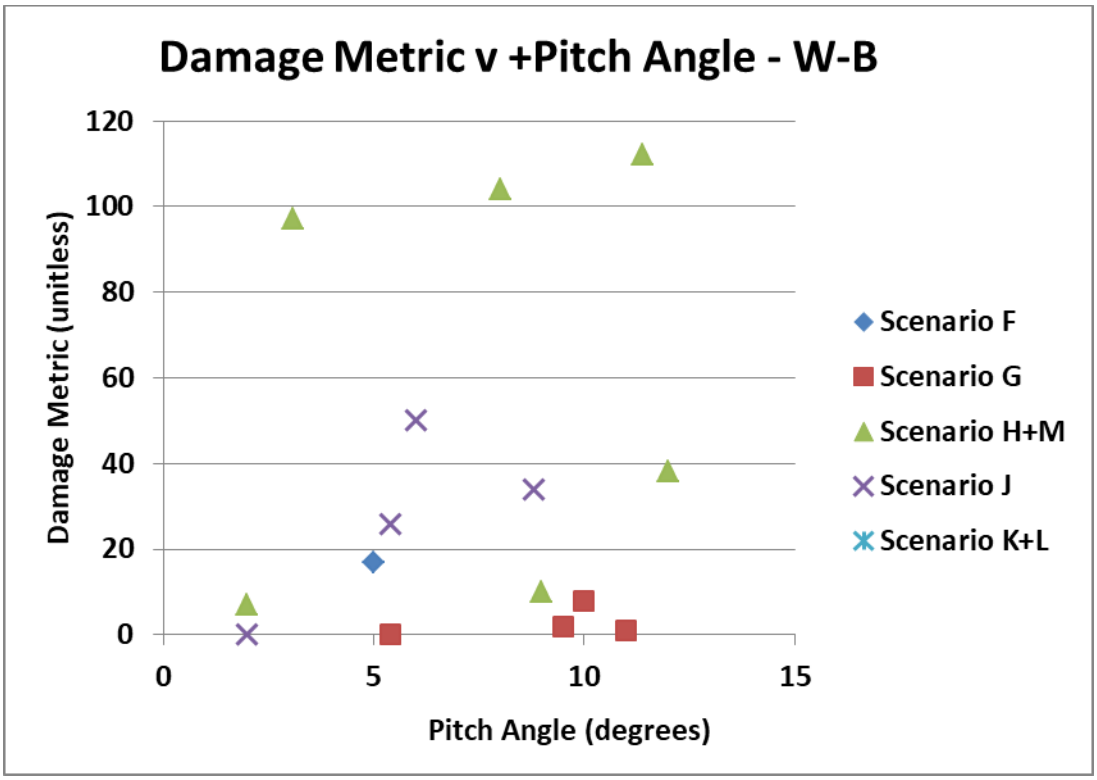

Figure 19. Damage metric vs. pitch angle—W–B

The correlation between peak vertical deceleration and damage metric for each scenario is generally poor, and only two of the five slopes are strongly in the anticipated direction (see figure 20). For the two acceleration parameters (longitudinal and vertical), a trend line was generated for each scenario. Scenario F does have a positive slope and a correlation factor (R^2) equal to 0.6. For scenario G, the slope is negative and the correlation is 0.38. The trend line for scenario H+M is only slightly positive, and the correlation factor equals zero. The scenario J data produced a negative slope with a correlation factor equal to 0.5. The two data points in scenario K+L produced perfect correlation, as any two points should. The slope was strongly positive.

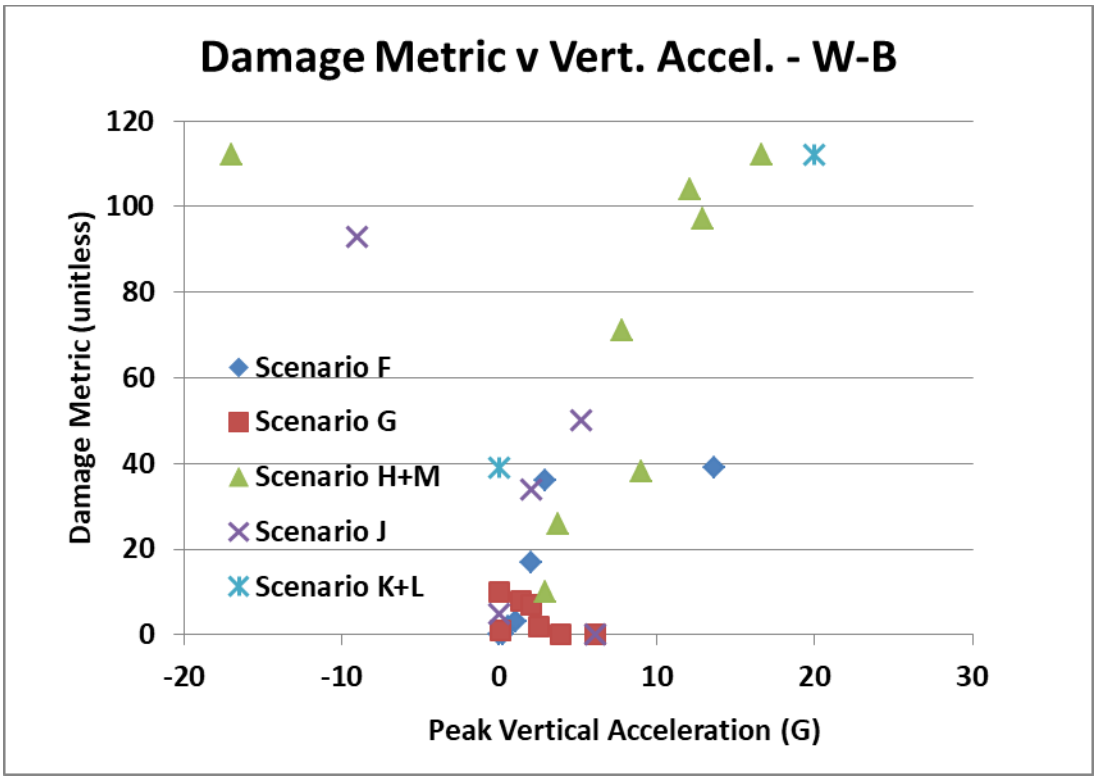

Figure 20. Damage metric vs. peak vertical deceleration—W–B

The damage metric displays better correlation to peak longitudinal acceleration (see figure 21) than to peak vertical deceleration (see figure 20). The anticipated slope for these trend lines is negative, although it is expected the damage metric would be higher at larger negative values of acceleration. Scenario F data display both a negative slope for the trend line and a correlation factor of 0.88, one of the highest correlation factors in this section of the analysis. The data for scenario G result in a steeply negative slope with a moderate correlation factor equal to 0.48. Scenario H+M data form a trend line with a negative slope and a correlation factor equal to 0.77. The data for the last two scenarios produce trend lines with positive slopes. Scenario J has a correlation of only 0.04, whereas scenario K+L again results in a correlation of 1.0 because the scenario has only two mishaps.

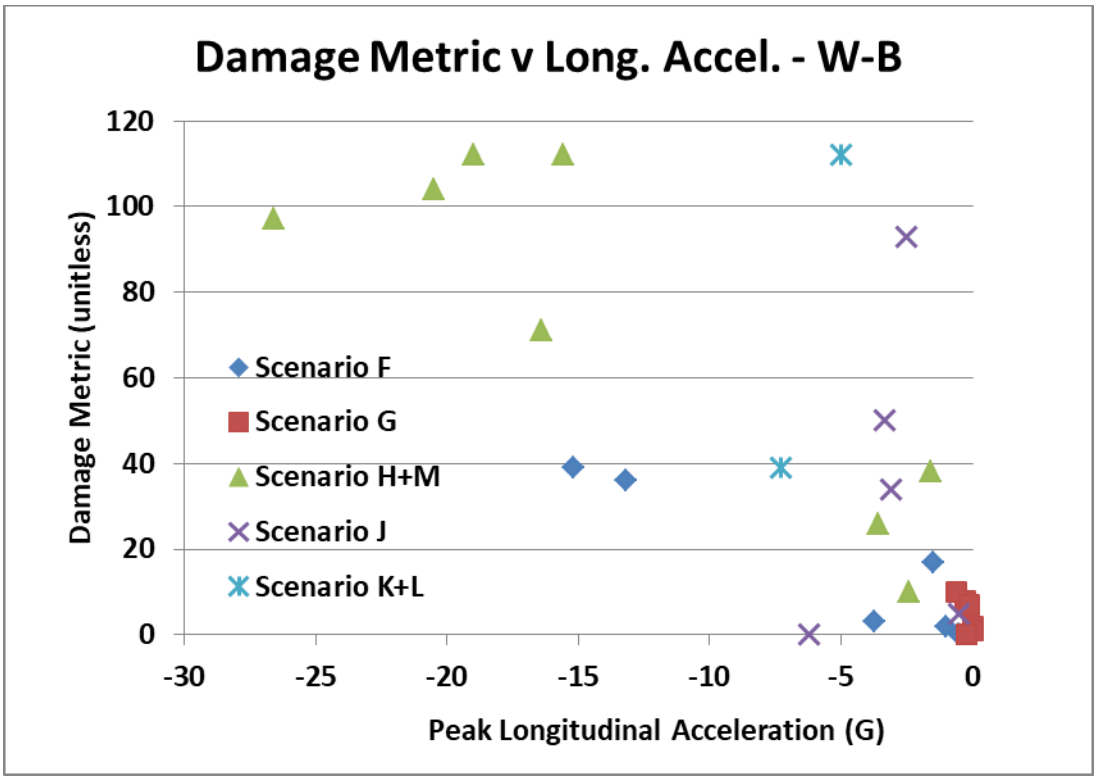

Figure 21. Damage metric vs. peak longitudinal deceleration—W–B

3.3.3.1 Effect of Vertical Impediment on Damage Metric—W–B

In reading the investigation reports for the W–B mishaps, the idea that an encounter with obstacles leads to greater damage was suggested. All of the W–B aircraft have engines under the wings; consequently, vertical impediments not only may cause the landing gear to shear off, but often may damage or completely remove one or more engines. The damage metric only quantifies mechanical damage to the fuselage portion of the aircraft and does not consider engine damage. To record whether the aircraft had encountered a vertical impediment, a yes/no (Y/N) field was added to the damage worksheet. The data in this field were used to explore the influence of obstacles on damage and injury outcome for the mishaps.

The field consists of a Y/N value for the aircraft encountering a vertical impediment as part of the impact sequence. A vertical impediment is loosely defined as any sharply upward discontinuity in the surface that the aircraft is traveling on or impacting. Such discontinuities include walls, structures (including lighting and antenna supports), berms, trees, poles, and the far sides of ditches and culverts. There is a difference in the average and median damage metric between those mishaps in which an impediment was encountered and those in which no impediment was encountered (see table 20). Breaking the data down by scenario (see table 21) highlights the fact that the severe damage mishaps occurred in scenarios H, M, J, and K. It appears that the overruns mishaps (see scenario F) were only damaging when an impediment was involved. Conversely, the four more damaging scenarios were not strongly affected by the presence of an impediment, possibly because these mishaps already involve the aircraft at more extreme attitudes.

Table 20. Damage metric dependence on vertical impediments

	Obstacle Encountered Damage Metric (unitless)	No Obstacle Encountered Damage Metric (unitless)
Average	42	31
Median	37	10
No. of Mishaps	12	17

Table 21. Damage metrics associated with impediments by scenario

	Vertical Impediment – Average Damage Metric (unitless)	No Vertical Impediment – Average Damage Metric (unitless)	No. of Mishaps With a Vertical Impediment (No.)	No. of Mishaps With No Vertical Impediment (No.)
Scenario F	20	6	4	3
Scenario G	8	3	1	6
Scenario H+M	75	64	5	3
Scenario J	5	44	1	4
Scenario K+L	39	112	1	1

Plots were created with the objective of spotting correlation between encounters with vertical obstacles and the damage metric. The frequency of vertical obstacles in a particular scenario is represented by the fraction of scenarios that involved vertical obstacles (number of mishaps with vertical obstacles/number of all mishaps in scenario). The parameter for comparison is the average damage metric for each scenario. It was first thought that the damage metric would be expected to increase as the fraction of vertical obstacles encountered increased (see figure 22). The trend is in the anticipated direction, but the correlation coefficient is not particularly high. Among the kinematic parameters, the peak longitudinal deceleration would be expected to correlate well with the damage metric (see figure 23). In this plot, the peak longitudinal deceleration is presented as the average value for the scenario. The trend is the one anticipated, and the average of the longitudinal deceleration increases as the fraction of mishaps involving vertical obstacles increases. However, the correlation coefficient indicates a weak correlation.

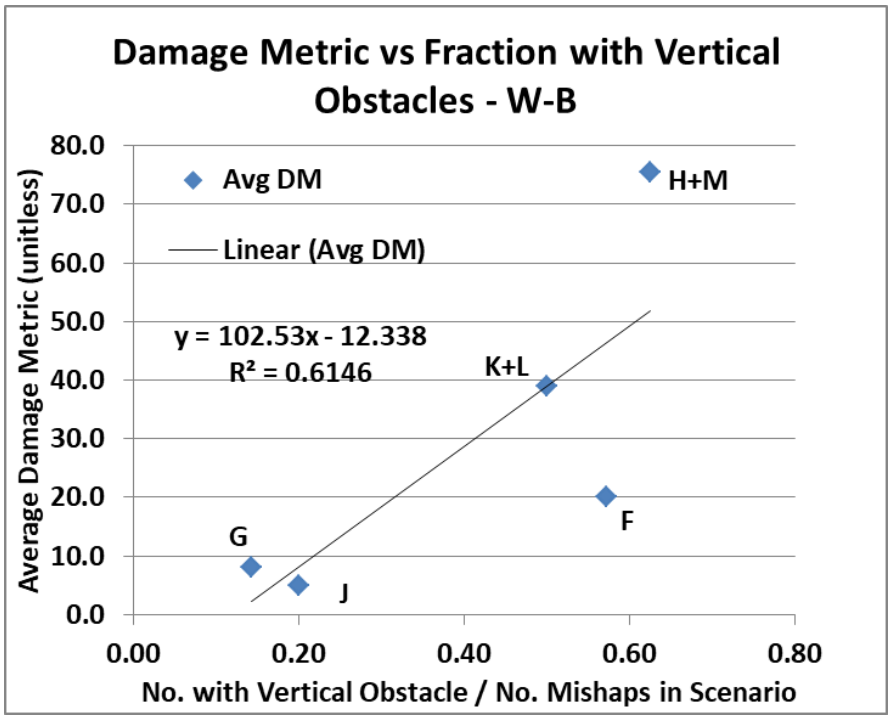

Figure 22. Correlation between damage metric and fraction of vertical obstacles W–B

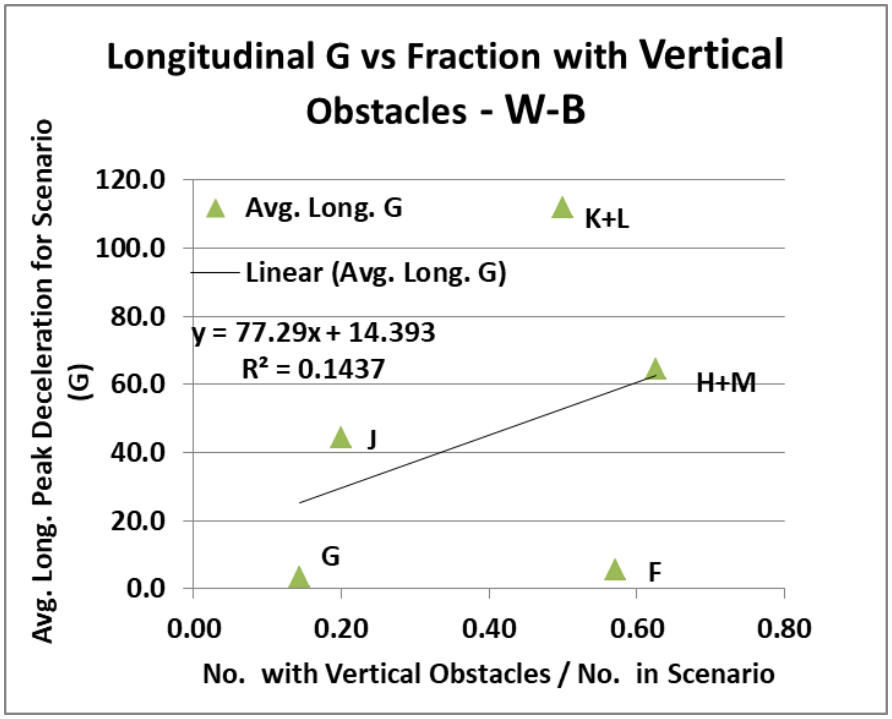

Figure 23. Correlation between damage metric and peak longitudinal deceleration—W–B

A two-sample T test was conducted on damage metric data for the whole W–B dataset of 29 mishaps—12 with impediments and 17 without. This test found no justification for stating that the

mean of the damage metric for the mishaps involving vertical impediments was higher than the mean for the mishaps without vertical impediments. The *p*-value for the test statistic is 0.44, whereas a value less than 0.100 is needed to support the difference in the means being significant. The 90 percent confidence interval for the difference between the two means (mean DM with impediment–mean DM without impediment) is -14.3 to +38.1, which includes the value 0, further confirming no difference. The boxplot (see figure 24) indicates asymmetry in the data. The upper and lower edges of the box depict the interquartile (25^{th} percentile to the 75^{th} percentile) range of the data; the line connects the mean of each dataset, whereas the horizontal bar within each box locates the median value for that dataset. The low position of the bar in the box without impediment indicates a large number of low values for the damage metric.

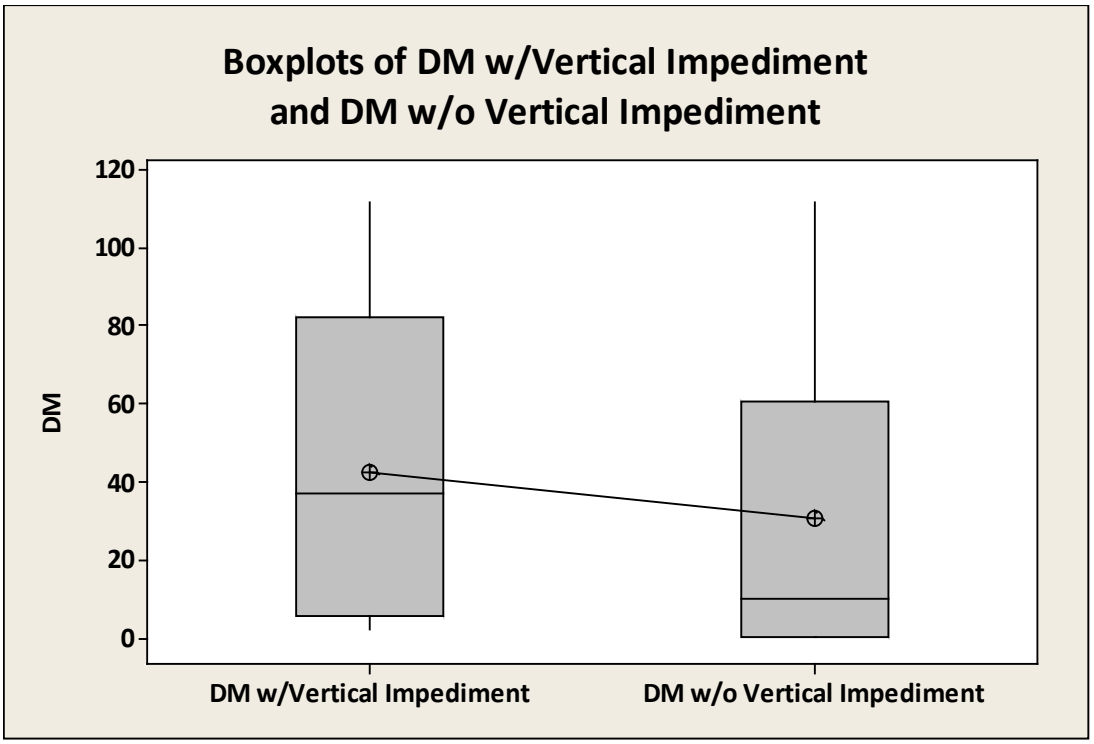

Figure 24. Boxplot of damage metric with and without impediment—W–B

3.3.3.2 Damage Dependence on Design Characteristics—W–B

There are just two engine configurations in the W–B dataset: engines on wing and engines on wing and fin. All of the aircraft with the wing-and-fin configuration had three engines. Among the engines on wing aircraft (see table 22), eight were two-engine aircraft and eight were four-engine aircraft. Comparing the two-engine position configurations, the engine-on-wing aircraft had higher median and higher average damage metrics than the aircraft with engines on wing and fin. The number of aircraft in each group is comparable, and the averages and medians confirm each other. Looking just at the aircraft with engines mounted on the wings, the average damage metric differs between two-engine and four-engine datasets. The number of aircraft in each of these two groups is equal, and the trend for the averages is the same as the trend for the medians.

Table 22. Damage metric related to engine configuration—W–B

	Wing-Mounted Engines (2 & 4)	Wing & Fin Mounted Engines (3)	Two Wing-Mounted Engines	Four Wing-Mounted Engines
Average Damage Metric	43	27	37	49
Median Damage Metric	30	10	22	31
No. of Mishaps	16	13	8	8

3.3.3.3 Damage Dependence on Gear up/Down—W–B

Of the 29 mishaps in the W–B dataset, only one mishap occurred with the gear in the up position. This mishap was a go-around, and the gear had been retracted. The aircraft lost control and descended from 600 feet AGL to crash. In all other mishaps, the landing gear was down.

3.3.4 Evacuation—W–B

All of the W–B aircraft in the study were equipped with doors, and none had Type-III exits. Three B767 aircraft are included in this group, and some variants of this aircraft type do use overwing exits. However, none of the three B767 mishaps led to an emergency evacuation, and therefore exits are not treated in this analysis. The accident database contained information on the functionality and usability of the doors and exits, but the reports were also read carefully for information on the evacuation. A door is deemed functional if it is mechanically operational post-crash. A door or an exit is deemed usable if it is both functional (or open) and able to be used for egress. In more than one mishap, one or more doors were reported to be found detached from their frames in the wreckage. If the resulting opening was reported to have been used as an escape route, then that door opening was counted as usable, although it was not counted as functional; therefore, there can be more ‘usable’ doors than ‘functional’ doors. However, a door that had fire beyond it or was blocked by terrain may have been functional, but was not usable for escape. Functionality or usability of all doors and exits was not necessarily documented in the investigation reports (see table 23). In less-severe mishaps in which the evacuation was not an emergency, only one door may have been used and the others left unreported (see table 23, second line). In some severe cases in which the aircraft was totally destroyed on impact, there was no emergency evacuation in the conventional sense. The few survivors were either found alive in their seats among the wreckage or were found wandering in or near the wreckage having exited through gaps in the fuselage. The numbers provided are for the doors on the 23 aircraft for which door conditions were reported (see table 24).

Table 23. Overall Door and Exit Availability—W–B

(29 Aircraft/23 Reported)	Doors (#)	Exits (#)
Installed on 23 Mishap Aircraft	196	NA
Portal Condition Reported	109	NA
Portal Reported as Functional	102	NA
Portal Reported as Useable	74	NA

Table 24. Post-crash door availability for emergency egress by scenario—W–B

Doors	Emergency Evacuations #/# of Mishaps	Doors on Aircraft Reported Condition (average #/minimum #)	Functional Doors (average #/minimum #)	Usable Doors (average #/ minimum #)
Scenario F	5/7	7.2/4	6.4/4	4.6/3
Scenario G	3/7	8.0/6	7.0/5	4.3/2
Scenario H+M	5/8	4.2/0	3.8/0	3.8/0
Scenario J	4/5	5.0/1	2.8/0	4.3/3
Scenario K	1/2	10.0/10	5.0/5	4.0/4

The presence of fire affects evacuation routes in important ways. First, the presence of fire near, and particularly inside, the cabin sets a very severe limit on the time available to evacuate occupants out of the cabin. Second, the presence of fire inside or outside may reduce the number of routes that are usable for evacuation. Post-crash fire was present in 17 of the 29 mishaps, and 11 of the 20 emergency evacuations were associated with post-crash fire. Four of the eleven fire-related emergency evacuations occurred in the scenario F mishaps (overruns), even though these were not the most severe in terms of damage. The scenario H+M had the second highest fraction of fire-related emergency evacuations (three of eight). Scenario K covers only two events, and one of these had a fire-related emergency evacuation. For each scenario, the average number and the minimum number of doors are shown in table 24. The third column indicates the average and minimum number of doors whose condition was reported for those mishaps in which an emergency evacuation occurred. The fourth column gives the average and minimum number of doors reported as functional. Similarly, the fifth column provides the average and minimum number of usable doors for each scenario. In scenario J, there is an apparent discrepancy in which more usable doors are reported than functional doors. In two mishaps, the impact ejected three doors on each aircraft; therefore, the doorways were available as exit routes, but the doors were not actually functional.

3.3.5 Injury Analysis—W–B

In analyzing the injuries resulting from the mishaps in this study, the distribution of injuries among the different types of mishaps are reviewed. The injuries are correlated with the kinematics and aircraft characteristics. The injuries for the entire aircraft are viewed first, and then the injury fraction will be looked at by aircraft segment.

In many of the reports, minor injuries are treated in one category with non-injuries. In other reports, two separate counts are provided for minor and non-injuries. Because the numbers from the combined figures cannot be separated again, minor injuries and non-injuries are reported together for all mishaps.

Viewing the injury fractions for the entire W–B dataset, just under 17 percent of all occupants were fatally injured (see table 25). Less than 8 percent were seriously injured. The remaining 75.5 percent had either minor or no injuries. The injury fractions shown below for the W–B mishaps are remarkably similar to those for the N–B mishaps.

Table 25. Number and percent of occupants injured in the entire study—W–B

	Number of Occupants	Percent of Occupants
Fatally Injured (all causes)	1163	16.9
Fatally Injured (identified as thermal)	373	5.4
Seriously Injured	535	7.8
Minor or Not Injured	5213	75.5
Total Occupants	6877	100

The overview for injuries in the W–B mishaps included in this study reveals that fatalities and serious injuries were confined to those mishaps occurring at extreme attitudes or on terrain away from the prepared surfaces around the airport. Based on the median values, the fraction of fatalities and serious injuries is low (see table 26) for both the overruns and all other mishaps. The median being zero indicates that at least half of the mishaps had no fatal injuries. The higher average values in the fatalities indicate that there were several severe accidents. Realizing that a limited number of accidents were quite severe recommends a further breakdown of the injury rates by scenario (see table 27). Among the scenarios in which the aircraft is coming from the air (G–M), scenario G and scenario J have low fatality rates. That scenario G, the compromised landings, has few fatalities is not surprising considering that the average aircraft damage metric for scenario G is low (see table 16). Therefore, a plot of the average severe-injury fraction against the average aircraft damage metric for each individual scenario (see figure 25) reveals a distinct trend and a good correlation for a linear trend line. A slightly better correlation coefficient is obtained with a quadratic trend line, but the two curves are so similar that the injury fraction value predicted for a given damage metric does not differ by very much.

Table 26. Injury severity for overrun mishaps compared to other mishaps—W–B

	Scenarios G–M Impact from Air (Median/Average)	Scenario F Overrun Impacts (Median/Average)
Fatal Injury (percent of aircraft occupants)	0/27	2/13
Serious Injury (percent of aircraft occupants)	5/9	4/5
Minor/No injury (percent of aircraft occupants)	89/64	96/93
No. of Aircraft Occupants (#)	211/221	284/282
Number of Mishaps in Scenario (#)	22	7

Table 27. Injury severity for each scenario—W–B

Scenario	Number of Mishaps (No.)	Number of Occupants (Med. No./ Avg. No.)	Frac. of Occupants Fatal Inj. (Med. %/ Avg. %)	Frac. of Occupants Serious Inj. (Med. %/ Avg. %)	Frac. of Occupants Minor/No Inj. (Med. %/ Avg. %)	Average Damage Metric for Aircraft (Unitless)
F	7	284/283	2/13	4/5	96/93	13.9
G	7	219/222	0/0	0/1	99/98	4.0
H	6	184/208	68/53	10/12	9/37	74.5
J	5	306/292	1/11	16/13	83/76	36.4
K	2	142†/142	73/73	11/11	16/16	75.5
L	0	-	-	-	-	-
M	2	165/165	41/41	5/5	53/53	61.5
H+M	8	172/197	68/50	10/12	9/37	71.3
K+L	2	142/142	73/73	11/11	16/16	75.5

† Excel calculates the average value for the median of two values.

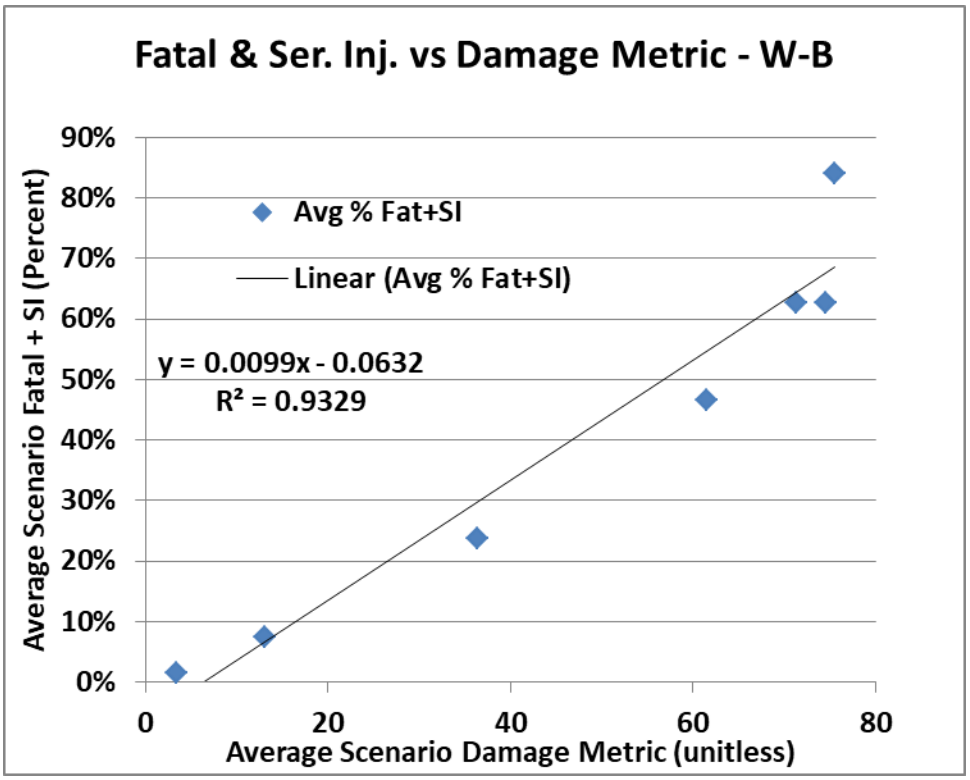

Figure 25. Average fatality and serious-injury fraction vs. damage metric—W–B

Comparing scenario H to scenario M (see table 27), the same scenario with localized wind influence, reveals that scenario M has lower average fatal and lower average serious injury rates. The comparison between scenario K and scenario L cannot be made in the W–B dataset because there were no scenario L mishaps. The comparison of scenario H to scenario M supports the earlier conclusion based on damage metric that the localized wind influence on the mishap does not cause the mishap to be more severe than other mishaps with similar characteristics.

3.3.5.1 Design Influence on Injury—W–B

The two design considerations investigated are engine location and engine number. Two configurations cover all of the W–B mishaps: engines on wing, and engines on wing and fin. All of the engine-on-wing-and-fin configurations were three-engine aircraft. The engine-on-wing aircraft included both two-engine and four-engine aircraft. Approximately 45 percent of the mishaps involved the engine-on-wing-and-fin configuration.

The average values for the fraction of severe injuries do not vary much (see table 28) between the two different engine configurations, nor between the three levels of engine number. However, the median values do vary. To further investigate the injury rates, the number of mishaps for each configuration and scenario were broken out by scenario (see table 29). One important consideration for this breakout is that each cell of the table has few mishaps. The most populous cell has five mishaps; therefore, the statistics can be strongly influenced by one extreme event. The first notable relationship is that the wing-fin configuration was involved in five of the seven overrun mishaps (scenario F), compared to only two for the engine-on-wing configuration. The

relationship for the other low-severity scenarios was reversed with five of the seven compromised-landing (scenario G) mishaps being associated with engine-on-wing aircraft. In Scenario H, which consists of landing short resulting in a severe impact, five of the six mishaps involved the engine-on-wing configuration. However, when one looks at the breakdown by the number of engines, the distribution is more even with three mishaps involving two-engine aircraft, two mishaps involving four-engine aircraft, and one mishap involving the three-engine aircraft. Because the trend to fewer engines has been a relatively recent one, the time element was included in table 28 by determining the median mishap date for each dataset.

Table 28. Fatal- and serious-injury fraction dependence on engine configuration—W–B

	Eng. On Wing	Eng. On Wing/Fin	2 Eng. Aircraft	3 Eng. Aircraft	4 Eng. Aircraft
Severe-Injury Fraction (Med. %/Avg. %)	4%/31%	17%/27%	1%/27%	17%/27%	5%/35%
Damage Metric (Med./Avg.)	30/43	10/27	22/37	10/27	31/49
No. Mishaps	16	13	8	13	8
Median Mishap Date	Sep. 1995	Nov. 1993	Oct. 2004	Nov. 1993	Sep. 1986

Table 29. Number of mishaps associated with design configurations—W–B

Scenario	Eng. On Wing No. Mishaps	Eng. On Wing/Fin No. Mishaps	2 Eng. Aircraft No. Mishaps	3 Eng. Aircraft No. Mishaps	4 Eng. Aircraft No. Mishaps
F—Overrun	2	5	0	5	2
G—Compromised Landing	5	2	3	2	2
H—Impact Short	5	1	3	1	2
M—Short Wind Influence	0	2	0	2	0
J—Control Loss after Landing	2	3	1	3	1
K—Takeoff Control Loss	2	0	1	0	1
All	16	13	8	13	8

A two-sample T-test was applied to the entire W–B dataset to determine if the difference in the mean for the engines-on-wing-and-fin configuration (mean=0.269) was different statistically from the mean for the engines-on-wing configuration (mean=0.312). The *p*-value for the test is 0.767, indicating that the two means are not significantly different. The measured difference in the means of +0.043 falls within the 90 percent confidence range covering -0.203 to +0.289, which includes the possibility of zero difference. Therefore, there is no statistical support for the idea that the means are actually different. The box plot for this T-test is shown in figure 26.

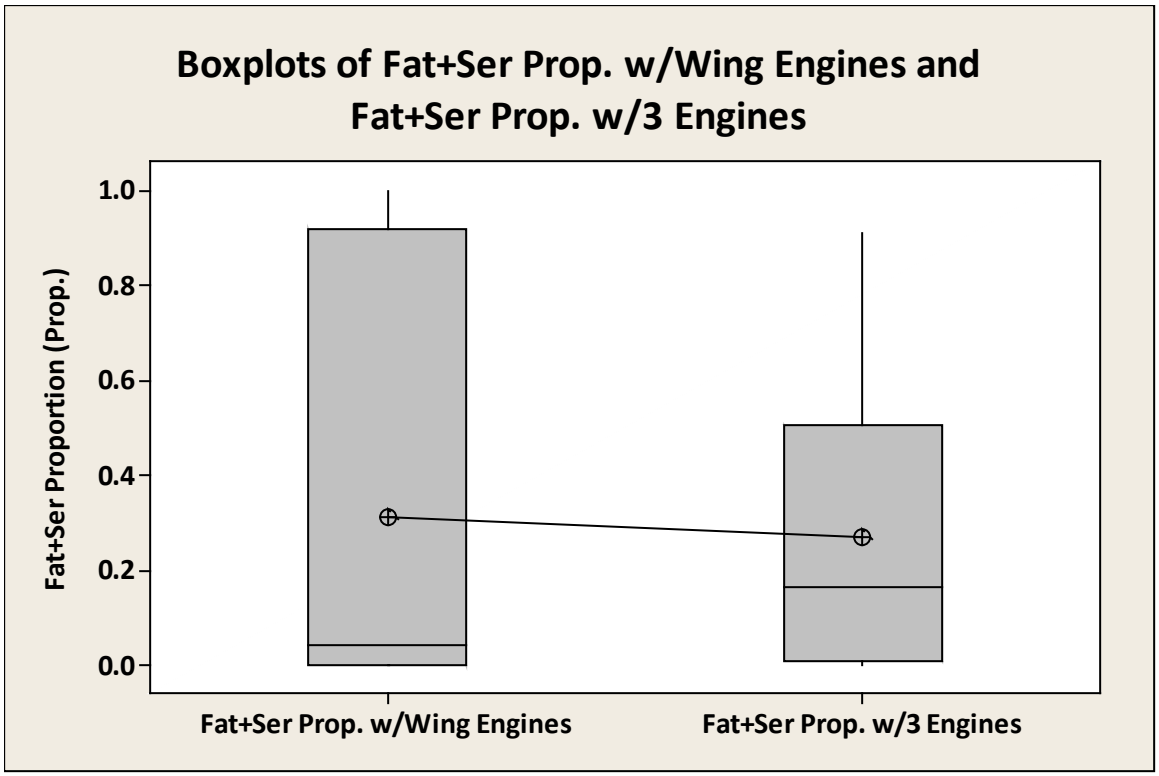

Figure 26. Means T-test of engines-on-wings and engines-on-wings-and-tail—W–B

The subset of data containing two-engine and four-engine aircraft was also tested for the difference in the means. The eight two-engine mishaps had a mean severe-injury fraction equal to 0.273, whereas the seven four-engine mishaps had a mean severe-injury fraction equal to 0.395. The *p*-value for the two-sample T-test on this data is 0.622, indicating that the means are not significantly different. Supporting this conclusion, the 90-percent confidence range for the real value of the difference between the two means covers from -0.553 to +0.308, which includes zero difference.

All aircraft in the W–B dataset were of the low-wing configuration; therefore, there is no basis for analyzing the survivability implications of differing wing configurations.

3.3.5.2 Injuries in Each Scenario and Segment—W–B

Transport aircraft fuselages and cabins have one long dimension (length) and two approximately equal dimensions (width and height). As a consequence of these dimensional differences, it is reasonable to expect that the impact conditions and, consequently, the injury outcomes may not be uniform throughout the aircraft. To see what effect this dimensional anisotropy has on the injury distributions throughout the aircraft, the data have been grouped by segment and scenario (see table 30).

Table 30. Fraction of severe injuries for each scenario and cabin segment—W–B

Scenario (no. of mishaps)	Cockpit (% of Occupants Fatal or Serious Injury)	Forward Cabin (% of Occupants Fatal or Serious Injury)	Over-Wing Cabin (% of Occupants Fatal or Serious Injury)	Rear-Cabin (% of Occupants Fatal or Serious Injury)	Tail (% of Occupants Fatal or Serious Injury)
Scenario F (7)	0%	2%	1%	17%	11%
Scenario G (7)	0%	0%	0%	0%	0%
Scenario H+M (8)	80%	74%	60%	66%	100%
Scenario J (5)	25%	12%	14%	17%	0%
Scenario K (2)	50%	56%	91%	44%	No occupants
Scenarios G–M (22)	50%	55%	47%	36%	6%

For the purpose of this analysis, fatalities and serious injuries have been grouped together and are referred to collectively as "severe injuries." The percentage of all occupants fatally or seriously injured is determined for each cabin segment. From the values in table 30, the results are not as might be expected in scenario F. The overrun scenario is anticipated to have a higher incidence of injuries in the cockpit and forward cabin, but the opposite is true. Most of the severe injuries are in the aft cabin and tail. The population of occupants in the tail is generally small, being limited to one or two rows of seats, or more commonly only the flight attendant seats. Surprisingly, the high-damage metric scenario J—loss of control after a hard landing—displays the strongest trend for more injuries forward. However, this scenario is dominated by two extreme events, one being the Sioux City DC-10 landing. The distinctly high severe-injury rate for the overwing segment in scenario K is also strongly influenced by a single mishap. Mishap 20001031B was an attempted takeoff for a trans-Pacific flight on a closed runway. The aircraft struck construction equipment, resulting in a post-impact fire that killed 54 in the overwing segment, but only 10 elsewhere in the aircraft. A general observation is that those scenarios resulting in more extreme attitudes, the loss-of-control scenarios J and K, tend to show a more uniform distribution of severe injuries along the length of the aircraft.

3.3.5.3 Injuries Dependence on Kinematics W–B

The influence by each of the kinematic parameters on the fraction of severe injuries is evaluated by plotting the severe-injury fraction for each mishap against the value of the kinematic parameter. The scenario of the mishap is coded into the point marker.

In the airspeed plot (see figure 27), the mishaps in scenarios F and G generally display low severe-injury fractions across all airspeeds. For the more violent scenarios, the anticipated pattern of increasing injury fraction with increasing airspeed is evident, although there is a great deal of scatter. In particular, for the landing-short scenario, H+M, four mishaps occur close to 200 ft/s, yet two of the four mishaps result in all occupants severely injured; the other two mishaps result in

less than 20 percent severely injured. For scenario J, there is a distinct trend upward from a mishap with very little airspeed and no severe injuries to one with more than 50 percent injuries at 360 ft/s. However, there is also a scenario J mishap at 340 ft/s with only 1 percent severe injuries.

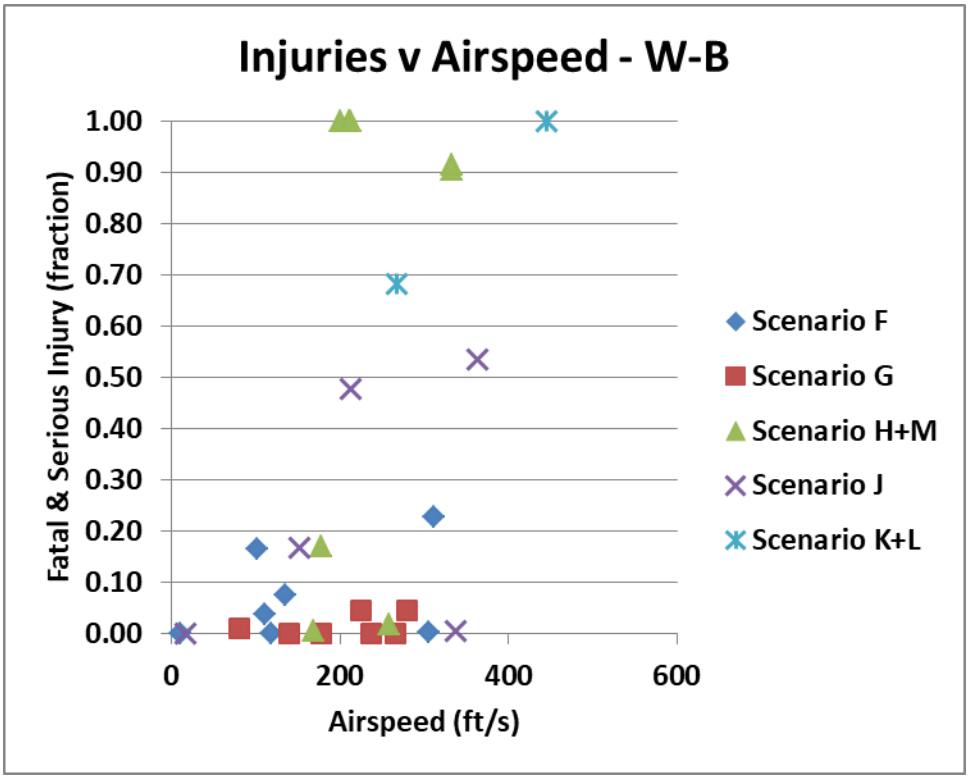

Figure 27. Severe-injury fraction dependence on airspeed—W–B

The anticipated vertical velocity trend is for the injury fraction to increase as the vertical velocity increases. Such a trend with a wide range of velocity is apparent in the scenario H+M data (see figure 28). Two of the H+M mishaps with high vertical velocity also have high injury fractions, but there are three mishaps with high injury fractions that occurred with low-to-moderate vertical velocities. Three mishaps occurred with negative (upward) vertical velocities, which have low injury fractions. The scenario G events all have very low injury fractions; therefore, the slight upward trend is barely perceptible. The scenario G event with a negative vertical velocity is a tail-strike during takeoff and, therefore, a rather innocuous event. The scenario F event with a negative vertical velocity is an overrun in which the aircraft hits a sharply rising road shoulder and is accelerated upward as it is longitudinally decelerated. The two scenario K events show the expected trend, but there are only the two values, and it may be by chance that the trend is the expected one.

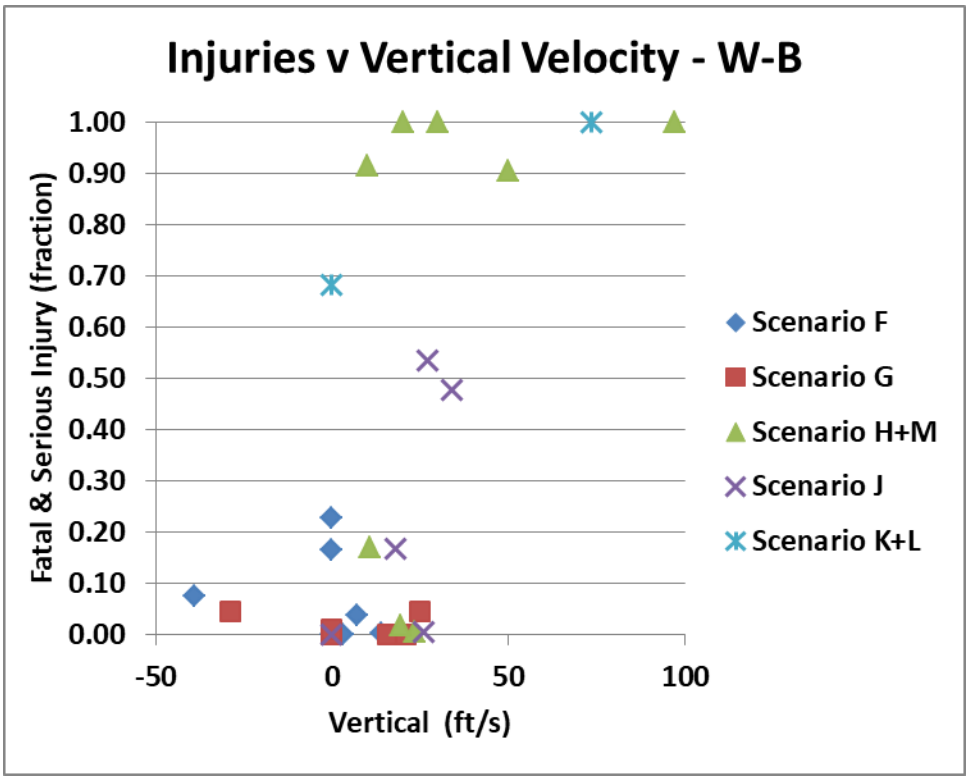

Figure 28. Severe-injury fraction dependence on vertical velocity—W–B

Most of the mishaps have the expected flight path: zero angle for the overrun mishaps and a negative flight path angle for the scenarios coming from in-flight. The range of flight-path angles is narrow (see figure 29); consequently, scatter in injury fraction is large relative to the range of the flight-path angle values. Scenario H+M is the only scenario that reveals a general trend toward a greater injury fraction with more negative flight-path angle, but the wide range of flight-path angles at high-injury fractions makes the trend difficult to discern.

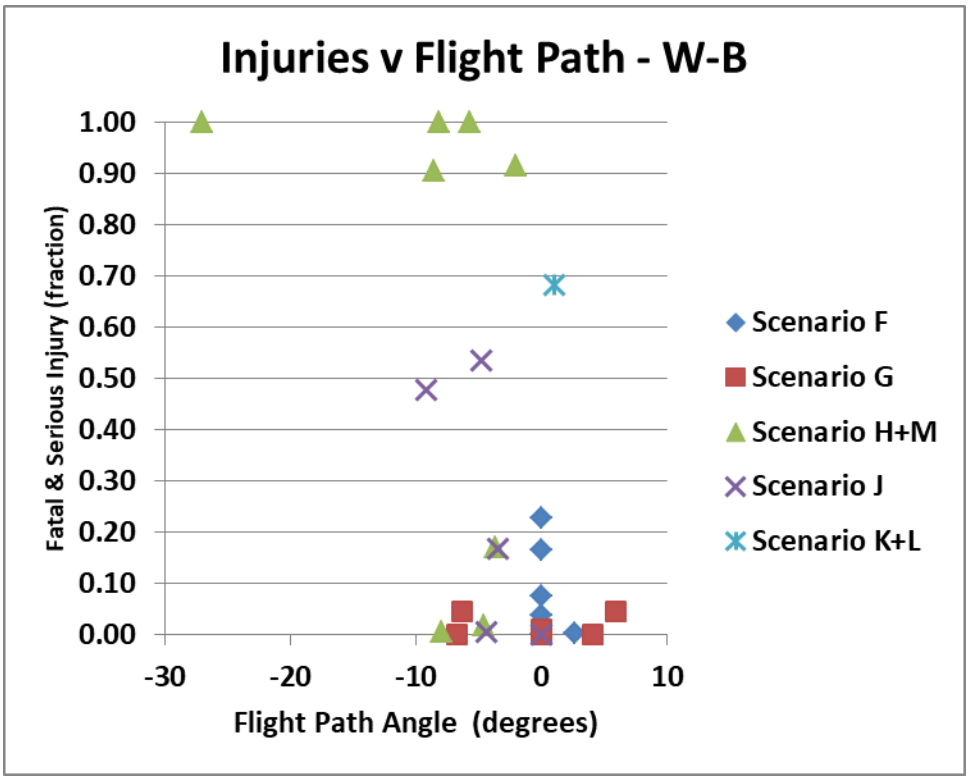

Figure 29. Severe-injury fraction dependence on flight-path angle—W–B

The pitch angle could be expected to exhibit two trends. As the pitch becomes either increasingly positive or increasingly negative, the number and severity of injuries would be expected to increase, although the crash develops in very different ways. With a positive pitch angle, the main gear or tail is expected to make first contact with the aircraft, then pivoting downward about that initial contact point to impact the nose gear and then bottom of the fuselage, if the nose gear fails. For the nose-down situation, the nose makes first contact. For small nose-down angles, initial damage would be to the nose, and the tail would rotate downward as the aircraft slides out. The nose gear often fails, even for small nose-down angles. For increasing nose-down angles, greater damage would be expected to be incurred to the cockpit and the forward cabin; for soft terrain, there would be a greater tendency for the nose to dig in and the aircraft to stop more abruptly. Scenario J is the only one to show evidence of this binary trend with two high-injury fraction mishaps on the nose-up side of the plot (see figure 30) and one on the nose-down side of the plot. Scenario H+M has three mishaps with high severe-injury fractions, and they all have pitch angles above +7 degrees. However, there is a point in this scenario with a 12-degree nose-up angle and zero injury fraction.

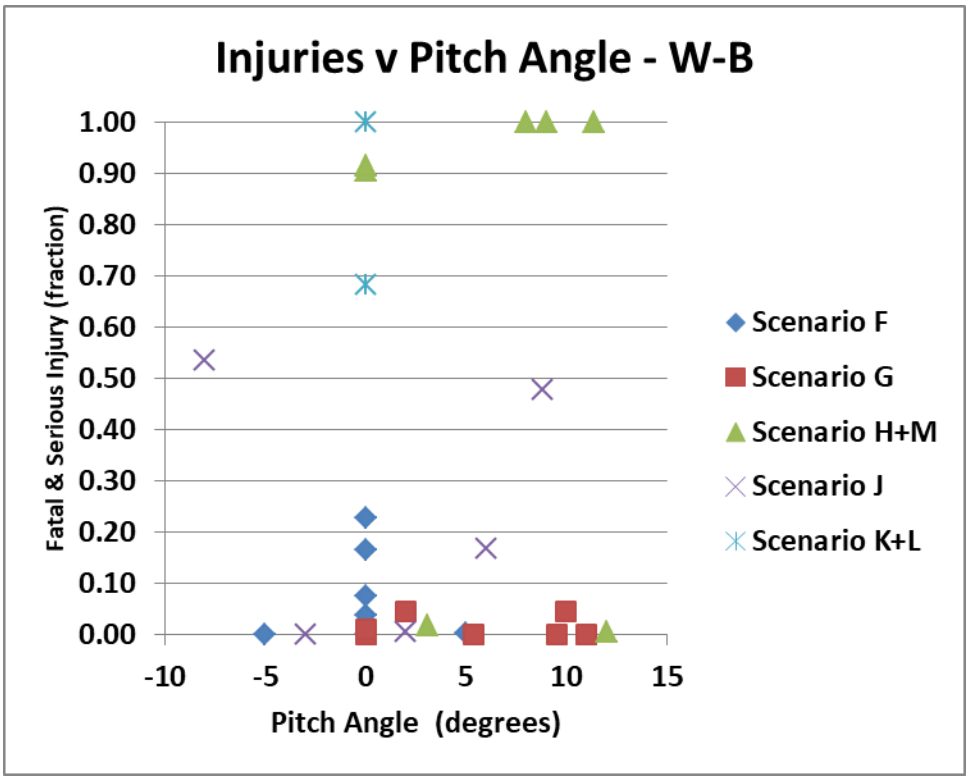

Figure 30. Severe-injury fraction dependence on pitch angle—W–B

To explore whether the pitch angle does affect the frequency of injuries, the mishaps were sorted into three groups: positive pitch, negative pitch, and zero pitch. The severe-injury (fatal plus serious injuries) fraction was determined for each segment in each mishap, and the average injury fraction was determined for each segment in each pitch group (see table 31). Analyzing the data for the scenarios in which the aircraft is coming to the ground from the air (scenario G–M), the values (see table 31) show a minimal variation along the length of the cabin. For the more common nose-up attitude, there are slightly higher fractions aft, but the difference is not dramatic. For the nose-down attitude, attitude is a higher fraction in the cockpit, but the next highest is the overwing cabin. However, the nose-down data are a very small sample with only two mishaps. The zero-pitch attitude also displays an unusual pattern with overwing and tail segments displaying the highest injury fractions. The average positive pitch angle is +7.4 degrees; the average negative pitch angle is -5.5 degrees. There are very little data in the mishaps for scenario F; consequently, these will not be discussed. The data are displayed in the lower part of table 31 for completeness.

Table 31. Injury fraction by cabin segment for positive and negative pitch—W–B

Scenario G–M	Cockpit	Forward Cabin	Overwing Cabin	Rear Cabin	Tail	No. of Samples
Pitch Angle > 0	0.33	0.25	0.31	0.35	0.56	14
Pitch Angle = 0	0.33	0.38	0.49	0.35	0.50	6
Pitch Angle < 0	0.70	0.57	0.63	0.51	0.50	2
Scenario F						
Pitch Angle > 0	0.00	0.06	0.04	0.24	0.00	2
Pitch Angle = 0	0.00	0.00	0.00	0.20	0.25	4
Pitch Angle < 0	0.00	0.00	0.00	0.00	0.00	1

Injury fraction is the sum of fatally injured and seriously injured occupants divided by the number of occupants expressed as a decimal value.

3.3.5.4 Injury Dependence on Combined Velocity—W–B

The two-axis velocity plot can be used to visualize the dependence of injuries on impact velocities. The plot (see figure 31) displays all of the mishaps in scenarios G–M. The mishaps were grouped into three clusters: mishaps with less than 0.1 fraction of severe injuries (11 mishaps), mishaps with greater than 0.9 fraction of severe injuries (6), and mishaps with the fraction of severe injuries between 0.1 and 0.9 (5). The ellipse is the same 90^{th} percentile survivable velocity ellipse as used in figure 15. All the mishaps with injury fractions of 0.9 or greater fall near or outside the ellipse, as would be expected. Two of the five mishaps with intermediate injury fractions fall well outside the ellipse. Looking back to figure 15, it can be seen which four mishaps were PS and which four were NS. Figures 15 and 31 display the same data, but with the data points labeled for different characteristics: scenario and severe-injury fractions.

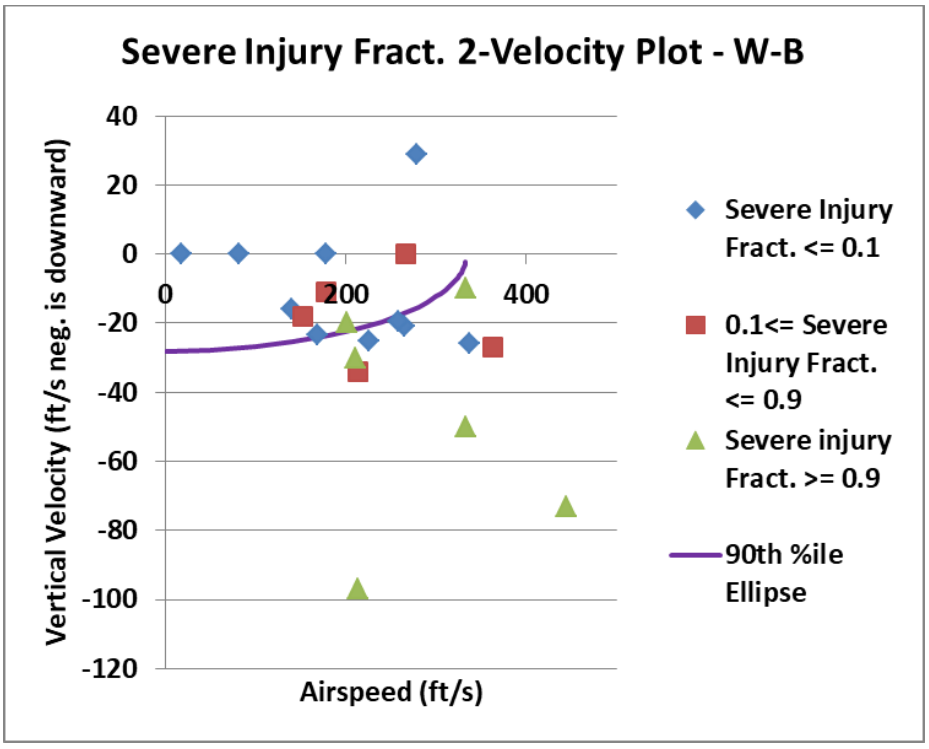

Figure 31. (G–M) severe-injury fraction on a two-velocity plot—W–B

3.3.5.5 Injuries Related to Damage Metric—W–B

The general trend is that as the aircraft damage metric increases, the fraction of occupants suffering severe injury also increases (see figure 32). The overrun scenario F and the compromised landing scenario G have low severe-injury fractions and low damage factors; consequently, discerning any trend within these scenarios is difficult. However, the other three scenarios generally exhibit the expected trend. Eliminating the overrun mishaps and plotting the injury fraction against the damage metric for the remaining events more clearly reveals the correlation (see figure 33). A trend line fit to the scenario G–M data results in a respectable correlation factor (R^2) value of 0.88. This plot clearly relates injury to damage, supporting the hypothesis that designing to minimize damage in a crash will reduce the number of severe injuries.

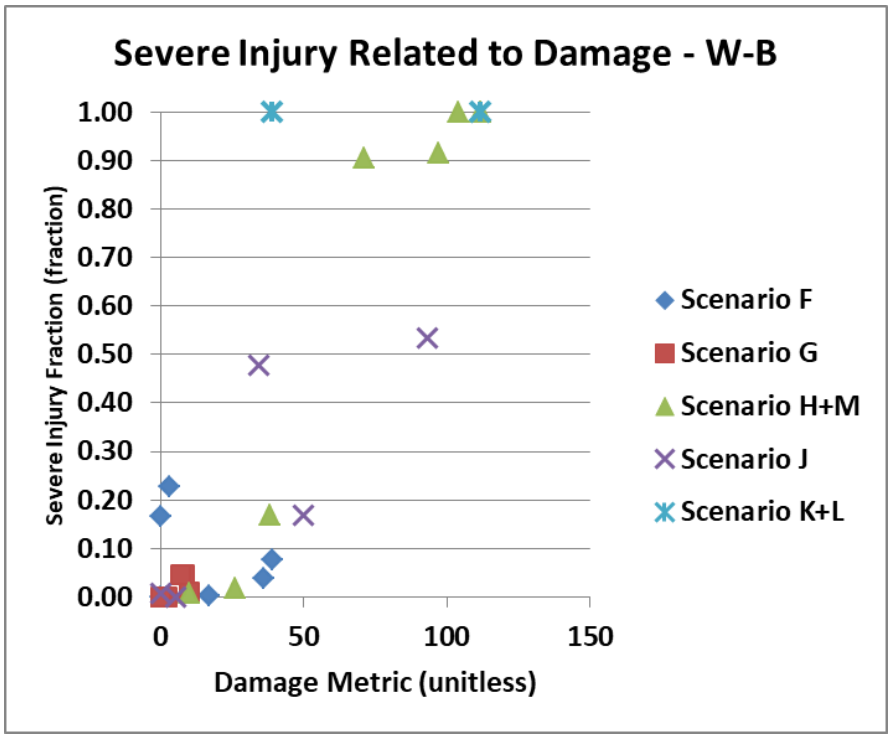

Figure 32. Severe-injury fraction dependence on damage metric—W–B

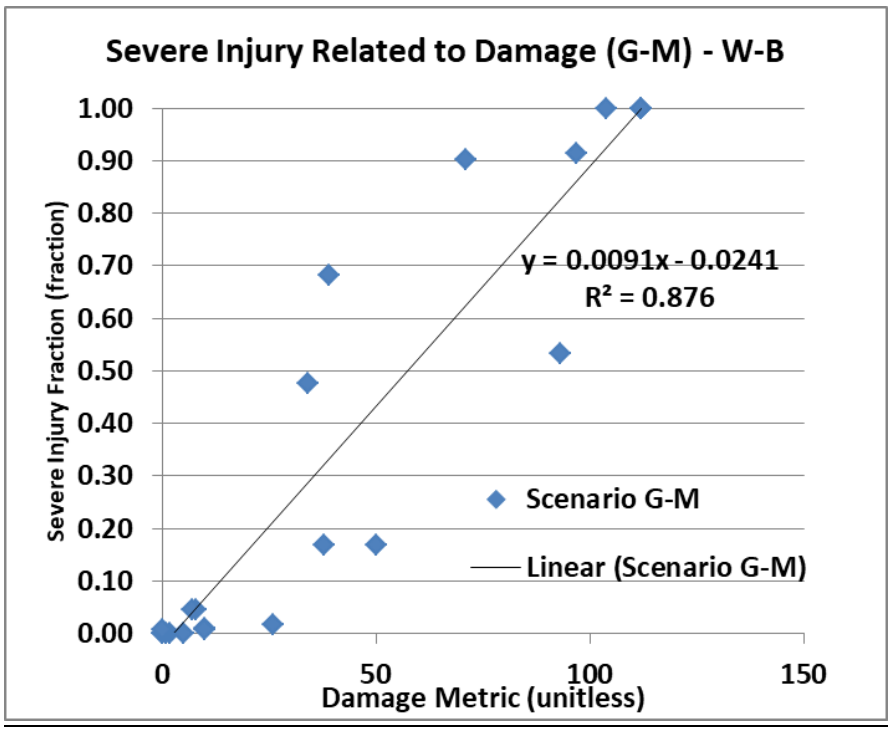

Figure 33. Severe injury vs. damage metric (G–M)—W–B

3.3.5.6 Injury Dependence on Obstacles—W–B

The effect of obstacles on the injury outcome is less clear than the effect on damage. In scenario F (the overruns), the presence of an obstacle raises the severe-injury fraction very modestly (see table 32) compared to no obstacle. The presence of an obstacle also raises the injury fraction for compromised landings (scenario G). For the remaining, more severe scenarios, the trend is actually counter to the anticipated effect; in each of these scenarios, the severe-injury fraction is higher in the absence of obstacles. The sample in each cell of the matrix is small, which reduces the validity of the conclusion.

Table 32. Influence of vertical impediments on severe-injury fraction—W–B

	Vertical Impediment—Average Fraction of Severe Injury (percent)	No Vertical Impediment—Average Fraction of Severe Injury (percent)	No. of Mishaps with a Vertical Impediment (No.)	No. of Mishaps with No Vertical Impediment (No.)
Scenario F	9%	6%	4	3
Scenario G	5%	1%	1	6
Scenario H+M	62%	64%	5	3
Scenario J	0%	30%	1	4
Scenario K+L	68%	100%	1	1

The injury data for all of the W–B mishaps was combined into one large dataset, and the severe-injury fraction means were determined. The mean severe-injury fraction for the 12 mishaps involving a vertical obstacle is 0.348, and the corresponding mean for the 17 mishaps without a vertical obstacle is 0.254. Therefore, the mean severe-injury fraction without obstacles is lower than the mean with obstacles, which is consistent with the trend seen in the damage metric. As with the damage metric, a two-sample T-test was applied to the data. The difference in the estimated means is 0.094, but the 90 percent confidence interval for the actual value of the difference is -0.167 to +0.355. This range includes the possibility of zero difference between the means. The *p*-value for the test is 0.544, whereas a value <0.100 is needed to confirm a statistically significant difference. The box plot (see figure 34) displays a similar effect to that seen in the damage metric box plot (see figure 24); the data are asymmetric with a few large values for the injury fraction increasing the mean values far above the median values. Therefore, the tracking of vertical impediments for W–B mishaps proved not to be indicative for either damage metric or for the severe-injury fraction.

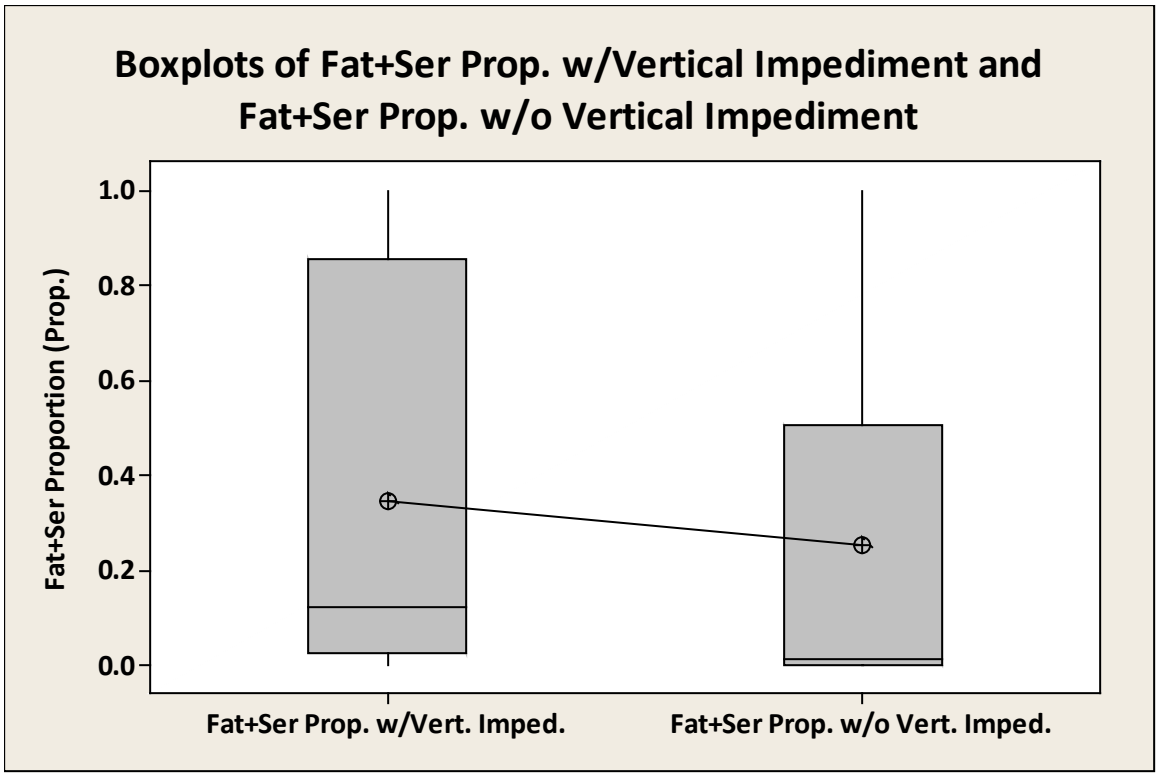

Figure 34. Box plot for severe-injury fraction with and without impediment—W–B

3.3.5.7 Thermal Injuries—W–B

The mishap investigations were not consistent in addressing the cause of death through autopsy. Many factors contributed to the lack of complete knowledge on fatal injury causation. The autopsy information of interest for this study is whether the fatality was caused by trauma or by thermal exposure. If by thermal exposure, then the question becomes whether trauma was a factor in not escaping or if it was the lack of an escape route. Unfortunately, there are very few events in which the data resolve either question. Of the 29 mishaps, seven had recorded thermal fatalities[†]. Of 6877 occupants in the study, 373 occupants were recorded as thermal fatalities, which is 5.4 percent of the occupants and one third of all the reported fatalities. The thermal fatalities were not uniformly distributed along the fuselage (see table 33). The greatest percentage of thermal injuries occurred to occupants in the overwing cabin, with the next most common occurrence in the aft cabin. One mishap (19721229A) had no thermal information; there were 96 fatalities in this mishap. Therefore, the 373 thermal fatalities could be undercounted by as many as 96.

[†] CSRTG ID nos. 20020415A, 20001031B, 19970806A, 19960613A, 19921221A, 19890719A, & 19820913A.

Table 33. Distribution of thermal injuries in aircraft—W–B

	Cockpit	Forward Cabin	Overwing Cabin	Aft Cabin	Tail
No. of Thermal Fatalities	0	52	176	144	1
Percent of All Occupants in Segment	0	3.1	6.8	5.9	1.6
No. of Mishaps With Reported Thermal Injuries	0	4	6	7	1

3.3.5.8 Injury Binary Logistic Regression Analysis—W–B

The binary logistic approach interprets the injury data as having just one of two outcomes for each occupant: severe injury (fatal or serious) or no injury (including minor injury). In this view for each parameter, the fraction of severe injuries will be low (near zero) for low values of the parameter, and the severe-injury probability will increase to the limit value of 1 as the value of the parameter increases. For example, the probability of severe injuries would be expected to increase as the impact velocity increases. (For details of the analysis, see section 2 of this report.) The equation that the logistic regression fits assumes that the dependence on the parameter is linear. Therefore, the equation being fitted is an exponential with a linear form to the exponent. The output variable '$\hat{p}$' is the estimated probability that an occupant in a similar crash scenario will be severely injured. In this analysis, the probability of severe injury to an individual is being used interchangeably with the fraction of severe injuries within a given mishap and over groups of mishaps. For an *n*-parameter model, the equation contains one constant and *n* coefficients. The linear form of the equation with one parameter is:

$$\hat{p} = \frac{1}{1+e^{-(\beta_0+\beta_1 x_1)}} \tag{2}$$

The analysis developed models to predict the probability that an occupant in a similar crash scenario will sustain a severe injury (serious or fatal) and, therefore, these models can be used to determine the fraction of occupants suffering serious or fatal injuries using the kinematic parameters of the mishaps. The prediction capability would then allow a value of the kinematic parameter to be associated with a probability of severe injury. For example, a successful model could assign a value for vertical impact velocity that would be associated with half of the occupants being seriously injured. One must be mindful that the model is valid only within the range of the parameter(s) used to create the model. Extrapolation beyond the lowest or highest input value of any parameter(s) may produce invalid results. Both single-parameter and multi-parameter models are created in this analysis.

In the following discussion, one evaluation for the success of the BLM is purely qualitative. This subjective evaluation by the author is in regard to the direction of the trend predicted by the model. The model-predicted trend (slope) is either "intuitive" (i.e., the slope expected by the author) or "counterintuitive" (i.e., opposite the slope expected by the author). The third possibility in this

column, “Bidirectional Response,” refers to parameters for which the injury response may increase on either side of a neutral value. For example, the injury fraction for a given mishap would be expected to be higher as the peak lateral acceleration increases to either side. If this parameter is modeled as a conventional monotonic parameter, the positive values of the parameter will tend to average out the negative values, and the injury fraction will appear to have no dependence on the parameter. Because an aircraft is symmetric left and right, it is argued here that the injury probability will also be symmetric left and right. Therefore, the peak lateral acceleration parameter has been revised for this analysis by taking the absolute value. This revision results in a parameter that is expected to cause an increasing injury fraction as the parameter value increases. Consequently, it is the absolute value of the lateral acceleration that will be modeled. The roll angle and yaw angle have been revised to the always positive off-nominal angle by adding together the absolute value of both angles. For the pitch angle, the crash dynamics vary between nose-up (positive pitch angle), wherein the main gear or tail strikes the ground first, and nose-down (negative pitch angle), wherein the nose or nose gear strikes the ground first. Using the absolute value approach for pitch angle will not resolve the issue for pitch because it cannot be argued that the injury outcomes are expected to be symmetric. Initially, pitch angle will be treated as a single parameter; later, treating the positive and negative values of the pitch angle as separate parameters will be investigated. In these initial single-parameter models for the W–B study, single-parameter models were generated for mishaps in each scenario in which there are sufficient mishaps; for scenarios G–M, that is all of the scenarios that were not runway overruns.

The seven mishaps in scenario F resulted in 53 occupants with fatalities, 95 occupants with serious injuries, and 1904 occupants with minor or no injuries. The results for the single-parameter analysis on the dataset for scenario F are shown in table 34. The *p*-value of the coefficient (in columns 2 and 3 of table 34) indicates whether the coefficient is likely to have a non-zero value. If the *p*-value is less than or equal to 0.100, then the coefficient’s value is likely a non-zero number and, therefore, the parameter influences the injury outcome. The fourth column, goodness-of-fit, is a *p*-value signaling the quality of fit between the data and the linear BLM. This measure of the validity of the model is uniformly low throughout the W–B analysis; even though the goodness-of-fit numbers are low, some models are showing statistical significance, and some are showing that predictions using the model can be useful based on summary measures of association. It is also important to note that the cause of the low goodness-of-fit values is known. The severe-injury fraction values vary widely and the outcome of the mishaps depend on an array of parameters (see figure 35). Figure 35 shows that the severe-injury fraction (blue data points are the observed values) does trend upward with increasing airspeed but that the values for the injury fraction vary widely within the range of mishap airspeeds. For example, there are two mishaps just above 300 ft/s—one with a severe-injury fraction equal to 0, and one with a severe-injury fraction of 0.23. As seen in tables 34 and 35, and figures 35 and 36, the multi-parameter models are generally more successful than the single-parameter models, indicating that the injury outcome of a mishap is not solely or even strongly determined by one parameter. Each point labeled “Prediction” is the injury probability predicted for the given parameter value (in this case, airspeed). The statistics predict that 90 percent of similar mishaps that occur with that parameter value will have injuries values between the upper and lower confidence limits (UCLs and LCLs), as shown in figure 35. The summary measures of association (values 0–1.0) are indicators of the model’s predictive capability (see table 34, sixth column). None of the single-parameter models for scenario F has strong predictive capability.

Table 34. Single-Parameter BLM for Scenario F—W–B

Parameter	Regressor Coefficient (*p*-value & coeff. value)	Constant Coefficient (*p*-value & coeff. value)	Goodness-of-Fit (*p*-value)	Summary Measures of Assoc.	Model Predictive Capability	Trend: Intuitive or Counter
Airspeed	*p*=0.000 +0.006	*p*=0.000 -3.815	0.000 0.000 0.000	0.37 0.43 0.05	Medium Medium Low	Intuitive
Vertical Velocity	*p*=0.008 -0.013	*p*=0.000 -2.597	0.000 0.000 0.000	0.31 0.51 0.04	Medium Medium Low	Counterintuitive
Flight-Path Angle	Model failed to converge				No model	No model
Pitch Angle	*p*=0.036 -0.077	*p*=0.000 -2.538	0.000 0.000 0.000	0.08 0.34 0.01	Low Medium Low	Bidirectional response[†]
Off-nominal Angle	*p*=0.000 +0.042	*p*=0.000 -2.674	0.443 0.452 0.443	0.12 0.27 0.02	Low Low Low	Intuitive
Vertical Peak Deceleration	*p*=0.637 +0.010	*p*=0.000 -2.527	0.000 0.000 0.000	0.06 0.06 0.01	Low Low Low	Intuitive
Longitudinal Peak Deceleration	*p*=0.872 -0.002	*p*=0.000 -2.567	0.000 0.000 0.000	0.20 0.25 0.03	Low Low Low	Intuitive
Absolute Value Lateral Peak Deceleration	*p*=0.000 -3.714	*p*=0.000 -2.137	0.000 0.000 0.000	0.31 0.63 0.04	Medium Medium Low	Counterintuitive

[†] Injury fraction may increase with increasing positive pitch angle and/or may increase as pitch angle is more negative.

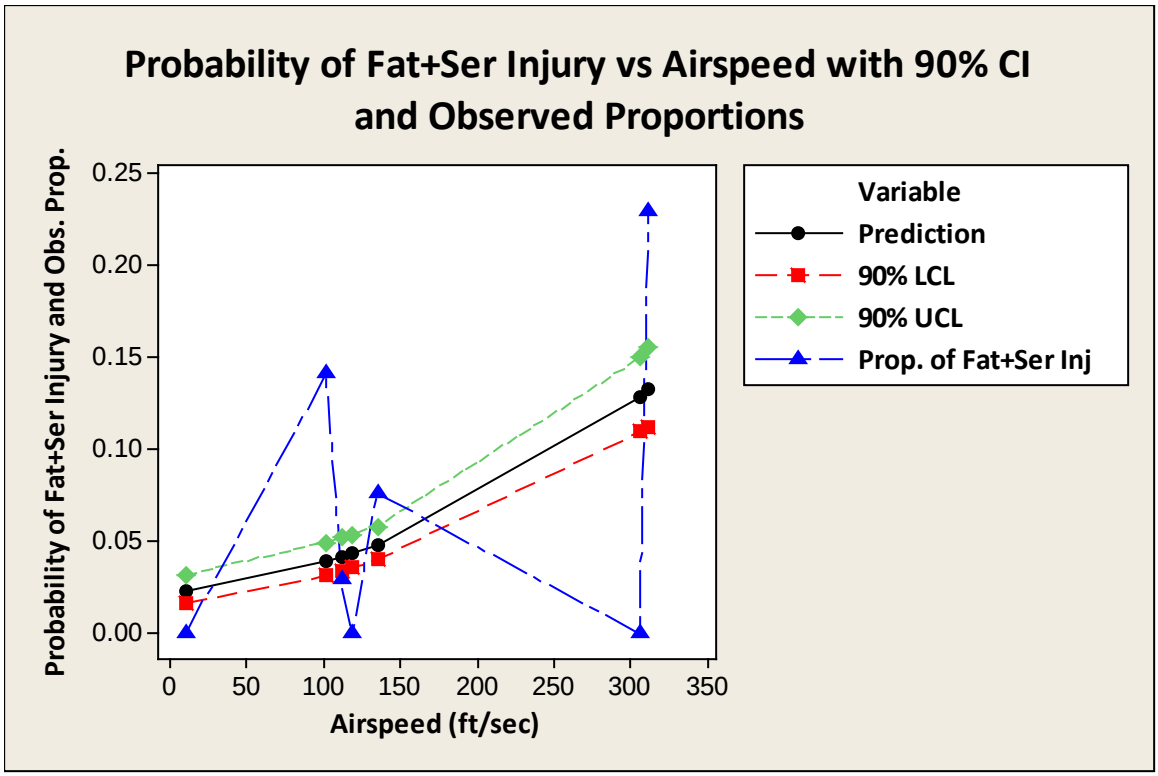

Figure 35. Airspeed BLM model for scenario F—W–B

The multi-parameter model for scenario F has a range of predictive capability depending on the statistic being used (see table 35); the summary measures of association range from a low of 0.09 to a high of 0.74, indicating good predictive capability by at least one measure. The full model with all of the parameters would not converge. Consequently, the non-significant parameters were removed one by one until the model converged. The remaining regressors are the airspeed, vertical velocity, and the off-nominal angle (summed absolute values of roll and yaw). Therefore, the model contains three linear coefficients and one constant. The model predicts the severe-injury probability, $\hat{p}$, for a specific set of input values; this severe-injury probability for a single occupant is taken to be equivalent to the fraction of all occupants severely injured in the mishap. The equation for evaluating $\hat{p}$ is equation (3). The coefficients and the useful range for each parameter are listed in table 35. As a means of presenting the prediction capability of the model (see figure 36), the model-predicted value for each observed injury fraction is plotted against the observed value. If the model predicted each value correctly, then each point would fall on the diagonal line (blue) representing that the two plotting coordinates are equal. It is evident that three of the six predicted points fall reasonably close to the ideal line. Figure 36 also shows that, because of the limited range of the severe-injury fractions in the scenario F mishaps, the predictive range of the model is also limited. The severe-injury fractions for scenario F fell within the range 0.0 to 0.28. For the reader's convenience, the corresponding usable range for the input parameters is provided in table 35 column "Goodness-of-Fit" as the "Useful Range" with the appropriate units.

Table 35. Multi-parameter, BLM scenario F – W–B

Parameter	Coefficient (coeff. value)	Coefficient (*p*-value)	Goodness-of-Fit (*p*-value)	Summary Measures of Assoc.	Predictive Capability
Model properties			0.000 0.000 0.000	0.64 0.74 0.09	Medium Medium Low
Constant	-7.532	*p*=0.000			
Regressors:			Useful Range		
Airspeed (x_1)	+0.019	*p*=0.000	+10 to +312 ft/sec		
Vertical Velocity (x_2)	-0.068	*p*=0.000	-39.1 to +14 ft/sec		
Off-nominal Angle (x_3)	+0.180	*p*=0.000	0 to +21 degrees		

$$\hat{p} = \frac{1}{1+e^{-(-7.53217+0.0191643x_1-0.0676750x_2+0.179960x_3)}} \quad (3)$$

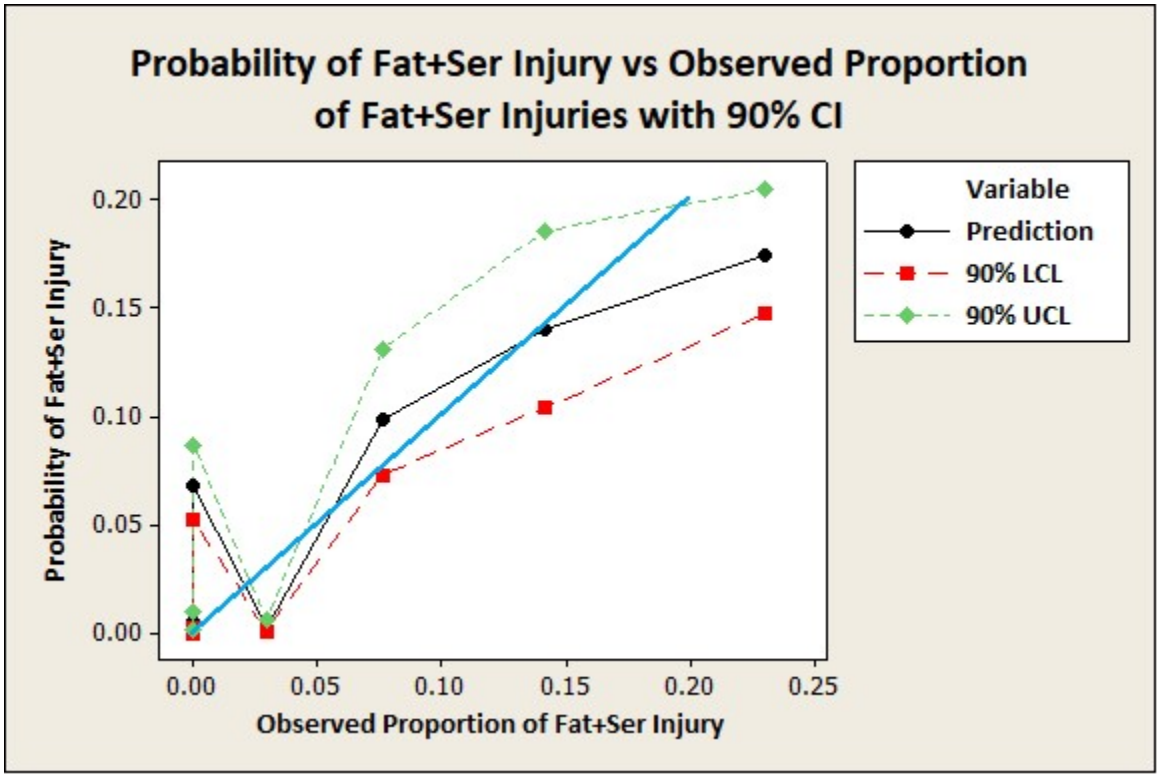

Figure 36. Scenario F multi-parameter model predicted vs. measured severe injury—W–B

Scenario G was the least-injurious scenario with only two serious injuries and zero fatalities in one mishap out of seven mishaps; there were 1546 occupants with minor or no injuries. Consequently,

the model had only a single, non-zero severe-injury fraction. The models for four of the parameters (e.g., airspeed, vertical velocity, flight path angle, and off-nominal angle) failed to converge (see table 36). The peak longitudinal acceleration and the pitch angle resulted in models that indicate the medium predictive capability, whereas peak vertical acceleration has low predictive capability.

The multi-parameter model did eventually converge after several parameters were removed. However, none of the remaining parameters had significance (all *p*-values exceeded the criteria by a wide margin).

Table 36. Single parameter BLM for scenario G—W–B

Parameter	Regressor Coefficient (*p*-value & coeff. value)	Constant Coefficient (*p*-value & coeff. value)	Goodness-of-Fit (*p*-value)	Summary Measures of Assoc.	Model Predictive Capability	Trend: Intuitive or Counter
Airspeed	Failed to converge.					
Vertical Velocity	Failed to converge.					
Flight-Path Angle	Failed to converge.					
Pitch Angle	*p*=0.286 +0.381	*P*=0.007 -9.809	0.247 0.262 0.299	0.46 0.54 0.00	Medium Medium Low	Bidirectional parameter
Off-nominal Angle	Failed to converge.					
Vertical Peak Deceleration	*p*=0.550 -0.240	*P*=0.000 -6.207	0.056 0.191 0.029	0.20 0.23 0.00	Low Low Low	Counter intuitive
Longitudinal Peak Deceleration	*p*=0.610 -1.756	*P*=0.000 -7.064	0.010 0.055 0.010	0.60 0.70 0.00	Medium Medium Low	Intuitive
Absolute Value Lateral Peak Deceleration	Failed to converge.					

The combined scenario H+M contains 763 fatalities, 193 serious injuries, and 603 minor/no injuries in 8 mishaps. All the single-parameter models converged (see table 37). Despite a well-populated dataset, only two of the single-parameter models (e.g., off-nominal angle and peak longitudinal deceleration) have high predictive capability. Most of the models do show medium predictive capability, and all have the expected slope direction. The multi-parameter model is significant with three parameters (see table 38). These three parameters are airspeed, flight path, and absolute value of lateral acceleration.

Table 37. Single parameter BLMs for scenario G+M—W–B

Parameter	Regressor Coefficient (p-value & coeff. value)	Constant Coefficient (p-value & coeff. value)	Goodness -of-Fit (p-value)	Summary Measures of Assoc.	Model Predictive Capability	Trend: Intuitive or Counter
Airspeed	*p*=0.000 +0.014	*P*=0.000 -2.602	0.000 0.000 0.000	0.51 0.53 0.24	Medium Medium Low	Intuitive
Vertical Velocity	*p*=0.000 +0.066	*P*=0.000 -1.137	0.000 0.000 0.000	0.44 0.45 0.21	Medium Medium Low	Intuitive
Flight-Path Angle	*p*=0.000 -0.197	*P*=0.000 -0.834	0.000 0.000 0.000	0.44 0.45 0.21	Medium Medium Low	Intuitive
Pitch Angle	*p*=0.000 -0.205	*P*=0.000 +1.926	0.000 0.000 0.000	0.52 0.54 0.24	Medium Medium Low	Bidirectional parameter
Off-nominal Angle	*p*=0.000 +0.460	*P*=0.000 -3.654	0.000 0.000 0.000	0.90 0.96 0.43	High High Medium	Intuitive
Vertical Peak Deceleration	*p*=0.310 +0.006	*P*=0.000 +0.426	0.000 0.000 0.000	0.43 0.45 0.21	Medium Medium Low	Intuitive
Longitudinal Peak Deceleration	*p*=0.000 -0.329	*P*=0.000 -2.968	0.000 0.000 0.000	0.86 0.89 0.41	High High Medium	Intuitive
Absolute Value Lateral Peak Deceleration	*p*=0.000 +0.179	*P*=0.136 -0.097	0.000 0.000 0.000	0.69 0.71 0.33	Medium Medium Medium	Intuitive

Table 38. Scenario H+M multi-parameter BLM scenario H+M—W–B

Parameter	Coefficient (coeff. value)	Coefficient (*p*-value)	Goodness-of-Fit (*p*-value)	Summary Measures of Assoc.	Predictive Capability
Model properties			0.000 0.000 0.000	0.72 0.74 0.34	Medium Medium Low
Constant	-4.038	*p*=0.000			
Regressors:			Useful Range		
Airspeed (x_1)	+0.005	*p*=0.000	169 to 333 ft/sec		
Flight Path (x_2)	-0.464	*p*=0.000	-2 to -27 degrees		
A.V. Lateral Deceleration (x_3)	+0.121	*p*=0.000	0 to 33 G		

$$\hat{p} = \frac{1}{1+e^{-(-4.03889+0.0054680x_1-0.464104x_2+0.121107x_3)}} \quad (4)$$

The equation for the probability of severe injury, $\hat{p}$, is shown in equation 4. The predictive capability of the model is medium for the multi-parameter model, as shown in figure 37, with three of eight points falling near the ideal line.

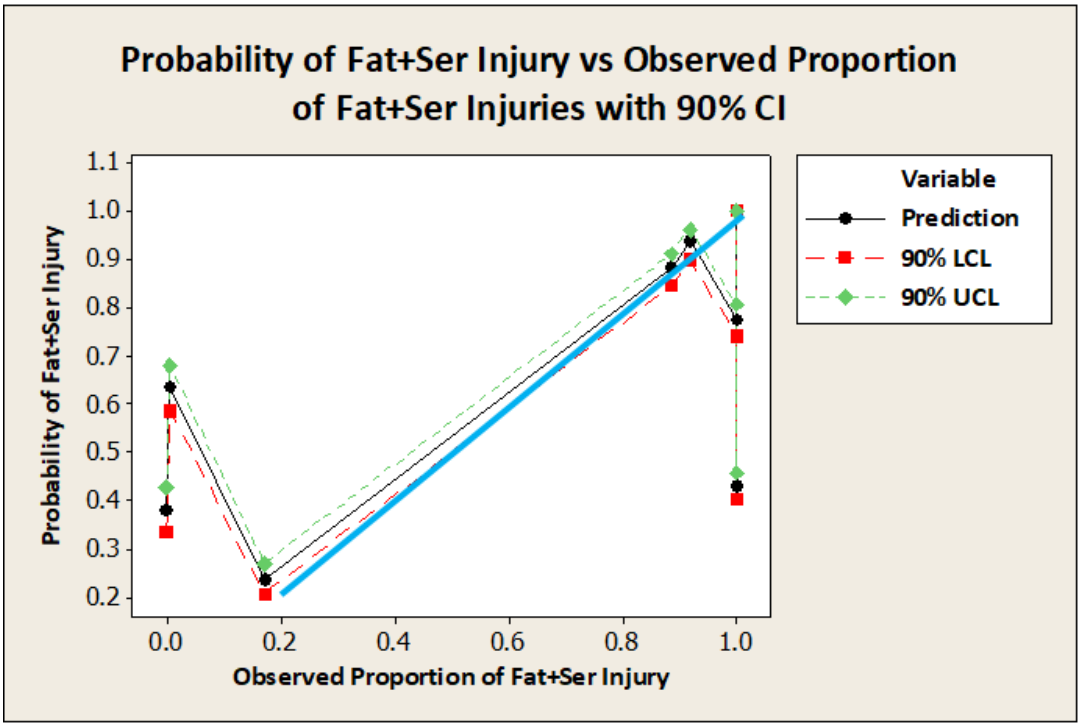

Figure 37. Scenario H+M multi-parameter model predicted vs. measured—W–B

Scenario J encompasses five mishaps with 167 fatalities, 201 serious injuries, and 1084 occupants with minor or no injury. Only the off-nominal angle of the single-parameter models (see table 39) has a high predictive capability, but most have medium predictive capability by at least some statistics.

Table 39. Single-parameter BLMs for scenario J—W–B

Parameter	Regressor Coefficient (p-value & coeff. value)	Constant Coefficient (p-value & coeff. value)	Goodness-of-Fit (p-value)	Summary Measures of Assoc.	Model Predictive Capability	Trend: Intuitive or Counter
Airspeed	*p*=0.000 +0.004	*p*=0.000 -2.104	0.000 0.000 0.000	0.33 0.39 0.12	Medium Medium Low	Intuitive
Vertical Velocity	*p*=0.000 +0.123	*p*=0.000 -4.235	0.000 0.000 0.000	0.55 0.65 0.21	Medium Medium Low	Intuitive
Flight-Path Angle	*p*=0.000 -0.311	*p*=0.000 -2.741	0.000 0.000 0.000	0.55 0.65 0.21	Medium Medium Low	Intuitive
Pitch Angle	*p*=0.109 -0.016	*p*=0.000 -1.054	0.000 0.000 0.000	-0.06 -0.07 -0.02	Low Low Low	Bidirectional parameter
Off-nominal Angle	*p*=0.000 +0.100	*p*=0.000 -2.541	0.000 0.000 0.000	0.66 0.78 0.25	Medium High Low	Intuitive
Vertical Peak Deceleration	*p*=0.000 -0.140	*p*=0.000 -1.043	0.000 0.000 0.000	0.44 0.52 0.17	Medium Medium Low	Counter Intuitive
Longitudinal Peak Deceleration	*p*=0.000 +0.208	*p*=0.001 -0.419	0.000 0.000 0.000	0.28 0.33 0.11	Low Medium Low	Counter Intuitive
Absolute Value Lateral Peak Deceleration	*p*=0.000 +0.329	*p*=0.000 -2.370	0.000 0.000 0.000	0.62 0.74 0.24	Medium Medium Low	Intuitive

The multi-parameter model (see table 40) has three regressors: airspeed, vertical velocity, and flight path. However, like the single-parameter models, the multi-parameter model has only medium predictive capability (see table 40 and figure 38). The equation for the probability of injury, $\hat{p}$, is provided in equation (5).

Table 40. Multi-parameter BLM scenario J—W–B

Parameter	Coefficient (coeff. value)	Coefficient (*p*-value)	Goodness-of-Fit (*p*-value)	Summary Measures of Assoc.	Predictive Capability
Model Properties			0.000 0.000 0.000	0.55 0.65 0.21	Medium Medium Low
Constant	-3.372	*p*=0.000			
Regressors			Useful Range		
Airspeed (x_1)	+0.012	*p*=0.000	17-363 ft/sec		
Vertical Velocity (x_2)	-0.222	*p*=0.009	0 to 34 ft/sec		
Flight Path (x_3)	-0.913	*p*=0.000	0 to -9.2 degrees		

$$\hat{p} = \frac{1}{1+e^{-(-3.37171+0.0117539x_1-0.221931x_2-0.913159x_3)}} \quad (5)$$

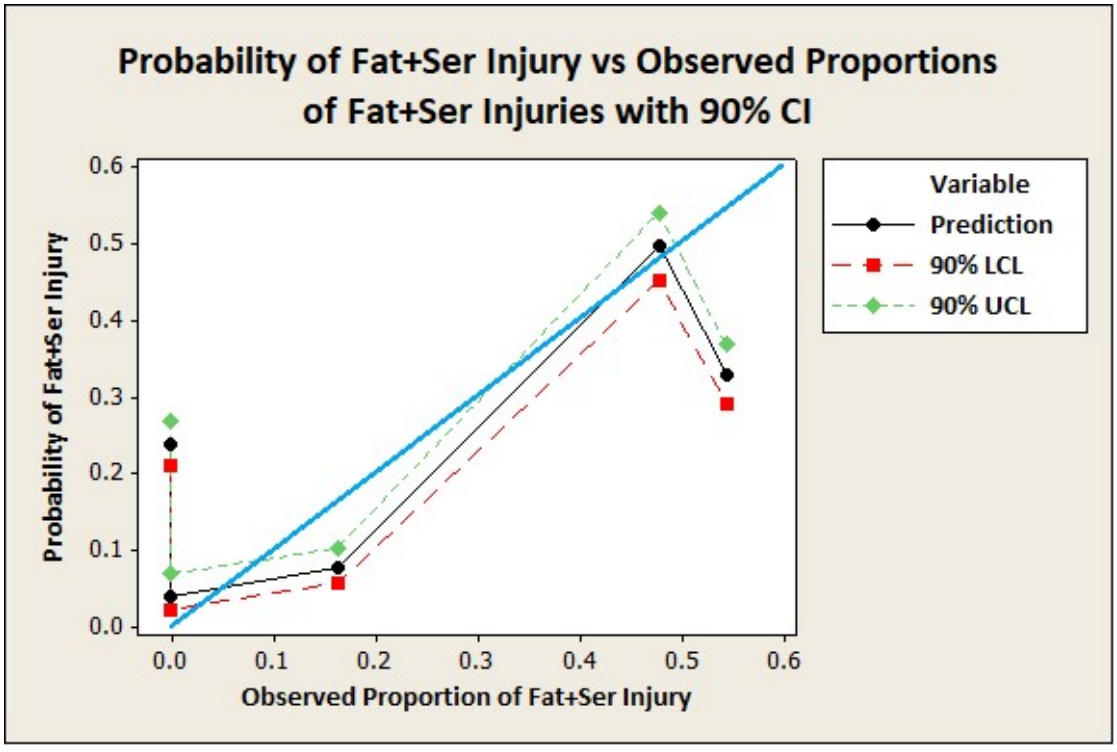

Figure 38. Scenario J multi-parameter model prediction vs. measured—W–B

Scenario K+L contained only two scenario K mishaps and zero scenario L mishaps. These two mishaps resulted in 181 occupants fatally injured, 42 seriously injured, and 55 with minor or no injury. Sufficient data were not available for the single-parameter models to converge, and there were not sufficient data for the multi-parameter model to run.

Treating all the mishaps except scenario F (overruns) as one dataset (scenario G–M) creates a larger dataset (22 mishaps), which has the potential for better statistics. The mishaps have commonality in that they are all impacts involving an aircraft attempting to fly or to land; therefore, the aircraft are arriving at the terrain from the air. Even so, just one single-parameter model (see table 41) has high predictive capability and five have medium predictive capability. The longitudinal peak deceleration model has high predictive capability, whereas airspeed, vertical velocity, flight path, and the absolute value of lateral peak deceleration have medium predictive capability.

Table 41. Single-parameter BLM for scenario G–M—W–B

Parameter	Regressor Coefficient (*p*-value & coeff. value)	Constant Coefficient (*p*-value & coeff. value)	Goodness-of-Fit (*p*-value)	Summary Measures of Assoc.	Model Predictive Capability	Trend: Intuitive or Counter
Airspeed	*p*=0.000 +0.008	*p*=0.000 -2.710	0.000 0.000 0.000	0.33 0.33 0.14	Medium Medium Low	Intuitive
Vertical Velocity	*p*=0.000 +0.064	*p*=0.000 -2.167	0.000 0.000 0.000	0.49 0.51 0.22	Medium Medium Low	Intuitive
Flight Path Angle	*p*=0.000 -0.256	*p*=0.000 -2.025	0.000 0.000 0.000	0.52 0.54 0.23	Medium Medium Low	Intuitive
Pitch Angle	*p*=0.000 -0.043	*p*=0.000 -0.571	0.000 0.000 0.000	0.14 0.15 0.06	Low Low Low	Bidirectional
Off-nominal Angle	*p*=0.000 +0.111	*p*=0.000 -1.902	0.000 0.000 0.000	0.63 0.72 0.28	Medium Medium Low	Intuitive
Vertical Peak Deceleration	*p*=0.000 +0.041	*p*=0.000 -0.913	0.000 0.000 0.000	0.27 0.28 0.12	Low Low Low	Intuitive
Longitudinal Peak Deceleration	*p*=0.000 -0.336	*p*=0.000 -2.530	0.000 0.000 0.000	0.81 0.82 0.35	High High Low	Intuitive
Absolute Value Lateral Peak Deceleration	*p*=0.000 +0.252	*p*=0.000 -1.364	0.000 0.000 0.000	0.63 0.68 0.27	Medium Medium Low	Intuitive

The multi-parameter model incorporates seven of the kinematic parameters and has high predictive capability by two of the three summary measures of association (see table 42).

Table 42. Multi-parameter BLM for scenario G–M—W–B

Parameter	Coefficient (coeff. value)	Coefficient (p-value)	Goodness-of-Fit (p-value)	Summary Measures of Assoc.	Predictive Capability
Model properties			0.000 0.000 0.000	0.90 0.91 0.39	High High Medium
Constant	-4.082	0.000			
Regressors:			Usable Range		
Airspeed (x_1)	+0.001	0.088	16.9 to 445 ft/sec		
Vertical Velocity (x_2)	+0.032	0.000	-29 to 97 ft/sec		
Flight Path (x_3)	+0.082	0.012	-27 to +5.9 degrees		
Vertical Peak Deceleration (x_4)	+0.058	0.001	-17 to 20 G		
Longitudinal Peak Deceleration (x_5)	-0.271	0.000	0 to -26.6		
Absolute Value Lateral Peak Deceleration (x_6)	+0.055	0.046	0 to 33 G		
Off-nominal Angle (x_7)	+0.087	0.000	0 to 155 degrees		

$$p\hat{} = 1/(1 + e\hat{}(-(-4.08189 + 0.0014424x_1 + 0.0317243x\_2 + 0.0816510x\_3 + 0.0580210x\_4 - 0.271034x\_5 + 0.0550172x\_6 + 0.0871654x\_7))) \quad (6)$$

The model equation for predicting the probability of severe injury, $\hat{p}$, or equivalently the severe-injury fraction in a given mishap, is shown in equation (6) below. The multi-parameter model predicted injury fractions are plotted against the observed values (see figure 39). In this plot, agreement between the prediction and the measured value is represented by a point falling on the diagonal blue line running from (0,0) to (1,1). This line represents the points where the predicted severe-injury fraction equals the measured severe-injury fraction. For the actual figure, the points are plotted in ascending order of measured value so that the 90 percent lower and upper confidence limits for each point can be displayed in a manner to create a confidence corridor. The statistics predict a range within which the actual value has a 90-percent chance of falling. This range is defined by the upper and LCL. The plot displays several mishap points near the ideal diagonal line, including those near the origin and up to approximately 0.55 on the observed fraction axis. These points are followed by an obvious under-prediction and then by an over-prediction. Near the limit at 1.0 (all severe injuries), there are two well-predicted points and one poorly predicted point (low).

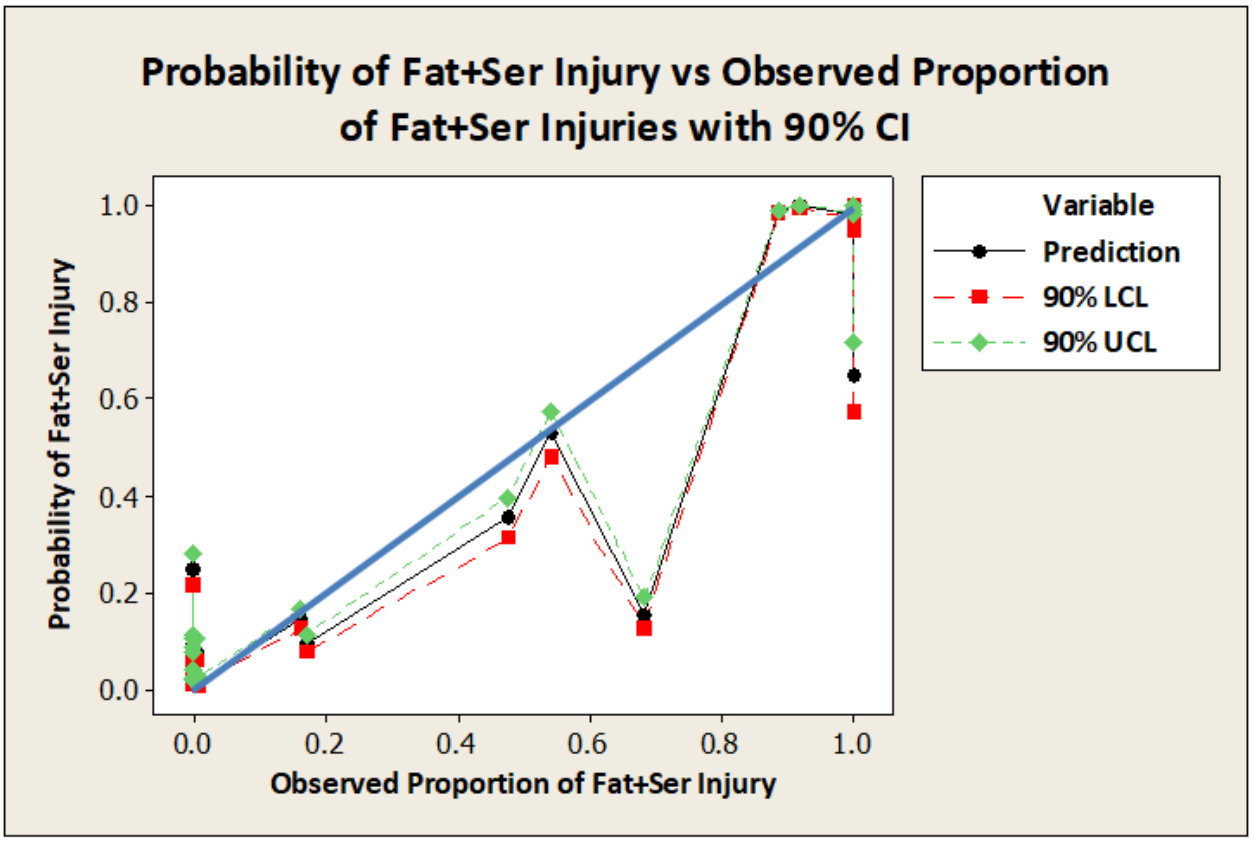

Figure 39. Scenario G–M multi-parameter predicted and observed injury fractions—W–B

The objective of the BLM analysis is to obtain models useful for selecting crashworthiness design criteria. However, only a few of the models in the single scenario analyses appear to be useful for that purpose. In scenario F, the multi-parameter model incorporates airspeed, vertical velocity, and off-nominal angle to give a model capable of predicting severe-injury fraction. The airspeed and vertical velocity are parameters of special interest to crashworthy design. For scenario H+M, two single-parameter models—longitudinal acceleration and off-nominal angle—resulted in high predictive capability. The multi-parameter model for scenario H+M contained only three parameters: airspeed, flight-path angle, and lateral acceleration. However, the model does have moderate predictive capability for these three parameters, which are useful for crashworthiness specification. Scenario G and scenario K+L produced no usable models because of either a lack of injuries or a low number of mishaps. Scenario J also produced no useful models, though not for lack of mishaps or injuries, but because the data were too scattered to give a clear correlation. Overall, in the rather small W–B dataset, the injury outcomes were too diverse relative to the kinematic parameters to develop anything but models valid for limited subsets of the data. The multi-parameter model for the combined scenario G–M is arguably the best model to use for crashworthiness considerations. The model contains all of the critical parameters except the pitch angle and has high predictive capability.

4. N–B IMPACT STUDY

4.1 SELECTING MISHAPS FOR THE STUDY—N–B

The term N–B has no formal definition in the regulatory environment, but generally, the term refers to aircraft with one lengthwise aisle. Aircraft with two aisles are also being studied (see section 3) and are referred to in this work as W–B aircraft. Rather than try to query the database by weight class or other database fields, a list of N–B aircraft was assembled (see table 43), and the CSTRG database was queried for each type on the list. Only western built N–B aircraft were included because experience with the RJ [1] study revealed that very few mishaps involving non-western-built aircraft were investigated and reported thoroughly enough to provide the information needed for this study. The series of N–B queries by specific aircraft type retrieved 719 candidate mishaps. Reviewing the summaries for applicability reduced the list to 219 that appeared to be suitable for the study. Reading the reports and other information on these 219 resulted in 86 mishaps being included in the study.

Table 43. Aircraft types queried for mishaps—N–B

A319	B757	MD83
A320	CV880	MD87
A321	CV990	MD88
B707	DC8	MD90
B717	DC9	Trident
B720	MD80	VC-10
B727	MD81	
B737	MD82	

4.2 ANALYSIS—N–B

The following sections describe how the analysis was conducted and present the results for the N–B dataset. To ensure consistent results, the same methods were used to analyze the datasets for the two classes of aircraft. The analysis method was modified out of necessity. In some cases, because the N–B dataset contains more mishaps than the W–B, the analysis was taken a bit further.

4.2.1 Aircraft Population—N–B

Although a diverse population of aircraft was sought, ultimately, the population available consists only of those airplanes that have crashed in mishaps with sufficiently well-documented investigations. The aircraft in the dataset are characterized by such design features as number of engines, location of engines, wing position, weight class, and seats per row. Tables 44–47 characterize the mishap aircraft in terms of these parameters. The types of aircraft, together with the number of mishaps in the study, are shown in table 44. All aircraft in this study were powered by nonprop turbine engines. The database differentiates between turboprop and turbojet, but does not differentiate turbofans from turbojets. The majority of aircraft (77 of 86) in this study were in

weight class C—100,000 to 250,000 lb (see table 45). The remaining nine aircraft are in weight class D—250,000 to 400,000 lb.

The N–B aircraft had one of three engine configurations (see table 46): engines on wings, engines on the tail, or engines on the tail plus one engine under the vertical stabilizer (referred to as "fin" for brevity). The eight aircraft with the tail and fin configuration had three engines (see tables 46 and 47). Sixty-eight aircraft in the study had two engines and ten aircraft had four engines (see table 47). All of the aircraft in the N–B study were of the low-wing configuration.

Table 44. Aircraft type and quantity in N–B study

A320 (1)	B737-600 (1)	DC9-30 (12)
A320-200 (4)	B737-700 (2)	DC9-80 (1)
A321-200 (2)	B737-800 (7)	MD81 (1)
B707-100 (2)	B737-900 (1)	MD82 (4)
B707-300 (2)	B727-000 (2)	MD83 (2)
B737 (1)	B727-200 (6)	MD88 (2)
B737-200 (12)	B757-200 (2)	DC8-60 (4)
B737-300 (4)	B717-200 (1)	CV880 (1)
B737-400 (3)	DC9 (1)	VC10 (1)
B737-500 (1)	DC9-10 (3)	

Table 45. Weight category populations—N–B

Weight Category	Number of Aircraft in the Dataset
C (100,000–250,000 lb)	77
D (250,000–400,000 lb)	9
E (> 400,000 lb)	0

Table 46. Aircraft engine configuration populations—N–B

Engine Configuration	Number of Aircraft With Configuration
Engines on Wing	50
Engines on Tail	28
Engines on Tail and Fin	8

Table 47. Number of engines on aircraft—N–B

Number of Engines	Number of Aircraft in the Dataset
2	68
3	8
4	10

Being one-aisle aircraft, the N–B aircraft generally have fewer seats across than do the W–B aircraft. All aircraft in the N–B study had a maximum of either five or six seats per row. Aircraft with a maximum number of six across were the most common configuration (see table 48). The number of passenger seats in the aircraft is shown in table 49 with the number of people aboard. The "total people aboard" is from the CSTRG database and includes crew members and infants. In the analysis, crew members were tracked separately from passengers; infants were not counted because they would normally not be restrained. The number of occupants involved in the N–B analysis is 10,335.

Table 48. Maximum seats per row—N–B

Total Seats per Row (Maximum)	Number of Aircraft
5	29
6	57

Table 49. Number of seats and occupants—N–B

	Total Passenger Seats	Total People Aboard†
Average Number	141	120
Median Number	137	118
Greatest Number	236	245
Least Number	83	26

† Total people aboard includes passengers and crew.

The mishaps included in the study cover a range of scenarios and severity. These mishaps occurred in several phases of flight, but approach and landing predominate (see table 50), together accounting for 69 percent of the mishaps. The study mishaps occur in the low-altitude phases of flight.

Table 50. Phase of flight—N–B

Phase of Flight	Number of Mishaps (No.)	Fraction of Mishaps (percent)
Aborted Takeoff	8	9
Takeoff	10	12
Climb	4	5
Flight	0	0
Approach	12	14
Go-around	5	6
Landing	47	55
Total	86	100
Characterized as 'Overrun,' including both takeoff and landing (included above)	26	30

From the CSTRG database query, 37 of the mishaps resulted in "substantial" damage, and 45 aircraft were considered "destroyed." The aircraft in four mishaps were rated as having minor damage. Fatalities occurred in 33 of the 86 mishaps, and serious injuries occurred in 50 of the 86 mishaps. The number of fatalities exceeded the number of serious injuries.

Injuries caused by the impact are of primary interest (see table 51). In many investigation reports, minor injury counts are combined with no-injury counts; consequently, these two counts are combined throughout this analysis for consistency. The distribution of injuries will be discussed later in the report. The injury numbers in this table are from the CSTRG database and include all aboard the aircraft.

Table 51. Overview severity of injuries—N–B

	Total Occupants/ Mishap	Total Fatalities/ Mishap	Total Severe Injuries/ Mishap	Total Minor-No Injury/ Mishap
Median	116.5	0	2	94.5
Average	120.0	21	9	89.0
Maximum	245.0	180	81	242.0
Minimum	26.0	0	0	0

An emergency evacuation was conducted in 57 of the 86 mishaps. Where an evacuation did not occur, there was either no danger of fire or the mishap was so catastrophic that the escape of the few survivors could not be characterized as an evacuation.

4.2.2 Mishap Scenarios—N–B

Like the W–B mishaps, the N–B mishaps cover a diverse range of circumstances. As with the W–B study, grouping the mishaps in the N–B study into scenarios for analysis proved to be useful. The same set of scenarios is used to describe the N–B mishaps. The 86 mishaps were classified into 7 scenarios (see table 52). Scenario F, runway overruns following either landing or an aborted takeoff, is the most common scenario in the N–B dataset (26 mishaps). The scenario characterized as "compromised landing with mild impact" (scenario G) includes landings in which a failure of some type occurred that damaged the aircraft, but the aircraft generally remained under control and on or near the runway (11 mishaps). Scenario H (11 mishaps) consists of impacting terrain short of the runway during an attempted approach or landing; these impacts are characterized by higher-than-normal but moderate descent rates and moderate-to-low airspeeds. Scenario J (16 mishaps) consists of hard landings that result in sufficient loss of control to cause excursion from the runway and severe damage to the aircraft. The differentiating characteristic between scenario G and scenario J is the extent of control loss and the severity of impact. Scenario K (7 mishaps) is loss of control on takeoff due to contaminated wings, mismanaged engine failure, or a misconfigured aircraft. Scenario K includes misjudged and mishandled go-around attempts, the common characteristic being the engines at high thrust, and the intent to fly rather than to land.

The two wind-related scenarios were created beyond those developed in the RJ study, but these two new scenarios are variations on two scenarios used in the RJ study. Scenario M is similar to scenario H, landing short, with the additional consideration of wind as a contributing influence.

As shown in table 52, five N–B mishaps were assigned to this scenario. The reason to identify the scenario M events separately was to reveal a possible trend related to wind-shear events. For many of the analyses in this report, the H & M mishaps are combined into a single scenario because the two scenarios are very similar. As with scenario K, seven mishaps were influenced, if not actually caused, by wind shear. Consequently, scenario L was created to identify loss of control on takeoff with a strong effect of wind shear (7 mishaps). The result of analyzing the wind-affected events is discussed in the report.

Table 52. Number of study mishaps by scenario—N–B

Scenario	Number of N–B Mishaps (no.)	Fraction of N–B Mishaps (percent)
Scenario F—Runway overrun (landing or takeoff)	26	30
Scenario G—Compromised landing (mild, but damaging impact)	11	13
Scenario H—Impacted terrain short of runway (reduced speed and thrust during approach)	14	16
Scenario J—Hard landing with loss of control post-impact	16	19
Scenario K—Loss of control during or following takeoff or go around attempt (includes wing contamination)	7	8
Scenario L—Loss of control on takeoff or go-around attempt contributed to by wind influence	7	8
Scenario M—Impacted terrain short of runway due to wind influence	5	6
Total	86	100
Scenarios H + M	19	22
Scenarios K + L	14	16

To determine how representative the study sample of the N–B mishaps is with regard to the frequency of each scenario, the larger population of mishaps returned by the original query (719) was reviewed. The summary descriptions were read, and each mishap was assigned to one of the scenarios in which sufficient information was present. There were 276 mishaps of a suitable type for inclusion that could be assigned a scenario. The remaining mishaps either had insufficient information or were not applicable to this study. The study sample tracks the larger population (see table 53) well in three of the seven scenarios, and the sample study is at most 6 percent off the larger sample. This similarity in fraction of mishaps indicates that the sample of mishaps analyzed is representative of the larger population of mishaps for these scenarios. The sample analyzed for scenarios G and H underrepresents these scenarios relative to the larger sample of mishaps. The analyzed samples for scenarios L and M over-represent the number of mishaps compared to the larger sample of mishaps. These over- and under-representations will have little effect on the statistics within a given scenario but could impact the result when making comparisons between scenarios.

Table 53. Number of study mishaps by scenario and larger sample—N–B

	86 Mishaps Studied in Detail (percent)	276 Mishaps From Query With Assignable Scenario (percent)
Scenario F—Runway overrun (landing or takeoff)	30	30
Scenario G—Compromised landing (mild impact)	13	17
Scenario H—Impacted terrain short of runway (during on approach)	16	22
Scenario J—Hard landing with loss of control post-impact	19	16
Scenario K—Loss of control on, during, or following takeoff (includes wing contamination)	8	7
Scenario L—Loss of control on takeoff or go-around due to wind influence	8	5
Scenario M—Impacted terrain short of runway due to wind influence	6	3
Scenarios H + M	22	25
Scenarios K + L	16	12

4.2.3 Mishap Kinematics Scenario (G–M)—N–B

A dataset of all mishaps except the overruns (scenario G–M) will be reviewed first, and then the individual scenarios will be analyzed. For the purpose of setting design guidelines and test conditions, knowledge of the larger set of data may be more beneficial. In this analysis, the data for scenarios G-M are grouped together (60 mishaps). These scenarios have the common attribute that the impact occurs from the air or in the attempt to become airborne. Being airborne causes at least two factors to be different compared to the overrun scenario F: 1) the velocity is generally higher, and 2) the attitude has an additional degree of freedom. The overrun scenario is analyzed in the subsequent section in which each scenario is reviewed separately.

The data are presented in several graphical ways to facilitate the reader's interpretation of where critical transitions may be occurring. In the following section, the kinematic data are presented as combined histogram frequency and cumulative percentile charts. The histograms are created to show the number of mishaps that occurred within ranges or "bins" for each parameter. In the percentile distribution curves, the value for each mishap is ranked in ascending order and then assigned a percentile value based on the number of events. The percentile value for a particular mishap means that "*N*" percent of the events occurred at a lower value of the parameter than the value for a particular mishap. Therefore, the plot can be used to determine either what percentile a given parameter value corresponds to, or for a particular percentile value, the corresponding parameter value can be read out. In the Excel incarnation of the histogram plot, the bin is labeled with the highest value in the range of the bin. The value range for a given bin is from the label value of the bin to the left to the label value of the bin of interest. In figure 40, the lowest bin contains all events with vertical velocity less than or equal to -50 ft/s (one mishap), and the second bin contains the mishaps with vertical velocity greater than -50 ft/s and less than or equal to

-25 ft/s (two mishaps). The third bin indicates six mishaps in the range -25 ft/s to and including 0 ft/s.

The first kinematic parameter analysis is for the vertical velocity (see figure 40). Vertical velocity is normally positive for the downward direction, but in six mishaps of the N–B study, the aircraft crashed inverted or rolled in such a way that the impact was upward as expressed in the aircraft reference frame. The third bin includes three mishaps with zero vertical velocity; therefore, there are six mishaps with negative vertical velocities (one in the first bin, two in the second, and three in the third). The red curve presents the cumulative percentile of crashes; approximately 70 percent of these 60 mishaps have vertical velocities between 0 and 30 ft/s.

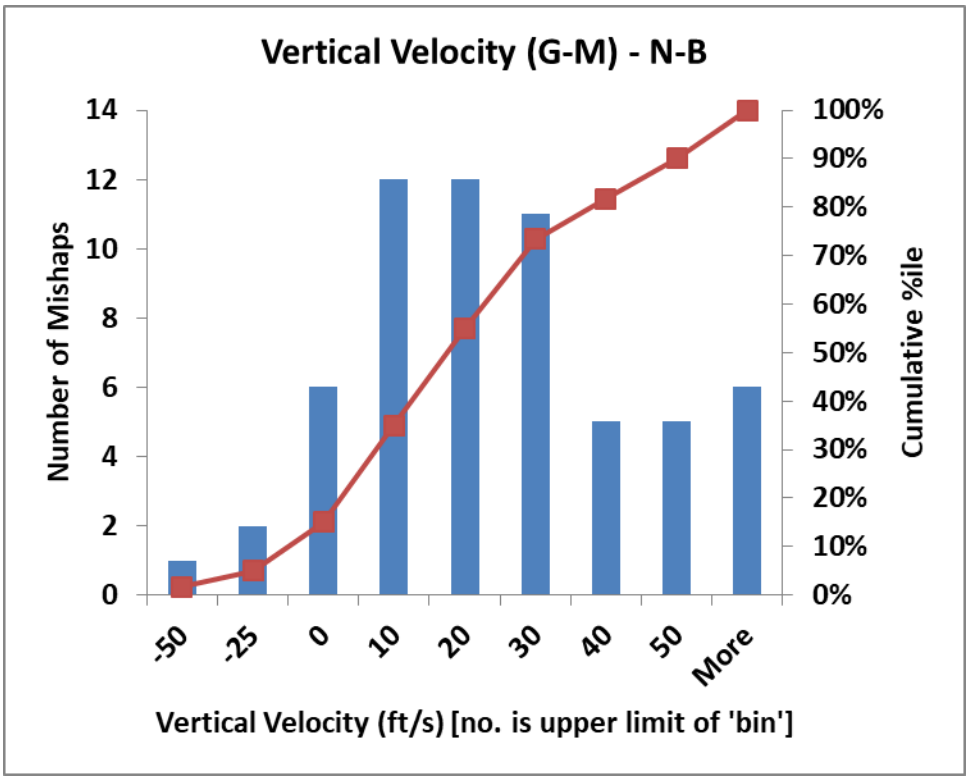

Figure 40. Vertical velocity distribution (G–M) – N-B

The Airspeed is the velocity along the flight path; the data for Scenarios G–M cover a wide range (figure 41), but are somewhat normally distributed. The median (225) and average (223) values for Airspeed both fall between 200 and 250 ft/s at the peak of the frequency. The fact that these metrics are approximately equal is a confirmation that the distribution of values is nearly symmetric. One zero velocity event occurred when the aircraft was improperly loaded and struck its tail when the engines were throttled up. The cumulative percentile curve indicates that approximately 76 percent of the mishaps in the dataset had Airspeeds of 250 ft/s or less.

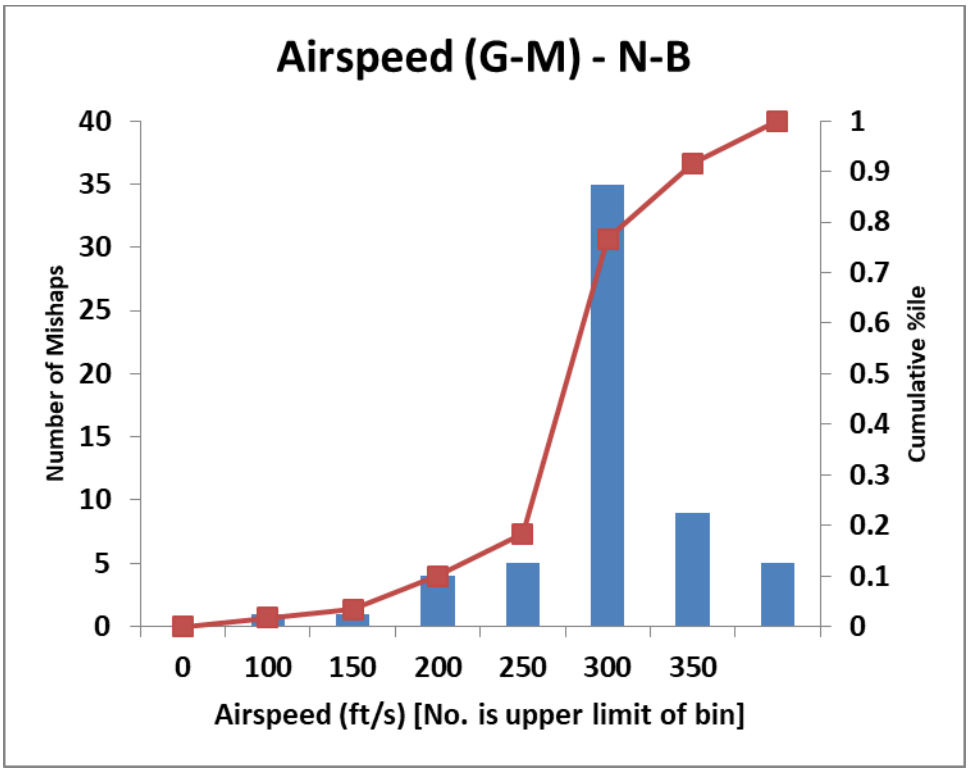

Figure 41. Airspeed distribution (G-M) – N-B

The flight path angle is the angle between the path of the aircraft's center of gravity and the horizon (see figure 42); descent is a negative angle. The flight-path angle can be estimated as the ratio between the airspeed and the vertical velocity (arcsine). The flight-path angle is expressed as a negative number indicating a downward impact in the aircraft reference frame. The N–B dataset for scenarios G–M (see figure 43) contained one positive value, which was a tail strike during takeoff.

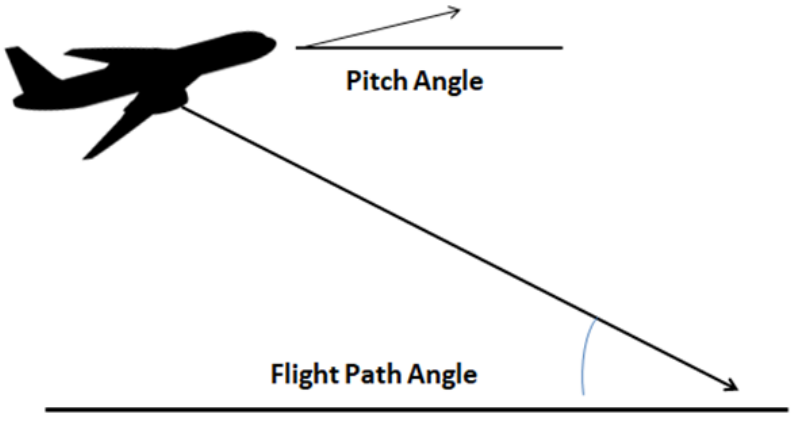

Figure 42. Flight path and pitch-angle relationship

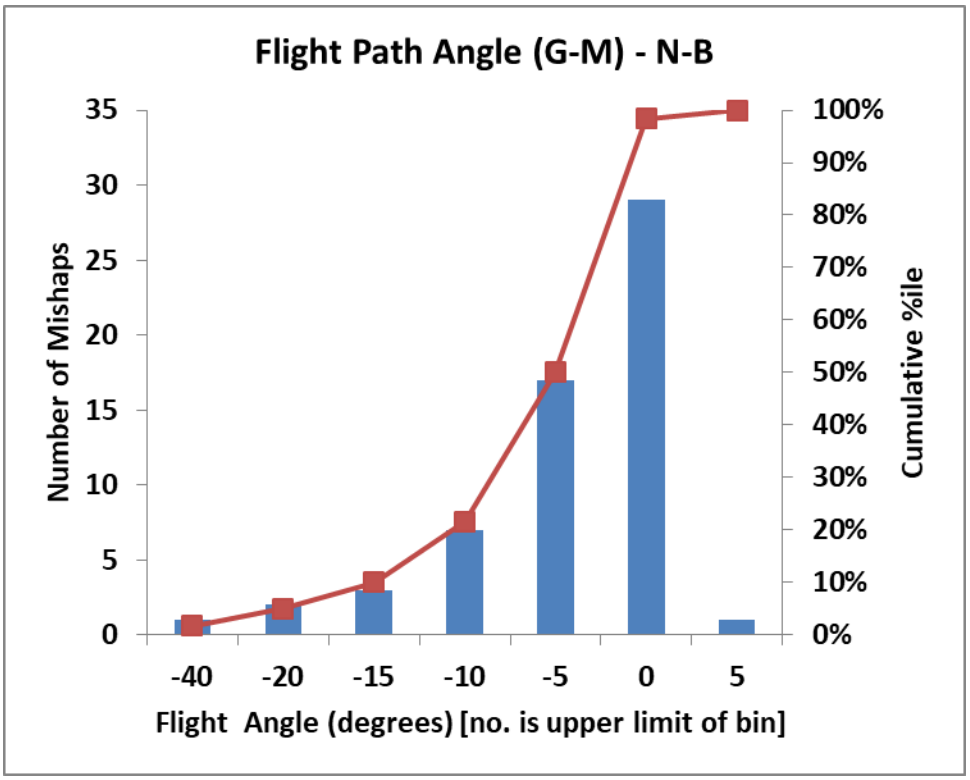

Figure 43. Flight-path angle distribution—N–B

The pitch angle is the angle between the longitudinal axis of the aircraft and the horizon; nose up is positive pitch angle. The pitch-angle chart (see figure 44) shows that, of the 59 mishaps with pitch data, only four impacted with the nose down (negative pitch) more than 5 degrees. There were 11 mishaps between -5 degrees and 0 degrees, and 4 mishaps at 0 pitch (as represented by the "0" bin having 15 mishaps). Therefore, the most common attitude was in the range 0 to +15 degrees nose up (bins labeled "5," "10," and "15" including 37 mishaps). There were only four mishaps with the nose pitched above +15 degrees. There was one mishap with no information available.

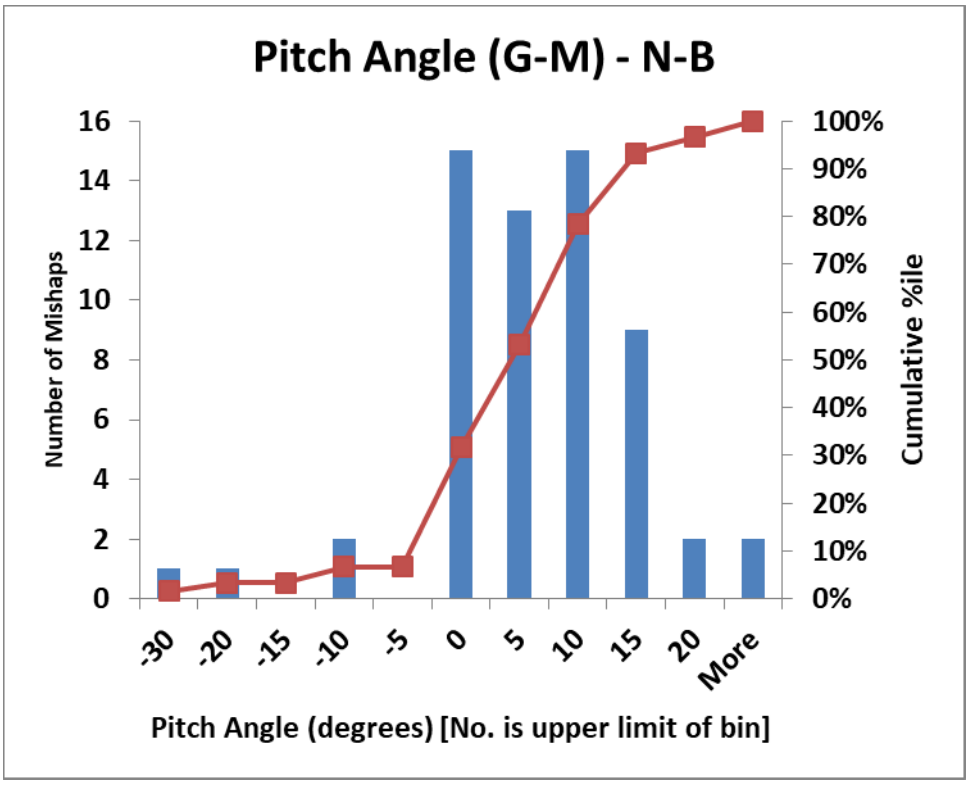

Figure 44. Distribution of pitch angles (G–M)—N–B

The roll (see figure 45) and yaw angles (see figure 46) at impact in many of these mishaps are very near neutral values because most of the aircraft impacted from controlled flight. The 33 mishaps in the 0-degree bin for roll angle (of 58 mishaps with roll data) and the 44 mishaps in the 0-degree bin for the yaw angle (of 56 mishaps with yaw data) are 0 angle. Even small positive values fall into the next bin up. Two of the three values in the roll "more" bin are extreme at 120 and 130 degrees. The two high values for the yaw angle are 35 and 90 degrees. The absolute values are plotted considering the symmetry of the airplane. The important quantity is the magnitude of deviation from nominal attitude; the effect on the airframe presumably will be equal, regardless of which side is affected.

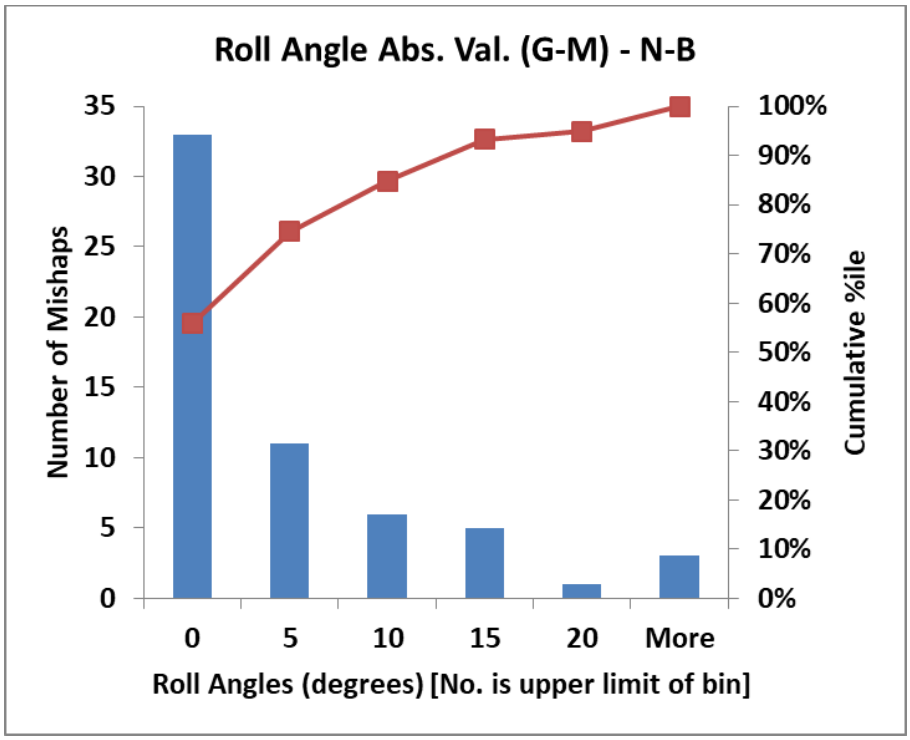

Figure 45. Distribution of roll angles (G–M)—N–B

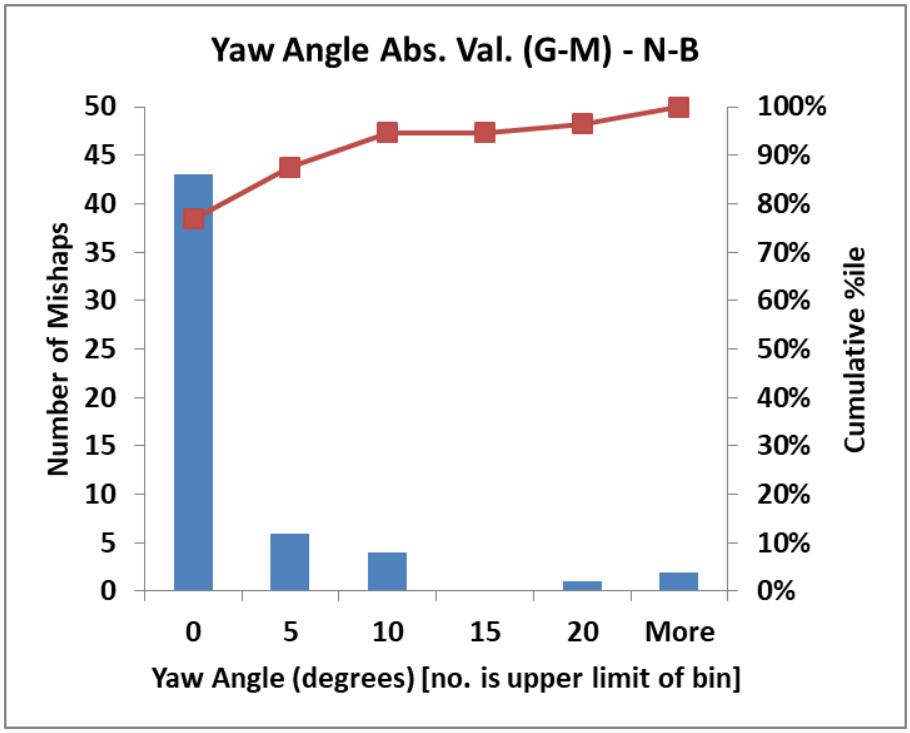

Figure 46. Distribution of yaw angles (G–M)—N–B

Because of the infrequency of occurrence and the generally small values for the roll and yaw angles in these mishaps, the two angles were combined into a single parameter. The combining was accomplished by taking the absolute value of each datum and then adding the two positive values together to create the new parameter designated "off-nominal angle." Only those mishaps with values for both angles are included (56 of 60). As is shown in figure 47, even in the combined, single parameter, small values predominate; 80 percent of the mishaps have a value less than 10 degrees, and 20 degrees encompass 93 percent.

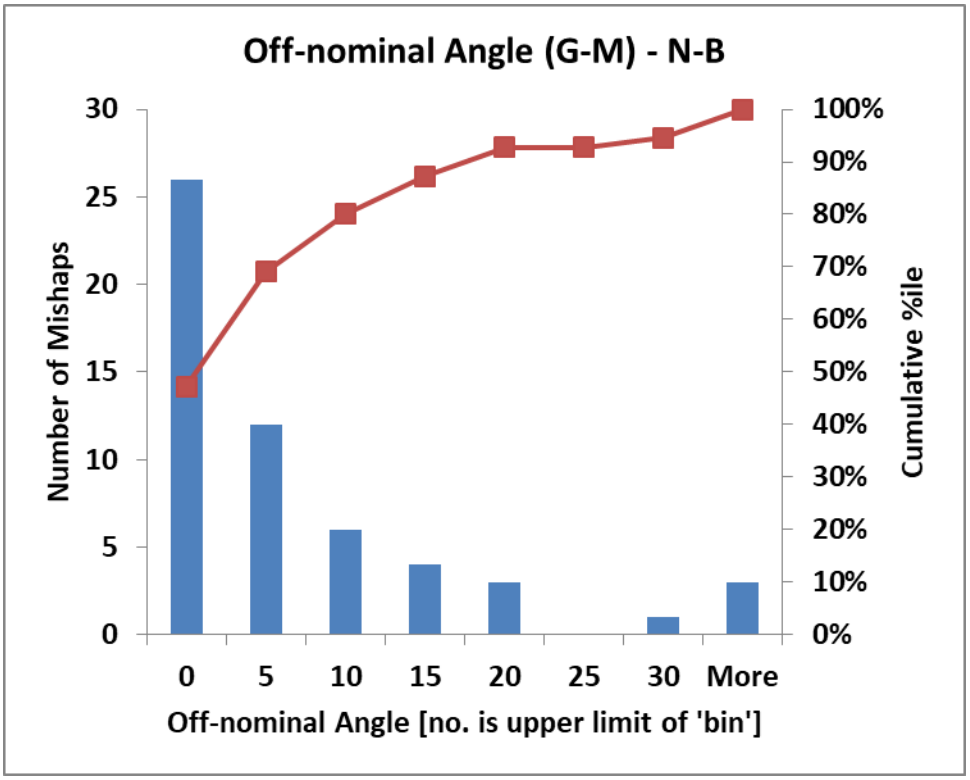

Figure 47. Distribution of off-nominal angle (G–M)—N–B

Most of the acceleration force values used in this study were estimated by impact reconstructions. The vertical acceleration (also referred to as "normal acceleration" in several reports) was recorded in a few aircraft. In those cases in which the impact was recorded, it should be noted that to capture the shape of the deceleration pulse in the actual impact, the recording frequency for the acceleration in each axis must be much higher than the recording frequency normally used to capture flight data. As can be seen in the vertical deceleration[†] histogram in figure 48, the vertical deceleration was between 0 and 5 G (inclusive) in 40 of the 60 mishaps. Four cases exceeded 15 G downward deceleration. Four mishaps resulted in inverted impact (negative values), and the other two mishaps had zero vertical deceleration.

[†] The aircraft reference frame convention takes Z positive downward; therefore, an aircraft crashing downward has positive vertical velocity and a negative vertical acceleration. The vertical acceleration is plotted with signs reversed here so that the majority of values are positive.

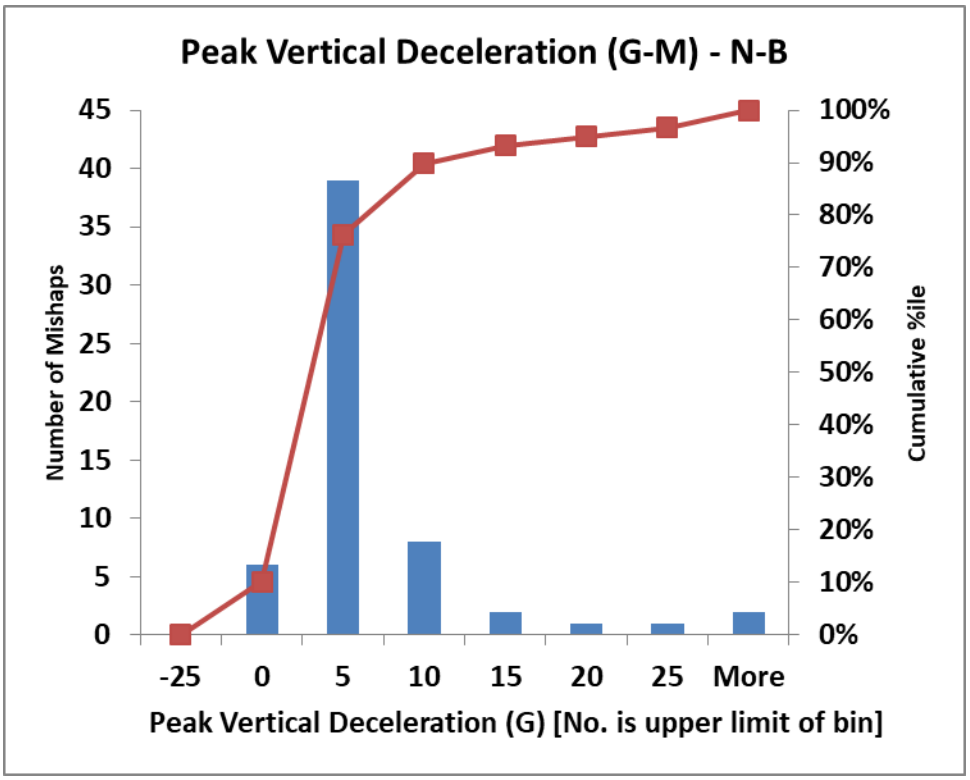

Figure 48. Distribution of vertical impacts (G–M)—N–B

The longitudinal deceleration data are presented in cumulative percentile format because the more severe mishaps are those with larger negative values. The histogram routine is not amenable to reversing the axis; consequently, just the cumulative percentiles for the N–B mishaps are presented (see figure 49). The plot indicates that four of the 50 mishaps with longitudinal deceleration data (10 mishaps had no longitudinal deceleration data) experienced positive deceleration forces (> 0 G), indicating an extreme angle and rearward deceleration. Roughly 60 percent of the mishaps fall in the range of 0 to -2.8 G. These low deceleration levels reflect the long distances over which transport aircraft are generally brought to rest in potentially S crashes. The few mishaps in which the deceleration is high represent events in which the aircraft strongly interacted with the terrain or a massive obstacle such as a building. In events in which only the landing gear interacted, such as striking shallow ditches or low vertical obstacles, the resulting deceleration on the aircraft was relatively modest. In this study and the W–B study, a new field was added to the damage worksheet to track how many of the mishaps involved the aircraft striking a vertical obstacle. Any obstacle with a vertical dimension equal to or greater than the radius of the nose wheel was considered such an obstacle, regardless of its mass relative to the aircraft. Therefore, light structures, antennas, and fences were included with sharp terrain discontinuities, trees, and buildings. Of the 60 N–B scenario G–M events, 21 involved interaction with a vertical obstacle. For the scenario G–M mishaps, the presence of a vertical impediment raised the magnitude of the average peak longitudinal deceleration from -1.3 to -7.6 G. The corresponding difference in average longitudinal deceleration for the runway overruns (scenario F) is -3.5 G for an impact involving an obstacle (16 mishaps) compared to -1.1 G for the mishaps without an obstacle (10 mishaps). Note that for scenario F, more mishaps involved vertical obstacles than did not involve obstacles, whereas for

the G–M scenarios, only approximately one-third involved obstacles. Longitudinal deceleration values were missing for two of the 26 scenario F mishaps and 10 of the 60 scenario G–M mishaps.

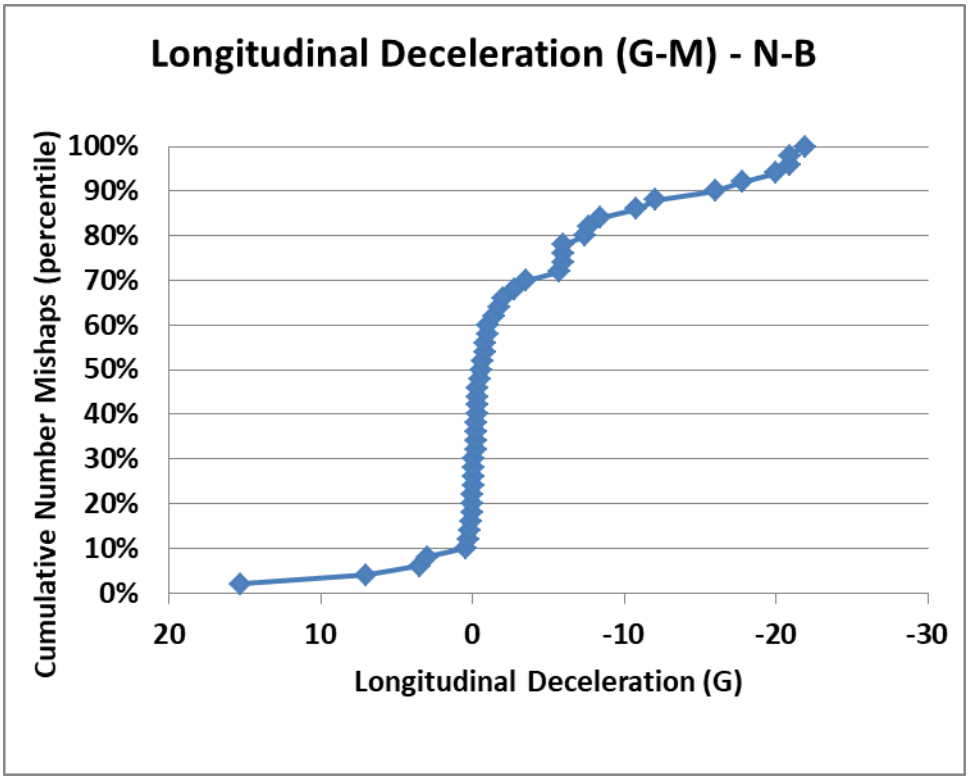

Figure 49. Distribution longitudinal decelerations (G–M)—N–B

The absolute value is taken for the lateral deceleration data in the analysis. The outcome of lateral acceleration in terms of number of injuries is assumed to be symmetrical; taking the absolute value assures that the results of positive and negative values for this parameter do not cancel each other out but are additive. The lateral deceleration is generally non-zero only when the roll or yaw angles have deviated from zero degrees. As was seen previously in the angle charts, relatively few of the mishaps occur at extreme angles, and that fact is reflected in lateral deceleration values (see figure 50). Only 3 of the 55 mishaps with lateral deceleration values (5 mishaps had no lateral deceleration data) experienced lateral deceleration greater than 4 G.

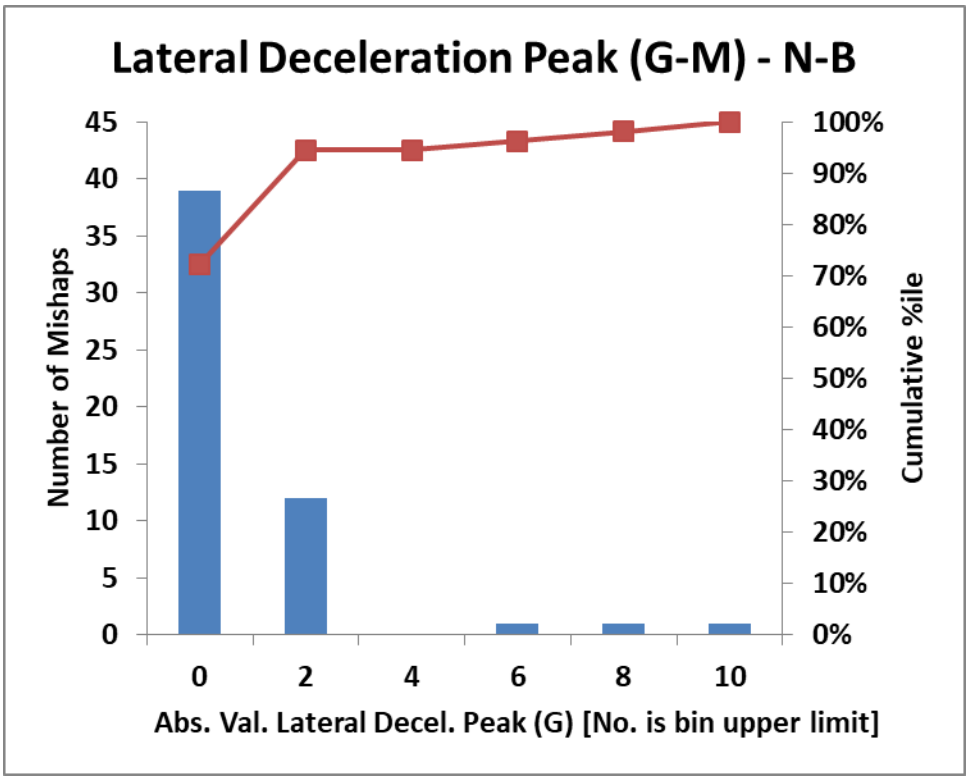

Figure 50. Distribution lateral decelerations—N–B

4.2.4 Kinematics of Each Mishap Scenario—N–B

The kinematic characteristics of the different scenarios are generally consistent with the nature of the scenario. The runway overruns (F) have a lower airspeed (longitudinal velocity) than the other scenarios (see table 54). A few of the overrun events also had a non-zero vertical-velocity component in the impact due to the terrain dropping off, ditches, or ravines. Both the median airspeed and the median longitudinal deceleration for scenario F have generally lower values than the other scenarios. The lower median deceleration is likely a direct consequence of the lower velocity and, therefore, less kinetic energy to be dissipated.

Table 54. Kinematics by scenario—N–B

Scenario {# of events in scenario}	Vertical Velocity Med./Avg. (ft/s)	Airspeed Med./Avg. (ft/s)	Flight Path Angle Med./Avg. (deg.)	Pitch Angle Med./Avg. (deg.)	Vert. Accel. Med./Avg. (G)	Long. Accel. Med./ Avg. (G)
F Runway overrun {26}	0/9.0	137/142	0/-3.1	0/-0.5	2.0/2.9	-1.6/-2.6
G Compromised landing, no impact {11}	1.0/-0.5	225/215	-0.8/-1.6	8.9/5.0	1.3/1.5	-0.2/-0.2
H Impact terrain, short {14}	23.8/28.2	218/222	-6.0/-8.7	4.8/5.3	3.8/8.3	-8.4/-9.8
M Loss of control landing due to weather influence. (H influenced by weather) {5}	25.0/26.8	248/245	-5.0/-5.9	4.5/8.7	2.0/1.1	-5.7/-4.7
J Hard landing, loss of control {16}	11.2/16.2	218/207	-3.8/-5.0	0.0/1.6	3.2/3.4	-0.3/0.2
K Loss of control takeoff {7}	30.0/42.5	260/243	-10.3/-15.3	14.0/7.3	0.8/3.8	-1.4/-4.5
L Loss of control takeoff due to weather influence (K influenced by weather) {7}	40.0/37.1	245/236	-9.8/-8.9	3.0/1.5	4.8/2.8	-4.4/-5.6
K + L Similar mishaps with and without wind {14}	30.5/39.8	248/239	-10.1/-12.1	10.0/4.4	2.5/3.3	-1.4/-5.1
H + M Similar mishaps with and without wind {19}	25.0/27.8	219/228	-5.4/-8.0	4.8/6.1	3.2/6.3	-6.0/-8.1
G–M inclusive {60}	17.7/22.3	224/223	-4.9/-7.0	5.0/4.3	2.1/3.9	-0.6/-3.5

Scenario G, the compromised landing scenario, is associated with some deficiency in the landing preparation, which leads to a poor landing outcome. Consequently, the kinematics (see table 54) approximate the kinematics of a near-normal landing. This scenario includes tail strikes on both landing and takeoff, and on gear-up landings.

Scenario H involves the aircraft impacting the terrain short of the runway. Although airspeeds (see table 54) in this scenario are similar to those for scenario G, the vertical velocity at impact is markedly higher, contributing to landing short. As a consequence of the higher descent rate, the magnitude of the median flight path angle is also greater for scenario H compared to scenario G. Because in many cases the terrain is other than a prepared surface, the median vertical and longitudinal accelerations are higher for scenario H than for scenario G.

Scenario M includes five mishaps in the N–B dataset. Scenario M mishaps are similar to scenario H mishaps with the presence of localized winds. The median airspeed for the scenario M mishaps is 30 ft/s higher than the median for the scenario H, whereas the average airspeed is 23 ft/s higher. The median and average vertical velocities between the two scenarios are very similar,

suggesting that the horizontal localized winds exhibit greater variation than do the vertical localized winds.

The hard landings with loss of control, scenario J, exhibits airspeeds comparable to those of scenario H. The average vertical velocities (see table 54) associated with scenario J are lower than those for scenario H, as reflected by the median and the average. The severity of the vertical impacts in scenario J are lower than those in scenario H, which is consistent with the vertical velocities. Comparing the longitudinal peak decelerations between scenario J and scenario H, the median and average values for scenario H are higher, likely because many of these impacts occur on unprepared (off-airfield) terrain. On looking into the individual mishaps within scenario J, the hard landings with loss of control were all poorly executed approaches that effectively led to stall situations over the runway.

The N–B dataset contains seven scenario K mishaps. Scenario K has both the highest median and average airspeed and the highest median and average magnitude pitch angles. Two of the seven scenario K mishaps impacted inverted, and consequently, had negative vertical velocities. These two negative vertical velocities reduce the value of the median and average velocity. Scenario K contains high flight path angles. However, the median and average vertical impact forces are not especially high compared to the other scenarios and, again, the median and the average values encompass two negative values.

The N–B dataset contains seven scenario L mishaps—loss of control on takeoff with wind shear as a contributing factor. Like scenario K, the mean and average vertical velocities for scenario L are high. The flight path angles are comparable. The vertical and longitudinal decelerations for scenario L are both higher than for scenario K, suggesting that the presence of wind increased the severity for this type of crash. The median and average airspeeds in scenario L are lower than those in scenario K. The slightly lower airspeed in scenario L suggests that localized shifts between head and tail winds may contribute to the mishap by suddenly dropping the airspeed at a critical point in the landing or takeoff.

4.2.4.1 Kinematics of Survivable Crashes—N–B

The basis for identifying the crashes as S, PS, or NS is discussed in section 2 of this report. The runway overrun mishaps (scenario F) are excluded from this analysis as there is generally only a longitudinal velocity, and the nature of the impacts is different from the impacts in which the aircraft has been airborne.

The scenarios G–M dataset includes 60 mishaps: 3 mishaps were NS, 14 mishaps were PS, and the remaining 43 mishaps were S. The three NS mishaps were one each from scenario H, scenario K, and scenario L. Seven of the PS mishaps were in scenario H, and one was in scenario M. Four of the PS mishaps were in scenario K and two in scenario L. Looking only at the vertical velocity (see figure 51), six of the mishaps had inverted impacts (i.e., the vertical velocity was negative); two of these six mishaps were PS. The remaining four negative vertical velocity mishaps were S. The 90th-percentile level[†] is marked with a reference line. Of the six mishaps above the 90th-percentile vertical velocity, two were PS and four were S. The corresponding plot

[†] The 90th percentile is selected only as a convenient reference point; there is no technical or regulatory reason for its selection.

for airspeed is shown as figure 52. Half of the six events above the 90th-percentile velocity were PS and the other half were S.

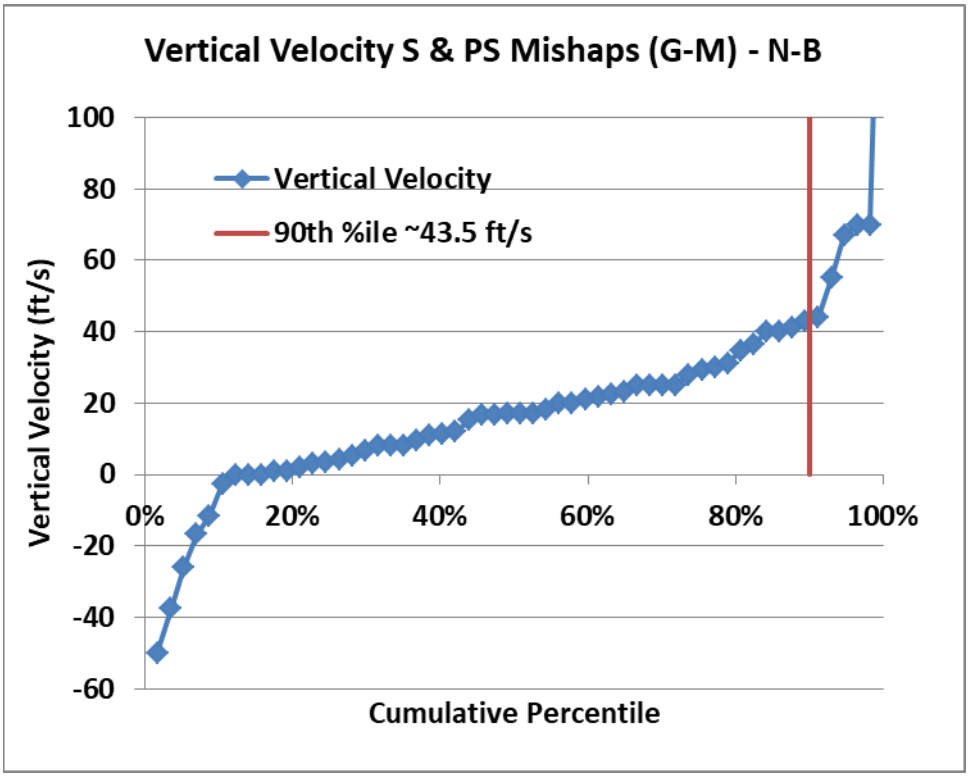

Figure 51. Vertical velocity for S and PS mishaps—N–B

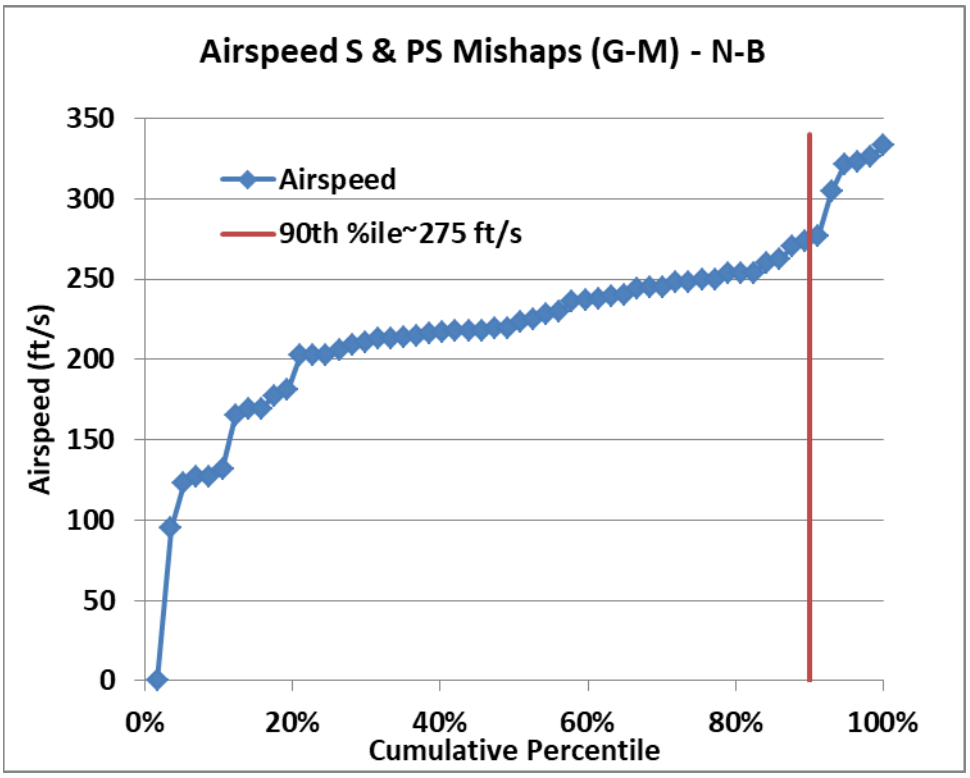

Figure 52. Airspeed for S and PS mishaps—N–B

The 90th-percentile velocity has been chosen as a reference velocity for creating a two-velocity plot (see figure 53) to illustrate how the two primary velocities interact in a mishap outcome. For each mishap, the airspeed is plotted as the *X* value, and the negative of the vertical velocity is plotted as the *Y* value. The sign of the vertical velocity is reversed because the resulting plot is more intuitive with downward velocity being down on the plot. The 90th-percentile curve is created just as the vector magnitude would be created—the square root of the sum of airspeed squared plus the vertical velocity squared. The result is the equation of an ellipse in which the *X* intercept is the 90th-percentile airspeed, and the *Y* intercept is the 90th-percentile vertical velocity. All three of the NS crashes fall outside the 90th-percentile curve (see figure 53), as do more than half of the PS mishaps. A first impression is that too many mishaps fall outside the 90th-percentile ellipse. However, looking back to the determination of the two 90th-percentile values (see figures 51–52), there are six mishaps on each curve greater than the 90th percentile, but they are not necessarily the same six mishaps. In both figure 51 and figure 52, the NS crashes are not included in determining the 90th percentile, and it is not surprising that they would all be beyond the ellipse in figure 53. Looking at only airspeed, there are six points beyond the 90th-percentile intercept. For the vertical velocity, there are six points below the level of the 90th-percentile vertical velocity.

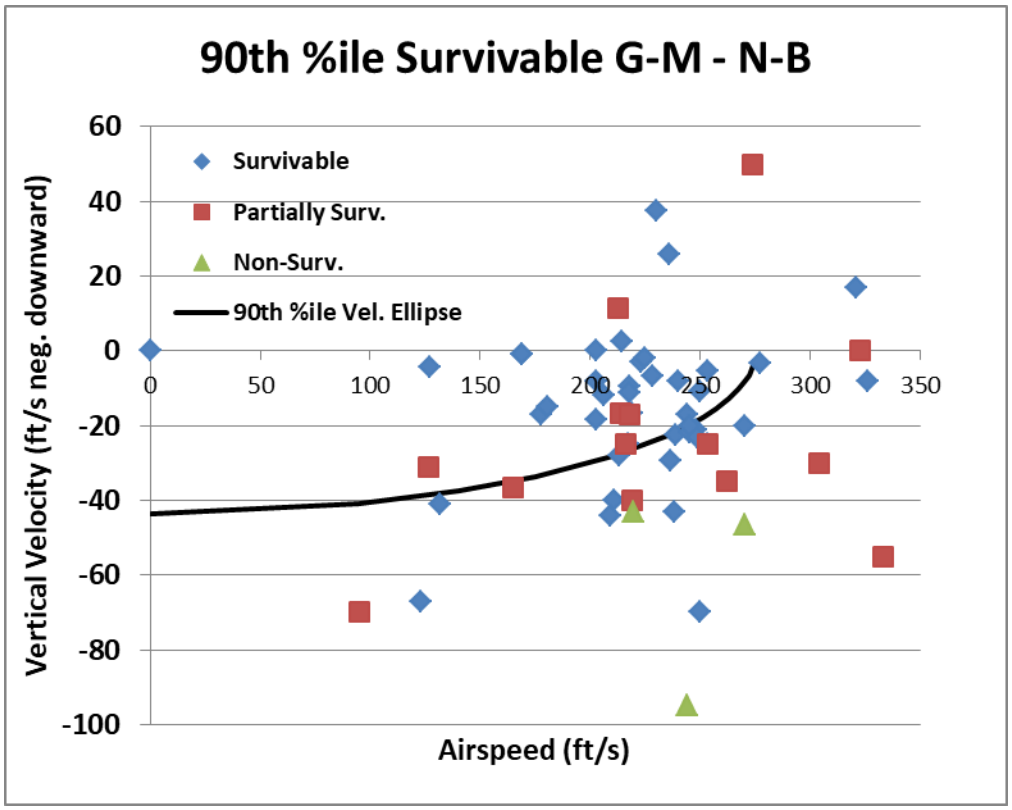

Figure 53. 90th-percentile survivable velocities—N–B

4.2.5 Quantifying Damage—N–B

The definition and construction of the damage metric is presented in the section 2 of this report. This metric is the same definition used for the RJ study and is the same used for the W–B study earlier in this report. The damage modes reported in the database are underside fuselage damage, floor disruption, seat failure, fuselage breaks, and loss of occupied volume. The information in the CSRTG database was supplemented by text from the investigation report and by photographs found both in the investigation reports and on the Internet. To record the severity for each mode of damage in each segment of the aircraft, a cell for each damage mode in each segment was populated with: "none," "local," or "widespread." These values are accumulated to form the damage metric for each segment. A table of the damage metric by segment for each N–B mishap is presented in appendix D. The damage for the N–B mishaps was thoroughly reported; only three mishaps of 86 had any missing information. The worst of these mishaps was missing 11 of 24 cells in a scenario-K mishap. The resulting damage metric of only 20 was the lowest value in that scenario and, consequently, may have materially affected the mean and the median. The effect of any missing cell is to reduce the value of the damage metric because no information (NI) is assigned a zero value. Several approaches for working around this missing data were considered, but none were deemed satisfactory. For the benefit of the reader, the column on the right of the table (appendix D) lists the number of cells containing no information; the total damage factor for these mishaps may be lower than would have been recorded had all of the information been available.

Each fuselage break (see table 55) that occurred was entered as damage to the segment on the aft side of the break. This allocation was based on the observation that injuries related to a break tend to occur in the seats behind the break rather than ahead of the break. Generally, the fuselage breaks in the N–B aircraft occurred at the segment interfaces. Consequently, breaks occurring in the center of the forward or the aft cabin were not tracked separately. Therefore, the maximum damage metric is 112. This observation about where the injuries occur is based on generalizing from those investigation reports in which detailed injury maps were provided. The lowest frequency of breaks is experienced in the least-severe scenario G, in which the aircraft lands and ends up on the prepared area of the airport. In scenario F, in which the aircraft departs the airfield, more breaks are experienced. For the remaining scenarios in which the aircraft makes contact with the obstacles or with the ground at more extreme angles and higher velocities, the number of breaks per mishap is markedly higher.

Table 55. Fuselage breaks by scenario

	Number of Fuselage Breaks	Fuselage Breaks/Mishap
Scenario F, Overruns (26 events)	20	0.8
Scenario G, Compromised Landing (11 events)	3	0.3
Scenario H+M, Short of Runway (19 events)	30	1.6
Scenario J, Hard Landing, Lost Control (16 events)	9	0.6
Scenario K+L, Lost Control during T-O (14 events)	27	1.9
Scenarios G–M (60 events)	71	1.2

The different types of damage used to construct the damage metric vary only slightly in frequency along the length of the aircraft (see table 56). The most frequent damage is underside skin damage. This form of damage occurs any time there is landing-gear failure or the aircraft goes over an impediment. The two forward segments have underside damage slightly more frequently than the overwing or aft cabin; this trend may be the result of frequent nose-gear failures (46 nose-gear failures; in 86 mishaps, there were also 11 gear-up mishaps). If the underside damage is very severe, it will cause floor disruption, typically pushing the floor upward. The floor damage may be localized, such as when a nose gear fails and folds rearward, pushing other structures and the floor upward. Floor disruption may also occur when an aircraft impacts a large impediment that deforms the fuselage inward. This type of damage not only reduces cabin volume but may also disrupt the floor. The trend in the floor-disruption occurrences indicates that the overwing segment experiences floor disruptions less frequently than the segment either ahead or behind it. The tail segment experiences the fewest floor disruptions, even though it experiences the most instances of skin damage. The skin damage for the tail includes several tail strikes. In severe cases of floor disruption, the seats do not remain attached. When the seats become detached from the floor, the occupant-restraint load path is broken, and the occupants can be subjected to more severe impacts with the seats in front of them, with other occupants, or with structure. The most extreme form of damage is the loss of occupant volume, in which the structure is pushed into the cabin volume containing the occupants. The moving structure causes widespread blunt-trauma injuries and leads to serious and fatal injuries. The overwing segment again experiences a lower rate than the cabin segment ahead or behind it. Not only is this segment structurally more robust, but the wings may serve to reduce the impingement of vertical obstacles into this segment and prevent rollover. The

tail shows the lowest frequency of volume loss; this may be due to the additional structure necessary to support and transfer the aerodynamic loads.

Table 56. Number and type of damage for each segment—N–B

All Mishaps (86)	Cockpit (# of Mishaps)	Forward Cabin (# of Mishaps)	Overwing Cabin (# of Mishaps)	Rear Cabin (# of Mishaps)	Tail (# of Mishaps)
Underside Skin Damage	62	61	56	56	63
Floor Disruption	33	34	27	33	24
Seat Failure	30	33	26	32	20
Loss of Occupant Volume	26	26	19	24	15
Breaks	–	20	24	26	19

There were several extreme mishaps in the N–B dataset. There are 10 mishaps with damage metrics greater than 90, and three of those have the maximum value of 112. These extreme mishaps have several general aspects in common (see table 57). In all cases, the aircraft either impacted a vertical obstacle or struck the ground at an extreme angle; these impacts led to high localized loads on the structure, which tore the aircraft apart. In all but one case, the severe structural damage was accompanied by post-crash fire. In this one exception (19820113A), after hitting a bridge, the aircraft fell into a river; the post-crash hazardous environment was freezing water rather than fire. In only a few mishaps were the post-mortems sufficiently detailed to identify those killed by trauma or thermal injury. In each of the extreme mishaps, the survivors were located in a segment of the aircraft that had retained cabin volume locally. In a couple of these cases, the survivors had the additional advantage that the survivable volume came to rest away from the fire.

Table 57. Extreme mishaps—N–B

CSRTG ID	Location	Damage Metric	Scenario	Survivors/Occupants	Damage/Survival Factors
20070717B	Congonhas, Brazil	112	F	0/187	Down an embankment, struck a building, fire
19770404A	New Hope, GA, US	93	H	62/85	Wing struck poles, fuselage broke up in large pieces
19730731A	Boston, US	112	H	0/89	Vertical obstacle, fire
19671120A	Constance, KY, US	94	H	12/82	Struck ground extreme angle, fire, 22 removed alive
19750624A	JFK, NY, US	95	M	11/124	Vertical obstacles, rocky ground, fire, most fatalities were identified as trauma
20080820A	Madrid, Spain	106	K	18/172	Over an embankment struck rising ground, fire, survivors in survivable volume separated from fire
20050905A	Medan, N. Sumatera	97	K	100/117	Hit embankments and roads beyond end of runway, post-crash fire
19820113A	District of Columbia, US	102	K	5/79	Vertical obstacle, cold water rather than fire, most fatalities were trauma, survivors from aft cabin with survivable volume
20061029A	Nnamdi, Abuja, Nigeria	104	L	9/105	Ground extreme angle, fire, survivors in small, intact tail section
20051210A	Port Harcourt, Nigeria	112	L	2/110	Vertical obstacle, fire

Of the five main scenarios, scenario H+M and scenario K+L have the highest whole aircraft damage metric values (table 58, right column). The average damage metric for each segment of the scenario F mishaps is higher than for the corresponding segment of the scenario G mishaps. This higher value may be due to the influence of the aircraft leaving the prepared area of the airfield in scenario F, whereas the aircraft remains on the prepared surface in scenario G. The damage metric values for scenario H+M are high; most of these mishaps occur short of the prepared surface of the airfield. The low average values for the damage metric in scenario J is somewhat unexpected because these mishaps are associated with loss of control of the aircraft after a hard landing. The explanation may be that the loss of control comes after the plane is on the ground and the aircraft

remains within the prepared area of the airfield. The reason for the damage metric being high for scenario K+L is that the loss of control occurs with the aircraft in the air, leading to impacts at more extreme angles. The trend of the damage metric for each scenario along the length of the fuselage is very similar to the trends seen in each type of damage (see table 56). The average damage metric for the whole aircraft reflects the same pattern as the average number of breaks for each scenario (see table 55).

Table 58. Damage metric of each segment by scenario—N–B

Scenario	Cockpit Average Damage Metric	Fwd Cabin Average Damage Metric	OW Cabin Average Damage Metric	Aft Cabin Average Damage Metric	Tail Average Damage Metric	Whole Aircraft Average Damage Metric
Scenario F	4.8	5.7	3.6	4.5	3.3	22.0
Scenario G	0.5	0.5	0.5	0.3	0.8	2.5
Scenario H+M	10.2	11.8	10.7	9.8	7.7	50.2
Scenario J	1.4	2.1	1.8	3.9	0.9	10.1
Scenario K+L	13.2	14.5	13.0	13.0	10.1	63.9
Scenario H	11.9	14.0	12.4	11.4	9.3	59.1
Scenario M	5.2	5.8	5.8	5.0	3.0	24.8
Scenario K	15.0	15.6	14.9	15.9	11.3	72.6
Scenario L	11.4	13.4	11.1	10.1	9.0	55.1

As noted earlier, two new scenarios were created in this study to investigate the effect of wind shear or localized winds. Scenario L consists of scenario K mishaps that involved localized wind, and scenario M consists of scenario H mishaps that involved localized wind. Comparing M to H and L to K provides some insight into whether the wind influence leads to more severe impacts. In each segment, the damage metric for scenario M (with wind influence) is less than half the damage metric for scenario H (without wind influence). The average whole aircraft damage metric for the 14 scenario H mishaps is 59.1, and the average whole aircraft damage metric for the five scenario M mishaps is 25.4. This relationship suggests that the wind's influence does not increase the amount of damage occurring. Comparing scenario K and scenario L reveals a similar trend; the average damage metric for scenario K is 72.6, whereas the average for scenario L is 55.1. These results indicate that the presence of the localized wind does not lead to a more severe accident outcome on average. However, the trend of higher damage metrics for the mishaps without wind does not preclude the possibility that these events were a consequence of the wind. That is to say, the presence of the wind could have caused this type of mishap to occur in a similar situation in which it would not have occurred had the wind been absent. Therefore, the effect of wind may create a mishap in which one would not otherwise have occurred, rather than to cause a mishap to have a more severe outcome.

The scenarios in table 59 are listed in descending order of average damage metric. The highest two scenarios for damage metric also have the highest vertical velocities by a wide margin. The pattern in the vertical velocity is not reflected by a similar pattern in the vertical acceleration, because

scenario F has surprisingly high vertical acceleration values despite low vertical velocity values. The scenario with the highest average damage metric also has the highest airspeed, but the relationship breaks down for the remaining scenarios. The damage metric for scenario H+M is much higher than for scenario G, yet the two scenarios have similar airspeeds. The difference in damage metrics is consistent with deceleration values for the two scenarios. Both the vertical and longitudinal deceleration values for scenario H+M are much higher than for scenario G. This lower average damage metric is consistent with the lower airspeed, and is consistent with the somewhat lower vertical and longitudinal deceleration. A related table (see table 60) for damage metric with the flight path and attitude angles is shown in table 59.

Table 59. Damage metric and kinematics by scenario—N–B

Scenario {# of events in scenario}	Aircraft Damage Metric (Avg. for Scenario)	Vertical Velocity Med./Avg. (ft/s)	Airspeed Med./ Avg. (ft/s)	Vert. Accel. Med./ Avg. (G)	Long. Accel. Med./ Avg. (G)	Vertical Impediments Impacted (% of Mishaps)
K+L Loss of control takeoff {14}	63.9	30.5/39.8	248/239	2.5/3.3	-1.4/-5.1	50
H + M Similar mishaps regardless of influence {19}	50.2	25.0/27.8	219/228	3.2/6.3	-6.0/-8.1	63
F Runway overrun {26}	22.0	0/9.0	137/142	2.0/2.9	-1.6/-2.6	62
J Hard landing, lose control {16}	10.1	11.2/16.2	218/207	3.2/3.4	-0.3/0.2[1]	13
G Compromised landing, no impact {11}	2.5	1.0/-0.5	225/215	1.3/1.4	-0.2/-0.2	0

Table 60 shows the relationship between the damage metric and the kinematic angles. As noted before, the absolute values have been used for roll and yaw because it is believed that the resulting extent of damage would be the same because of the structural symmetry of the aircraft. In this table, the two angles have been added together to create a single parameter—off-nominal angle—representing the deviation from normal flight attitude. The two scenarios with the high damage metrics also have the largest median and average flight path angles. The trend with decreasing damage metric is less clear for the off-nominal angle in which scenario H+M exhibits a low median value with a high average roll and yaw angle. This contrast between median and average suggests that most mishaps have zero or low values, but a few severe cases have raised the average. Scenario J, which has a low average damage metric, also has a moderately high average off-nominal angle.

Table 60. Damage metric and kinematic angles by scenario—N–B

Scenario {# of events in scenario}	Aircraft Damage Metric (Avg. for Scenario)	Flight Path Angle Med./Avg. (degr.)	Pitch Angle Med./Avg. (degr.)	Off-nominal Angle Med./Avg. (degr.)	Vertical Impediments Impacted (% Mishaps)
K+L Loss of control takeoff {14}	63.9	-10.1/-12.1	10.0/4.4	3.5/18.6	50
H + M Similar mishaps regardless of influence {19}	50.2	-5.4/-8.0	4.8/6.1	1.3/11.0	63
F Runway overrun {26}	22.0	0/-3.1	0.0/-0.5	0.0/7.4	62
J Hard landing, lose control {16}	10.1	-3.8/-5.0	0.0/1.6	2.1/11.4	13
G Compromised landing, no impact {11}	2.5	-0.8/-1.6	8.9/5.0	0.0/0.5	0

The pitch angle has been treated differently because the interaction between the aircraft and the ground is different depending on whether the aircraft strikes nose up (+) or nose down (-). To determine if this difference is reflected in the damage metric, the average damage metric is calculated for the nose-up condition and for the nose-down condition of each scenario (see table 61). Similarly, the average positive and negative pitch angles were calculated with the zero values dropped. The scenario column in table 61 lists the number of mishaps and the number of nose-up and nose-down mishaps; the number of nose-level events is the difference between the number of mishaps and the sum of nose-up plus nose-down events. For the nose-up data, four of the five scenarios have average pitch angles near the value of 8 degrees, despite the damage metric range being from 4 to 65. The highest and lowest angle values correspond to the two highest damage metrics. The conclusion is that the damage metric is not sensitive to variation in positive pitch angle; other factors are more important. For the nose-down mishaps, there is a trend of high damage metrics being associated with greater pitch downward, though the trend is not uniform. A trend line fitted to the negative data has a correlation R^2=0.602.

Table 61. Damage metric and pitch angle for each scenario—N–B

Scenario {# of events in scenario}	Aircraft Damage Metric Nose-up (Avg. for Scenario)	Nose-up Pitch Angle Avg. (degr.)	Aircraft Damage Metric Nose-down (Avg. for Scenario)	Nose-down Pitch Angle Avg. (degr.)	Vertical Impediments Impacted (%)
K+L Loss of control takeoff {14, 10+, & 4-}†	64	11.6	66	-13.7	50
H + M Similar mishaps regardless of influence {19, 15+, & 1-}	43	8.0	81	-11.5	63
J Hard landing, lose control {16, 7+, & 7-}	65	7.4	38	-3.8	60
F Runway overrun {26, 4+, & 5-}	35	7.7	18	-8.6	13
G Compromised landing, no impact {11, 8+, & 3-}	4	8.0	3	-3.0	0

† The first value in the brackets is the number of mishaps, the second value is the number of mishaps with positive pitch angles, and the third value is the number of mishaps with negative pitch angles. The remainder of mishaps had zero pitch angle.

One difficulty in plotting the damage metric against the various kinematic parameters for the N–B dataset is the large number of points in the dataset. The plots are densely populated with points. To try to visualize trends, one must focus on one set of plot markers to the exclusion of the others. The plots are presented to give the reader some idea of the scatter in the data and the trends where they exist. During the analysis, a trend line (linear least squares) was computed for each scenario dataset with an R^2 correlation value. In general, the correlation values were low; the lowest was zero, and none exceeded 0.45 where 1.0 is perfect correlation and 0 is no correlation. All of the scenario G damage metric values were low (<20) and, consequently, small variations in assigning the individual damage scores have a large effect. On a relative basis, the “noise” has a larger impact on this scenario than the others.

The damage metric plotted against airspeed (see figure 54) reveals poor correlation between the two variables. The damage metric value would be expected to increase with increasing airspeed. Of the five scenarios, only scenario J has a coefficient of determination (R^2 value) (see table 62) indicative of a good correlation and a slope of the anticipated sign. As can be seen in table 62, the correlation is very weak in the other scenarios. These low correlation values essentially mean that the damage metric is random relative to the airspeed.

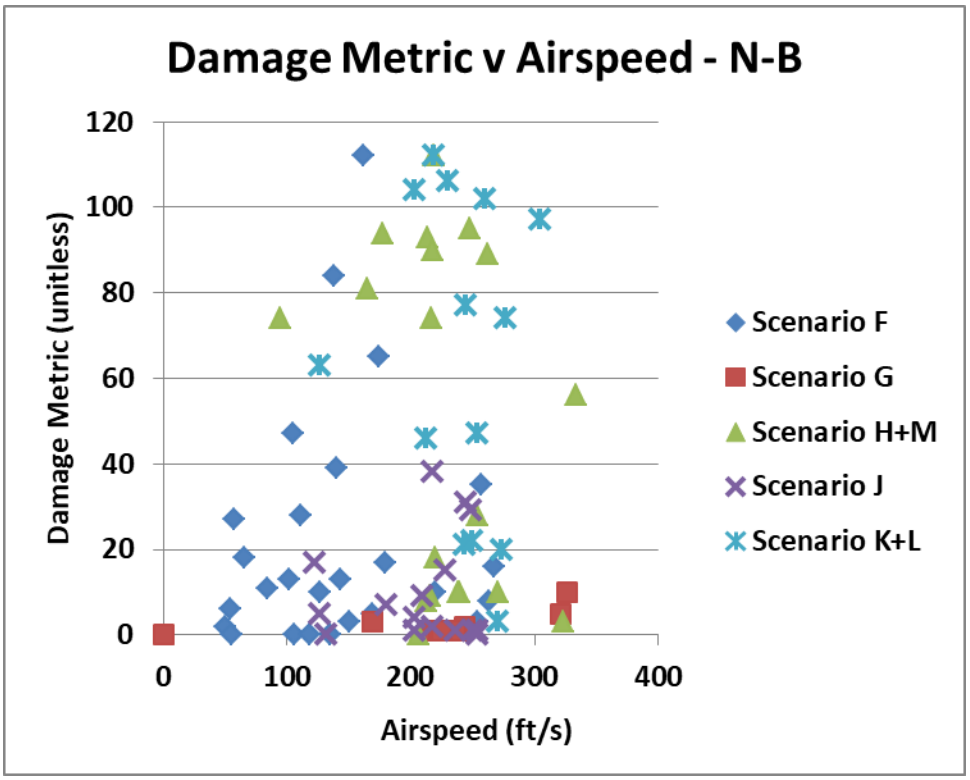

Figure 54. Damage metric vs. airspeed—N–B

Table 62. Correlation statistics for damage metric with airspeed—N–B

Airspeed	Scenario F	Scenario G	Scenario H+M	Scenario J	Scenario K+L
Coefficient of Determination R^2	0.01	0.36	0.01	0.69	0.00
Slope sign	(+)	(+)	(-)	(+)	(-)

In as much as the vertical velocity is positive downward, the expected relationship is for the damage metric values to increase with increasing vertical velocity. This trend (see figure 55) is reflected in the data for all five scenarios (see table 63). However, all of the coefficients of determination values were 0.07 or less, which indicates poor correlation.

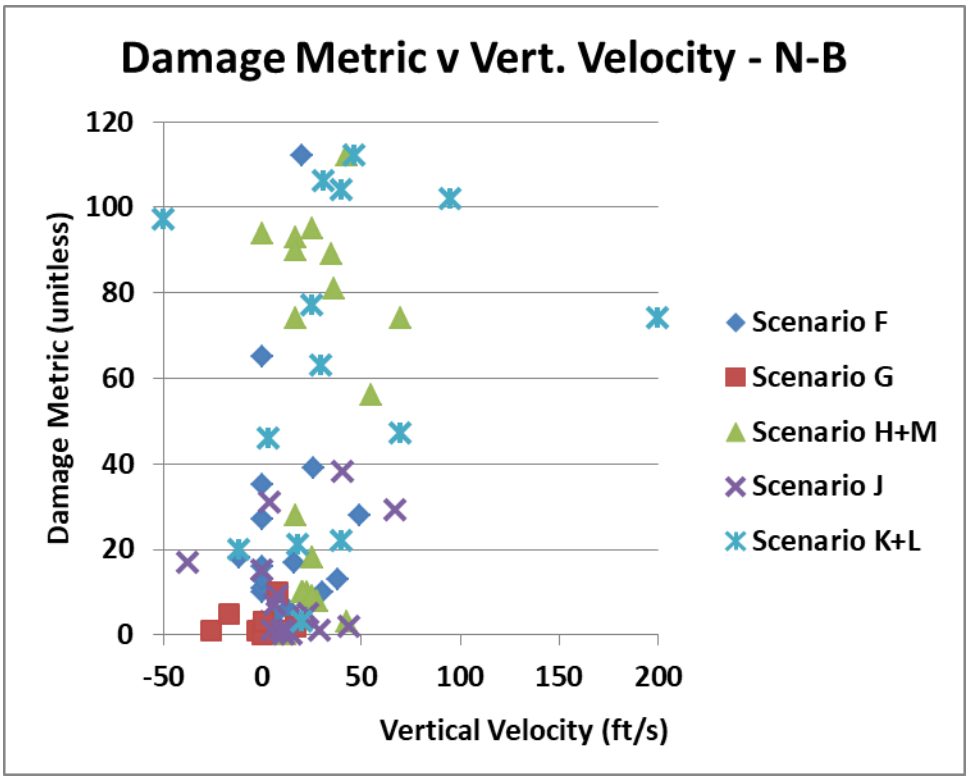

Figure 55. Damage metric vs. vertical velocity—N–B

Table 63. Correlation statistics for damage metric with vertical velocity—N–B

Vertical Velocity	Scenario F	Scenario G	Scenario H+M	Scenario J	Scenario K+L
Coefficient of Determination R^2	0.04	0.07	0.06	0.04	0.03
Slope sign	(+)	(+)	(+)	(+)	(+)

The damage metric does not show a clear correlation (see figure 56) with the flight path angle. Flight path is negative for downward impacts and, consequently, the expected slope for a linear trend line is expected to be negative. Scenarios F and G have essentially zero correlation coefficients (see table 64) and flat slopes, as would be expected from the nature of these mishaps. The remaining three scenarios (see table 64) have negative slopes, but very low correlation coefficients, with scenario J being the highest correlation at 0.14.

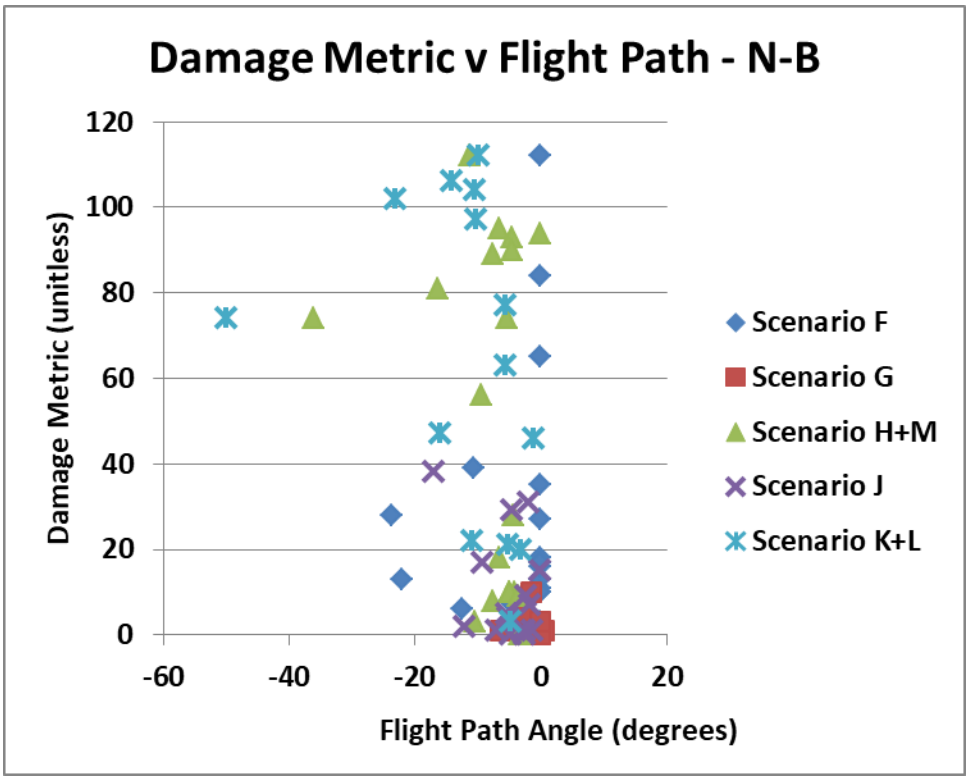

Figure 56. Damage metric vs. flight path angle—N–B

Table 64. Correlation statistics for damage metric with flight path—N–B

Flight Path	Scenario F	Scenario G	Scenario H+M	Scenario J	Scenario K+L
Coefficient of Determination R^2	0.00	0.03	0.06	0.14	0.10
Slope sign	(+)	(0)	(-)	(-)	(-)

Plotting the damage metric against the pitch angle, the difference in crash mechanics between positive and negative pitch angles must be considered. The damage metric may be expected to increase for larger values of the pitch angle in either a positive or negative sense. Therefore, either a positive or negative slope for the trend line is credible. When all the pitch angles for each scenario are plotted, the best correlation coefficient is 0.35 for scenario G with a negative slope. Because of the nature of these mishaps, all the pitch angles fall within a narrow range, and all of the damage metrics are low. Scenario J has a correlation factor of 0.29 with a positive slope. The remaining three scenarios have correlations ≤ 0.14, and two of the three have negative slopes. More crashes occur with positive pitch than with negative, so a positive slope could be expected, but only when the damage factors and the number of mishaps with positive pitch outnumber the mishaps with negative pitch. The correlation would never be expected to be very good, because the damage metric would be expected to increase as the pitch angle increases, either positively or negatively from zero. A positive slope is expected for the positive pitch angle mishaps and a negative slope for the negative pitch angle mishaps. Considering that there were more mishaps with positive slopes (44 > 0, 20 < 0, and 20 = 0), a plot was made using only the mishaps with positive pitch angles (see figure 57) to determine if the correlation coefficients would be improved. The result of

this revised analysis was not fruitful (see table 65). All slopes for the positive pitch angle mishaps are negative counter to the anticipated outcome. The best coefficient of determination is 0.48 for scenario J. As a single parameter, pitch angle, even selecting values, does not correlate well with the damage metric.

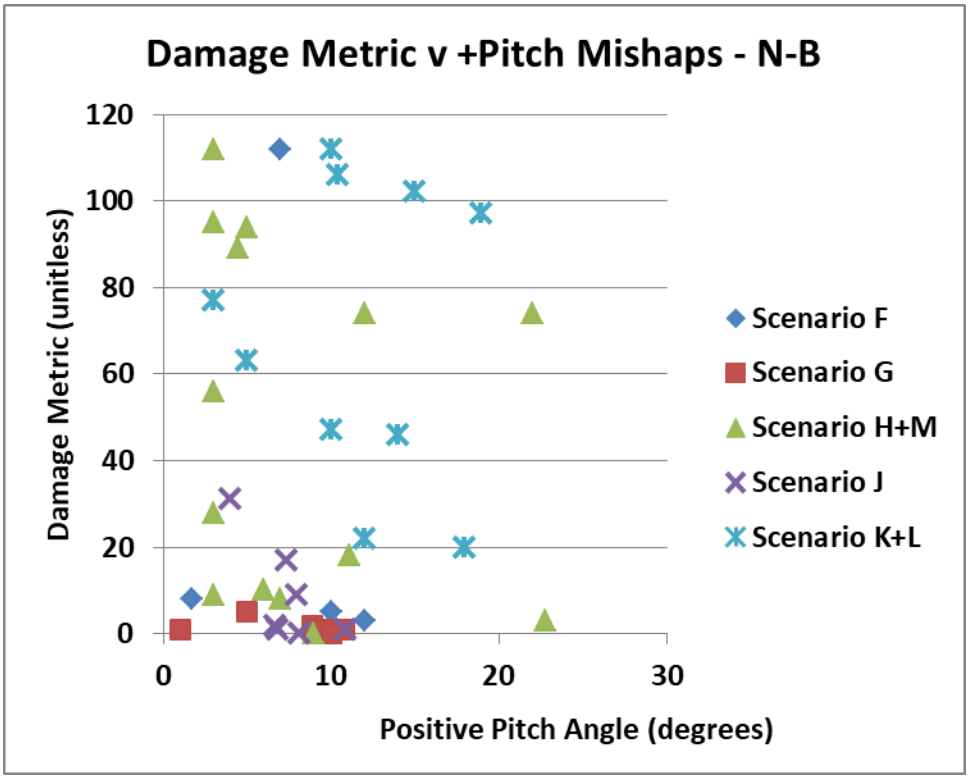

Figure 57. Damage metric vs. positive pitch angles—N–B

Table 65. Correlation statistics for damage metric with positive pitch angle—N–B

Nose-up Pitch	Scenario F	Scenario G	Scenario H+M	Scenario J	Scenario K+L
Coefficient of Determination R^2	0.02	0.14	0.04	0.48	0.01
Slope sign	(-)	(-)	(-)	(-)	(-)

The two deceleration parameters have slightly better correlation with the damage metric, but neither proved to be strong. The damage metric is plotted against peak vertical deceleration in figure 58. All scenarios have generally low values of the coefficient of determination for the peak vertical deceleration (see table 66). Only scenario J has the anticipated positive slope.

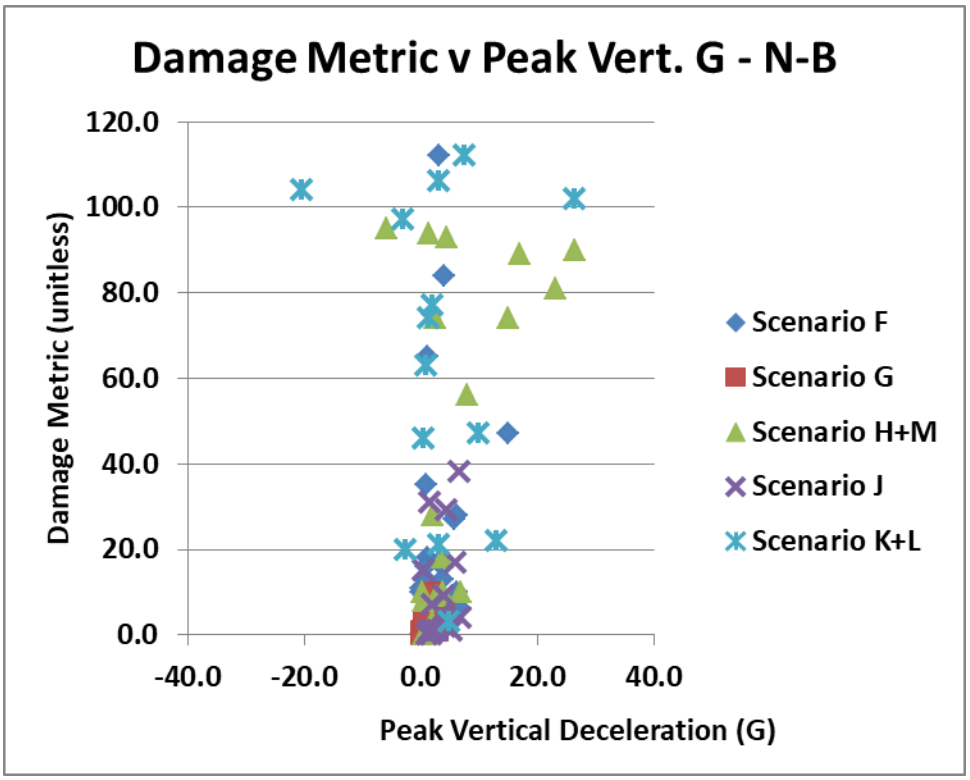

Figure 58. Damage metric vs. peak vertical deceleration—N–B

Table 66. Correlation statistics for damage metric with peak G vertical—N–B

Peak G Vertical	Scenario F	Scenario G	Scenario H+M	Scenario J	Scenario K+L
Coefficient of Determination R^2	0.07	0.14	0.20	0.08	0.01
Slope sign	(-)	(-)	(-)	(+)	(-)

The peak longitudinal deceleration has arguably the strongest single-parameter correlation with the damage metric (see figure 59). Considering that the normal sign of the deceleration is negative, the expected slope of the damage metric to longitudinal acceleration is negative. Only scenario J does not have negative slopes for the trend line (see table 67). All of the correlation coefficients are 0.30 and greater, but none are near 1.0.

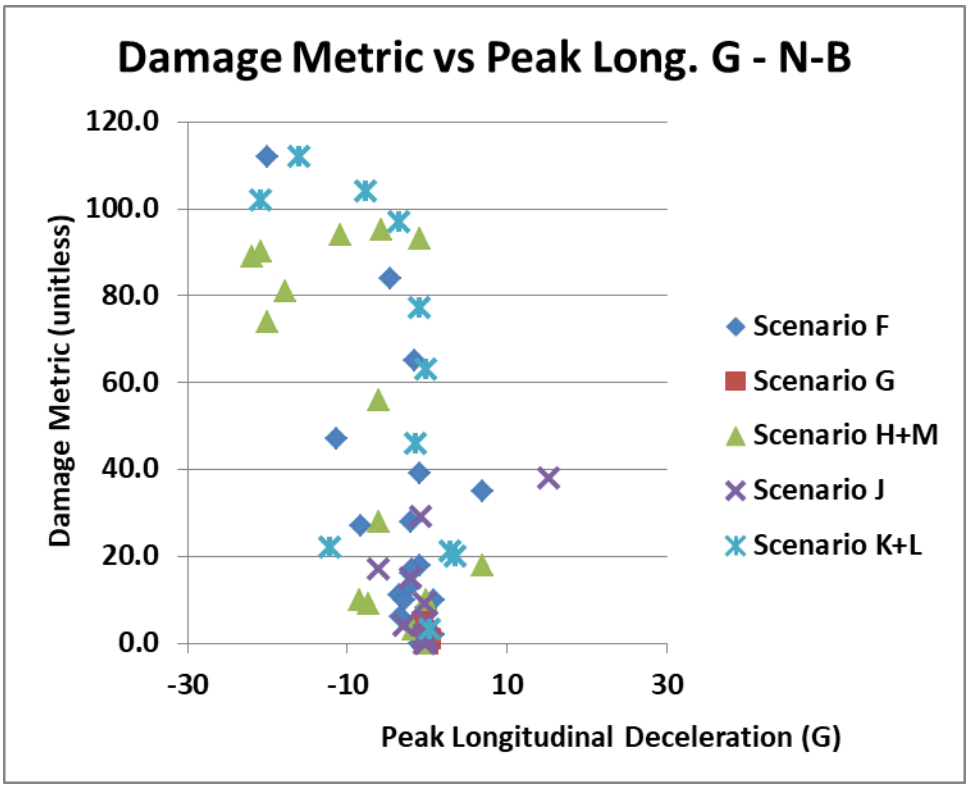

Figure 59. Damage metric vs. peak longitudinal deceleration—N–B

Table 67. Correlation statistics for damage metric with peak G longitudinal—N–B

Peak G Longitudinal	Scenario F	Scenario G	Scenario H+M	Scenario J	Scenario K+L
Correlation Coefficient R^2	0.41	0.53	0.39	0.30	0.37
Slope sign	(-)	(-)	(-)	(+)	(-)

4.2.5.1 Effect of Vertical Obstacles on Damage Metric

A yes/no field was added to the damage worksheet to record whether the aircraft encountered vertical impediments during its deceleration. Although the damage metric records only damage to the fuselage, a vertical impediment struck by any part of the aircraft including the engines was recorded as a yes. Looking first at the entire dataset, the striking of vertical obstacles has a strong effect on the damage to the aircraft fuselage, as quantified by the damage metric (see table 68). Where vertical obstacles are encountered (43 percent of all mishaps), both the average and median damage metric are higher.

Table 68. Damage metric with and without vertical obstacles

	Obstacle Encountered Damage Metric (unitless)	No Obstacle Encountered Damage Metric (unitless)
Average	52	14
Median	46	5
No. of Mishaps	37	49

The means for these two datasets were determined, and the difference between the means was tested for significance using the two-sample T-test (see figure 60). The difference in the means is found to be significant. The means are represented by the two + symbols, and the line connecting them is only to highlight the difference in vertical position. Confirming that the means differ, the 90 percent confidence interval on the difference between the two means does not include zero. The lower and upper edges of the grey areas (i.e., boxes) are the first and third quartiles of each dataset, respectively. The T-test assumes the two sample datasets are normally distributed, but both of these datasets fail the normality test. Consequently, the median values were also tested for a significant difference, even though they are also dramatically different. The nonparametric Mann-Whitney Test was applied to the two datasets to test for significance in the difference between the medians. The *p*-value is less than or equal to 0.000 and confirms that the two medians are significantly different at the 0.100 level of significance.

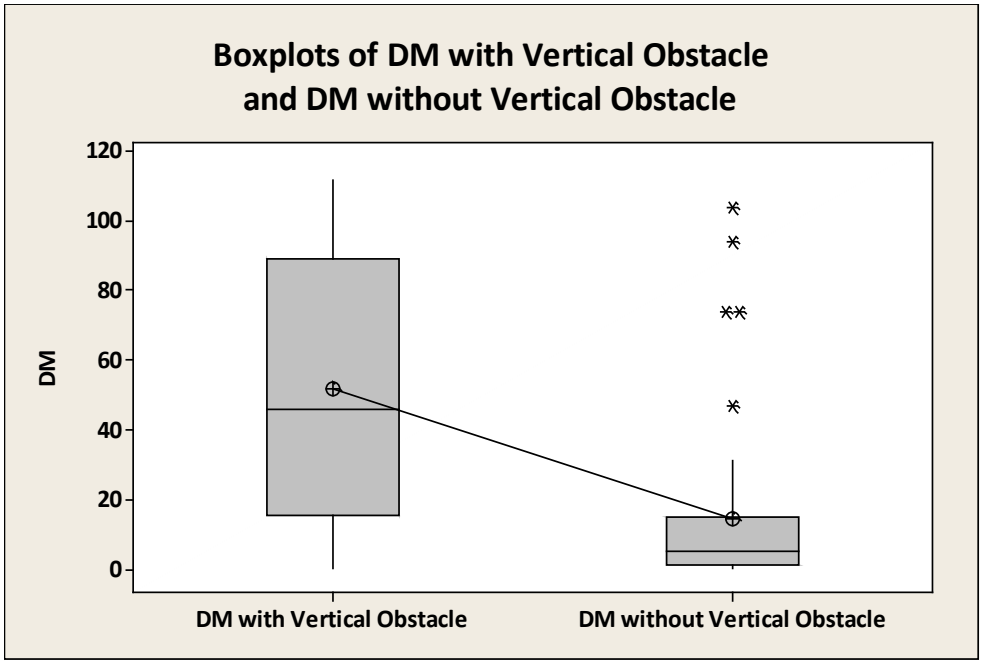

The * symbol indicates outliers identified by the statistical package as being beyond a distribution criterion.

Figure 60. Mean damage metric with and without obstacles—N–B

When the dataset is divided into scenarios (see table 69), the trend of higher damage metric with obstacles continues to hold for all but scenario G. In scenario G, no vertical obstacles were struck; consequently, there is no corresponding average damage metric, but the damage metric equals just 3 for the 11 mishaps in which there were no vertical obstacles struck. Even in scenario J, in which only 2 of 16 mishaps involved vertical obstacles, the average damage metric for the mishaps involving vertical obstacles is substantially higher than the average for those not involving vertical obstacles.

Table 69. Damage metric for each scenario with and without obstacles—N–B

	Vertical Impediment—Average Damage Metric (unitless)	No Vertical Impediment—Average Damage Metric (unitless)	No. of Mishaps With a Vertical Impediment (No.)	No. of Mishaps Without Vertical Impediment (No.)
Scenario F	32	6	16	10
Scenario G	-	3	0	11
Scenario H+M	62	30	12	7
Scenario J	27	8	2	14
Scenario K+L	86	42	7	7

In looking at the damage metric values for scenarios F and G (see tables 68–69), it is notable that the average damage metrics are substantially higher for scenario F than for scenario G, even though many of the kinematics parameters are similar. Part of the explanation for that relationship is shown in table 69, where it is evident that none of the scenario-G mishaps involved vertical obstacles. In as much as aircraft involved in scenario F mishaps generally went beyond the bounds of the prepared airfield, and the aircraft involved in scenario G mishaps did not, one possible cause for the higher damage metrics in scenario F could be a greater number of interactions with vertical obstacles. If interacting with vertical obstacles increased the damage metric in a mishap, then it would be expected that the average damage metric for a scenario is high when the fraction of mishaps that involve vertical obstacles is also high (see figure 61). The trend in the data indicates that the higher the fraction of mishaps involving vertical obstacles, the higher the average damage metric. Although the correlation factor is not strong, the trend is evident (see figure 61). This result suggests inquiring whether the presence of vertical obstacles affects or correlates with a kinematic parameter, such as a peak longitudinal deceleration (see figure 62). The correlation between the peak longitudinal deceleration and the fraction of mishaps with obstacles is somewhat better than the correlation of the damage metric with the mishap obstacle fraction. Therefore, encountering a vertical obstacle plays a significant role in the longitudinal deceleration experienced by the aircraft and, correspondingly, the acceleration experienced by its occupants. Encountering a vertical obstacle also influences the severity of the damage to the aircraft. This idea will be pursued further in the injury discussion.

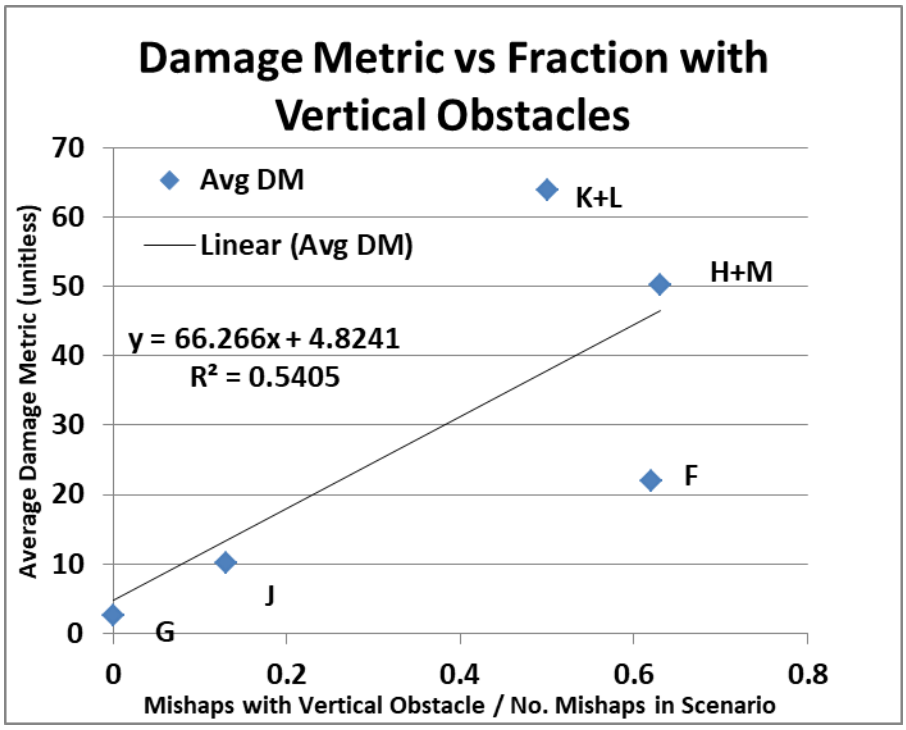

Figure 61. Damage metric correlation with vertical obstacles—N–B

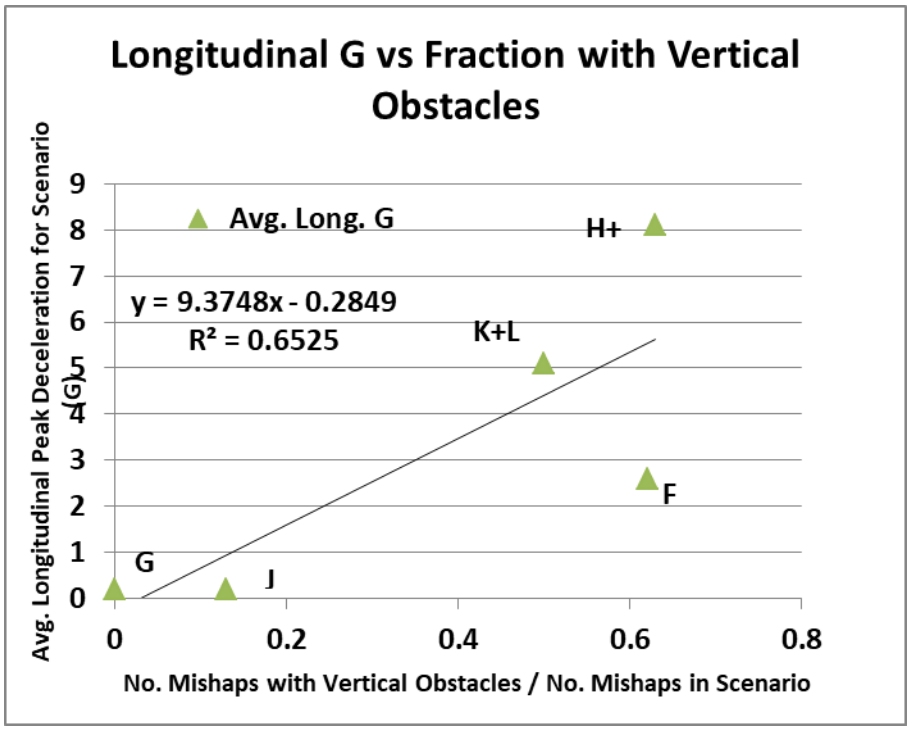

Figure 62. Average longitudinal deceleration correlation with vertical obstacles—N–B

4.2.5.2 Damage Dependence on Design Characteristics—N–B

There are three engine configurations represented in the N–B dataset: engines on wing, engines on tail, and engines on tail and fin. All eight of the engine-on-tail-and-fin aircraft are B727 three-engine aircraft (see table 70). Among the engines on wing aircraft, 41 are 2-engine aircraft, and 10 are 4-engine aircraft (see table 70). Only one of the engine-on-tail aircraft had four engines (VC-10); the remaining 27 aircraft had two engines.

Table 70. Damage metric for various engine configurations

	Eng. On Wing—2 Eng. Damage Metric (Unitless)	Eng. On Wing—4 Eng. Damage Metric (Unitless)	Eng. On Tail/Fin 3 Eng. Damage Metric (Unitless)	Eng. On Tail—2 Eng. Damage Metric (Unitless)	Eng. On Tail—4 Eng. Damage Metric (Unitless)
Mean Damage Metric	23	38	45	35	28
Median Damage Metric	6	18	37.5	13	28
No. of Mishaps	41	9	8	27	1

Taking into account that the engine-on-wing configuration has both two-engine and four-engine variations, there are four engine configurations of interest. There being only one mishap, the four-engine-on-tail mishap is excluded from this analysis. A one-way analysis of variance (ANOVA) was performed on the four datasets to test whether there is a significant difference in mean damage metric between the four configurations (see figure 63). The *p*-value for the test at the 0.10 significance level is 0.269; consequently, there is no basis for claiming that the means of any two or more configurations are significantly different. The 90^{th}-percentile confidence intervals for the value of each mean all overlap substantially, further suggesting that the means do not differ. The positions of the median lines in the box plots (see figure 63) indicate asymmetry in three of the four datasets. When tested, the datasets contain serious departures from normality. Therefore, a nonparametric test equivalent to the ANOVA is called for to be applied to the medians. The Kruskal-Wallis test requires only that the sample populations be independent and continuous, conditions that are both satisfied here. The *p*-value for the Kruskal-Wallis test is 0.025 less than the 0.100 level of significance selected. Therefore, there is a significant difference between the medians of at least two of these populations. From inspection of the boxplot (see figure 63), the significantly different pairs are the two-engine-on-wing configuration and the engines-on-tail-and-fin configuration. Given concerns about the validity of the ANOVA test, the Kruskal-Wallis test prediction is preferred.

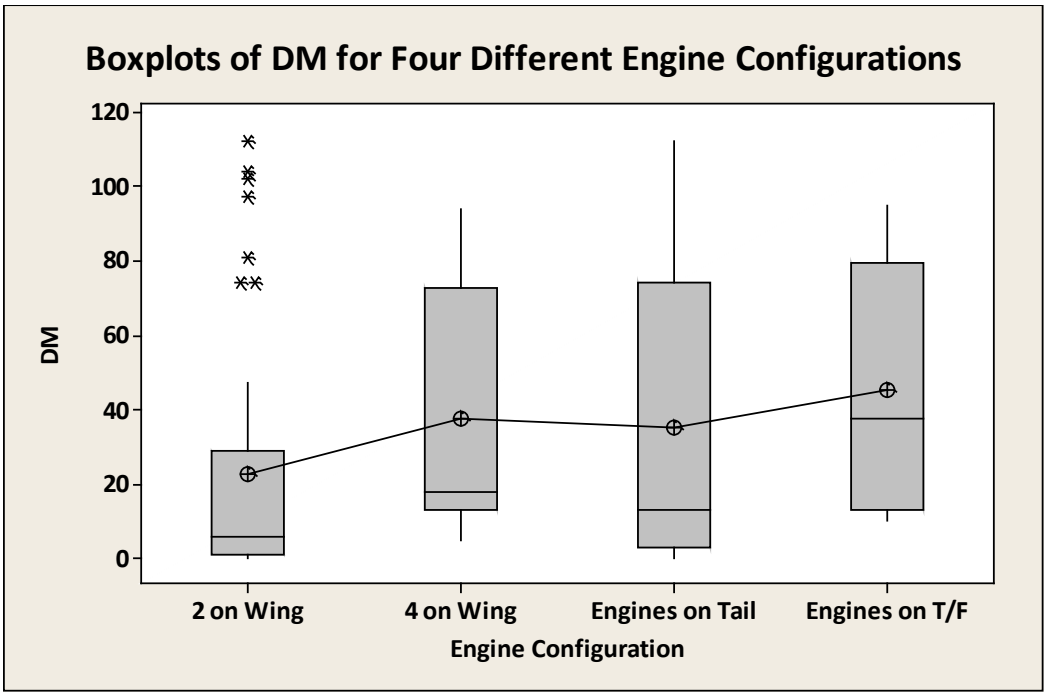

Figure 63. Damage metric comparison between engine configurations—N–B

The aircraft with tail- and fin-mounted engines have both higher average and median damage metrics than either two-on-wing or four-on-wing configurations. The median and average values are similar for the three-engine configuration, suggesting that the average is not distorted by extreme values. In looking for an explanation for why this configuration would experience a higher damage metric, it is noted that two of the eight events are scenario F, but both have damage metric values well above the average of 22 for scenario F. None of the scenario-G mishaps was a tail-and-fin configuration; therefore, there are no low-damage-metric mishaps in the dataset. Of the eight mishaps involving the tail-and-fin aircraft, five of eight (63 percent) were in the two most damaging scenarios—H+M and K+L. Having 63 percent of tail-and-fin aircraft in these two scenarios is in marked contrast to these two scenarios accounting for only 39 percent of all mishaps.

The two more populous engine configuration datasets both contain two-engine aircraft. These two datasets offer the opportunity to determine if there is a difference in the damage metrics based only on engine location without being confounded by engine numbers. Comparing these, the aircraft with tail-mounted engines have a higher average and higher median damage metric than the aircraft with two wing-mounted engines (see figure 64). The mean damage metric for the two-engines-on-tail configuration is 35, compared to 22.8 for the two-engines-on-wing configuration. The two-sample T-test finds that these two means do not differ significantly. The 90 percent confidence interval on the difference of the two means includes the value zero, which further supports the prediction of the two means not being significantly different. The boxplots (see figure 64) indicate asymmetry in the datasets, and the normality assumption is violated. A Mann-Whitney test was made to compare the two sample medians. The Mann-Whitney test finds that the two medians are just statistically different (p-value = 0.0815) at the 0.100 level of significance. Consistent with the view in figure 64, the two-engine-on-tail is identified as the higher median.

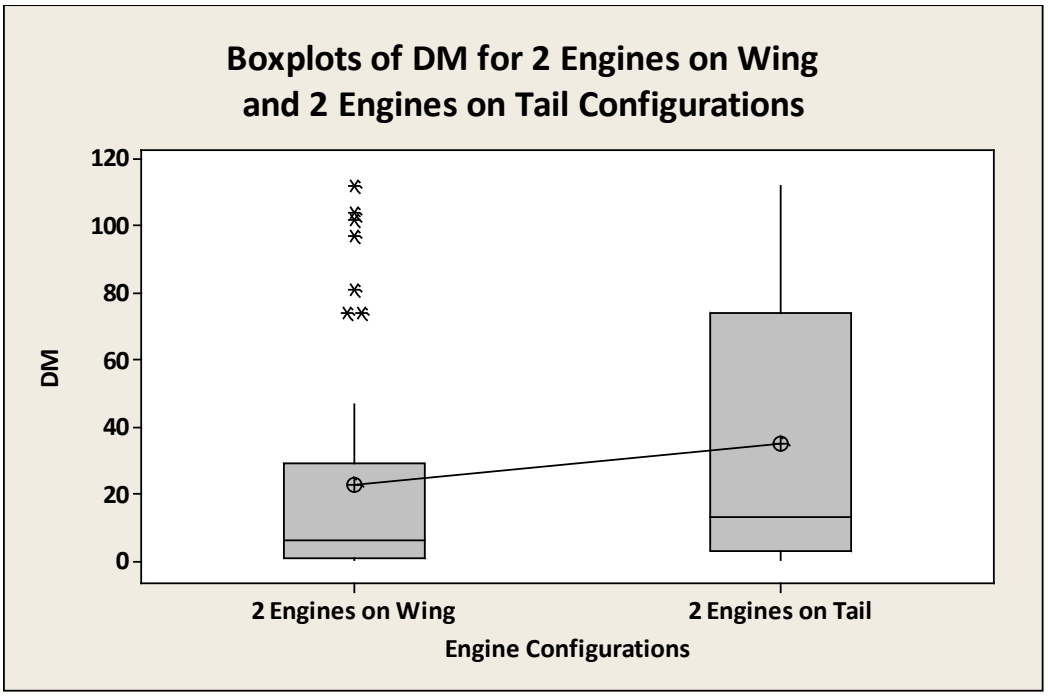

Figure 64. Damage metric of two-engine configurations compared—N–B

Making the same comparison for the four-engine aircraft is not advisable because there is only a single mishap involving four tail-mounted engines.

A third comparison is made of the engine-in-tail-and-fin to engines-on-the-wings. For this assessment, the two-engine and four-engine-on-wing datasets are combined. Giving 50 mishaps in the engine-on-wing dataset and eight mishaps in the tail-fin configuration, the mean damage metric for the engines-on-wings dataset is 25.5 compared to 45.1 for the tail fin dataset. The two-sample T-test gives a *p*-value of 0.155, which indicates that the two means do not significantly differ at the 0.100 level of significance. The 90-percent confidence interval for the difference between the two means includes the value zero, which supports that the two means do not significantly differ. From figure 65, the indication is that the engine-on-wing dataset is asymmetric. Applying the Mann-Whitney nonparametric test generates a *p*-value of 0.035, which indicates a statistically significant difference between the medians. This is a different conclusion than that predicted by the T-test, but in view of the validity concerns for the T-test, the result of the Mann-Whitney test is given preference.

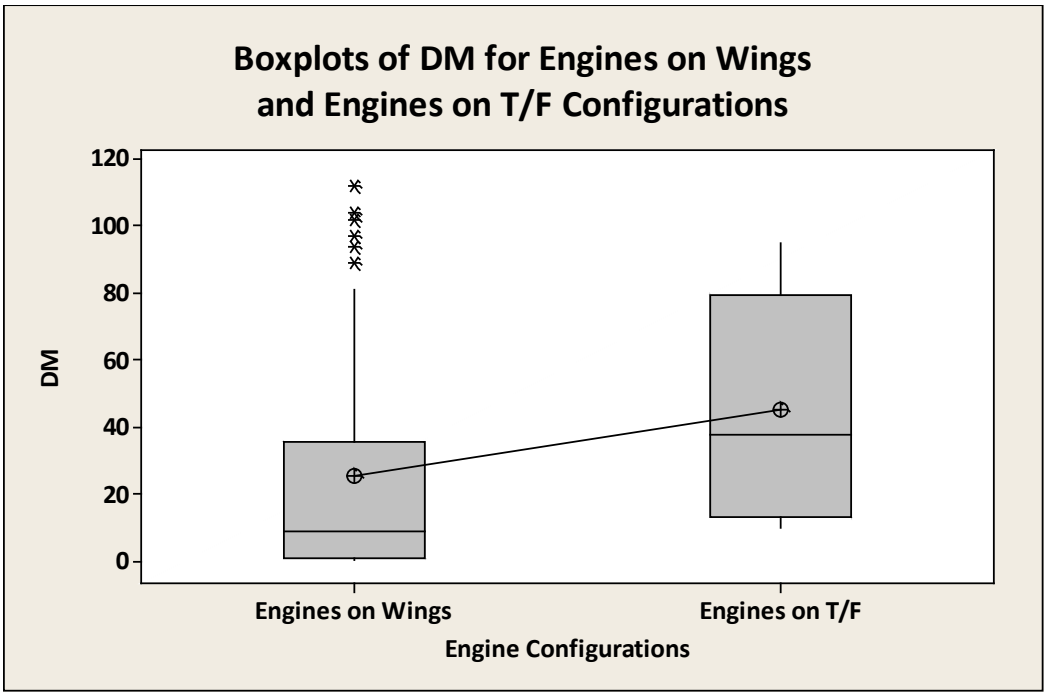

Figure 65. Damage metric of engine-on-wings to three-engine configuration compared—N–B

4.2.5.3 Damage Dependence on Gear up/Down—N–B

The status of the landing gear was noted for each mishap. Of the 86 mishaps, 11 occurred with the landing gear up. Only 1 of the 26 scenario-F mishaps occurred with the landing gear up, and this was an aborted takeoff. The aircraft had contaminated wings, but was back down on the runway before going beyond the threshold; therefore, the mishap was counted as scenario F rather than scenario K. Of the 11 scenario-G mishaps, 2 occurred with the gear up. The fact that the landing occurred with the gear up is the mishap itself (i.e., the crew landed with the gear up; otherwise, it would have been a successful landing). Of 15 scenario-H mishaps, 2 occurred with the gear up; of the 16 scenario-J mishaps, 1 occurred with the landing gear up, and 0 of the 5 scenario-M mishaps occurred. One of seven scenario-K mishaps and four of seven scenario-L mishaps occurred with the gear up. The large fraction of scenario-L mishaps with gear up may reflect the crew's lack of anticipation for the wind. Two of these four mishaps were among the oldest (1975 and 1976) and occurred within the U.S., ''whereas the other two occurred in 2005 and 2006 in Africa.

This is the end of the analysis on damage metric as the outcome. After considering evacuation, the analysis will address injuries as the outcome and the dependence on kinematics, and as the damage metric.

4.2.6 Evacuation—N–B

The N–B aircraft in the study were equipped with doors and at least two different overwing exit types. Any portal that is intended for occupants and that is a floor-to-standing-height opening is considered a door; any portal of smaller dimensions is considered an exit. The accident database contained information on the functionality and usability of the doors and exits, but the reports were

also read carefully for information on the evacuation. A door is deemed functional if it was mechanically operational post-crash. A door or an exit is deemed usable if it is both functional (or open[†]) and able to be used for egress. Therefore, a door that had fire beyond it or was blocked by terrain may have been functional but was not usable for escape; similarly, a door with a slide that failed or did not reach the ground was designated "unusable." The functionality or usability of all doors and exits was not documented, as shown in table 71. The numbers provided in table 71 are for those mishaps in which an emergency evacuation was carried out (58/86 mishaps). For mishaps in which the evacuation was not an emergency, only one door may have been used and the others left unreported. In some severe cases in which the aircraft was totally destroyed on impact, there was no emergency evacuation in the conventional sense. The few survivors were found either still alive in their seats among the wreckage or wandering in or near the wreckage. In these severe breakups, some occupants left the aircraft by going out through gaps in the fuselage.

Table 71. Number of doors and exits—N–B

86 Aircraft	Doors: 82 Mishaps Reported (#)	Exits: 80 Mishaps Reported (#)
Installed on Mishap Aircraft	248	196
Condition Reported	197	138
Reported as Functional	157	134
Reported as Useable	131	120

The presence of fire affects evacuation routes in important ways. First, the presence of fire near, and particularly inside, the cabin sets a very severe limit on the time available to evacuate the occupants from the cabin. Second, the presence of fire inside or outside may reduce the number of routes usable for evacuation. Post-crash fire was present in 35 of the 86 mishaps, and 26 of the 57 emergency evacuations were associated with post-crash fire. The number of available doors and exits is critical in successfully evacuating the aircraft in the regulated 90 seconds. This timing requirement is set primarily by survival time in the event of fire but is also a consideration in water landings in which flotation time can become the limit on escape. Therefore, survivability depends on the number of portals useable for occupant egress. Looking first at the doors (see table 72, upper portion), the table presents the number of fires and the number of emergency evacuations in the scenario (second column). The third column reports the average number of doors whose conditions were reported in that scenario and the lowest number of doors whose conditions were reported in that scenario. For mishaps in which no emergency evacuation occurred, it was not unusual to report only the door that was used to deplane the passengers and not to report anything about the condition of the other doors. The fourth column identifies the average number of functional doors in each scenario and the lowest number of functional doors reported for a single mishap. In three scenarios, there was at least one mishap with zero functional doors. The fifth column reports the usable doors; normally, the average number of usable doors would be expected to be lower than the average

[†] In more than one mishap, one or more doors were reported to be found detached from their frames in the wreckage. If the resulting opening was reported to have been used as an escape route, then that door opening was counted as usable; thus, there can be more 'usable' doors than 'functional' doors.

number of functional doors, and this is the case. Again, there are three scenarios with at least one mishap in which there were zero usable doors consistent with the zero functional doors.

In the lower portion of table 72, the data for the exits are presented. The third column in the table shows the average and minimum number of exits on the aircraft involved in mishaps whose condition was reported. Column four shows the average and minimum number of functional exits. Column five shows the average and minimum number of usable exits. Once again, the average number of usable doors is slightly less the average number of functional doors.

Table 72. Number of doors and exits for emergency egress by scenario—N–B

Doors (86 Aircraft/82 Reported)	Emergency Evacuations (# of Fires/# of Evacuations)	Doors on Aircraft with Reported Condition (average #/minimum #)	Functional Doors (average #/minimum #)	Usable Doors (average #/minimum #)
Scenario F (26)	9/22	3.6/0	3.1/0	2.6/0
Scenario G (11)	2/3	3.0/2	2.7/2	1.7/1
Scenario H+M (19)	9/13	3.9/1	3.1/0	2.3/0
Scenario J (16)	5/11	4.5/2	3.7/2	3.5/2
Scenario K+L (14)	10/8	2.2/0	1.5/0	1.1/0
Exits (86 Aircraft/80 Reported)	Emergency Evacuations (# of Fires/# of Evacuations)	Exits on Aircraft With Reported Condition (average #/minimum #)	Functional Exits (average #/minimum #)	Usable Exits (average #/minimum #)
Scenario F (26)	9/22	3.1/1	3.1/0	2.8/0
Scenario G (11)	2/3	1.7/0	2.5/1	2.5/1
Scenario H+M (19)	9/13	2.9/0	3.0/0	2.4/0
Scenario J (16)	5/11	2.7/0	2.4/0	2.1/0
Scenario K+L (14)	10/8	2.1/0	2.4/0	1.9/0

Of the 26 mishaps in scenario F (overruns), 9 involved fires, and there were 22 emergency evacuations. The less-severe scenario G experienced only 2 fires in 11 mishaps, and there were just 3 emergency evacuations. The 19 mishaps in scenario H+M led to 9 fires and 13 emergency evacuations. Scenario K+L encompasses 14 events; 10 involved fires, but only 8 emergency evacuations were conducted. This lower number was because several crashes were so severe that there was no organized evacuation. Of the 16 scenario J mishaps, only 5 involved fire, but 11 mishaps led to emergency evacuations.

For both the doors and the exits, the minimum usable number equal to zero appears several times. Of particular interest are cases in which both zero doors and zero exits were usable. This occurs in at least three mishaps with survivors (19770404A[†], 50050905B, and 19940702A). In each of these cases, the impact led to the breakup of the fuselage, and the survivors either escaped through the gaps or were extracted by rescue personnel working through the fuselage gaps. Mishap 19770404A

[†] CSTRG ID identifier numbers.

was a scenario H with a damage metric equal to 93, and a fraction of fatal plus serious injuries equal to 0.95. Mishap 20050905B was a scenario K with a damage metric equal to 97, and a fatal- and serious-injury fraction equal to 0.98. Mishap 19940702A was a scenario L with a damage metric equal to 77, and a fatal- and serious-injury fraction equal to 0.93.

4.2.7 Injury Analysis—N–B

In analyzing the injuries resulting from the mishaps in this study, the distribution of injuries among the different scenarios will be investigated. The injuries will be correlated with the kinematics and aircraft characteristics. The injuries for the entire aircraft will be viewed first, and then the injury fraction will be examined by aircraft segment.

In many of the investigation reports, minor injuries are treated in one category with non-injuries. In other reports, two separate counts are provided for minor and non-injuries. In as much as the numbers from the combined reports cannot be separated again, minor injuries and non-injuries are reported together for all mishaps in this study.

Viewing the injury fractions for all of the occupants in the study, including two aircraft in which the injuries could not be assigned to specific cabin segments, 17.6 percent of all occupants were fatally injured (see table 73). A further 7.6 percent of all passengers were seriously injured. The remaining 74.7 percent had either minor or no injuries. The investigation reports were not consistent in autopsy reporting; therefore, the thermal fatalities represent only a fraction of the total. The injury fractions shown below for the N–B mishaps are remarkably similar to those for the W–B mishaps.

Table 73. Number and percentage of occupants injured in the entire study—N–B

	Number of Occupants	Percent of Occupants
Fatally Injured (all causes)	1818	17.6
Fatally Injured (identified as thermal)	517	5.0
Seriously Injured	788	7.6
Minor or Not Injured	7704	74.7
Total Occupants	10,310	100

Even though approximately 18 percent of the occupants in the study were fatally injured (see table 73), the median value being zero for both scenarios G–M and for scenario F (see table 74) reveals that more than half of the mishaps in each group had zero fatalities. Similarly, the percentage of serious injuries was low. The higher average values for both fatalities and serious injuries indicate that in mishaps in which fatalities and serious injuries do occur, the numbers are well above zero. For the N–B dataset, the overrun scenario (F) and the other scenarios as a group (i.e., the impacts from the air) have similar injury percentages. The average being higher than the median values in the fatalities indicates that there are several accidents with high fractions of fatalities. A further breakdown of the injury rates to each scenario (see table 75) reveals that two scenarios (H and K) account for a large portion of the fatalities.

Table 74. Injury severity for overrun mishaps compared to all other scenarios

	Scenarios G–M Impact from Air (Median/Average)	Scenario F Overrun Impacts (Median/Average)
Fatal Injury (percent of aircraft occupants)	0/24	0/11
Serious Injury (percent of aircraft occupants)	1/8	2/8
Minor/No injury (percent of aircraft occupants)	98/67	98/81
No. of Aircraft Occupants (#)	116/121	118/118
Number of Mishaps in Scenario (#)	60	26

Table 75. Injury severity for each scenario—N–B

Scenario	Number of Mishaps (No.)	Number of Occupants (Med. No./Avg. No.)	Frac. of Occupants Fatal Inj. (Med. %/Avg. %)	Frac. of Occupants Serious Inj. (Med. %/Avg. %)	Frac. of Occupants Minor/No Inj. (Med. %/ Avg. %)	Average Damage Metric for Aircraft (Unitless)
F	26	118/118	0/9	2/11	98/81	22
G	11	136/136	0/0	0/0	100/100	2.5
H	14	90/104	22/37	10/15	46/48	59.1
J	16	140/137	0/2	0/6	100/92	10.1
K	7	108/114	85/69	13/16	2/15	72.6
L	7	108/109	0/36	5/12	66/52	55.1
M	5	101/106	0/37	1/3	99/60	25.4
H+M	19	93/106	7/37	6/12	83/51	50.2
K+L	14	108/112	67/53	11/14	9/33	63.9

Scenarios F, G, and J are characterized by low fatality and serious injury rates. The strong difference between scenarios suggests looking for a correlation with the degree of damage in each scenario. Therefore, a plot of the average severe-injury fraction for each scenario (F through M) against the average aircraft damage metric for each scenario (see figure 66) reveals a distinct trend and a good correlation for a linear trend line (a quadratic fit gives a very small improvement in the correlation coefficient, but there is no obvious physical justification). The two trend lines are so close that the predicted injury value for a given damage metric value is not very different.

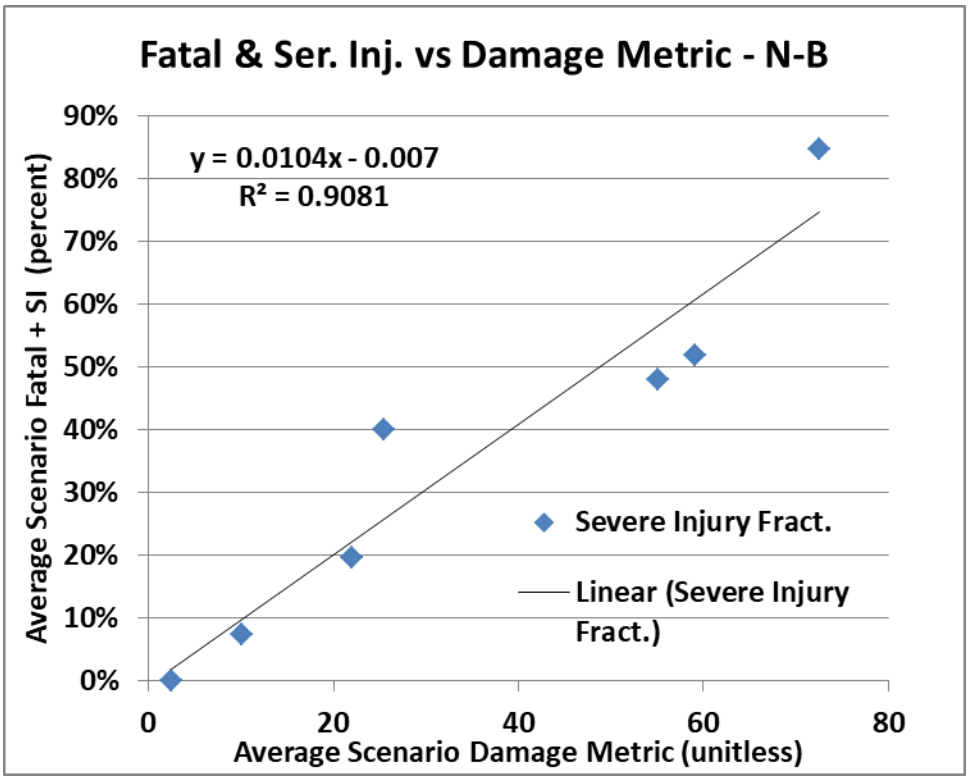

Figure 66. Average fatality and serious injury rate vs. damage metric—N–B

Comparing scenario H to scenario M (see table 75), the same scenario with localized wind influence, reveals that scenario M has similar average fatal rates but lower average serious injury rates. Similarly, for scenarios K and L, the wind-influenced scenario L has lower average fatality and lower average serious injury rates. These two results support the earlier conclusion based on damage metric that the localized wind influence on a mishap does not cause the mishap to be more severe than other mishaps with similar characteristics.

4.2.7.1 Configuration Influence on Injury—N–B

Two design considerations—engine location and engine number—were investigated. Three engine configurations cover all of the N–B mishaps: engines-on-wing, engines-on-tail, and engines-on-tail-and-fin. All of the engine-on-tail-and-fin configurations were three-engine B727 aircraft. The only engine-on-tail aircraft with four engines was a VC10. Approximately 59 percent of the mishaps involved aircraft with the engines on the wing. The most recent four-engines-on-the-wing mishap occurred in 1990 in the U.S. involving a South American airline. All other mishaps in the study involving four-engine-on-the-wing aircraft occurred prior to 1980.

The average values for the percent of fatal and serious injuries vary according to the engine configuration (see table 76). Excluding the single instance of four engines mounted on the tail (VC10), four engines on the wings has the highest mean and median rates of fatal plus serious injury. Although not the highest, the mean and median damage metrics for this configuration are also high, indicating that mishaps involving this configuration were severe. The two-engine-on-the-tail configuration has the second-highest mean severe-injury rate, but the low value for the

median injury fraction of this dataset indicates that there are many low-injury-fraction mishaps in the dataset; the average has been raised by severe events. The damage metric for this configuration does not show as large of a difference as do the average and median for the injury fractions. Although the three-engines-on-tail-and-fin configuration experienced the most severe crashes, as indicated by mean and median damage metric, it had only the third-highest mean severe-injury fraction. This relationship could suggest that there may be injury mitigating advantage to having the engines at the rear. However, if there were an advantage to positioning the engines behind the cabin, then the injury rate for the two-engines-on-tail configuration would be expected to be lower than for the two-engines-on-the-wing configuration. The opposite is true; the severe-injury fraction for the two-engines-on-tail is higher than for two-engines-on-wing. The relationship between the two average injury fractions is consistent with the damage metric being higher for the two-engines-on-tail. The lowest mean and median severe-injury fractions are exhibited by the two-engines-on-wing configuration. The mean and median damage metrics are also low, suggesting that the low injury fraction may be due to a less severe set of mishaps. To investigate the differences in injury fractions further, the number of mishaps for each configuration and scenario were broken out (see table 77).

Table 76. Fatal- and serious-injury fraction dependence on engine configuration—N–B

	Eng. On Wing – 2 Eng. Median /Average	Eng. On Wing – 4 Eng. Median /Average	Eng. On Tail/Fin 3 Eng. Median /Average	Eng. On Tail – 2 Eng. Median /Average	Eng. On Tail – 4 Eng. Median /Average
% Severe Injury	0%/19%	17%/41%	13%/29%	2%/34%	55%/55%
Damage Metric	6/23	18/38	38/45	13/35	28/28
No. Mishaps	41	9	8	27	1
Median Mishap Date	Dec. 2003	Jun. 1973	Jan. 1976	Jan. 1996	Apr. 1972

The breakout of the mishaps by scenario provides some support for the idea that the difference in injury fractions is because of the difference in the types of crashes in which the aircraft were involved. The three-engines-on-the-tail configuration was involved in three scenario H+M mishaps and two scenario K+L mishaps, which are generally the more severe mishaps, as indicated by mean damage metric. The two-engines-on-wing configuration, which has the lowest severe-injury fraction and lowest damage metric, experienced 32 of 41 mishaps in the relatively mild scenarios F, G, and J.

Table 77. Number of mishaps associated with design configurations—N–B

Scenario	Eng. On Wing – 2 Eng. No. of Mishaps	Eng. On Wing – 4 Eng. No. of Mishaps	Eng. On Tail/Fin 3 Eng. No. of Mishaps	Eng. On Tail – 2 Eng. No. of Mishaps	Eng. On Tail – 4 Eng. No. of Mishaps
Scenario F (26)	15	2	2	6	1
Scenario G (11)	7	0	0	4	0
Scenario H+M (19)	3	5	3	8	0
Scenario J (16)	10	2	1	3	0
Scenario K+L (14)	6	0	2	6	0
All (86)	41	9	8	27	1

All of the aircraft in the N–B dataset were of the low-wing configuration; therefore, there is no basis for analyzing the survivability implications of differing wing configurations.

4.2.7.2 Injuries in Each Scenario and Segment—N–B

Transport aircraft fuselages and cabins have one long dimension (length) and two approximately equal dimensions (width and height). As a consequence of these dimensional differences, it is reasonable to expect that the impact conditions and, consequently, the injury outcomes may not be uniform throughout the aircraft. To see what affect this dimensional anisotropy has on the injury distributions in aircraft, the data have been grouped by segment and scenario (see table 78). For the purpose of this analysis, fatalities and serious injuries have been grouped together and are referred to as "severe injuries." The percentage of all occupants that were either fatally or seriously injured is determined for each cabin segment.[†] From the values in table 78, the results are not as might be expected in scenario F. The overrun scenario would be expected to have a higher incidence of injuries in the cockpit and forward cabin, but actually only the cockpit exhibits a slightly higher rate of serious injury. The overwing cabin shows a slightly lower rate of injuries. Scenario G has no severe injuries and, therefore, no pattern. Scenario J, the other mild scenario, experiences slightly more severe injuries in the cockpit, as might be expected for the most vulnerable area of a vehicle moving forward. For the two severe scenarios, the frequency of severe injuries is remarkably uniform along the length of the aircraft. The rates of severe injury are slightly higher at the cockpit and the tail. In these two severe scenarios, there appears to be no advantage to being in the structurally more robust overwing cabin. The population of occupants in the tail is generally small, being limited to one or two rows of seats (infrequent) or, more commonly, exclusively flight attendant seats. A general observation is that those scenarios

[†] The injury information for one scenario F mishap (19760427) was incomplete; only 2 fatalities of the 37 could be located (cockpit and tail), whereas the remaining fatalities, serious injuries, and minor/no injuries could not be located. This missing information does not affect those analyses in which the whole aircraft is treated together and the correct numbers were used. However, the missing information does mean that these distribution percentages for Scenario F could be off slightly. One Scenario-K mishap (19880831A) provides locations for the 14 fatalities, but the 26 serious injuries and the 68 minor/no injuries could not be located; consequently, there is also some uncertainty in the segment percentages for Scenarios K+L and G-M. Because the number of mishaps in each scenario is large, the effect can be expected to be relatively small.

resulting in more extreme attitudes—the loss of control scenarios J and K—tend to show a more uniform distribution of severe injuries along the length of the aircraft.

Table 78. Fraction of severe injuries for each scenario and cabin segment

Scenario (no. of mishaps)	Cockpit (% of Occupants Fatal or Serious Injury)	Forward Cabin (% of Occupants Fatal or Serious Injury)	Over-Wing Cabin (% of Occupants Fatal or Serious Injury)	Rear-Cabin (% of Occupants Fatal or Serious Injury)	Tail (% of Occupants Fatal or Serious Injury)
Scenario F (26)	23%	17%	13%	18%	19%
Scenario G (11)	0%	0%	0%	0%	0%
Scenario H+M (19)	61%	45%	48%	47%	51%
Scenario J (16)	9%	4%	3%	3%	0%
Scenario K+L (14)	74%	70%	63%	56%	79%
Scenarios G–M (60)	40%	31%	28%	23%	36%

4.2.7.3 Injuries Related to Kinematics—N–B

The influence by each of the kinematic parameters on the fraction of severe injuries is reviewed by plotting the severe-injury fraction for each mishap against the value of the kinematic parameter. The scenario of the mishap is coded into the point marker.

In the airspeed plot (see figure 67), the mishaps in scenario G all have zero severe-injury fractions. For the more-violent scenarios—H+M and K+L—the anticipated pattern of increasing injury fraction with increasing airspeed is evident, although there is a great deal of scatter in the data. Looking in particular at the severe-injury fractions for scenario H+M mishaps, it is evident that the wide range of airspeeds for the high-injury fraction mishaps substantially overlaps the wide range of airspeeds for the low-injury fraction mishaps within the same scenario. The H+M mishaps are remarkable for the absence of intermediate values of injury fraction.

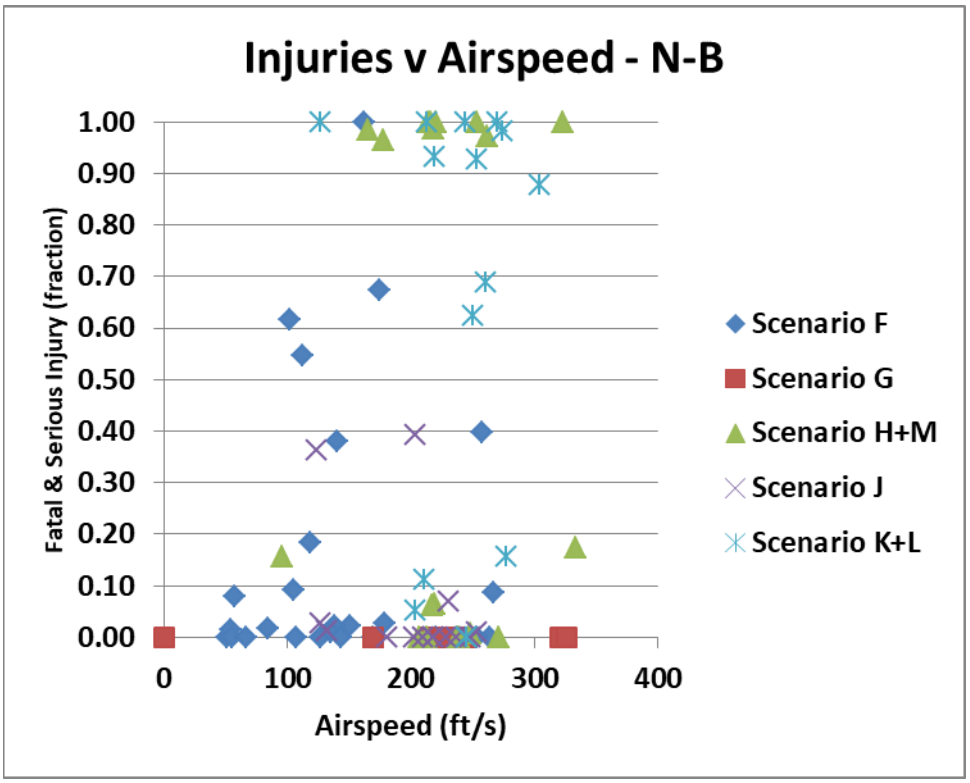

Figure 67. Severe-injury fraction dependence on airspeed—N–B

Higher vertical velocity would be expected to lead to more severe damage and, consequently, higher severe-injury fractions (see figure 68). As with the airspeed, this is generally true for the vertical velocity, but the trend is by no means clear. All scenario G mishaps were without severe injury. Scenario F would be expected to have only small values of vertical velocity because the aircraft is already on the ground when it overruns. However, it does appear that in those instances in which a vertical velocity develops, the vertical velocity leads to an increased injury fraction. The combined scenarios H+M exhibit both high- and low-injury fractions over the same range of vertical velocity and, therefore, there is no trend. Only in the combined scenario K+L does there appear to be a clear trend, although again, with wide scatter.

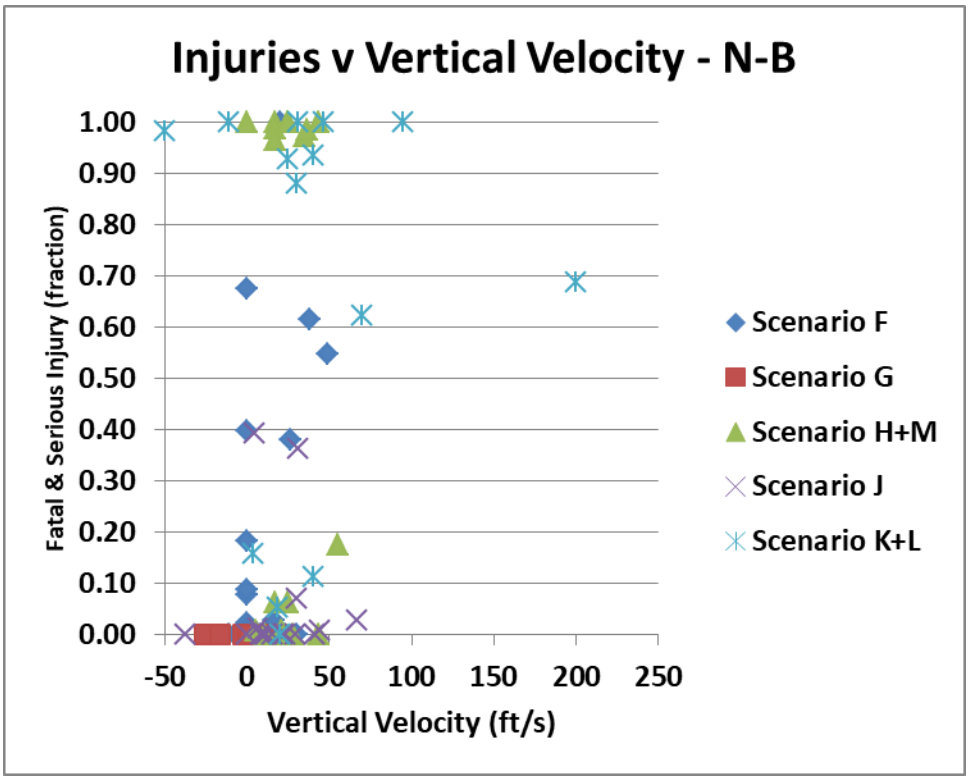

Figure 68. Severe-injury fraction dependence on vertical velocity—N–B

The flight path is the angle between the aircraft's velocity vector and the ground. Normal landings have a flight path in the range of 2 to 4 degrees. Steeper flight-path angles would be expected to lead to harder landings and, consequently, to greater damage and injuries. For scenario F, the flight path is generally zero because the aircraft is already on the ground. It is only when the aircraft goes down a slope or drops off a discontinuity that a flight-path angle develops. Most of the flight-path angles for scenario F are zero, but where an angle develops, the injury fraction is higher (see figure 69). However, a non-zero flight-path angle is not the only reason for a high severe-injury fraction. As can be seen in figure 69, there are values of the injury factor exceeding 0.4 in mishaps with zero flight-path angle. The combined scenario H+M has both high and low values for the injury fraction, but they occur over roughly the same range of flight-path angles; therefore, there is no clear trend. Similarly, for combined scenario K+L, except that there is one extreme flight-path angle. This extreme angle might be expected to lead to a very severe mishap, and yet more than 30 percent of the occupants were not severely injured.

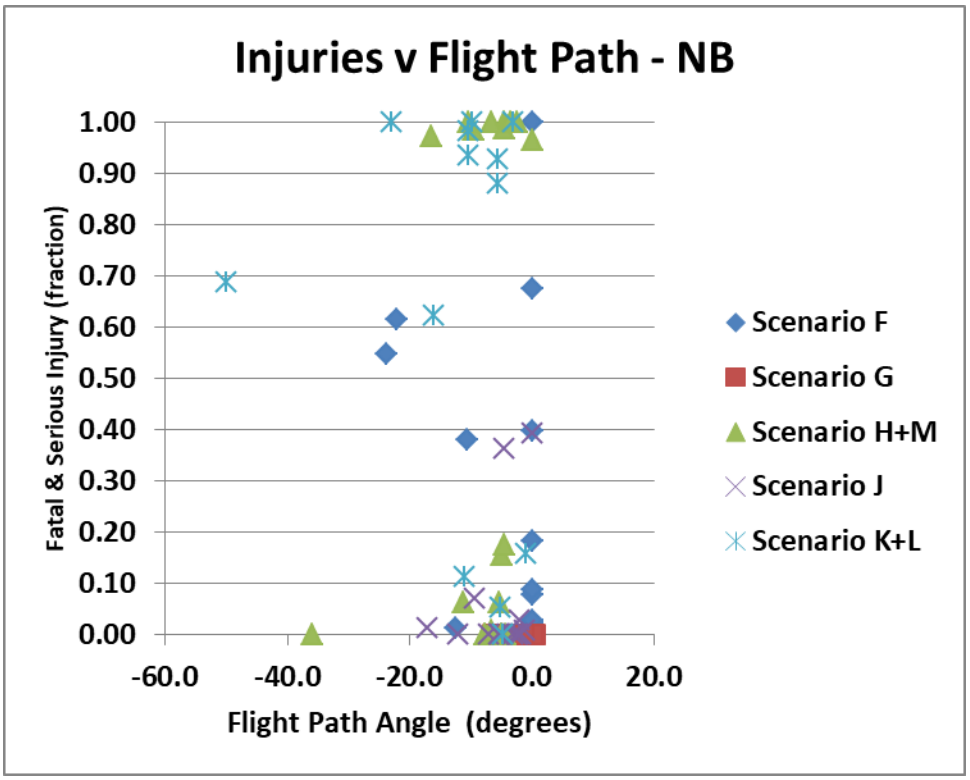

Figure 69. Severe-injury fraction dependence on flight-path angle—N–B

The expectation for the trend in pitch angle is somewhat different than the other kinematic parameters. Rather than a monotonically increasing trend, the zero value for pitch angle might be expected to be the least injurious, with the rate of injury increasing as the pitch angle becomes either more positive or more negative. The evidence (see figure 70) for such a bimodal trend is not clear from the data. If one views only the points on the positive side of zero, none of the scenarios exhibits a clear trend of increasing injury with increasing pitch angle. Similarly, viewing only the negative values of pitch, there is not a clear trend for any of the scenarios. The range in pitch angle data points at the higher injury fractions is certainly broader than the range in pitch angle of points at the low injury fractions, but there are not two distinct curves forming a "V" shape. There is not even a roughly triangular area of data points; rather, the data show a broad spread of pitch angles, even at a low-injury fraction.

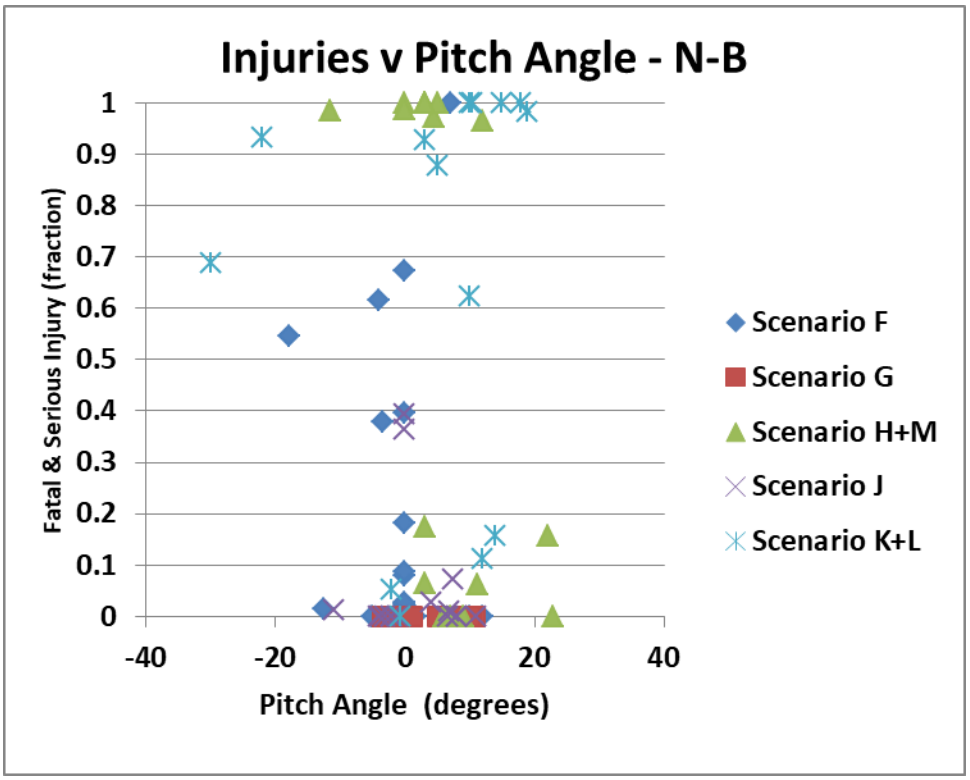

Figure 70. Severe-injury fraction dependence on pitch angle—N–B

The idea of two separate trends for positive and negative pitch angle also elicits the idea of different impact sequences for the two different cases. For positive pitch (nose up), the tail will strike first, followed by the fuselage rotating downward before impacting the ground, and then the aircraft sliding to a stop. Based on these crash mechanics, more injuries of a vertical nature might be expected forward compared to rearward. Unfortunately, the investigation reports generally only include numbers of injuries at two or three levels, not the detail on the nature of the injury. For the negative pitch angle (nose down) mishaps, the aircraft will impact nose first, followed by the tail falling to the ground. The degree of damage to the nose and forward cabin will depend on the firmness of the surface. For a runway, there will be less damage as the nose impacts and slides out; conversely for soft terrain, the nose may tend to dig in and cause a higher deceleration rate. So again, the pattern is likely to be more injuries toward the front.

To explore whether the pitch angle does affect the frequency of injuries, the mishaps were sorted into three groups: positive pitch, negative pitch, and zero pitch. The severe-injury (fatal plus serious injuries) fraction was determined for each segment in each mishap, and the average injury fraction was determined for each segment in each pitch group (see table 79). Analyzing the data for the scenarios in which the aircraft is coming to the ground from the air (G–M), the values in table 79 show a minimal variation along the length of the cabin. There are slightly higher fractions toward the front, but the difference is not dramatic. Two observations are unexpected. The pitch angle equal to zero mishaps (small sample) as a group have much higher injury fractions than either nose-up or nose-down. Secondly, the injury fractions for the nose-down mishaps are even lower than those for the nose-up. The average positive pitch angle is +8.8 degrees; the average negative pitch angle is -6.8 degrees.

Table 79. Injury fraction by cabin segment for positive and negative pitch—N–B

Scenario G–M	Cockpit	Forward Cabin	Overwing Cabin	Rear Cabin	Tail	No. of Samples
Pitch Angle > 0	0.42	0.36	0.34	0.34	0.38	41
Pitch Angle = 0	0.77	0.80	0.68	0.63	0.67	4
Pitch Angle < 0	0.20	0.21	0.19	0.13	0.15	15
Scenario F						
Pitch Angle > 0	0.20	0.24	0.20	0.22	0.20	5
Pitch Angle = 0	0.14	0.12	0.07	0.08	0.07	15
Pitch Angle < 0	0.5	0.33	0.33	0.17	0.16	5 †

† In scenario F, one mishap was missing pitch angle data; therefore, only 25 mishaps are reported.

The scenario F mishaps were excluded from the initial analysis because the aircraft is already on the ground, and pitch angle zero predominates. However, the trichotomous analysis was applied to the scenario F data with an interesting result. For the nose-down condition (average -8.6 degrees), the injury fractions are high at the forward segments of the aircraft. For the overrun scenario F, a nose-down condition means that the aircraft left the runway and went downward to impact. In one of these mishaps, the aircraft went downward and the forward fuselage struck a lighting structure; in another mishap, a post-crash fire caused a high-fatality rate. For the nose-up cases (average +7.7 degrees), the aircraft encountered rising terrain, which led to slightly more injuries, probably due to higher deceleration and greater damage. The zero pitch cases had the lowest injury fractions, likely because these aircraft continued decelerating at a uniformly low rate.

4.2.7.4 Injury Dependence on Combined Velocity—N–B

The two-axis velocity plot is used to visualize the dependence of injuries on impact velocities (see figure 71). The plot displays all of the mishaps in scenarios G–M. The mishaps are grouped into three clusters: mishaps with less than 0.1 fraction of severe injuries (35), mishaps with greater than 0.9 fraction of severe injuries (17), and the mishaps with the fraction of severe injuries between 0.1 and 0.9 (8). The ellipse is the same 90^{th}-percentile survivable velocity ellipse as used to investigate damage metric in figure 53. Although the mishaps with injury fractions of 0.9 or greater tend to fall near or outside the ellipse, there are four of these high-injury fraction mishaps with velocities within the 90^{th}-percentile survivable velocity. Of the 17 mishaps with intermediate injury fractions, 6 fall well outside the ellipse. Looking back to figure 53, one can see that only three of the high-fraction mishaps were actually labeled as NS; the remainder had some degree of survivability.

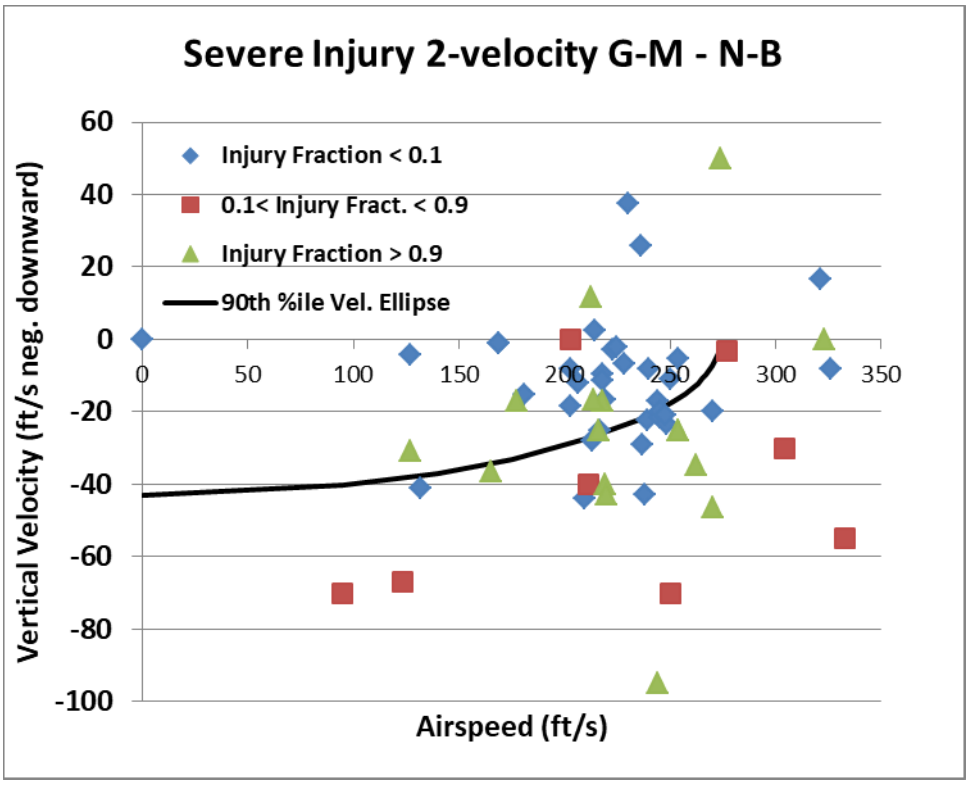

Figure 71. (G–M) Severe-injury fraction on a two-velocity plot—N–B

Although the limits for the three injury fraction intervals in figure 71 were chosen somewhat arbitrarily, the fact that the lowest 10 percentage points contain the most mishaps, and the upper 10 percentage points contain the second greatest number of mishaps, is striking. Creating a histogram for the severe-injury fraction of scenario G–M (see figure 72) reveals the polarized distribution. Including the scenario F mishaps does not materially change the distribution. There are very few mishaps with intermediate injury outcomes.

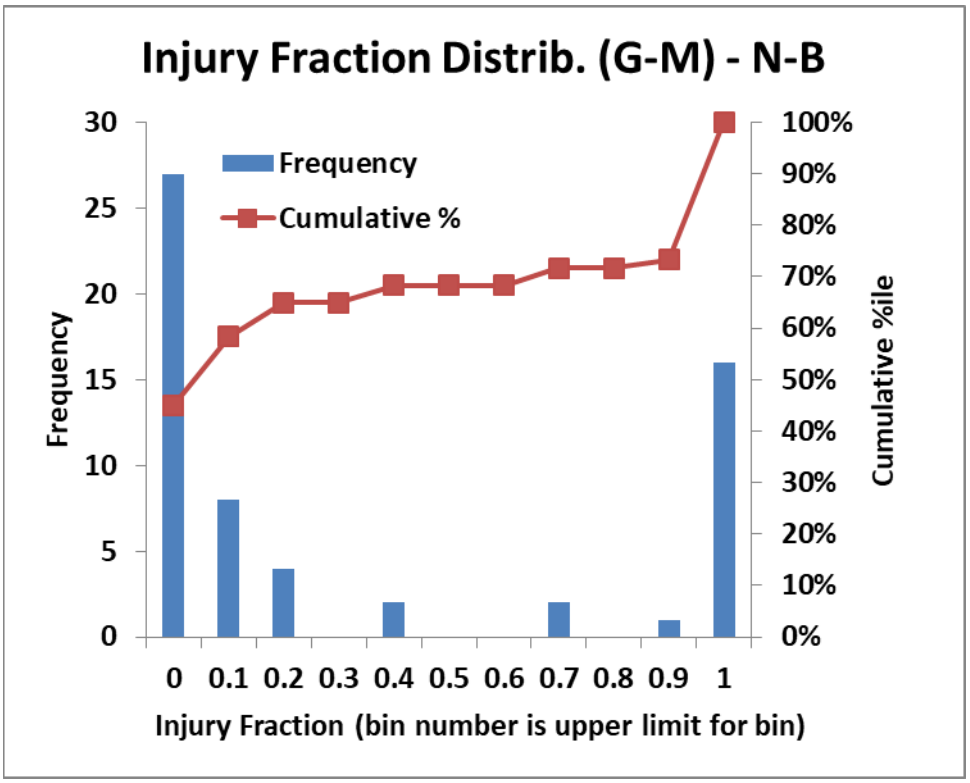

Figure 72. Severe-injury fraction distribution scenario (G–M)—N–B

4.2.7.5 Injury Related to Damage Metric—N–B

The general trend is that as the aircraft damage metric increases, the fraction of occupants suffering severe injury also increases (see figure 73). The highest injury fraction in the overrun scenario F is 0.70 and the other mishaps generally show an upward injury trend with increasing damage metric. The linear trend line had a coefficient of determination, R^2, equal to 0.45 and a slope equal to 0.0065. With the exception of scenario G, the other scenarios have trend-line slopes with similar values. Scenario G had no injuries. Scenario H+M has a coefficient of determination equal to 0.64, and the slope is 0.0096. This slope can be interpreted as an approximately 1% increase in injury fraction for each unit increase in damage metric. Scenario J has a limited range of damage and injury fraction; the coefficient of determination is low at 0.18, but the slope is within the same order of magnitude as the other scenarios at 0.0044, or approximately half the slope of scenario H+M. Scenario K+L has a coefficient of determination equal to 0.60 and a slope equaling 0.0083, which is similar in value to scenario H+M.

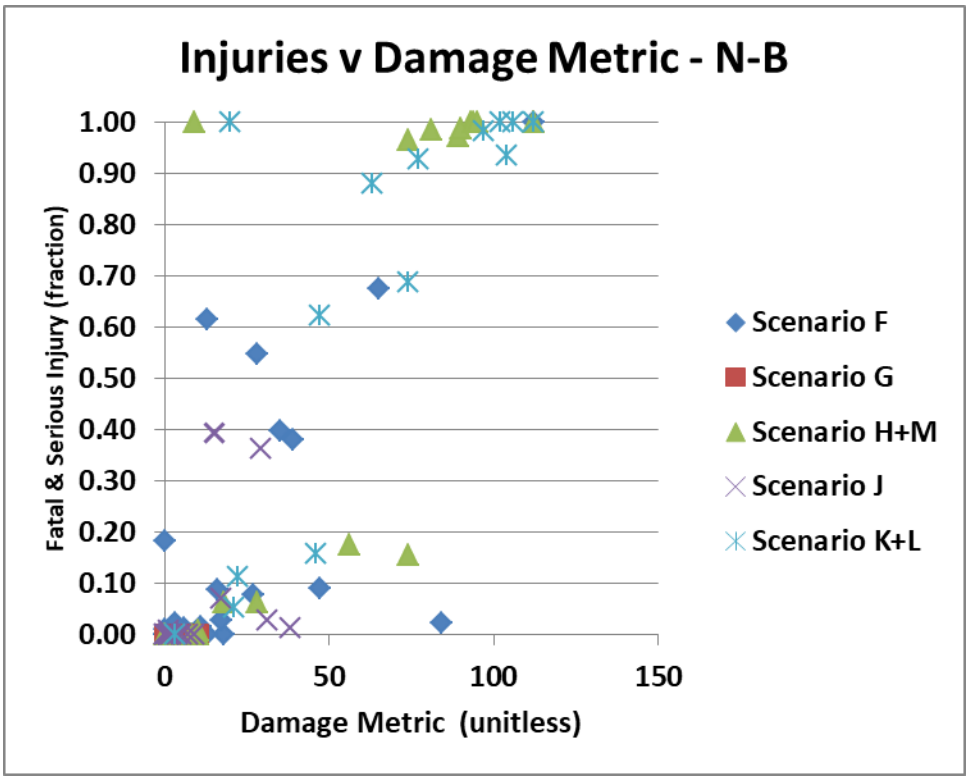

Figure 73. Severe-injury fraction dependence on damage metric—N–B

In view of the polarized severe-injury distribution identified in the previous section (see figure 72), the same plot will be considered for the damage metric. The polarization for the damage metric is not so extreme as that for the severe injury fraction (see figure 74). In as much as these are "mishaps," there are very few where zero damage has occurred. Therefore, the lowest damage level with a substantial population of mishaps is 0–10; this range of damage encompasses 43 percent of the mishaps. At the upper end of the damage metric scale, the mishaps are not so concentrated in the one highest "bin." However, there is a concentration of mishaps (27 percent above damage metric = 70), with high levels of damage that correspond to the top 10 percent of the severe-injury range (also 27 percent of the mishaps). This comparison would indicate that a mishap involving a damage metric greater than 70 will likely lead to greater than 90 percent severe injuries.

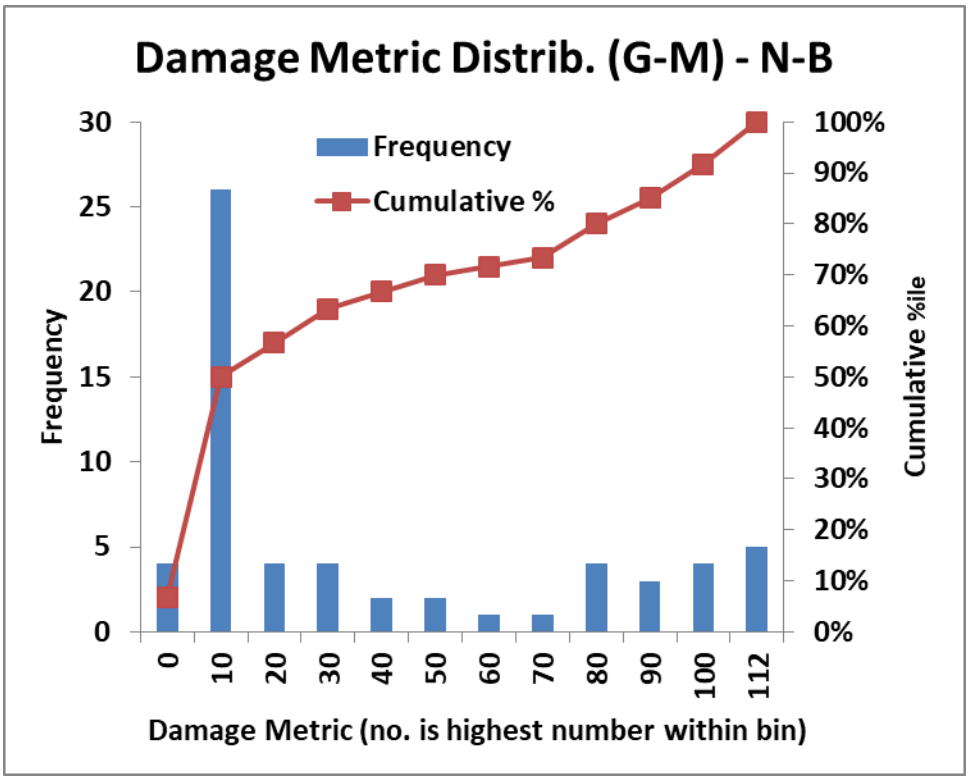

Figure 74. Damage metric distribution scenario G–M—N–B

4.2.7.6 Injury Dependence on Obstacles—N–B

In the N–B dataset, the presence of obstacles has a clear effect on the injury outcome. In scenario F, the overruns, the presence of an obstacle doubles the average severe-injury fraction (see table 80) compared to no obstacle. For the compromised landings, scenario G, the effect cannot be discerned because there are no cases of a vertical obstacle in the scenario-G dataset. For the remaining, more injurious scenarios, the effect is quite distinct. In the case of the landing-short scenarios (H+M), the presence of vertical obstacles increases the average injury fraction by a factor of four. Scenario J also has a much higher injury fraction for the aircraft encountering obstacles, but there are only two mishaps within the scenario involving obstacles. For scenario K+L, the injury fraction for the mishaps with obstacles is nearly double the fraction in mishaps without obstacles, and there are an equal number of mishaps for each condition. These trends for the effect of obstacles on the injury fraction reflect the same trends in the damage metric data (see table 69).

Table 80. Influence of vertical impediments on severe-injury fraction—N–B

	Vertical Impediment—Average Fraction of Severe Injury (percent)	No Vertical Impediment—Average Fraction of Severe Injury (percent)	No. of Mishaps with a Vertical Impediment (No.)	No. of Mishaps with No Vertical Impediment (No.)
Scenario F	21%	9%	16	10
Scenario G	-	0%	0	11
Scenario H+M	68%	14%	12	7
Scenario J	20%	4%	2	14
Scenario K+L	85%	47%	7	7

Looking at the entire dataset for all mishaps, the mean injury fraction for the 49 mishaps without obstacles is 0.121; this is much lower than the mean equal to 0.483 for the 37 mishaps that involved vertical obstacles (see figure 75). The two-sample T-test applied to these two means finds that the mean for mishaps with obstacles is larger than the mean without obstacles. The means are presented as "+" symbols on each side of figure 75; the line connecting them is for visual reference only. The boxplots (see figure 75) indicate a very strong asymmetry in the data; consequently, the normality assumption in the T-test is violated. The first quartile and the median for the data without obstacles are both zero. Therefore, the grey box on the right side of the figure represents the third quartile of the data, not solely the interquartile range, as is usually the case. It is difficult to see, but the mean value is just below the end of the top whisker. This view is expected because the dataset of 49 observations includes 32 values equal to zero. This large number of zero values has led to the interquartile range, which is the distance between the first quartile upper limit and the third quartile lower limit, being valued at 0.0595. The top of the upper whisker extends to the largest datum in the dataset above the third quartile + 1.5*interquartile range (i.e., the third quartile minus the first quartile). Any point beyond that value (1.5*interquartile range) is designated an outlier; therefore, the first outlier in this case appears very close to the top of the third quartile because the interquartile range is very narrow. Considering the failure of the normality assumption, a Mann-Whitney nonparametric test was applied to compare the two medians. The test found the median severe-injury fraction to be 0.3933 for the mishaps encountering a vertical obstacle. This value is significantly different from the median value of 0.0000 for the mishaps not encountering obstacles with a *p*-value less than or equal to 0.0000.

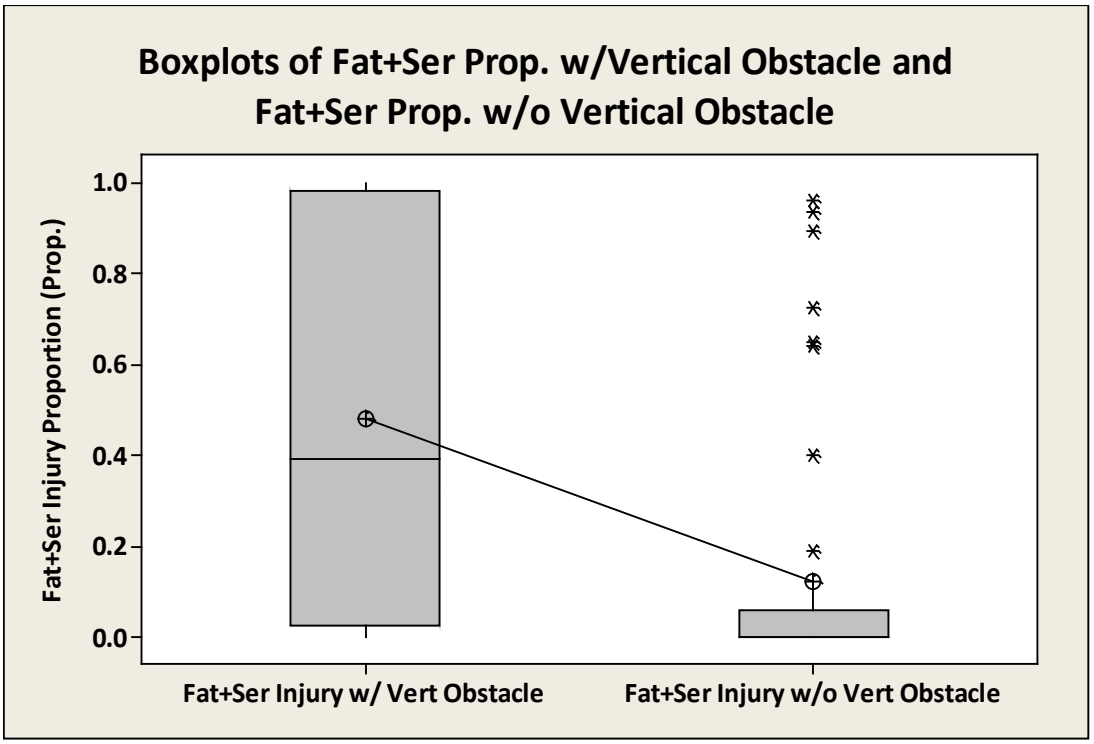

Figure 75. Severe-injury fraction with and without obstacles compared—N–B

4.2.7.7 Thermal Injuries—N–B

A question of interest for this study is whether the fatality was caused by trauma or by thermal exposure. If by thermal exposure, the question then becomes "was trauma a factor in not escaping or was it lack of an escape route?" Unfortunately, there are very few mishaps for which the data are present to resolve the latter question, and the data are not complete even in regard to the cause of death being thermal or trauma. Therefore, the data presented here are likely an under-accounting of the thermal injuries. Of the 86 mishaps, 13 had recorded thermal fatalities; unfortunately, five mishaps recorded no information about thermal fatalities. Of 10,294 occupants in the analysis, 517 occupants were recorded as thermal fatalities (5.0 percent of the occupants and 27 percent of all the reported fatalities). The thermal fatalities were not uniformly distributed along the fuselage (see table 81). The greatest percentage of thermal injuries occurred to occupants in the overwing cabin, with the next-most-common occurrence being in the aft cabin, a similar pattern to the W–B mishaps. Five mishaps had fires, but insufficient information to assign location or cause of death to fire or trauma. The number of fatalities with insufficient information is 474, or approximately 4.6 percent of the total occupants in the study. Therefore, the number of thermal fatalities could be as high as 1011, rather than the 517 previously stated.

Table 81. Thermal fatalities distribution in fuselage—N–B

	Cockpit	Forward Cabin	Overwing Cabin	Aft Cabin	Tail
No. of Thermal Fatalities	16	142	186	160	13
Percent of All Occupants in Segment	4	4	6	5	9
No. of Mishaps With Reported Thermal Injuries	5	10	13	12	6

4.2.7.8 Injury Binary Logistic Regression Analysis—N–B

The binary logistic approach interprets the injury data as having just one of two outcomes for each occupant: severe injury (fatal or serious) or no injury (including minor injury). In this view, the expectation is that for each kinematic parameter, the fraction of severe injuries will be low (near zero) for the less-injurious values of the parameter, and the severe-injury fraction will increase to the limit value of 1 as the value of the parameter changes toward a more injurious value. For example, the fraction of severe injuries would be expected to increase as the impact velocity increases. For details of the analysis, see section 2 of this report. The equation that the logistic regression fits assumes that the dependence on the parameter is linear. Therefore, the equation being fitted is an exponential with a linear form to the exponent. The output variable $\hat{p}$ is the estimated probability that an occupant in a similar crash scenario will be severely injured. For an *n*-parameter model, the equation contains one constant and *n* coefficients. The linear form of the equation with one parameter is:

$$\hat{p} = \frac{1}{1+e^{-(\beta_0+\beta_1 x_1)}} \tag{2}$$

The analysis strives to develop models that are capable of predicting the fraction of occupants suffering serious or fatal injuries using the kinematic parameters of the mishaps as input. The prediction capability would then allow a value of the kinematic parameter to be associated with a selected probability of severe injury. Both single-parameter and multi-parameter models are sought in this analysis.

In the following discussion, an evaluation for the success of the BLM is purely qualitative. This subjective evaluation by the author is in regard to direction of the trend predicted by the model. The model predicted trend (slope) is either “intuitive” (i.e., the trend expected by the author) or “counterintuitive” (i.e., opposite the trend expected by the author). The third possibility in this column, “bidirectional,” refers to parameters in which the injury response may increase as the parameter becomes farther removed from a neutral value, such as zero. For example, the injury fraction for a given mishap would be expected to be higher as the peak lateral acceleration increased to either side. If this parameter is modeled as a conventional monotonic parameter, the positive values of the parameter will tend to average out the negative values, and the injury fraction will appear to have no dependence on the parameter. Because an aircraft is symmetric left and right, it is argued here that the injury probability will also be symmetric left and right. Therefore, the peak lateral acceleration parameter has been revised by taking the absolute value. This revision

results in a kinematic parameter that is always positive and is expected to increase injury fraction as the parameter value increases. Consequently, it is the absolute value of the peak lateral acceleration that will be modeled. For the pitch angle, the crash dynamics vary between nose-up (positive pitch angle) wherein the tail strikes the ground first, and nose down (negative pitch angle) wherein the nose or nose gear strikes the ground first. Using the absolute value approach for pitch angle will not resolve the issue for pitch because it cannot be argued that the injury outcomes are expected to be symmetric. Initially, pitch angle will be treated as a single monotonic parameter, which is partially justified by the majority of values being positive, but later, treating the positive and negative values of the pitch angle as separate parameters will be investigated. In these initial single-parameter models for the N–B study, single-parameter models were generated for mishaps in each scenario in which there are sufficient mishaps and for the combined scenario G–M, which is all the scenarios that were not runway overruns.

Scenario F covers runway overrun mishaps wherein 354 occupants were fatally injured, 191 were seriously injured, and 2513 experienced minor or no injuries. The single-parameter models for scenario F predict the intuitively correct trends or no trends for the fraction of occupants receiving either fatal or serious injuries for each parameter. However, the goodness-of-fit tests all have *p*-values of 0.000 or less, indicating that the BLM is not a good fit for the data, and the predictive capabilities are also generally low (see table 82).

Table 82. Single parameter BLMs for scenario F—N–B

Parameter	Regressor Coefficient (*p*-value & coeff. value)	Constant Coefficient (*p*-value & coeff. value)	Goodness -of-Fit (*p*-value)	Summary Measures of Assoc.	Model Predictive Capability	Trend: Intuitive or Counter
Airspeed	*p*=0.000 +0.00513	*p*=0.000 -2.30	0.000 0.000 0.000	0.30 0.30 0.09	Medium Medium Low	Intuitive
Vertical Velocity	*p*=0.000 +0.0603	*p*=0.000 -2.25	0.000 0.000 0.000	0.42 0.53 0.12	Medium Medium Low	Intuitive
Flight-Path Angle	*p*=0.000 -0.0541	*p*=0.000 -1.67	0.000 0.000 0.000	-0.01[2] -0.02 -0.00	Low Low Low	Intuitive
Pitch Angle	*p*=0.630 -0.00379 [1]	*p*=0.000 -1.50	0.000 0.000 0.000	-0.04[2] -0.06 -0.01	Low Low Low	No trend
Off-nominal Angle	*p*=0.409 -0.00271[1]	*p*=0.000 -1.51	0.000 0.000 0.000	-0.20[††] -0.28 -0.06	Low Low Low	No trend
Vertical Peak Deceleration	*p*=0.003 +0.0388	*p*=0.000 -1.71	0.000 0.000 0.000	0.32 0.36 0.09	Medium Medium Low	Intuitive
Longitudinal Peak Deceleration	*p*=0.000 -0.139	*p*=0.000 -2.02	0.000 0.000 0.000	0.33 0.34 0.10	Medium Medium Low	Intuitive
Absolute Value Lateral Peak Deceleration	*p*=0.943 +0.00424[†]	*p*=0.000 -1.53	0.000 0.000 0.000	-0.01[2] -0.40 -0.00	Low Low Low	No trend

[†] The *p*-value >0.1 indicates that this parameter does not significantly differ from zero, where zero is a useful value indicating the parameter does not significantly affect the probability of an occupant being severely injured in like crashes.

[††] The negative sign indicates a poor predictive capability, as explained in section 2.8.

The problem with fit to the model can be seen in figure 76, in which the outcomes as measured by injury fraction values vary dramatically from one mishap to the next, even for mishaps with similar airspeeds (i.e., the dataset exhibits large variation, making it very difficult to achieve an adequate fit). As can be seen from the "Prediction" curve, the model predicts the intuitive expectation that the injury fraction will increase as airspeed increases, but many of the data points fall on either side and well away from the "Prediction" curve. The vertical velocity is the only parameter with moderate predictive capability (see figure 77). It is evident comparing figure 77 to figure 76 that the BLM for vertical velocity is a better predictor, but both are poor fits to the model. Several vertical velocity values are notably high in this dataset; the reason is that there were several mishaps in which the end of the runway was a drop-off. Two of the parameters, pitch angle and absolute value of the lateral acceleration, had no trend prediction as indicated by the *p*-value for

the coefficient being >0.1. A *p*-value greater than 0.1 for an estimated coefficient indicates that the value of the coefficient is unlikely to differ from zero; therefore no significant dependence on the applicable variable. This result is not surprising for scenario F, considering that few mishaps have non-zero pitch angles because of the nature of the scenario.

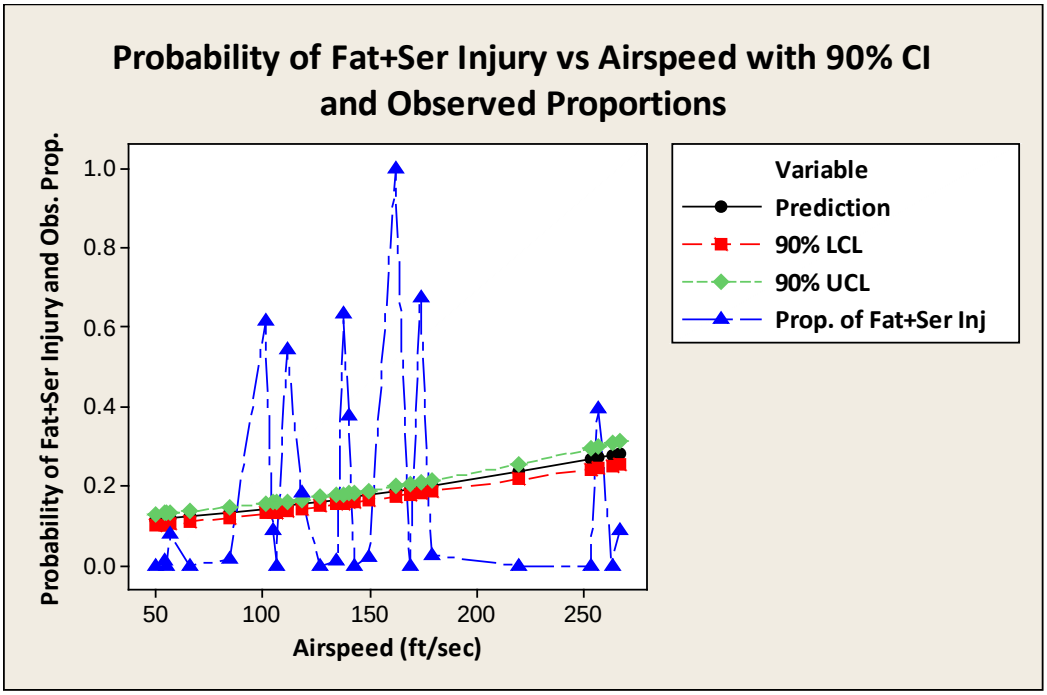

Figure 76. BLM injury fraction vs. airspeed for scenario F—N–B

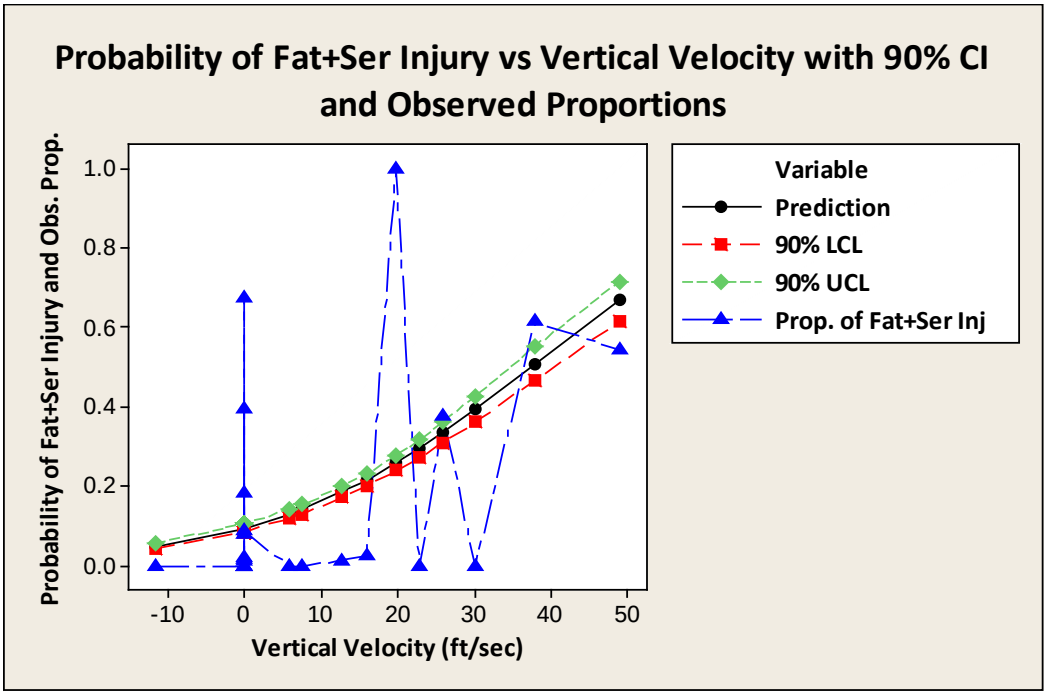

Figure 77. BLM injury fraction vs. vertical velocity for scenario F—N–B

The multi-parameter BLM for scenario F (see table 83) has statistics indicating good predictive capability, but again the goodness-of-fit statistics are indicating a poor fit. The model is presented in equation form (Eq. 7). Less reassuring is the fact that the trends (that is the dependence of the injury fraction on the parameter) indicated by the coefficients are mostly counterintuitive.

Table 83. Multi-parameter BLM for scenario F—N–B

Parameter	Coefficient (coeff. value)	Coefficient (*p*-value)	Goodness-of-Fit (*p*-value)	Summary Measures of Assoc.	Predictive Capability
Model properties			0.000 0.000 0.000	0.85 0.88 0.23	High High Low
Constant	-13.4	*p*=0.000			
Regressors:			Useful Range	Trend	
Airspeed (x_1)	+0.0814	*p*=0.000	50 to 267 ft/sec	Intuitive	
Vertical Velocity (x_2)	-0.126	*p*=0.000	-11.5 to 49 ft/sec	Counter-intuitive	
Flight Path (x_3)	+0.639	*p*=0.000	0 to -23.7 degrees	Counter-intuitive	
Pitch Angle (x_4)	-1.67	*p*=0.000	+12 to -18 degrees	Bidirectional	
Vertical Deceleration (x_5)	-1.11	*p*=0.000	0 to 15 G	Counter-intuitive	
Longitudinal Deceleration (x_6)	-1.06	*p*=0.000	7 to -20 G	Intuitive	
Abs. Val. Lateral Deceleration (x_7)	-2.15	*p*=0.000	0 to 5.33 G	Counter-intuitive	
Off-Nominal Angle (x_8)	-0.0135	*p*=0.024	0 to 52 degrees	Counter-intuitive	

$$p\hat{} = 1/(1 + e\hat{}(-(-13.3640 + 0.0813582x\_1 - 0.126478x\_2 + 0.639289x\_3 - 1.67146x\_4 - 1.11245x\_5 - 1.05959x\_6 - 2.14716x\_7 - 0.0135000x\_8))) \quad (7)$$

To present the predictive capability of the model in another way, the BLM predicted severe-injury fraction can be plotted versus the observed severe-injury fraction (see figure 78). For a perfect model, all the predicted points would equal the observed points and, therefore, would fall on the diagonal line corresponding to points (x, y) where $y = x$ (blue segment inserted for reader's reference). The plot (see figure 78) suggests that the model is reasonably good at predicting the severe-injury fraction despite several of the trends not being the expected relationship.

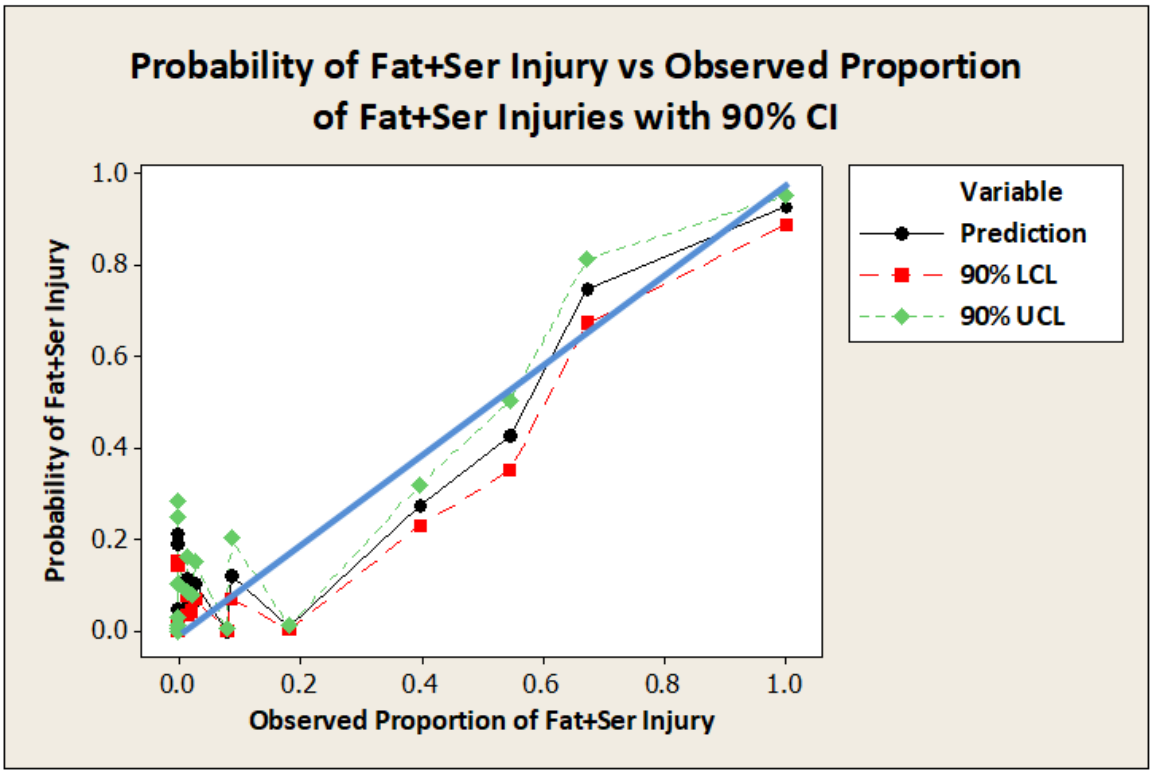

Figure 78. Scenario F multi-parameter BLM predicted probability vs. observed severe-injury fraction—N–B

Scenario G contained no severe injuries; consequently, none of the single-parameter models or the multi-parameter model had any variability to explain. The 1496 occupants in these mishaps all experienced minor or no injury as a result of the modest impacts characteristic of these mishaps.

The 19 scenario H+M mishaps involving landing short of the runway fatally injured 667 occupants, seriously injured 273 occupants, and inflicted minor or no injury to 1050 occupants. The BLM for airspeed showed no significant dependence on the parameter, and both vertical velocity and flight-path angle produced counterintuitive trends (see table 84). Two of these models have medium-strength predictive capability, but the rest have only low-strength predictive capability. The statistics for the pitch-angle model indicate medium-strength predictive capability, yet this bidirectional parameter is treated as a mono-directional parameter in the model.

Table 84. Single-parameter BLMs for scenario H+M—N–B

Parameter	Regressor Coefficient (*p*-value & coeff. value)	Constant Coefficient (*p*-value & coeff. value)	Goodness-of-Fit (*p*-value)	Summary Measures of Assoc.	Model Predictive Capability	Trend: Intuitive or Counter
Airspeed	*p*=0.278 -0.000862†	*p*=0.641 0.0880[1]	0.000 0.000 0.000	0.07 0.08 0.04	Low Low Low	No trend
Vertical Velocity	*p*=0.000 -0.0202	*p*=0.000 +0.500	0.000 0.000 0.000	0.06 0.07 0.03	Low Low Low	Counter-intuitive
Flight Path Angle	*p*=0.000 +0.0272	*p*=0.063 +0.125	0.000 0.000 0.000	0.02 0.02 0.01	Low Low Low	Counter-intuitive
Pitch Angle	*p*=0.000 -0.221	*p*=0.000 +1.25	0.000 0.000 0.000	0.64 0.71 0.32	Medium Medium Medium	Bidirec-tional
Abs. Val. Off-nominal Angle	*p*=0.000 +0.0172	*p*=0.004 -0.144	0.000 0.000 0.000	-0.11 -0.15 -0.05	Low Low Low	Intuitive
Vertical Peak Deceleration	*p*=0.000 +0.0690	*p*=0.000 -0.700	0.000 0.000 0.000	0.23 0.23 0.11	Low Low Low	Intuitive
Longitudinal Peak Deceleration	*p*=0.000 -0.235	*p*=0.000 -1.61	0.000 0.000 0.000	0.64 0.65 0.32	Medium Medium Medium	Intuitive
Absolute Value Lateral Peak Deceleration	*p*=0.000 +0.409	*p*=0.000 -0.374	0.000 0.000 *	0.03 0.10 0.01	Low Low Low	Intuitive

† The *p*-value >0.1 indicates that this parameter does not significantly differ from zero, where zero is a useful value indicating the parameter does not significantly affect the probability of an occupant being severely injured in like crashes.

* Not determined.

The multi-parameter BLM for scenario H+M (table 85) indicates high-strength predictive capability; that indication is supported by the predicted versus observed plot (see figure 79), although most of the mishaps fall at the extremes of either very few severe injuries or a great many serious injuries. The equation for the model is shown in (Eq. 8).

Table 85. Multi-parameter BLM for scenario H+M—N–B

Parameter	Coefficient (coeff. value)	Coefficient (*p*-value)	Goodness-of-Fit (*p*-value)	Summary Measures of Assoc.	Predictive Capability
Model properties			0.000 0.000 0.000	0.96 0.97 0.47	High High Medium
Constant	+8.86	*p*=0.000			
Regressors:			Useful Range	Trend	
Airspeed (x_1)	-0.0200	*p*=0.000	95 to 333 ft/sec	Counter-intuitive	
Vertical Velocity (x_2)	+0.147	*p*=0.001	0 to 70 ft/sec	Intuitive	
Flight Path (x_3)	+1.11	*p*=0.000	-36 to 0 degrees	Counter-intuitive	
Pitch Angle (x_4)	-0.802	*p*=0.000	-11.5 to +22.8 degrees	Bidirectional	
Vertical Deceleration (x_5)	-0.197	*p*=0.003	-6.0 to +26.3 G	Counter-intuitive	
Longitudinal Deceleration (x_6)	-0.460	*p*=0.000	-21.9 to +7 G	Intuitive	
Abs. Val. Lateral Deceleration (x_7)	-2.21	*p*=0.000	0 to 6.7 G	Counter-intuitive	
Off-Nominal Angle (x_8)	+0.132	*p*=0.000	0 to +125 degrees	Intuitive	

$$\hat{p} = 1/(1 + e\text{^}(-(8.85688 - 0.0199555\text{x\_1} + 0.146744\text{x\_2} + 1.11173\text{x\_3} - 0.802387\text{x\_4} - 0.197119\text{x\_5} - 0.460026\text{x\_6} - 2.21194\text{x\_7} + 0.132022\text{x\_8}\ )\ )\ ) \quad (8)$$

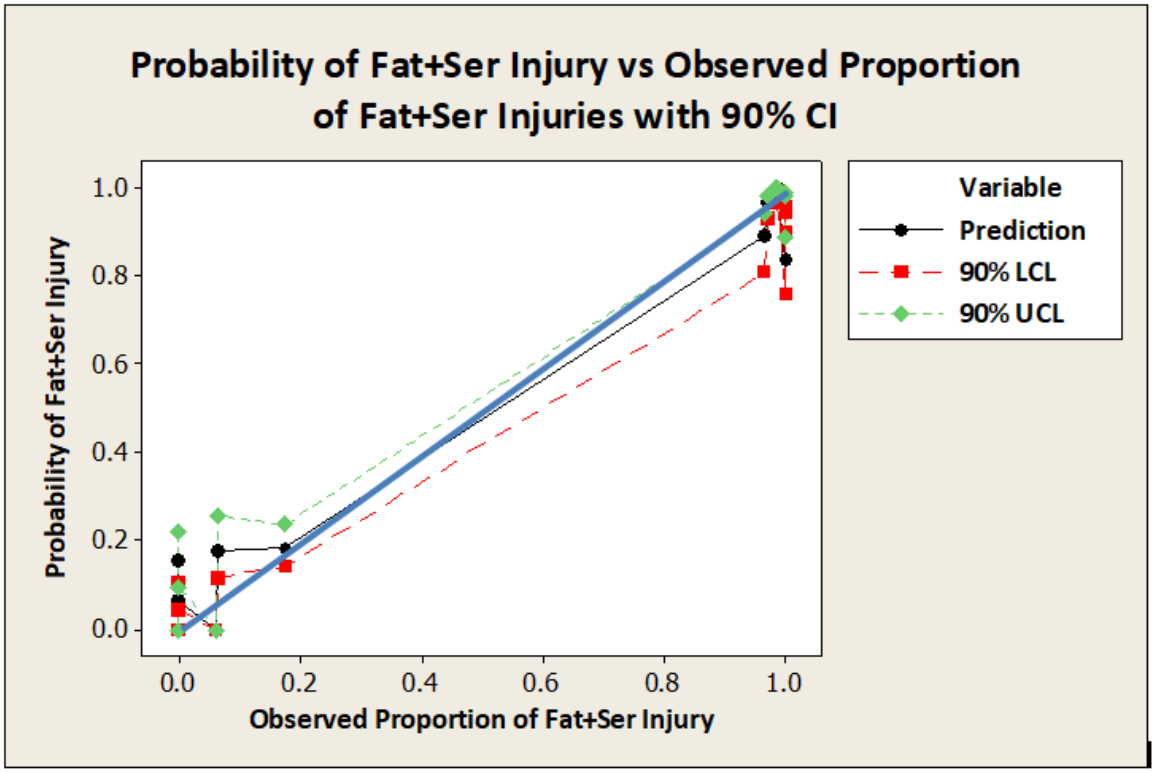

Figure 79. Scenario H+M multi-parameter BLM predicted probability vs. observed severe-injury fraction—N–B

The 16 hard landings with loss of control included in scenario J resulted in 25 fatal injuries, 49 serious injuries, and 2114 minor or non-injuries. The few severe injuries occurred in just four mishaps. In the single-parameter BLMs, three parameters have medium strength predictive capability—airspeed, flight path angle, and longitudinal deceleration (see table 86). The predicted trend for airspeed is counterintuitive. Three parameters were found to have no statistically significant trend—vertical velocity, pitch angle, and the absolute value of lateral acceleration.

Table 86. Single-parameter BLMs for scenario J—N–B

Parameter	Regressor Coefficient (*p*-value & coeff. value)	Constant Coefficient (*p*-value & coeff. value)	Goodness-of-Fit (*p*-value)	Summary Measures of Assoc.	Model Predictive Capability	Trend: Intuitive or Counter
Airspeed	*p*=0.000 -0.014	*p*=0.172 -0.631	0.000 0.000 0.000	0.50 0.54 0.03	Medium Medium Low	Counter-Intuitive
Vertical Velocity	*p*=0.861 +0.000988†	*p*=0.000 -3.37	0.000 0.000 0.000	-0.28 -0.30 -0.02	Low Low Low	No trend
Flight Path Angle	*p*=0.001 +0.112	*p*=0.000 -2.87	0.000 0.000 0.000	0.33 0.34 0.02	Medium Medium Low	Counter-intuitive
Pitch Angle	*p*=0.898 -0.002[1]	*p*=0.000 -3.35	0.000 0.000 0.000	-0.11 -0.11 -0.01	Low Low Low	No trend Bidirectional
Off-Nominal Angle	*p*=0.000 +0.0300	*p*=0.000 -3.76	0.000 0.000 0.000	0.04 0.05 0.00	Low Low Low	Intuitive
Vertical Peak Deceleration	*p*=0.001 -0.239	*p*=0.000 -2.61	0.000 0.000 0.000	0.26 0.27 0.02	Low Low Low	Counter-intuitive
Longitudinal Peak Deceleration	*p*=0.000 -0.161	*p*=0.000 -3.30	0.000 0.000 0.000	0.62 0.65 0.05	Medium Medium Low	Intuitive
Absolute Value Lateral Peak Deceleration	*p*=0.190 +0.0898[1]	*p*=0.000 -3.43	0.000 0.000 0.000	0.12 0.18 0.01	Low Low Low	No trend

† The p-value >0.1 indicates that this parameter does not significantly differ from zero, where zero is a useful value indicating the parameter does not significantly affect the probability of an occupant being severely injured in like crashes.

The multi-parameter BLM for scenario J shows more promise than the single-parameter models, although it contains only five of the available eight parameters (see table 87). The statistics indicate a high-strength predictive capability, but three of the five parameters indicate counterintuitive trends.

Table 87. Multi-parameter BLM for scenario J—N–B

Parameter	Coefficient (coeff. value)	Coefficient (*p*-value)	Goodness-of-Fit (*p*-value)	Summary Measures of Assoc.	Predictive Capability
Model Properties			0.000 0.000 0.000	0.86 0.92 0.06	High High Low
Constant	23.1	p=0.000			
Regressors:			Useful Range	Trend	
Airspeed (x_1)	-0.120	p=0.000	123 to 254 ft/sec	Counter-intuitive	
Vertical Velocity (x_2)	-0.118	p=0.000	-37.5 to 67 ft/sec	Counter-intuitive	
Flight Path (x_3)	+0.293	p=0.000	-17 to 0 degrees	Counter-intuitive	
Pitch Angle (x_4)	-0.240	p=0.000	-11 to +10.9 degrees	Bi-directional	
Longitudinal Deceleration (x_5)	-0.308	p=0.000	-6 to +15.3 G	Intuitive	

$$\hat{p} = 1/(1 + e\text{^}(-(23.1479 - 0.119745\text{x\_1} - 0.117972\text{x\_2} + 0.293155\text{x\_3} - 0.239534\text{x\_4} - 0.307720\text{x\_5}))) \quad (9)$$

The values predicted by the model plotted against the observed values (see figure 80) indicate good agreement, as the prediction curve is close to the ($y = x$) reference line. It should be noted that there are several points (mishaps) with zero observed serious injuries; also, the highest injury fraction in the model is 0.4, which further limits the model's usefulness.

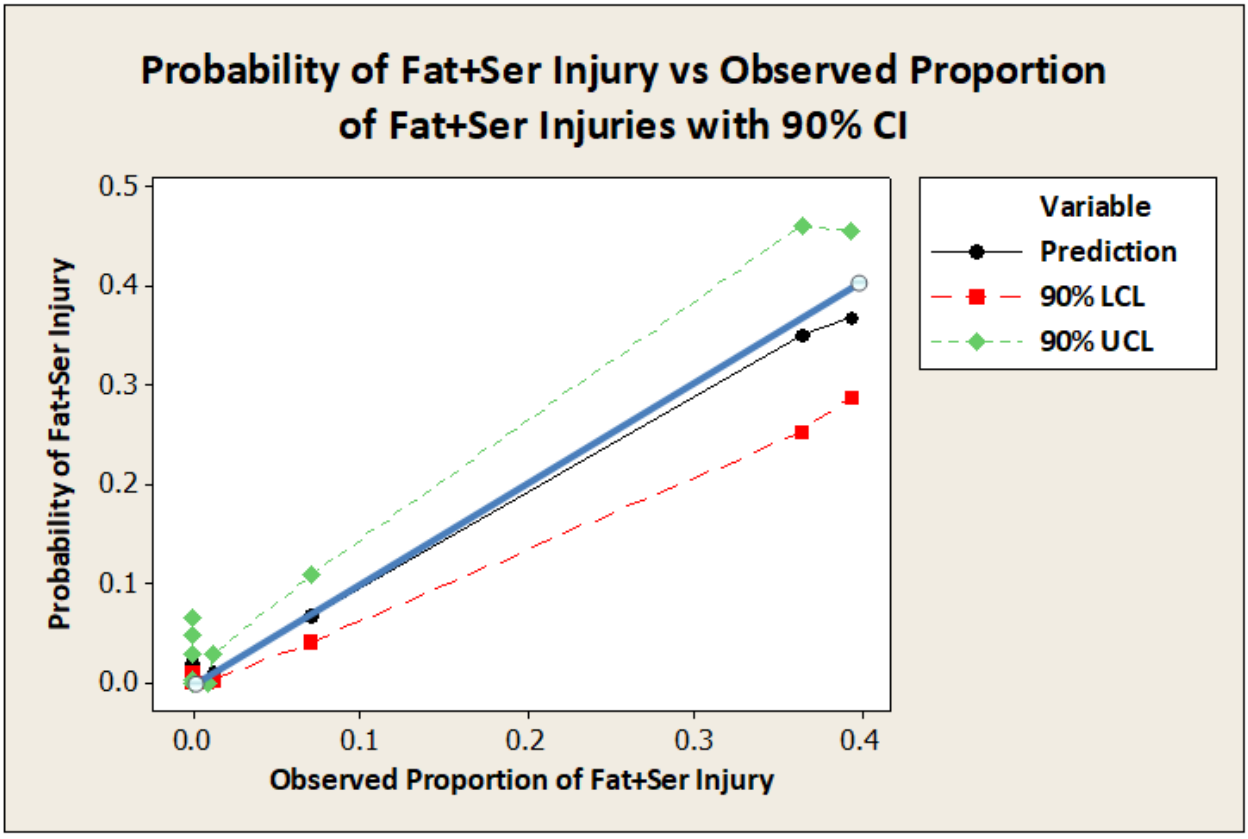

2000

Figure 80. Scenario J multi-parameter BLM predicted probability vs. observed severe-injury fraction—N–B

Scenario K+L, loss of control on takeoff, included 14 mishaps. These mishaps resulted in 803 fatalities, 225 serious injuries, and 534 minor or non-injuries. Despite a large number of mishaps and a substantial number of severe injuries, just four of eight single-parameter models have medium-strength predictive capability (see table 88). Four of the eight parameters led to coefficients with the expected trend; two were counterintuitive and two had no trend.

Table 88. Scenario K+L single-parameter BLMs—N–B

Parameter	Regressor Coefficient (*p*-value & coeff. value)	Constant Coefficient (*p*-value & coeff. value)	Goodness-of-Fit (*p*-value)	Summary Measures of Assoc.	Model Predictive Capability	Trend: Intuitive or Counter
Airspeed	*p*=0.604 -0.000582[1]	*p*=0.003 +0.792	0.000 0.000 0.000	-0.17 -0.20 -0.08	Low Low Low	No trend
Vertical Velocity	*p*=0.854 +0.000199†	*p*=0.000 +0.648	0.000 0.000 0.000	-0.06 -0.11 -0.03	Low Low Low	No trend
Flight Path Angle	*p*=0.000 -0.0448	*p*=0.026 0.194	0.000 0.000 0.000	0.33 0.34 0.15	Medium Medium Low	Intuitive
Pitch Angle	*p*=0.000 +0.0179	*p*=0.000 +0.570	0.000 0.000 0.000	0.29 0.30 0.13	Low Medium Low	No trend Bidirectional
Off-nominal Angle	*p*=0.000 +0.0165	*p*=0.000 +0.442	0.000 0.000 0.000	0.38 0.47 0.17	Medium Medium Low	Intuitive
Vertical Peak Deceleration	*p*=0.000 -0.0465	*p*=0.000 +0.823	0.000 0.000 0.000	0.34 0.35 0.15	Medium Medium Low	Counter-intuitive
Longitudinal Peak Deceleration	*p*=0.000 -0.0699	*p*=0.022 +0.158	0.000 0.000 0.000	0.30 0.31 0.14	Medium Low Low	Intuitive
Absolute Value Lateral Peak Deceleration	*p*=0.000 +0.307	*p*=0.002 +0.196	0.000 0.000 0.000	0.07 0.11 0.03	Low Low Low	Intuitive

† The *p*-value >0.1 indicates that this parameter does not significantly differ from zero, where zero is a useful value indicating the parameter does not significantly affect the probability of an occupant being severely injured in like crashes.

The Scenario K+L multi-parameter model has statistics indicating high-strength predictive capability (see table 89); however, only two of the five usable parameters have intuitive trends. The model uses only 10 of 14 mishaps because of incomplete data for four of the mishaps.

Table 89. Scenario K+L Multi-parameter BLM—N–B

Parameter	Coefficient (coeff. value)	Coefficient (*p*-value)	Goodness-of-Fit (*p*-value)	Summary Measures of Assoc.	Predictive Capability
Model properties			0.000 0.000 0.000	0.93 0.97 0.45	High High Medium
Constant	-5.93	*p*=0.000			
Regressors:			Useful Range	Trend	
Vertical Velocity (x_1)	+0.139	*p*=0.000	-50 to +200 ft/sec	Counter-intuitive	
Flight Path Angle (x_2)	-1.27	*p*=0.000	-50.0 to -1.0 degrees	Intuitive	
Vertical Deceleration (x_3)	-1.30	*p*=0.000	-20.4 to +26.3 G	Counter-intuitive	
Abs. Val. Lateral Deceleration (x_4)	-11.8	*p*=0.000	0 to +8.6 G	Counter-intuitive	
Abs. Val. Off-nominal Angle (x_5)	+0.482	*p*=0.000	0 to +135 degrees	Intuitive	

$$\hat{p} = \frac{1}{1+e^{-(-5.92620+0.138585x_1-1.27264x_2-1.30186x_3-11.8427x_4+0.481537x_5)}} \quad (10)$$

The predicted injury fraction plotted against the observed injury fraction (see figure 81) shows that most of the points predicted by the model are close to the actual values and, therefore, fall close to the reference line of perfect agreement between the model's prediction and the observed value. The equation form of the model is shown in (Eq 10).

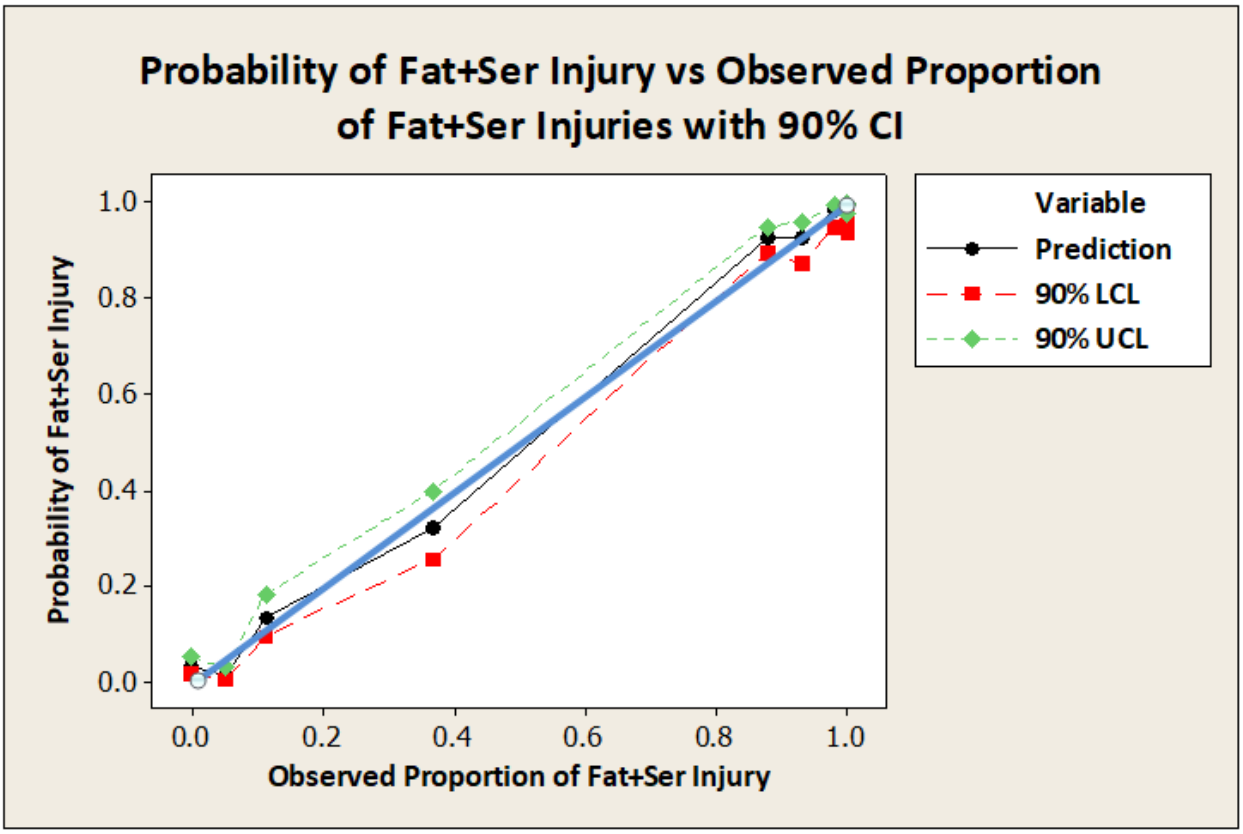

Figure 81. Scenario K+L multi-parameter BLM predicted probability of severe injury vs. observed severe-injury fraction—N–B

Grouping scenarios G–M provides a large sample of 60 mishaps. These 60 mishaps resulted in 1443 fatal injuries, 599 serious injuries, and 5194 minor and non-injuries. However, even this large sample led to only three single-parameter models (see table 90) with medium strength predictive capability—the vertical velocity, the flight path angle, and the longitudinal deceleration all had intuitive trends. All of the single parameter models except pitch angle produced coefficients with the anticipated trends. Pitch angle, which is a bidirectional parameter, had a statistically insignificant coefficient (i.e., a zero value coefficient).

Table 90. Single-parameter BLMs for scenarios G–M—N–B

Parameter	Regressor Coefficient (*p*-value & coeff. value)	Constant Coefficient (*p*-value & coeff. value)	Goodness-of-Fit (*p*-value)	Summary Measures of Assoc.	Model Predictive Capability	Trend: Intuitive or Counter
Airspeed	*p*=0.000 +0.00366	*p*=0.000 -1.75	0.000 0.000 0.000	0.13 0.13 0.05	Low Low Low	Intuitive
Vertical Velocity	*p*=0.000 +0.0163	*p*=0.000 -1.29	0.000 0.000 0.000	0.35 0.36 0.14	Medium Medium Low	Intuitive
Flight Path Angle	*p*=0.000 -0.0690	*p*=0.000 -1.44	0.000 0.000 0.000	0.44 0.45 0.18	Medium Medium Low	Intuitive
Pitch Angle	*p*=0.305 -0.00306†	*p*=0.000 -0.895	0.000 0.000 0.000	-0.08 -0.08 -0.03	Low Low Low	No Trend Bidirectional
Off-nominal Angle	*p*=0.000 +0.0215	*p*=0.000 -1.11	0.000 0.000 0.000	0.16 0.20 0.07	Low Low Low	Intuitive
Vertical Peak Deceleration	*p*=0.000 +0.0419	*p*=0.000 -1.16	0.000 0.000 0.000	0.04 0.04 0.02	Low Low Low	Intuitive
Longitudinal Peak Deceleration	*p*=0.000 -0.228	*p*=0.000 -1.88	0.000 0.000 0.000	0.67 0.67 0.26	Medium Medium Low	Intuitive
Absolute Value Lateral Peak Deceleration	*p*=0.000 +0.233	*p*=0.000 -1.29	0.000 0.000 0.000	0.03 0.05 0.01	Low Low Low	Intuitive

† The *p*-value >0.1 indicates that this parameter does not significantly differ from zero, where zero is a useful value indicating the parameter does not significantly affect the probability of an occupant being severely injured in like crashes.

The multi-parameter BLM (see table 91) for the combined scenarios G–M is developed using 46 of the 60 available mishaps because 14 mishaps contain missing data. The BLM includes all eight available parameters.

Table 91. Scenarios G–M multi-parameter BLM—N–B

Parameter	Coefficient (coeff. value)	Coefficient (*p*-value)	Goodness-of-Fit (*p*-value)	Summary Measures of Assoc.	Predictive Capability
Model properties			0.000 0.000 0.000	0.81 0.82 0.33	High High Medium
Constant	-4.72	p=0.000			
Regressors:			Useful Range	Trend	
Airspeed (x_1)	+0.0112	*p*=0.000	0 to +333 ft/sec	Intuitive	
Vertical Velocity (x_2)	-0.0220	*p*=0.000	-50 to +200 ft/sec	Counter-intuitive	
Flight Path (x_3)	-0.121	*p*=0.000	-50 to +0.5 degrees	Intuitive	
Pitch Angle (x_4)	-0.0293	*p*=0.000	-30 to +23 degrees	Bidirectional	
Vertical Deceleration (x_5)	-0.239	*p*=0.000	-20.4 to +26 G	Counter-intuitive	
Longitudinal Deceleration (x_6)	-0.437	*p*=0.000	-22 to +15 G	Intuitive	
Abs. Val. Lateral Deceleration (x_7)	-1.56	*p*=0.000	0 to +9 G	Counter-intuitive	
Abs. Val. Off-nominal Angle (x_8)	+0.0913	*p*=0.000	0 to +135 degrees	Intuitive	

$$\hat{p} = 1/(1 + e\text{^}(-(-4.71718 + 0.0111624x_1 - 0.0220482x_2 - 0.120820x_3 - 0.0292914x\_4 - 0.238648x\_5 - 0.437108x\_6 - 1.55648x\_7 + 0.0912716x\_8))) \quad (11)$$

The statistics indicate that the predictive strength of this model is high. However, the plot of predicted values against observed values (see figure 82) shows the wide range of predicted values for mishaps with low observed values (~0) and, similarly, a wide range of predicted values for mishaps with high observed severe-injury fractions (~1).

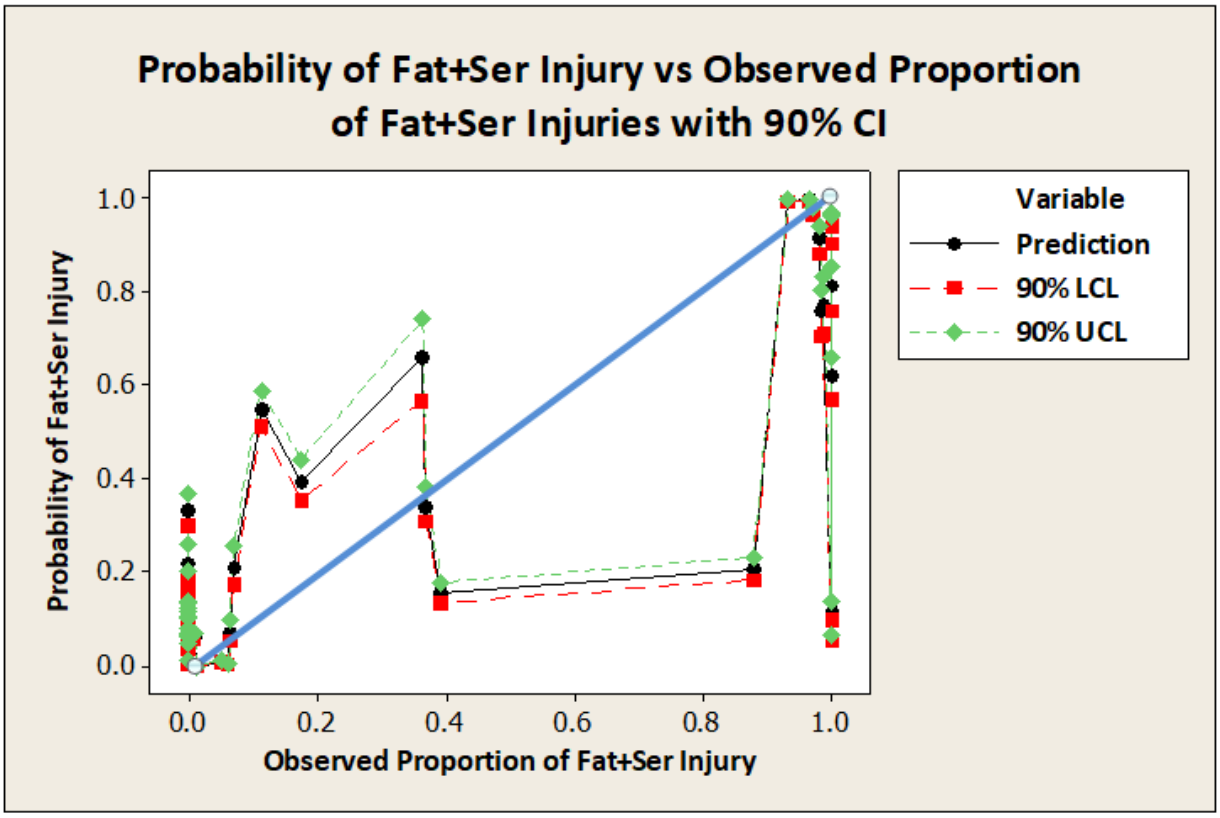

Figure 82. Scenario G–M multi-parameter BLM predicted probability of severe injury vs. observed severe-injury fraction—N–B

It was anticipated that the combined scenarios G–M had the best chance of producing a useful model capable of predicting the severe-injury fraction based on the kinematic parameters. As discussed earlier, the difficulty is a lack of intermediate values for injury fractions and the high degree of variability. For many of the kinematic parameters, there are mishaps with both high and low severe-injury fractions at similar values for the kinematic parameter.

The single-parameter models for each scenario generally had low predictive capability (see table 92), as indicated by the summary measures of association statistics. Even the combined scenario G–M had only three models with medium predictive capability.

Table 92. Predictive capability strength summary for single parameter BLMs—N–B

	Scenario F	Scenario G	Scenario H+M	Scenario J	Scenario K+L	Scenario G–M
Airspeed	Medium		Low	Medium	Low	Low
Vertical Velocity	Medium		Low	Low	Low	Medium
Flight Path	Low		Low	Medium	Medium	Medium
Pitch Angle	Low		Medium	Low	Medium	Low
Off-nominal Angle	Low		Low	Low	Medium	Low
Vertical Deceleration	Medium		Low	Low	Medium	Low
Longitudinal Deceleration	Medium		Medium	Medium	Low	Medium
Lateral Deceleration	Low		Low	Low	Low	Low

The multi-parameter models resulted in stronger predictive capability (see table 93). These models all have high predictive capability, but they do not all incorporate the same set of regressors. The model for scenario G–M does incorporate all the parameters. Therefore, the analysis has created one model capable of making predictions for each scenario given kinematic data.

Table 93. Parameters included in multi-parameter BLMs by scenario—N–B

	Scenario F	Scenario G	Scenario H+M	Scenario J	Scenario K+L	Scenario G–M
Strength of Predictive Capability	High	No Model	High	High	High	High
Airspeed	In model		In model	In model		In model
Vertical Velocity	In model		In model	In model	In model	In model
Flight Path	In model		In model	In model	In model	In model
Pitch Angle	In model		In model	In model		In model
Off-nominal Angle	In model		In model		In model	In model
Vertical Deceleration	In model		In model		In model	In model
Longitudinal Deceleration	In model		In model	In model		In model
Lateral Deceleration	In model		In model		In model	In model

5. DISCUSSION OF BOTH N–B AND W–B

The aircraft in the two classes were quite distinct in their characters. The W–B aircraft weighed in excess of 400,000 lb, whereas 77 of 86 N–B aircraft weighed less than 250,000 lb. The N–B aircraft had either five or six seats across, whereas the W–B aircraft had from seven to as many as ten seats across. The W–B aircraft averaged 238 occupants with an average occupancy factor (number of all occupants/number of passenger seats) equal to 0.77. The N–B aircraft averaged 120 occupants and an average occupancy factor equal to 0.85. The N–B dataset was dominated by two-engine aircraft (68/86), whereas the predominate configuration in the W–B dataset was two engines on the wing and one in the tail (13/29).

Whereas the configurations and occupancies differed, the kinematics of the mishaps were quite similar. All eight kinematic parameters had similar average values between the two types for scenario G–M. The largest difference in a single parameter for the two classes was in peak longitudinal acceleration (W–B -6.0 G compared to N–B -3.5 G). The damage metric values by scenario reveal a couple of different trends. First, the relative severity of the scenarios is similar with the two most damaging scenarios in the same order for both W–B and N–B (see table 94). The third and fourth scenarios ranked by most damage reverse positions between the two classes, and scenario G is the least damaging scenario for both classes of aircraft. Second, with the exception of scenario F, each of the N–B scenarios has a lower average damage metric than the corresponding W–B scenario. This relationship between the damage metrics is in spite of the N–B dataset experiencing slightly more fuselage breaks (1.6 per mishap) than the W–B dataset (1.2 breaks per mishap). Scenario F constituted 24 percent of W–B mishaps compared to 30 percent of N–B mishaps.

Table 94. Comparison of damage metrics—W–B to N–B

W–B Scenario	W–B Average Damage Metric	N–B Scenario	N–B Average Damage Metric
Scenario K+L	75.5	Scenario K+L	63.9
Scenario H+M	71.3	Scenario H+M	50.2
Scenario J	36.4	Scenario F	22.0
Scenario F	13.1	Scenario J	10.1
Scenario G	3.3	Scenario G	2.0
Average Fuselage Breaks per Mishap for Scenario G–M	1.2		1.6

Although the two classes have similar average kinematics, when the 90th percentile velocities for S and PS crashes are considered, differences between the two classes appear. The W–B dataset has a 90th percentile vertical velocity of 28 ft/sec, quite a bit lower than the 43.5 ft/s determined for the N–B dataset. However, the W–B average airspeed was 334 ft/s compared to 275 ft/s for the N–B dataset. Using the two sets of average velocity to estimate an "average" 90th-percentile flight path angle [inverse sin(vertical velocity/airspeed)], the W–B dataset value is 4.8 degrees compared to 9.1 degrees for the N–B. These 90th-percentile velocity values were developed after identifying crashes as S, PS, or NS. Reviewing the outcomes of these determinations for the two datasets, the N–B dataset has a higher fraction of S mishaps (see table 95) than does the W–B dataset. Additionally, the N–B dataset contains a larger fraction of PS mishaps and a smaller fraction of NS mishaps. Combining the kinematics with survivability suggests that the N–B class mishaps are more survivable, even though the vertical velocity is substantially higher, as is the flight path angle.

Table 95. Comparison of survivability W–B to N–B

	W–B (percent of Scenario G–M mishaps)	N–B (percent of Scenario G–M mishaps)
Survivable	64	72
Partially Survivable	18	23
Non-Survivable	18	5

Despite the apparent differences in survivability, the fractions of fatal, serious, and minor/no injury are similar for the two datasets. The fatality fraction for the W–B dataset is 16.9 percent compared to 17.6 for the N–B dataset. Serious injuries are 7.8 percent for the W–B dataset compared to 7.6 percent for the N–B dataset. The minor- and no-injury fractions are within 1 percent of each other—75.5 percent for W–B and 74.7 percent for N–B.

The range of aircraft included in the analysis, the age of the aircraft designs, and the time since the mishaps occurred cover a wide span. In conducting the work, a dramatic evolution in the quality of the investigations and reports was seen. The oldest N–B mishap occurred in November 1967, and the oldest W–B mishap occurred in July 1971. The latest of the mishaps in both datasets occurred in the summer of 2014. It is shown in table 96 which engine configurations are current and which are passing out of favor. The median mishap date for the four-engine-on-wing

configuration was 1973 for the N–B dataset and 1986 for the W–B dataset. Interestingly, the median mishap date for three-engine W–B dataset is later than the median date for the four-engine W–B dataset, even though four-engine W–B aircraft are still commonly flying passengers, whereas few three-engine W–B are still transporting passengers.

Table 96. Comparison of median mishap dates for engine configurations—W–B to N–B

	2 Eng. on Wing	4 Eng. on Wing	3 Eng. in Tail (B727)	2 Eng. on Tail	2 Eng. on Wing, 1 on Tail
Narrow-Body Median Mishap Date	Dec. 2003	Jun. 1973	Jan. 1976	Jan. 1996	
Wide-Body Median Mishap Date	Oct. 2004	Sep. 1986			Nov. 1993

5.1 WIND-INFLUENCED MISHAPS

In the course of reading the investigation reports for the W–B and N–B studies, it was noted that quite a few mishaps were influenced or even caused by wind effects, especially wind shear. It was decided to identify these wind-influenced scenarios with separate designations. The short landings in which the wind had influenced the outcome were designated scenario M rather than scenario H. The takeoffs affected by wind were labeled scenario L rather than scenario K. These separately identified scenarios could then be compared to the corresponding non-wind-influenced mishaps for trends in the damage metric and injury fraction. These findings are discussed separately in the N–B and the W–B sections. In this section, the frequency of these mishaps over the duration of the study period is investigated. In response to several serious accidents caused by wind shear, terminal-based and aircraft-based systems were developed to detect the presence of severe localized winds. The aircraft systems were certified for use by the FAA in September 1994.

In the N–B dataset, there were 12 wind-influenced mishaps: 7 scenario-L mishaps and 5 scenario-M mishaps. The latest scenario-M (landing) mishap occurred in January 1996, whereas the latest scenario-L mishap (takeoff) was in December 2008. One way to look for a trend is to break the time period of the study into shorter, equal time intervals and compare the number of mishaps in each interval. N–B scenario L mishaps covered the entire study period (see table 97). There is no trend evident in the number of mishaps in each interval.

Table 97. Timing of wind-influenced mishaps

	1/1974 to 12/1983 No. of Mishaps	1/1984 to 12/1993 No. of Mishaps	1/1994 to 12/2003 No. of Mishaps	1/2004 to 12/2013 No. of Mishaps
N–B Scenario M	3	0	3	0
N–B Scenario L	2	0	2	3
W–B Scenario M	1	1	0	0
W–B Scenario L	0	0	0	0

In the W–B dataset, there were insufficient mishaps to identify a trend. There were two scenario-M mishaps, and zero scenario-L mishaps. Of the two scenario-M mishaps, the later one occurred in 1985. Therefore, it could be argued that the wind-influenced events stopped after 1993, but there was only a single event in each of the earlier intervals.

Because the data are sparse, the two W–B scenario-M mishaps have been combined with the N–B data (see table 98). Rather than look at the number occurring in a particular period, this analysis looks at the interval between events. The mishaps occurring within the US have been grouped together and ordered chronologically. Although the data are sparse, it does appear that the general trend in the US has been a reduction in these types of accidents. The column on the right (see table 98) shows the number of days since the prior wind-influenced mishap in the dataset. The table shows that there were five such mishaps in the 1970s, one in the 1980s, three in the 1990s, and one in the 2000s. The fact that there were three events within 18 months in the mid-1990s may not look like an improvement. However, compared to the three events within one year during the mid-1970s, it is an improvement. It must also be remembered that the mishaps in the study are not a sample of all mishaps, and the mishaps were selected for a different purpose. Although the validity of the sample with respect to scenario types was discussed, the validity of the sample for chronology has not been checked. The reason for there being no wind-related mishaps in Africa prior to 2005 may simply reflect the availability of thorough mishap investigations from that continent and fewer commercial flights operated using the aircraft of interest.

Table 98. Wind influenced mishaps—combined

CSTRG ID	Date	Scenario	Aircraft Type	General Location†	Interval (days)
19731217A	17-Dec-73	M	W–B	US	
19750624A	24-Jun-75	M	N–B	US	554
19750807A	07-Aug-75	L	N–B	US	44
19751112A	12-Nov-75	M	N–B	US	97
19760623A	23-Jun-76	L	N–B	US	224
19850802A	02-Aug-85	M	W–B	US	3,327
19940702A	02-Jul-94	L	N–B	US	3,256
19951112A	12-Nov-95	M	N–B	US	498
19960107A	07-Jan-96	M	N–B	US	56
20081220A	20-Dec-08	L	N–B	US	4,731
19740130A	30-Jan-74	M	N–B	PO	
20010207A	07-Feb-01	L	N–B	EU	
20051210A	10-Dec-05	L	N–B	AF	
20061029A	29-Oct-06	L	N–B	AF	323

† US=United States, PO= Pacific Ocean (Pago-Pago), EU= Europe, AF=Africa

5.2 SEVERE-INJURY FRACTION—DAMAGE METRIC RELATIONSHIP

One way to quantify the correlation between the severe-injury fraction and the damage metric is to determine the average value for each of the two parameters for each scenario, and then plot the average value of the severe injury fraction against the average value of the damage metric. This plot (see figure 83) was initially created for the N–B dataset in which the larger number of mishaps (86) results in each scenario including several events. The correlation coefficient for this dataset is very good at 0.908, suggesting that this approach to quantify the correlation is promising. Consequently, the same plot was prepared (see figure 84) using the W–B dataset (29 mishaps). The slope for the W–B trend line is equal to the slope for the N–B trend line in four significant digits and the coefficient of correlation is even higher than that for the N–B. The results of these two plots would suggest the following interpretation: for either class of aircraft, a 10-unit reduction in damage metric will lead to reducing the severe-injury fraction by 10 percentage points. Further, because the data points are evenly spread across the plot, the trend lines appear usable for damage metric values from 5 to 73, which corresponds to predicted severe injury fractions from 0 to 0.75. Such a relationship is potentially very useful for justifying crashworthiness requirements or for justifying any regulation with the potential to reduce the damage to an aircraft involved in a mishap. However, considering that two of the W–B scenarios (K and M) each contain only two mishaps, the quality of the relationship in the W–B dataset seems surprising. On close inspection of scenario M, the average value (0.47) severe injury fraction consists of the average of 0.02 and 0.93, which suggests that the relationship may merely be fortuitous.

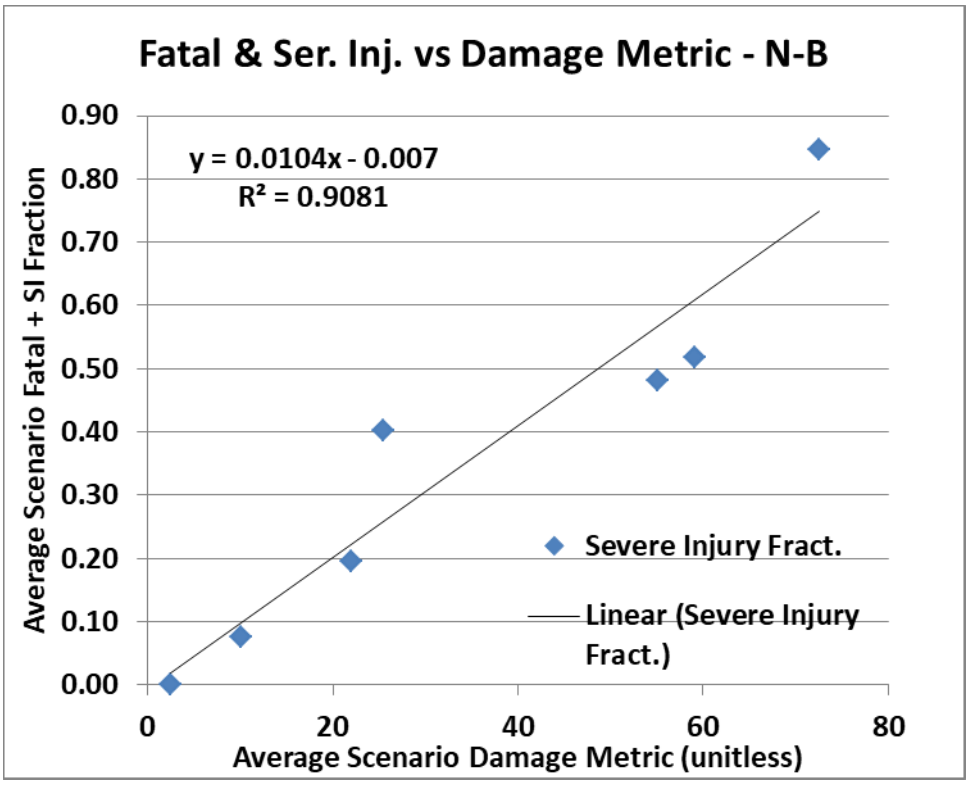

Figure 83. Severe-injury fraction vs. damage metric by scenario—N–B

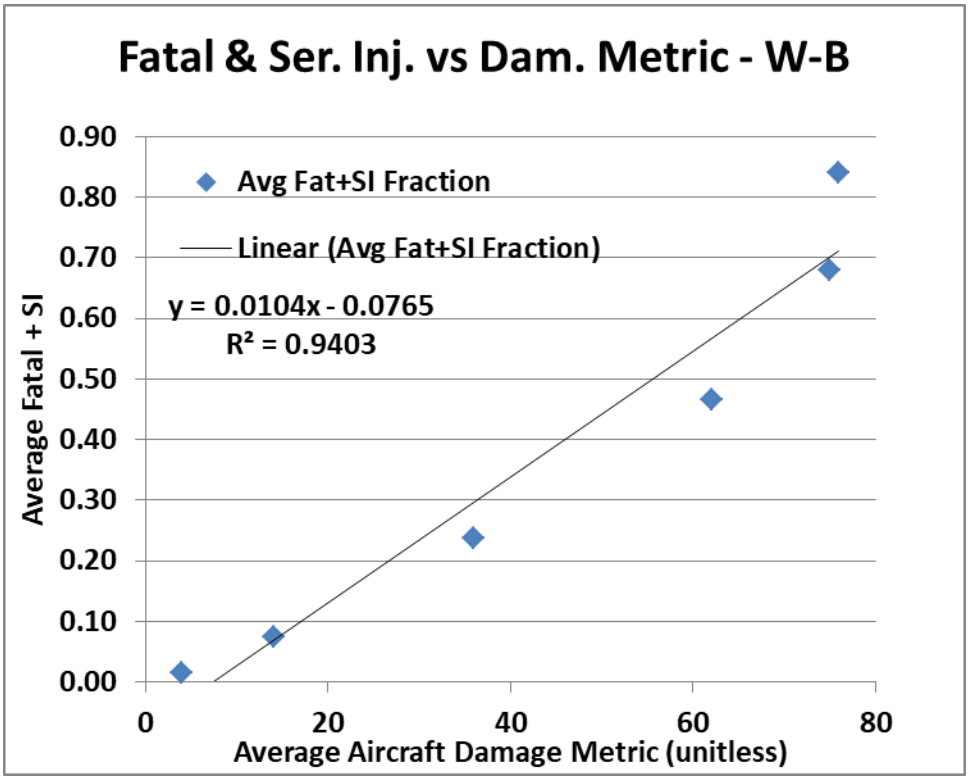

Figure 84. Severe-injury fraction vs. damage metric by scenario—W–B

To verify that the interpretation of the slope is really representative of the system response, histograms were created for the two severe-injury fraction datasets. The histogram of the N–B injury data (see figure 85) shows a very polarized (bimodal) distribution of severe-injury fraction values; 63 percent of the mishaps have an injury fraction of 0.1 or less, and 20 percent have a value greater than 90 percent. These two concentrations of mishaps leave only 17 percent of the mishaps spread across the intervening 80 percentage points. Creating the same plot for the W–B dataset (see figure 86) yields a similar result. The severe-injury fractions are not uniformly distributed but are grouped at the two extremes. These distributions for the severe injury fractions raise the question as to the cause of this bimodal distribution. The distribution of damage metric values for the two damage datasets being similar in distribution would at least partially explain the distribution of the mishap average severe-injury fractions. The N–B distribution of damage metric values (see figure 87) is not so clearly bimodal, but there is a cluster of mishaps above damage metric 80. The W–B distribution (see figure 88) is not quite as clearly polarized as the corresponding severe injury fraction distribution. Forty-eight percent of the mishaps with damage metric are less than 10, and 21 percent with damage metric are greater than 90.

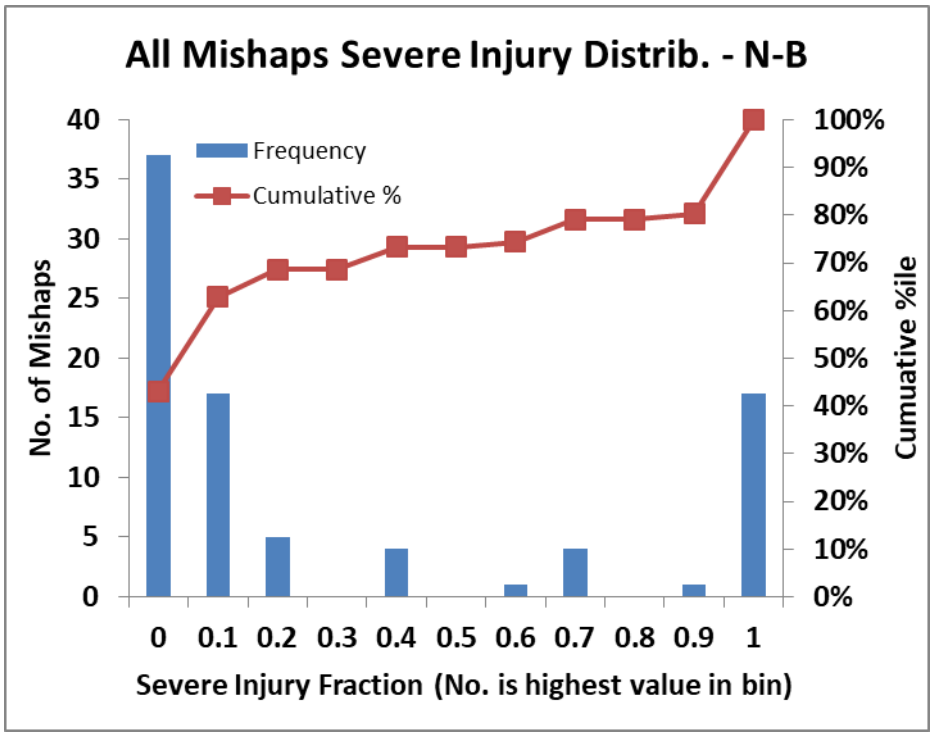

Figure 85. Distribution of severe-injury fractions across mishaps—N–B

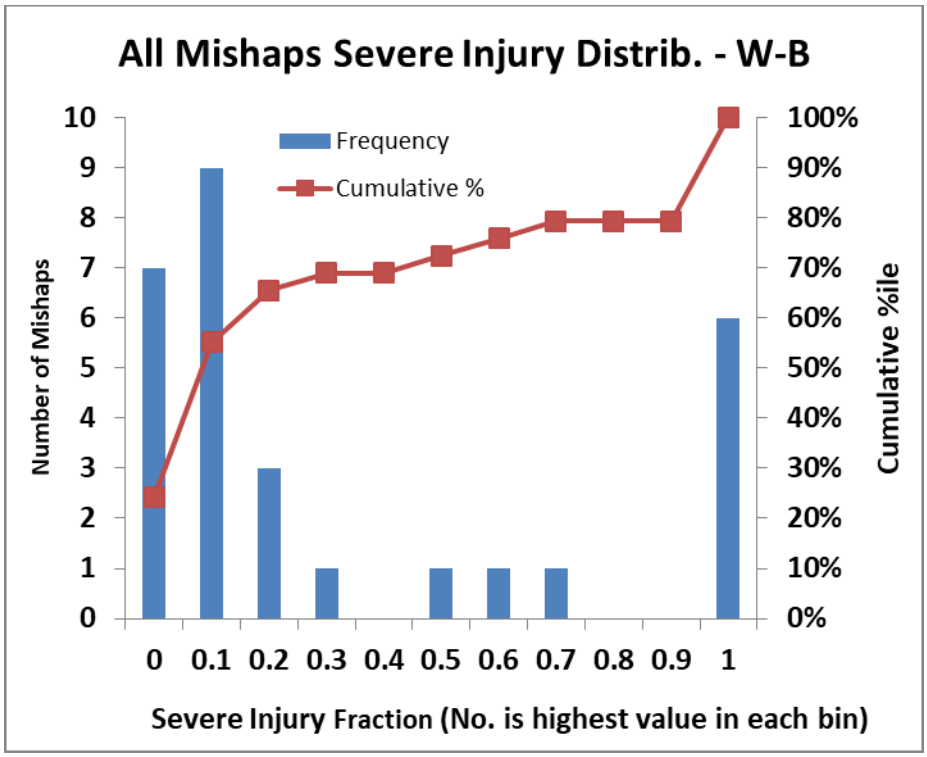

Figure 86. Distribution of severe-injury fractions across mishaps—W–B

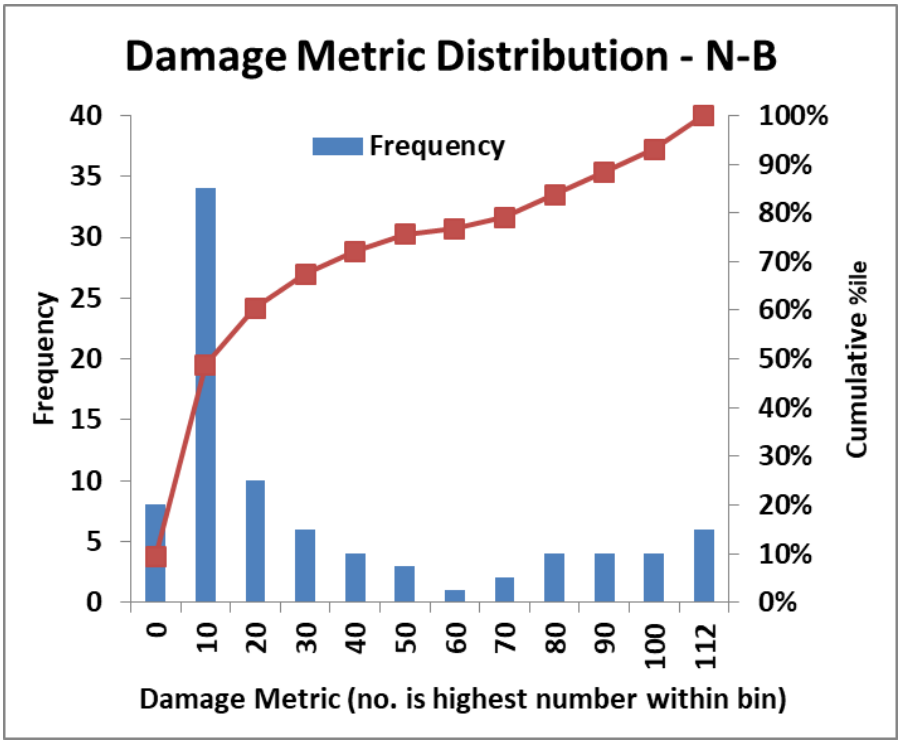

Figure 87. Damage metric distribution for all mishaps—N–B

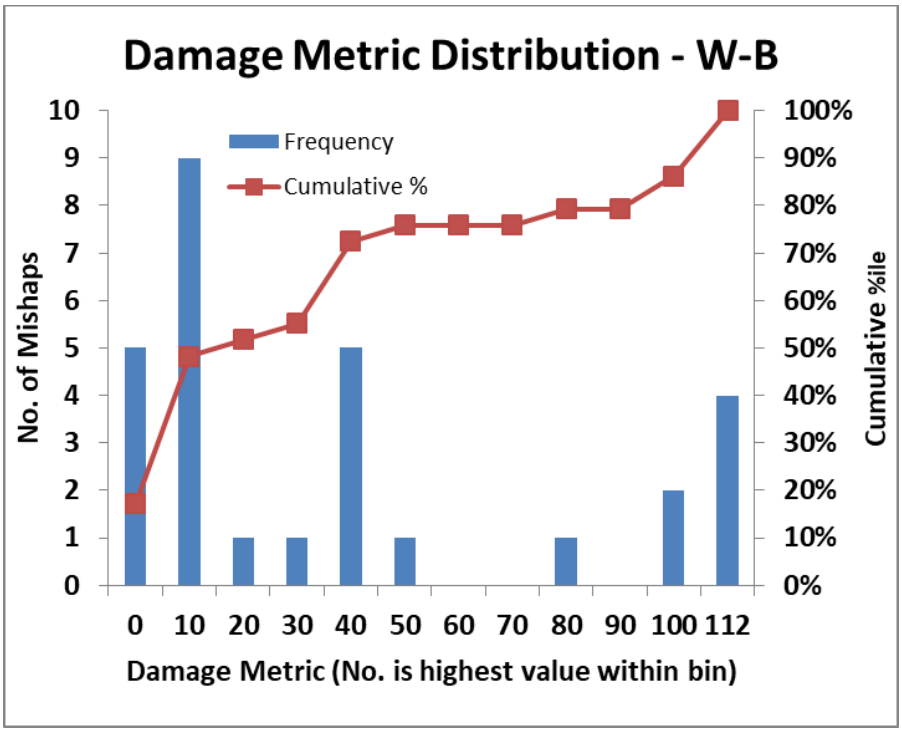

Figure 88. Damage metric distribution for all mishaps—W–B

Even though the severe-injury fractions have a bimodal distribution and the damage-metric values have a somewhat less-distinct bipolar distribution, grouping and averaging them by scenario results in a uniform distribution of values as reflected in the original plots (see figures 83–84). These uniform distributions seem to reflect the nature of the scenarios rather than the individual mishaps. That is to say, each of the scenarios has a characteristic "severity" and the outcomes of the different scenarios measured either in terms of severe injury fraction or in terms of damage metric are uniformly distributed, even though each scenario may contain mishaps mainly at the extremes of both injury fraction and damage metric.

5.3 INJURY PREVENTION OPPORTUNITIES

Although the purpose of this report is to provide quantitative information to support updating aircraft crashworthiness requirements, the results also support other possibilities. The approach has been to look at the kinematics of the mishaps to determine thresholds below which crashworthiness has the potential to reduce injuries without undue cost, weight, or capacity burdens. The analysis indicates that occupant survivability depends on a complex interaction of the kinematic variables. The separation of the mishaps into scenarios, and the consideration of novel effects, such as the presence of vertical obstacles, confirm that the outcomes have a complex dependence. The study quantitatively links the fraction of occupants receiving severe injuries to the severity of the damage incurred by the aircraft. The outcomes of the different scenarios combined with the effect of vertical obstacles suggest that there may be opportunity for reducing damage inflicted on the aircraft by controlling the surroundings and prudent design of the aircraft.

The outcomes of the different scenarios suggest that terrain for the final aircraft deceleration is critical. In scenario G, in which the aircraft remains on the prepared surface of the airfield, predominately on the runway, damage and injuries are exceedingly low, even though the "impact" velocity is approximately landing speed. By comparison, the overruns (scenario F) experience a higher degree of damage and more injuries, even though the velocity at impact is typically much lower. The difference seems to be that the overruns go beyond the prepared surface of the airfield and encounter rougher terrain and more vertical obstacles. Similarly, in scenario H, the landing-short mishaps, terrain, and vertical obstacles are often factors, even for mishaps close to threshold.

In considering revisions to the aircraft crashworthiness requirements, the consequences of crashworthy design must be balanced against the benefits. In the transport arena, mishaps are very infrequent. The costs of crashworthiness, as realized in added weight or reduced capacity, are incurred during every flight, whereas the benefits of crashworthiness accrue only rarely, if ever, for a given aircraft. Making the same reduction in injuries by modifying the airfield surroundings offers a possible alternate approach that does not directly penalize the aircraft performance. This is not to say that the airport design aspect has been neglected; effective design improvements, such as those completed under the Runway Safety Area program, have been implemented by the FAA. Rather, as future actions to improve occupant survival in mishaps are considered, aircraft design is not the only opportunity.

6. SUMMARY AND CONCLUSIONS

This section summarizes the results for the two aircraft classes and presents the conclusions for each class with conclusions on the combined classes.

6.1 W–B SUMMARY

The W–B dataset was homogeneous in several respects. Of the 29 aircraft, all but 2 weighed more than 400,000 lb. There were only three design configurations: two engines on wing, four engines on wing, and two engines on wing plus a single engine in the fin. All of the aircraft had at least seven seats across, with a maximum ten across. This meant that the W–B aircraft seating did not overlap with the N–B seating, in which none of the aircraft exceeded six across. The average number of occupants in the W–B dataset was 238.

For the W–B dataset, overruns (scenario F) and compromised landings (scenario G) were the two most-frequent types of mishaps. Scenario G was the least severe in terms of both damage metric (4.0 for scenario G compared to 13.9 for scenario F) and injury fraction (0.01 for scenario G compared to 0.18 for scenario F)

The kinematic parameters for the scenarios G–M subset of the W–B dataset provide general information potentially useful for design. The average vertical velocity is 22.2 ft/s, which is well above the landing-gear capability. Even so, the average peak vertical deceleration rate for the same set of mishaps is 4.0 G. The average flight-path angle is -5.0 degrees, which is consistent with the average vertical velocity and the average airspeed of 232 ft/s. The average longitudinal peak deceleration is -6.0 G.

The severity of damage, as quantified by the damage metric, correlates well with the vertical and longitudinal velocities by scenario. Ranking the scenarios from the highest to lowest based on

average damage metric (see table 17) results in the same ranking order for the top-three scenarios by average vertical velocities, airspeeds, and peak vertical accelerations. Important factors affecting the peak longitudinal deceleration are the terrain impacted (on or off the airport's prepared surface), and the presence of obstacles. Seeking the dependencies of the damage metric using conventional plotting and regression techniques on the individual kinematic parameters within the different scenarios did not produce useful results. Investigating the effect of vertical obstacles proved to be indicative, but not statistically significant. The mean damage metric for mishaps involving vertical obstacles was consistently higher than the mean damage metric for those mishaps without vertical obstacles. However, the differences identified were not statistically significant. Similarly for severe-injury fraction, those mishaps involving obstacles had consistently higher severe-injury fractions, yet the difference in the means was not statistically significant. Despite the lack of statistical significance, the large difference in mean damage metrics suggests that obstacles deserve consideration in establishing crashworthiness design requirements.

The injury data exhibited substantial variability. Some mishaps with low kinematics parameter values exhibited high fatality rates, especially where fire was present. Similarly, a few crashes with apparently severe kinematics parameter values resulted in some survivors. The possibility of a few localized survivors in a severe crash seems to be more likely in the W–B mishaps. These localized survivors occur when a small portion of intact cabin floor separates, experiences tolerable loads, is not crushed, and is isolated from the post-crash fire. Within this small volume, the occupants survive. In more general terms, the values of the severe-injury fraction for the three major segments (i.e., forward cabin, overwing cabin, and aft cabin) were quite consistent. Larger variation in the severe-injury fraction was found in comparing the same cabin segment across different impact scenarios. Therefore, the severity of individual injuries had more dependence on the crash conditions than on seating location.

Fatalities recorded as due to thermal exposure were 5.4 percent of all occupants, and approximately one third of all fatalities. Seven of 29 mishaps reported thermal injuries.

Whereas the severe-injury fraction failed to show strong correlation to any one kinematic parameter, some generalizations were observed. For the combination of vertical and longitudinal velocity, six of the six mishaps that resulted in injury fractions greater than 90 percent fell outside the 90^{th}-percentile velocity ellipse on the two-velocity plot. The severe-injury fraction did show a strong positive correlation ($R^2 = 0.86$) to the damage metric. This strong correlation implies that designing to reduce the types of damage incorporated into the metric should reduce severe injuries. The damage factors integrated in the damage metric include: underside skin damage, floor disruption, failure of seat attachment, and loss of occupant volume.

The analysis developed models to predict the probability that an occupant in a similar crash scenario will sustain a severe injury (serious or fatal) and, therefore, can be used to determine the fraction of occupants suffering serious or fatal injuries from the kinematic parameters of the mishaps. The prediction capability would then allow a value of the kinematic parameter to be associated with a probability of severe injury.

Tracking the wind-related mishaps separately from the non-wind-related mishaps was hampered by the small W–B dataset. There were no scenario-L (wind-influenced takeoff) mishaps to compare to scenario K (non-wind-influenced takeoffs). The six scenario-H mishaps had a higher

(38.5 ft/s) average vertical velocity than the two wind-influenced scenario-M (average vertical velocity 14.8 ft/s) mishaps. The relationship for airspeed was reversed, wherein the wind-affected scenario M had an average airspeed of 276 ft/s compared to 218 ft/s for scenario H. Using the ratio of the vertical velocity to the airspeed to estimate the flight-path angle reveals that scenario H has a much higher average impact angle of 10.7 degrees compared to 2.9 degrees for scenario M. The average damage metric for scenario H is 74.5 compared to 61.5 for scenario M. Consistent with scenario H having the higher damage metric, scenario H also had the higher injury fraction of 63 percent compared to 47 percent for scenario M.

6.2 N–B SUMMARY

The N–B dataset contains greater diversity in terms of aircraft models and configurations than the W–B dataset. The N–B dataset contains 86 mishaps. Eleven different aircraft models are represented, including five engine configurations. Most (77 of 86) of the aircraft were in the 100,000–250,000 weight category, with just 9 aircraft in the next heavier category. The seating width was also homogenous with all aircraft having either five- or six-wide seating. The number of occupants in the dataset is 10,335, giving an average number of 120 occupants in each mishap. Additionally, there was diversity in the configurations with 50 of the aircraft having engines on the wings compared to 36 with engines at the tail. No aircraft in this dataset had engines on the wing and the tail.

The kinematics for the large-scenario G–M subset of the N–B mishaps provide general information about the events. The average vertical velocity is 22.3 ft/s, which is greater than the normal vertical landing speed of 1–3 ft/s and beyond the landing gear capability. The average peak vertical deceleration is 3.9 G. The average airspeed at impact, 223 ft/s, is consistent with most of the included mishaps occurring during attempted landings or takeoffs. The average peak longitudinal deceleration is -3.5 G, which is consistent with long stopping distances and few obstacles. Consistent with the higher than normal descent rate, the average flight-path angle is a rather steep -7 degrees. The average pitch angle is +4.3 degrees, which is reduced by being averaged with a few negative values, as was discussed in the text. The mishaps included a few aircraft that came to rest inverted.

The damage severity, as represented by the damage metric, is consistent with the kinematics for the two most severe scenarios. Scenario K+L has the highest average damage metric of 63.9 and both the highest average vertical velocity, 39.8 ft/s, and the highest average airspeed, 228 ft/s. Similarly, scenario H+M has the second-highest average damage metric of 50.2, with the second-highest average vertical velocity 27.8 ft/s and second-highest airspeed 228 ft/s. However, scenario F, the runway overruns, contains the mishaps with the third-highest average damage metric, yet had lower average vertical velocity and airspeed than scenario J. The damage metric does not correlate well to the individual kinematic parameters in the various scenarios based on the use of conventional plotting and regression techniques. Investigation into the influence of vertical obstacles revealed a substantial difference in the average and median damage metrics for the subset of mishaps with obstacles compared to the subset without obstacles. However, the differences in the means with and without obstacles were not supported statistically.

In the N–B mishaps, 17.6 percent of the occupants received fatal injuries, and a further 7.6 percent were seriously injured; therefore, almost 75 percent of occupants had no injuries or only minor

injuries. This high fraction of minor injury is reflected in the injury data in which the median severe injury fraction for many of the scenarios is zero or near zero. The average severe-injury fraction values are raised by the few severe accidents. The aircraft design did make a difference in the outcome as measured by the severe injury (fatal + serious) fraction. The dominant engine configuration in numbers has a lower injury fraction than the other configurations. The most common configuration, two engines on the wing, was involved in 41 mishaps, having an average damage metric of 23 and an average severe-injury fraction of 19 percent. The less-common two-engines-on-tail configuration was involved in 27 mishaps; this configuration has a higher average damage metric of 35 and a correspondingly higher average severe injury fraction of 34 percent. The distribution of injuries among the three cabin segments—forward cabin, overwing cabin, and aft cabin—were within a few percent of each other for each scenario. No one cabin segment stood out as either safer or less safe than the others, nor was there a consistent pattern along the sequence of the three cabin segments.

The injury data contain substantial variability in relation to the kinematic data. The injury fraction was highly polarized, with more than half of the G–M mishaps having an injury fraction less than 0.1 and nearly 30 percent having an injury fraction in excess of 0.9. Looking for trends in the injury data as a function of individual kinematic parameters by conventional plotting and linear regression methodology was not productive. The correlation (R^2) values were generally low and, in many cases, the slope of the trend line was not the anticipated sign (+/-). Contact with obstacles did influence the outcome of mishaps as measured by the severe-injury fraction. Looking at the influence of obstacles in each scenario, the presence of obstacles at least doubled the severe-injury fraction in all scenarios in which the injury fraction was non-zero.

The binary logistic regression analysis applied to the injury data and single kinematic parameters did not produce models with strong predictive capability. These models were developed with four primary scenarios: F, H+M, J, and K+L. Scenario-G mishaps had no severe injuries; consequently, the models for this scenario could not be created. Of 32 possible models (four scenarios and eight parameters), only five had medium strength predictive capability and one, the pitch angle for scenario H+M, had high-strength predictive capability according to the statistics. The multi-parameter models for all of the scenarios have a high-strength predictive capability according to the summary measures of association statistics. In all but three cases, to get these models to converge and have high-strength predictive capability, one or more of the available parameters was eliminated from the model dataset because they were not significantly different than zero. When these eliminations were done, the reduced model was refit and analyzed. Therefore, only scenarios F, H+M, and G–M use all of the available parameters.

The separate tracking of the wind-related mishaps revealed that the mishaps associated with localized winds were slightly less severe in terms of damage and injury than those not associated with localized winds. The average airspeed for the scenario-M mishaps is 30 ft/s higher than the average airspeed for scenario H, but the vertical velocities are similar. In spite of the higher airspeed for scenario M, the average damage metric for scenario H is twice (59) the damage metric for scenario M (24.8). Despite this big difference in damage metric, scenario H and scenario M have similar fatality rates and scenario M had a slightly higher average serious injury rate. The comparison of scenario K and scenario L demonstrates consistent small differences, but with the mishaps in scenario L being the less-severe events. Scenario L has lower average vertical velocity and airspeed than does scenario K. These kinematics resulted in scenario L's damage metric (55.1)

being slightly lower than that for scenario K (63.9). The difference in damage metrics is reflected in the injury rates with scenario L having the lower rates for both fatalities and serious injuries.

6.3 CONCLUSIONS

In this study, the damage and injury characteristics for mishaps involving narrow-body (N–B) aircraft (single-aisle) and wide-body (W–B) aircraft (two-aisle) are investigated. The objective is to better understand and quantify the occupant survivability for the two classes of aircraft. The study will contribute to the larger objective of defining the crashworthiness of transport aircraft with metal fuselage structures on at least a semi-quantitative basis. The ability to describe the crashworthiness of these metal aircraft will set expectations for the crashworthiness of polymer-composite fuselages and other non-traditional materials or designs in current and future transport aircraft.

6.3.1 W–B Conclusions

The kinematic parameters for scenarios G–M provide useful design information. The average vertical velocity is 22.2 ft/s, which is well above the landing-gear capability; however, the average peak vertical deceleration rate for the same set of mishaps is only 4.0 G. The average flight path angle is a -5.0 degrees, which is consistent with the average vertical velocity and the average airspeed of 232 ft/s. The average longitudinal peak deceleration is -6.0 G.

The severity of damage, as quantified by the damage metric, correlates well with the vertical and longitudinal velocities by scenario. Ranking the scenarios from the highest to lowest based on average damage metric results in the same ranking order for the top three scenarios by average vertical velocities, average airspeeds, and average peak vertical accelerations. Important factors affecting the peak longitudinal deceleration are the terrain impacted (on or off the airport's prepared surface) and the presence of obstacles. The damage metric for each scenario did not correlate well to any of the single kinematic parameters. The mean damage metric for mishaps involving vertical obstacles was consistently higher than the mean damage metric for those mishaps without vertical obstacles. However, the differences identified were not statistically significant. Similarly for the severe-injury fraction, those mishaps involving obstacles had consistently higher severe-injury fractions, yet the difference in the means was not statistically significant. Despite the lack of statistical significance, the large difference in mean damage metrics suggests that obstacles deserve consideration in establishing crashworthiness design requirements. The aircraft with the engine-on-wing-and-tail configuration was involved in more overrun mishaps than the other configurations and overall had a lower average damage metric, possibly because more of the mishaps were of the overrun type. The aircraft with four on-wing engines had a higher average damage metric than those with two on-wing engines.

Among the different mishaps, overruns (scenario F) and compromised landings (scenario G) were the most common types at 24 percent each. These two were also the lowest in terms of average damage metric and average injury fraction.

The injury data exhibited substantial variability between mishaps. In all the W–B mishaps studied, 16.9 percent of occupants experienced fatal injuries, 7.8 percent were seriously injured and, therefore, 75.5 percent experienced minor or no injury. Some mishaps with low kinematics

parameter values exhibited high fatality rates, particularly where fire was present. Similarly, a few crashes with severe kinematics parameter values resulted in a few survivors. The possibility of a few survivors is more pronounced in the W–B mishaps, in particular when a small portion of the cabin becomes isolated from the post-crash fire. In more general terms, the values of the severe-injury fraction for the three major segments (i.e., forward cabin, overwing cabin, and aft cabin) were similar, indicating that no one segment of the fuselage has greater survivability than another. Larger variation in the severe-injury fraction was found in comparing the same cabin segment across different impact scenarios. Therefore, the severity of individual injuries had more dependence on the crash conditions than on seating location. No differences were found in the injury fractions based on aircraft engine configuration.

Whereas the severe-injury fraction failed to show strong correlation to any one kinematic parameter, some generalizations were observed. For the combination of vertical and longitudinal velocity, six of the six mishaps that resulted in injury fractions greater than 90 percent fell outside the 90th-percentile velocity ellipse on the two-velocity (vertical and longitudinal) plot. The severe-injury fraction did show a strong positive correlation ($R^2 = 0.86$) to the damage metric. This strong correlation implies that designing aircraft to reduce the types of damage incorporated into the damage metric will reduce severe injuries.

The analysis did develop multiple kinematic parameter models to predict the probability that an occupant in a similar crash scenario will sustain a severe injury (serious or fatal). Therefore, these models can be used to predict the fraction of occupants suffering serious or fatal injuries using the kinematic parameters characteristic of the mishap type. This prediction capability will then allow a set of kinematic parameter values to be associated with a probability of severe injury.

6.3.2 N–B Conclusions

The kinematics for the large scenario G–M subset of the N–B mishaps provide general information about the events. The average vertical velocity is 22.3 ft/s, greater than the normal vertical landing speed of 1–3 ft/s and beyond the landing gear capability. Even so, the average peak vertical deceleration is 3.9 G. The average airspeed at impact, 223 ft/s, is consistent with most of the included mishaps occurring during attempted landings or takeoffs. The average peak longitudinal deceleration is -3.5 G, which is consistent with long stopping distances and few encountered obstacles. Consistent with the higher than normal descent rate, the average flight path angle is a rather steep -7 degrees. The average pitch angle is +4.3 degrees, which is reduced by being averaged with a few negative values, as was discussed in the text. The mishaps included a few aircraft that came to rest inverted.

The damage severity, as represented by the damage metric, is consistent with the kinematics for the two most severe scenarios. Scenario K+L has the highest average damage metric of 63.9 and both the highest average vertical velocity, 39.8 ft/s, and the highest average airspeed, 228 ft/s. Similarly, scenario H+M has the second-highest average damage metric, 50.2, with the second-highest average vertical velocity, 27.8 ft/s, and second highest airspeed, 228 ft/s. However, scenario F, the runway overruns, contains the mishaps with the third-highest average damage metric, yet had lower average vertical velocity and airspeed than scenario J. The damage metric does not correlate well to the individual kinematic parameters in the various scenarios. Investigation of the influence of vertical obstacles revealed a substantial difference in the average

and median damage metrics for the subset of mishaps with obstacles compared to the subset without obstacles. However, the differences in the means for mishaps encountering obstacles compared to mishaps not encountering obstacles were not supported statistically.

In the N–B mishaps, 17.6 percent of the occupants received fatal injuries, and a further 7.6 percent were seriously injured; therefore, almost 75 percent of occupants had no injuries or only minor ones. This high fraction of minor injury is reflected in the injury data in which the median severe injury fraction for many of the scenarios is zero or near zero. The average severe injury fraction values are raised by the few more severe accidents. The aircraft design did make a difference in the outcome as measured by the severe injury (fatal + serious) fraction. The most common engine configuration, two engines on the wing, was involved in 41 (of 86) mishaps having an average damage metric of 23 and an average severe injury fraction of 19 percent. The less common two-engines-on-tail configuration was involved in 27 mishaps, with an average damage metric of 35 and a correspondingly higher average severe-injury fraction of 34 percent. The distribution of injuries among the three cabin segments—forward cabin, overwing cabin, and aft cabin—were within a few percent of each other for each scenario. No one cabin segment stood out as either safer or less safe than the others, nor was there a consistent pattern along the sequence of the three cabin segments.

The injury data contain substantial variability in relation to the kinematic data. The severe-injury fraction for each scenario showed weak correlation with individual kinematic parameters. The correlation (R^2) values were generally low and, in many cases, the slope of the trend line was not the anticipated sign (+/-). Contact with obstacles did influence the outcome of mishaps, as measured by the severe-injury fraction. Looking at the influence of obstacles in each scenario, the presence of obstacles at least doubled the severe-injury fraction in all scenarios in which the injury fraction was non-zero. Testing both the difference in means and the difference in medians for significance found both the mean- and median-injury fraction were higher when the mishap involved obstacles.

The binary logistic regression analysis applied to the injury data and single kinematic parameters did not produce models with strong predictive capability. These models were developed with four primary scenarios: F, H+M, J, and K+L. Scenario-G mishaps had zero severe injuries; consequently, the models for this scenario could not be created. Of 32 possible models (four scenarios and eight parameters), only five had medium strength predictive capability and one, the pitch angle for scenario H+M, had high strength predictive capability according to the statistics. The multi-parameter models for all of the scenarios have a high strength predictive capability according to the summary measures of association statistics. The multi-parameter models for predicting severe-injury fraction were generally successful. These models can be used to predict the fraction of severe injuries in a given scenario by inputting a set of kinematic parameters within the range for that scenario.

6.3.3 Combined Conclusions

The separate tracking of the wind-related mishaps reveals that the mishaps associated with localized winds are less severe in terms of both damage and injury factions. For the N–B class of aircraft, both scenario L and scenario M mishaps experienced a lower damage metric when compared with the non-wind influenced scenario K and scenario H. The trend was the same in

comparing the W–B aircraft when comparing scenario M to scenario H. The comparison could not be made between scenario K and scenario L for the W–B dataset because there were no scenario L W–B mishaps. Although the presence of localized winds does not increase the damage or injury severity of these types of mishaps, this does not mean that efforts to mitigate the wind-influenced mishaps were misspent. The mitigation effort does appear to have effectively reduced the number of these mishaps. Consequently, even though these mishaps were relatively less severe, they nonetheless did cause damage and injury. Therefore, preventing them not only reduces the number of mishaps but also reduces aircraft losses and human injuries.

The injury outcome of the studied mishaps correlates well to the amount of damage to the aircraft. The injury outcome has been quantified by the fraction of severe injuries (fatalities plus serious injuries divided by the total occupants). The damage to the aircraft has been quantified by the damage metric, a parameter developed specifically to quantify damage experienced by the aircraft fuselage. The types of damage selected for inclusion in the damage metric address the basic concepts of crashworthiness: maintenance of a survivable volume, and effective restraint of the occupants. The fact that the correlation between the injury fraction and the damage metric is strong reinforces the precept that designing aircraft to minimize these types of damage will lead to fewer injuries in future mishaps.

7. REFERENCES

1. FAA Report. (2017). Study of Transport Aircraft Water Mishap Kinematics and Regional Jet Mishap Kinematics. (DOT/FAA/TC-17/52).

2. US Army Aviation Systems Command. (1989). Aircraft Crash Survival Design Guide. (USAAVSCOM TR 89-D-22A).

3. Etkin, B. (1959). *Dynamics of Flight*. Edison, NJ: John Wiley & Sons.

4. Turnbow, S. T., (1997) Summary of Equations of Motion for Several Pulse Shapes, International Center for Safety Education and Arizona State University, Appendix pp. 62-84.

APPENDIX A—LIST OF DATA FIELDS FOR WIDE-BODY AND NARROW–BODY MISHAP STUDY

List of Column Headers and Meanings by worksheet. This appendix includes the fields of data exported from the Cabin Safety Technical Research Group (CSTRG) database and fields added during the analysis to record data from the reading of the investigation reports. More fields were added as the analysis progressed to document subsets of data, to sort and operate on data for analysis and, in some cases, to facilitate plotting. Each of the four topic worksheets (i.e., Mishap Data, Kinematics, Damage, and Injury) had two versions: one with the mishaps ordered reverse chronologically and the second sorted by scenario first, then by reverse chronology. The column titles listed below may not be exactly the same for both versions of the worksheet.

Fields for Mishap Data worksheet.

Col.	Header	Explanation
A	REF	CSTRG ID number: YEARMOnthDAyL(L = sequence letter)
B	NICKNAME	Typically place, short description of event and/or plane type
C	AC_TYPE	Aircraft type
D	DATE	Date of mishap
E	Scenario	Mishap assigned to a category of similar events (F-M)
F	NO_ENGS	Number of engines
G	ENG_CONFIG	Position of engines: wings, tail, fin
H	ENG_TYPE	Turbojet, turboprop, reciprocating
I	WT_CAT	Weight category A, B, C, D, E
J	HW_LW	Wing configuration, high or low
K	MAX_SPR	Maximum number of seats between aisles (modified in study to be maximum number of seats across the airplane)
L	NUM_SEATS	Number of passenger seats
M	DATE	Date of mishap, (duplicate field)
N	ACC_REPORT	Accident report source: NTSB number or Internet link
O	IMPACT_REL	Impact related, Y/N; all mishaps used were impact related
P	FUSE_RUPT	Fuselage ruptured, Y/N

Q	FTANK_RUPT	Fuel tank rupture, Y/N
R	PHASE_FLT	Phase of flight during which mishap initiated
S	OVERRUN	Mishap involved runway overrun, Y/N
T	AC_DAMAGE	Severity of damage: destroyed, substantial, minor, none
U	TOT_ABORD	Total occupants from CSTRG database
V	FAT_TOT	Total fatalities onboard from CSTRG database
W	SER_TOT	Total serious injuries onboard from CSTRG database
X	MN_TOT	Total on board with minor or no injury, number
Y	EVACUATION	Was the evacuation an emergency, Y/N
Z	Exits	Coded information about the exits from CSTRG

Fields for kinematics data worksheet. Data for some of these fields came from the kinematic reconstructions.

Col.	Header	Explanation
A	Reference #	Identification date: YEARMOnthDAyL(L = sequence letter)
B	IDENTIFIER	Typically place and plane type
C	Aircraft Type	Aircraft type
D	Date	Date of mishap
E	Scenario	Each mishap assigned to category of similar events (F-M)
F	Pk G Vert	Peak vertical deceleration aircraft ref. frame (G)
G	Pk G Lat	Peak lateral deceleration aircraft ref. frame (G)
H	Pk G Long	Peak longitudinal deceleration aircraft ref. frame (G)
I	Vert Vel	Vertical velocity in earth reference frame
J	Airspeed	Speed along the flight path
K	Flt Path	Angle between horizon and velocity vector of aircraft c.g.
L	Pitch	Aircraft pitch angle, + is nose up
M	Roll	Aircraft roll angle to horizon, + is right wing downward

N	Yaw	Aircraft yaw angle to flight path, + is nose moving right
O	Thrust	At least one engine was operating at impact, Y/N/Reverse
P	Reconstr	Whether a reconstruction was required for kinematic data, Y/N
Q	P-FP	(Pitch angle—flight path angle) algebraic angle to characterize aircraft attitude relative to flight path

Fields for damage data worksheet

Col.	Header	Explanation
A	Reference #	Identification date: YEARMOnthDAyL(L = sequence letter)
B	Identifier	Typically place and plane type
C	Aircraft Type	Aircraft type
D	Date	Date of mishap
E	Scenario	Each mishap assigned to category of similar events, (F-M)
F	FUSE_RUPT	Fuselage ruptured, Y/N
G	FTANK_RUPT	Was the fuel tank ruptured, Y/N
H	AC_DAMAGE	Four levels: none, minor, substantial, destroyed
I	EXITS	Coded information about the exits from CSTRG
J	DAM_GROUND	Related to ditching, damage due to ground prior to water, Y/N
K	STOW_DETACHD	% of overhead bins that became detached due to impact
L	STOW_NRET	% of cabin baggage that was NOT retained
M	OHEAD. STOW	Overhead storage state, D/R/N: disrupted, retained, none
N	STOW_CONT	Contents of bins, D/R/N: disbursed, retained, not fitted
O	BULKHEADS	Bulkhead D/R/N: disrupted, retained, not fitted
P	FLOOR_Failure	Floor disrupted, associated with loss of occupied volume, Y/N
Q	SEAT_Failure	Seat disrupted, associated with restraint chain failure, Y/N

All LofV fields are filled from investigation reports and photos.

R	C-LofV	Cockpit loss of volume, widespread/local /none
S	FC-LofV	Forward cabin loss of volume W/L/N
T	OW-LofV	Overwing cabin loss of volume W/L/N
U	RC-LofV	Rear cabin loss of volume W/L/N
V	T-LofV	Tail loss of volume W/L/N

Floor disruption fields are filled from CSTRG combined with investigation reports and photos.

W	C-Fl Dis	Cockpit floor disruption W/L/N
X	FC-Fl Dis	Forward cabin floor disruption W/L/N
Y	OW-Fl Dis	Overwing cabin floor disruption W/L/N
Z	RC-Fl Dis	Rear cabin floor disruption W/L/N
AA	T-Fl Dis	Tail floor disruption W/L/N

Seat fail fields are filled from CSTRG combined with investigation reports.

AB	C-Seat Fail	Cockpit segment seat failure W-L-N
AC	FC-Seat Fail	Forward cabin seat failure W-L-N
AD	OW-Seat Fail	Overwing cabin seat failure W-L-N
AE	RC-Seat Fail	Rear cabin seat failure W-L-N
AF	T-Seat Fail	Tail seat failure W-L-N
AG	C-Skin Dmg Udrs	Cockpit segment skin damage underside W-L-N
AH	FC-Skin Dmg Udrs	Forward cabin underside skin damage W-L-N
AI	OW-Skin Dmg Wtr	Overwing cabin underside skin damage W-L-N
AJ	RC-Skin Dmg Wtr	Rear cabin underside skin damage W-L-N
AK	T-Skin Dmg Wtr	Tail underside skin damage W-L-N
AL	Emerg. Evac.	An emergency evacuation was conducted Y/N
AM	Doors on the Aircraft	Number of doors; Door = stand up height, no step-over
AN	Exits on the Aircraft	Number of exits on the aircraft; Exit = all portals not doors

AO	Doors used to evac.	Number of doors actually used during evacuation
AP	Exits used in evac.	Number of exits actually used during evacuation
AQ	Doors-Frac of Reprtd	Number of doors whose condition is stated in the investigation divided by number of doors on aircraft
AR	Exits-Frac of Reprtd	Number of exits whose condition is stated in the investigation divided by number of exits on aircraft

Functional = portal or exit is mechanically operable

Usable = portal is not blocked by fire or terrain; slide deployed and is usable, if needed

AS	Doors- Frac of All Usab	Fraction of all doors usable after impact
AT	Exits- Frac of All Usab	Fraction of all exits usable after impact
AU	Doors-Frac of All Func	Doors fraction of all usable as escape path
AV	Exits-Frac of All Func	Exits fraction of all usable as escape path
AW	Fuse Brk C-FC	Fuselage break between cockpit and forward cabin Y/N
AX	Fuse Brk FC-OW	Fuselage break between forward cabin and overwing Y/N
AY	Fuse Brk OW-RC	Fuselage break between overwing and rear cabin Y/N
AZ	Fuse Brk RC-T	Fuselage break between rear cabin and tail Y/N
BA	Gear	Landing gear up or down (partial deployment = up)
BB	Landed on Runway	Initial touchdown was on runway Y/N
BC	Gear Fails	Which, if any, landing gears failed

N = nose gear; LMG = left main; RMG = right main; CM = center main,

BD	# of Brks	Total number of breaks recorded (sum of AW-AZ)
BE	Impacted Vertical Imped	Aircraft impacted a vertical impediment during deceleration (includes berms, ditches, fences, lighting or antenna structures and buildings). Field populated from reports and photographs. Y/N
BF	Survivability	S/PS/NS. Based only on damage, deceleration

Survivable = occupied volume maintained and deceleration forces within tolerance throughout the entire aircraft. Partially Survivable = some areas of the aircraft had survivable conditions. Non-survivable = no areas of the aircraft that had survivable conditions.

BN	Cockpit Damage Metric	Damage factor for cockpit

Damage Metric = {Skin Damage (2 or 1 or 0)*1 + Floor Disruption (2 or 1 or 0)*2 + Seat Failure(2 or1 or 0)*3 + Loss of Volume (2 or 1 or 0)*4}.

BF	Fwd Cab Damage Metric	Damage metric for forward cabin
BG	OW Cab Damage Metric	Damage metric for overwing cabin
BH	Rr Cab Damage Metric	Damage metric for rear cabin
BI	Tail Damage Metric	Damage metric for tail segment
BJ	Total Damage Metric	Sum of damage metrics from each segment

Fields for Injury Data worksheet

Col.	Header	Explanation
A	Reference #	Identification date: YEARMOnthDAyL(L=sequence letter)
B	Identifier	Typically place and plane type, brief description
C	Aircraft Type	Aircraft type
D	Date	Date of mishap
E	Scenario	Each mishap assigned to category of similar events (F-M)
F	TOT_ABORD	Total occupants on board, crew + passengers
G	FAT_CREW	Number of crew with fatal injuries
H	FAT_PAX	Number of passengers with fatal injuries (infants excluded)
I	FAT_TOT	Total number of occupants with fatal injuries
J	SER_CREW	Number of crew with serious injuries
K	SER_PAX	Number of passengers with serious injuries (infants excluded)
L	SER_TOT	Total number of occupants with serious injuries
M	MN_CREW	Number of crew with minor/no injuries
N	MN_PAX	Number of passengers with minor/no injuries (infants excluded)
O	MN_TOT	Total number of occupants with minor/no injuries
P	PAX_TOT	Total number of passengers

Q	CREW_TOT	Total number of crew
R	Seat Inj Map	Was a seat and injury map provided in the report, Y/N

The following fields were populated from a combination of the CSTRG data and the information in the report. Where no seat map was available, the allocation of occupants and injuries to cabin segments were based first on information from the report and second by assuming a uniform distribution of occupants.

S	C Occup	Number of occupants in the cockpit
T	FC Occup	Number of occupants in the forward cabin
U	OW Occu	Number of occupants in the overwing cabin
V	RC Occup	Number of occupants in the rear cabin
W	T Occup	Number of occupants in the tail
X	C Fatal	Number of fatalities in the cockpit
Y	FC Fatal	Number of fatalities in the forward cabin
Z	OW Fatal	Number of fatalities in the overwing segment
AA	RC Fatal	Number of fatalities in the rear cabin
AB	T Fatal	Number of fatalities in the tail
AC	C Ser Inj	Number of occupants seriously injured in the cockpit
AD	FF Ser Inj	Number of occupants seriously injured in the forward cabin
AE	OW Ser Inj	Number of occupants seriously injured in the overwing cabin
AF	RC Ser Inj	Number of occupants seriously injured in the rear cabin
AG	T Ser Inj	Number of occupants seriously injured in the tail
AH	C Fire Fatals	Number of cockpit occupants estimated to have died of fire-related injuries who were prevented from evacuating by injury or lack of available exits. Estimated based on report.
AI	FC Fire Fatals	Number of forward-cabin occupants estimated to have died of fire-related injuries who were prevented from evacuating by injury or lack of available exits.

AJ	OW Fire Fatals	Number of overwing cabin occupants estimated to have died of fire-related injuries who were prevented from evacuating by injury or lack of available exits.
AK	RC Fire Fatals	Number of rear-cabin occupants estimated to have died of fire-related injuries who were prevented from evacuating by injury or lack of available exits.
AL	T Fire Fatals	Number of tail occupants estimated to have died of fire-related injuries who were prevented from evacuating by injury or lack of available exits.
AM	C M/N Inj	Number of occupants with minor/no injuries in cockpit
AN	FC M/N Inj	Number of occupants with minor/no injuries in forward cabin
AO	OW M/N Inj	Number of occupants with minor/no injuries in overwing cabin
AP	RC M/N Inj	Number of occupants with minor/no injuries in rear cabin
AQ	T M/N Inj	Number of occupants with minor/no injuries in tail
AR	C % Fatal	Percent of Cockpit occupants fatally injured
AS	FC % Fatal	Percent forward cabin of occupants fatally injured
AT	OW % Ftl	Percent overwing cabin of occupants fatally injured
AU	RC % Ftl	Percent rear cabin of occupants fatally injured
AV	T % Ftl	Percent tail of occupants fatally injured
AW	C % Ser Inj.	Percent of cockpit occupants seriously injured
AX	FC % Ser Inj	Percent of forward cabin occupants seriously injured
AY	OW % Ser Inj	Percent of overwing cabin occupants seriously injured
AZ	RC % Ser Inj	Percent of rear cabin occupants seriously injured
BA	T % Ser In	Percent of tail occupants seriously injured
BB	C % M/N Inj.	Percent of cockpit occupants minor/no injury
BC	FC % M/N Inj	Percent of forward cabin occupants minor/no injury
BD	OW % M/N Inj	Percent of overwing occupants minor/no injury
BE	RC % M/N Inj	Percent of rear cabin occupants minor/no injury

BF	T % M/N Inj	Percent of tail occupants minor/no injury
BG	Seat Inj Map	Seat Injury Map available in report Y/N
BH	All Occ. % Fatal	Percent of all occupants fatally injured in mishap
BI	All Occ. % Ser. Inj.	Percent of all occupants seriously injured in mishap
BJ	All Occ. % Min.-No	Percent of all occupants with minor/no injury in mishap
BK	Total Aircraft Occupants	Total number of aircraft occupants = sum of segment occ.
BL	Fatal + Serious Injury	Sum of fatalities + serious injuries for each segment
BM	Fatal + Serious Injury Fraction	(Sum of Fatal + Serious Injury)/Total occupants

APPENDIX B—LIST OF WIDE-BODY MISHAPS INCLUDED IN THE ANALYSIS

Reverse chronological order:

REFERENCE	SHORT NAME	AIRCRAFT TYPE	SCENARIO
20140620A	Kabul Omni Air B767	B767-36N	G
20130706A	SAN FRANCISCO B777	B777-200ER	H
20120331A	Tokyo B777 Tail-strike	B777-200	G
20100512A	TRIPOLI A330	A330-202	K
20090420B	JFK Royal Air Maroc hrd ldg	B767-300	G
20080117A	HEATHROW B777	B777-236ER	H
20050802A	TORONTO A340	A340-313	F
20020415A	PUSAN B767	B767	H
20010824C	LAJES A330	A330-243	G
20001224A	Tahiti DC-10 overrun	DC10-10	F
20001105A	PARIS B747	B747-200	G
20001031B	TAIPEI B747	B747-412B	K
19990923A	BANGKOK B747	B747-438	F
19990822A	HONG KONG MD11	MD11	J
19970806A	NIMITZ HILL B747	B747-3B5B	H
19960613A	FUKUOKA DC10	DC10-30	F
19930414A	DALLAS DC10	DC10-30	G
19921221A	FARO DC10	DC10-30CF	J
19920730A	NEW YORK L1011	L1011-385-1	F
19900324A	TOKYO L1011	L1011	G
19890719A	SIOUX CITY DC10	DC10-10	J
19850802A	DALLAS L1011	L1011-385-1	M
19831127A	MADRID B747	B747-283B	H
19820913A	MALAGA DC10	DC10-30CF	F
19780301A	LOS ANGELES DC10	DC10-10	F
19731217A	BOSTON DC10 (2)	DC10-30	M
19721229A	MIAMI L1011	L1011	H
19710730A-T	SAN FRANCISCO B747	B747-121	F
19710730A-L	SAN FRANCISCO B747	B747-121	G

‘Reference’ refers to the CSTRG identifier, which is the date of the mishap as “YEARMOnthDAy.” The letter is a sequential indicator for that day; therefore, A is the first accident on that date. For 19710730A, two impacts occurred, one on takeoff and a second on landing. For this study, the two were treated separately and identified as “T” and “L” with a trailing letter.

APPENDIX C—LIST OF NARROW-BODY MISHAPS INCLUDED IN THE ANALYSIS

86 mishaps sorted by Scenario, then in reverse chronological order:

REFERENCE	SHORT NAME	AIRCRAFT TYPE	SCENARIO
20140313A	PHILADELPHIA A320	A320-214	F
20111220A	YOGYAKARTA A/p	B737	F
20101102B	SUPADIO A/p overrun	B737-4YO	F
20091222A	MANLEY A/p JAMAICA	B737-823	F
20070717B	CONGONHAS A/p SAO PAULO	A320-233	F
20051208A	CHICAGO B737	B737-700	F
20030617A	GRONINGEN A/p ABORTED T-O	MD88	F
20010317A	DETROIT ABT T-O	A320-200	F
20000305A	BURBANK CA 737	B737-300	F
19990601A	Little Rock Overrun	MD82	F
19980521A	IBIZA AP Overrun	A320-212	F
19951113A	KADUNA A/p., NIGERIA	B737-200	F
19940302A	FLUSHING NY T-O Overrun	MD82	F
19890920A	LA GUARDIA B737	B737-400	F
19861025A	CHARLOTTE B737	B737-222	F
19761116A	DENVER DC9	DC9-14	F
19760427A	ST THOMAS B727	B727-95	F
19760405A	KETCHIKAN B727	B727-81	F
19750331A	CASPER B737	B737-200	F
19731127B	AKRON-CANTON DC9	DC9-31	F
19731028A	GREENSBORO B737	B737-222	F
19720418A	ADDIS ABABA, ETHIOPIA	VC10	F
19701127A	ANCHORAGE, ALASKA, U.S.A.	DC8-63F	F
19700719B	PHILADELPHIA B737	B737-222	F
19681227B	SIOUX CITY IA DC9	DC9-15	F
19671106A	CINCINNATI B707	B707-131	F
20140729A	STANSTED AIRPORT, tailstrike	B737-800	G
20140217B	FUNCHAL A/p, MADEIRA	B737-800	G
20120414A	CHAMBERY A/p T-O tailstrk	B737-33A	G
20060620A	O'HARE INTL A/p Nose gear up landing	DC9-83	G

REFERENCE	SHORT NAME	AIRCRAFT TYPE	SCENARIO
20051119A	UNIVERSITY PARK A/p	B737-800	G
20050918A	FT LAUD A/p, FL, tailstrike	A321-231	G
20040101A	TOKUNOSHIMA A/p JAPAN	MD81	G
20031213A	LIMA, PERU - Gear up landing	B737-200	G
20030112A	ROTTERDAM, TAIL STRK T-O	B737-800	G
20010809A	MASCOUTAH, IL NG Up landing	B717-200	G
19960219A	HOUSTON DC9	DC9-32	G
20120124A	KANDAHAR A/p wing tip grounded	MD83	H
20090225A	SCHIPHOL AIRPORT Turkish Air Land Short	B737-800	H
19980209A	CHICAGO B727	B727-223	H
19900125B	COVE NECK, LONG ISLAND, NY, U.S.A.	B707-321B	H
19890108A	KEGWORTH, EAST MIDLANDS A/p, U.K.	B737-400	H
19781228A	PORTLAND, OREGON	DC8-61	H
19770404A	NEW HOPE DC9	DC9-31	H
19740911A	CHARLOTTE DC9	DC9-31	H
19731127A	CHATTANOOGA DC9	DC9-32	H
19730731A	LOGAN INT'L A/p, MASSACHUSETTS,	DC9-31	H
19730623A	KENNEDY A/p, NY.	DC8-61F	H
19721208A	CHICAGO B737	B737-222	H
19671120A	CONSTANCE, KY	CV880	H
19960107A	NASHVILLE, DC9	DC9-32	M
19951112A	BRADLEY A/p landing short	MD83	M
19751112A	RALEIGH B727	B727-225	M
19750624A	NEW YORK B727	B727-225	M
19740130A	PAGO PAGO, AMERICAN SAMOA	B707-321B	M
20140222A	TERCEIRA-LAJES A/p, AZORES	B737-800	J
20140201A	SURABAYA, INDONESIA	B737-900	J
20130722A	LAGUARDIA hard landing, nose	B737-700	J
20110926A	PUERTO ORDAZ A/p	DC9	J
20070221A	JUANDA A/p hard landing	B737-33A	J

REFERENCE	SHORT NAME	AIRCRAFT TYPE	SCENARIO
20060318A	SEVILLE, SPAIN	B737-6D6	J
20010418A	FUNCHAL, MADEIRA, PORTUGAL	A321-211	J
19990914A	GIRONA hard landing lost control	B757-204	J
19990909A	NASHVILLE Main landing gear fail	DC9-31	J
19971224A	SCHIPHOL A/p, AMSTERDAM,	B757-236	J
19910201A	LOS ANGELES B737	B737-300	J
19871227A	PENSACOLA DC9	DC9-31	J
19810217A	SANTA ANA B737	B737-293	J
19740116A	LOS ANGELES A/p,	B707-131B	J
19701228A	ST THOMAS B727	B727-200	J
19700915A	KENNEDY A/p, NY	DC8-62	J
20080820A	MADRID BARAJAS INTL A/p, SPAIN	MD82	K
20070916A	PHUKET INTL A/p, THAILAND	MD82	K
20050905B	MEDAN, INDONESIA	B737-200	K
20030306B	TAMANRASSET ENG FAIL on T-O	B737-2T4	K
19880831B	DALLAS B727	B727-232	K
19871115A	DENVER DC9	DC9-14	K
19820113A	WASHINGTON B737	B737-222	K
20081220A	DENVER Intl A/p,	B737-500	L
20061029A	NNAMDI A/p Nigeria	B737-200	L
20051210A	PORT HARCOURT, NIGERIA	DC9-31	L
20010207A	BILBAO A/p, SPAIN	A320	L
19940702A	CHARLOTTE DC9	DC9-31	L
19760623A	PHILADELPHIA DC9	DC9-31	L
19750807A	STAPLETON B727	B727-224	L

APPENDIX D—DAMAGE METRIC BY CABIN SEGMENT, NARROW-BODY MISHAPS

The following table is too large to be practically included in the body of the report. It is intended to appear after the first paragraph under the heading "Quantifying Damage – N–B". The reference number ID is the CSTRG identifier, as explained in the report. The assignment of scenario is explained in section 2 of the report as is the creation of the Damage Metric values. The column labeled "No. of NI" refers to the number of cells in the worksheet that had missing damage information for a particular mishap.

Reference # ID	Scenario (F-M)	Cockpit Damage Metric	Fwd Cabin Damage Metric	OW Cabin Damage Metric	Rr Cabin Damage Metric	Tail Damage Metric	Total Damage Metric	No. of NI
20140313A	F	2	1	0	0	2	5	0
20111220A	F	1	2	2	2	1	8	0
20101102B	F	0	0	0	0	0	0	0
20091222A	F	13	11	5	11	7	47	0
20070717B	F	20	23	23	23	23	112	0
20051208A	F	2	0	0	0	0	2	0
20030617A	F	2	2	2	2	2	10	0
20010317A	F	0	0	0	1	2	3	0
20000305A	F	5	1	0	0	0	6	0
19990601A	F	11	14	10	2	2	39	0
19980521A	F	0	0	0	0	0	0	0
19951113A	F	0	0	0	0	0	0	0
19940302A	F	10	7	1	0	0	18	0
19890920A	F	7	7	3	9	1	27	0
19861025A	F	2	7	2	0	0	11	0
19761116A	F	2	1	0	0	0	3	0
19760427A	F	11	23	17	23	10	84	0
19760405A	F	11	16	12	19	7	65	0
19750331A	F	0	0	0	0	0	0	0
19731127B	F	2	2	2	2	5	13	0
19731028A	F	2	2	2	2	5	13	0
19720418A	F	4	10	2	5	7	28	0
19701127A	F	8	9	2	11	5	35	0
19700719B	F	2	2	2	2	2	10	0
19681227B	F	5	5	2	2	2	16	0
19671106A	F	4	4	5	2	2	17	0
20140729A	G	0	0	0	0	2	2	0

Reference # ID	Scenario (F-M)	Cockpit Damage Metric	Fwd Cabin Damage Metric	OW Cabin Damage Metric	Rr Cabin Damage Metric	Tail Damage Metric	Total Damage Metric	No. of NI
20140217B	G	0	0	0	0	1	1	0
20120414A	G	0	0	0	0	1	1	0
20060620A	G	2	1	0	0	0	3	0
20051119A	G	0	0	0	0	1	1	0
20050918A	G	0	0	0	0	1	1	0
20040101A	G	0	0	1	0	0	1	0
20031213A	G	0	1	2	1	1	5	0
20030112A	G	0	0	0	0	0	0	0
20010809A	G	2	1	0	0	0	3	0
19960219A	G	2	2	2	2	2	10	0
20120124A	H	0	0	0	0	0	0	0
20090225A	H	17	16	14	11	16	74	0
19980209A	H	2	2	2	2	2	10	0
19961019A	H	1	1	2	2	2	8	0
19900125B	H	20	20	19	19	11	89	0
19890108A	H	14	20	19	19	9	81	0
19781228A	H	20	23	7	4	2	56	0
19770404A	H	20	23	16	19	15	93	1
19740911A	H	11	23	23	19	14	90	0
19731127A	H	7	2	5	7	7	28	0
19730731A	H	20	23	23	23	23	112	0
19730623A	H	1	1	2	7	7	18	0
19721208A	H	14	19	19	14	8	74	0
19671120A	H	20	23	23	14	14	94	0
19960107A	M	0	0	0	1	2	3	0
19951112A	M	2	2	2	2	2	10	0
19751112A	M	2	2	2	2	2	10	0
19750624A	M	20	23	23	19	10	95	0
19740130A	M	2	2	2	2	1	9	0
20140222A	J	0	0	0	0	0	0	0
20140201A	J	0	0	0	0	1	1	0
20130722A	J	1	0	0	0	0	1	0
20110926A	J	0	0	0	0	2	2	0
20070221A	J	0	0	0	9	0	9	0

Reference # ID	Scenario (F-M)	Cockpit Damage Metric	Fwd Cabin Damage Metric	OW Cabin Damage Metric	Rr Cabin Damage Metric	Tail Damage Metric	Total Damage Metric	No. of NI
20060318A	J	0	0	1	0	0	1	0
20010418A	J	0	0	0	0	1	1	0
19990914A	J	4	14	2	14	4	38	0
19990909A	J	0	0	0	0	0	0	0
19971224A	J	2	2	1	2	0	7	0
19910201A	J	10	5	0	0	0	15	0
19871227A	J	0	0	0	3	1	4	0
19810217A	J	2	2	11	14	2	31	0
19740116A	J	1	2	2	0	0	5	0
19701228A	J	2	7	10	8	2	29	0
19700915A	J	1	1	1	13	1	17	0
20080820A	K	20	17	23	23	23	106	0
20070916A	K	20	23	11	4	5	63	0
20050905B	K	20	20	23	23	11	97	0
20030306B	K	2	5	2	2	9	20	11
19880831B	K	7	7	4	16	12	46	0
19871115A	K	16	14	18	20	6	74	0
19820113A	K	20	23	23	23	13	102	0
20081220A	L	10	5	2	2	2	21	0
20061029A	L	20	23	23	19	19	104	0
20051210A	L	20	23	23	23	23	112	0
20010207A	L	0	1	1	1	0	3	0
19940702A	L	16	23	13	15	10	77	0
19760623A	L	12	12	12	7	4	47	0
19750807A	L	2	7	4	4	5	22	0